

Forschungszentrum Karlsruhe
in der Helmholtz-Gemeinschaft

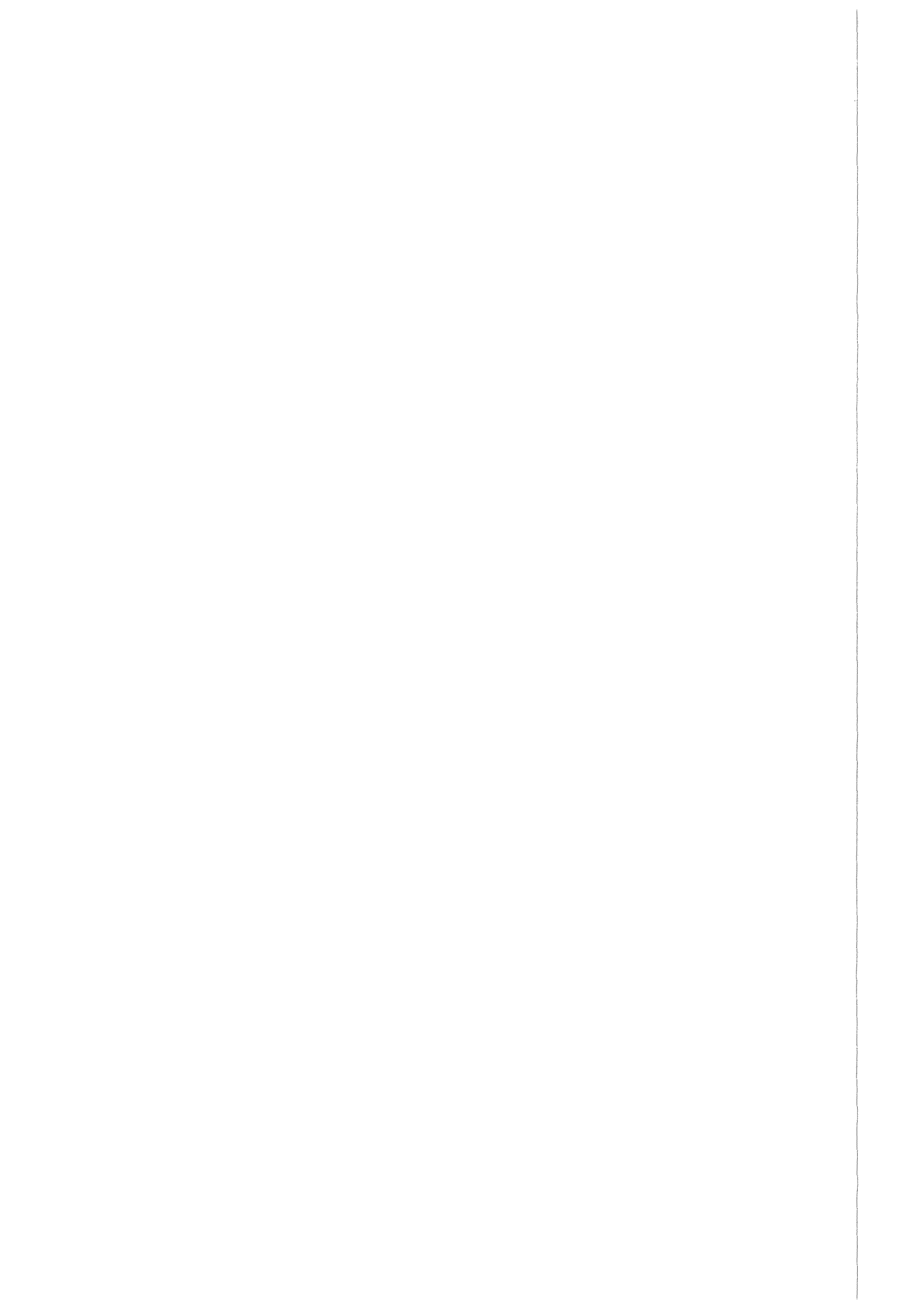
Wissenschaftliche Berichte
FZKA 6124

**Effects of Humic Substances
on the Migration of
Radionuclides: Complexation
and Transport of Actinides
First Technical Progress Report**

G. Buckau (Editor)

Institut für Nukleare Entsorgungstechnik

August 1998



**Forschungszentrum Karlsruhe
Technik und Umwelt**

**Wissenschaftliche Berichte
FZKA 6124**

**EFFECTS OF HUMIC SUBSTANCES ON THE MIGRATION
OF RADIONUCLIDES: COMPLEXATION AND TRANSPORT
OF ACTINIDES**

FIRST TECHNICAL PROGRESS REPORT

EC Project No.: FI4W-CT96-0027

(Work Period 01.97 - 12.97)

G. BUCKAU (Editor)

Institut für Nukleare Entsorgungstechnik

**Forschungszentrum Karlsruhe GmbH, Karlsruhe
1998**

- Partner No. 1 (Coordinator): FZK/INE, D**
Partner No. 2: BGS, UK
Partner No. 3: CEA-SGC, F
Partner No. 4: FZR-IfR, D
Partner No. 5: KUL, B
Partner No. 6: LBORO, UK
Partner No. 7 (Associated to Partner No. 3): CEA-LSLA, F
Partner No. 8 (Associated to Partner No. 3): GERMETRAD, F
Partner No. 9: RMC-E, UK
Partner No. 10: NERI, Dk
Partner No. 11 (Associated to Partner No. 1): GSF-IfH, D

Als Manuskript gedruckt
Für diesen Bericht behalten wir uns alle Rechte vor

Forschungszentrum Karlsruhe GmbH
Postfach 3640, 76021 Karlsruhe

Mitglied der Hermann von Helmholtz-Gemeinschaft
Deutscher Forschungszentren (HGF)

ISSN 0947-8620

Foreword

The present report describes progress within the first year of the EC-project "Effects of Humic Substances on the Migration of Radionuclides: Complexation and Transport of Actinides". The project is conducted within the EC-Cluster "Radionuclide Transport/Retardation Processes". Contrary to formal requirements of the Commission, this report with a great deal of detail is established already after one year of project work. It is scheduled to be followed by a second technical progress report covering the second year of the project. In agreement with the contractual obligations a final report of similar technical detail will also be generated.

The report contains an executive summary written by the coordinator (FZK/INE) with strong support from the other three task leaders (BGS, CEA-SGC and RMC-E). More detailed results are given by individual contributions of the project partners in 13 annexes. In the executive summary report the origin of results presented is given, also serving as guidance for finding more detailed results in the annexes. Not all results are discussed or referred to in the executive summary report and thus readers with a deeper interest also need to consult the annexes.

Content	<u>Page</u>
Executive Summary (G. Buckau, FZK/INE)	1
Annexes:	
Sampling and Characterization of Gorleben Groundwater/Sediment Systems for Actinide Migration Experiments (Artinger R. et al., FZK/INE)	23
Complexation of Np(V) with Humic Acid: Intercomparison of Results from Different Laboratories (Marquardt, C.; Kim J.I., FZK/INE)	43
Effects of Humic Substances on the ²⁴¹ Am Migration in a Sandy Aquifer: Batch and Column Experiments with Gorleben Groundwater/Sediment Systems (Artinger R. et al., FZK/INE)	69
Modeling of Humic Colloid Mediated Transport of Americium(III) by a Kinetic Approach (Schüssler W. et al., FZK/INE)	91
Extraction, Purification and Characterization of Fulvic Acid (Higgo, JJW et al., BGS)	103
Uranium Inorganic Speciation Determined by Time-Resolved Laser-Fluorescence (Laszak I. et al., CEA)	129
Mobility of Am, Eu and Tc in the Presence of Humic Acids (Fleury Ch. et al., GERMETRAD)	147
Isolation and Characterization of Aquatic Humic Substances from the Bog "Kleiner Kranichsee" (Schmeide K. et al., FZR-IfR)	161
Reduction of Technetium in Solution: Influence of Ferrous Iron, Mineral Phases and Organic Matter (Maes A.; Capon, L., KUL)	197
Studies of Metal Complexation with Humic and Fulvic Acid (King S.; Warwick P., LBORO)	217
A Modelling Study of Humate Mediated Metal Transport (Bryan N., RMC-E)	245
Interaction of Humic Acids with Mineral Surfaces (Carlsen L, NERI)	263
Effects of Humic Substances on the ¹⁵² Eu Migration in a Sandy Aquifer: First Results from Column Experiments with 10 m Flow Distance (Klotz D.; Wolf M., GSF/IfH)	269

EXECUTIVE SUMMARY

**EFFECTS OF HUMIC SUBSTANCES ON THE MIGRATION OF
RADIONUCLIDES: COMPLEXATION AND TRANSPORT OF
ACTINIDES**

FIRST TECHNICAL PROGRESS REPORT

EC Project No.: FI4W-CT96-0027

(Work Period 01.97 - 12.97)

**G. Buckau
(FZK/INE)**

Content of Executive Summary

	<u>Page</u>
INTRODUCTION	5
1. OBJECTIVES	7
2. PARTNERS AND PROJECT STRUCTURE	7
3. SUMMARY OF RESULTS	7
3.1 TASK 1 (Sampling and Characterization)	9
3.1.1 Objectives and General Achievements	9
3.1.2 Summary of Characterization Results	9
3.1.3 Characteristic Properties of Humic and Fulvic Acids	10
3.2 TASK 2 (Complexation)	12
3.2.1 Objectives and General Achievements	12
3.2.2 Summary of Complexation Studies	13
3.3 TASK 3 (Actinide Transport)	15
3.3.1 Objectives and General Achievements	15
3.3.2 Experimental Systems	16
3.3.4 Summary of Results	16
<Mobility of the redox sensitive technetium>	16
<Mobility of Am(III)/Eu(III)>	17
<Sorption of humic acid on mineral surfaces>	18
3.4 TASK 4 (Migration Model Development and Testing)	18
3.4.1 Objectives and General Achievements	18
3.4.2 Modeling based on Equilibrium Approach	18
3.4.3 Modeling based on Kinetic Approach	19
3.4.3 Joint Database on Humate Complexation	20
4. REFERENCES	21

INTRODUCTION

The project started 01.97 and has a duration of three years. This report covers the first year, i.e. the period 01.97 - 12.97. Work has been conducted on Task 1 ("Sampling and Characterization"); Task 2 ("Complexation"); Task 3 ("Actinide Transport") and Task 4 ("Migration Model Development and Testing"). Work on Task 5 ("Assessment of Impact on Long-Term Safety") will commence at a later stage of the project. Nevertheless, initial studies on the origin and fate of humic substances in the Gorleben aquifer have already been performed providing input for site-specific assessment of the impact of humic substances on the radionuclide migration.

The project encompasses development of the necessary input to judge upon the influence of humic substances on the long-term safety of radioactive waste disposal. The project focuses on long-lived radionuclides with high radiotoxicity, i.e. actinides and technetium, and their behavior in the far-field. To assess the impact of humic substances on the radionuclide migration in the far-field relevant processes need to be introduced into models. These models rest on a step-wise approach where data of individual processes from relatively well defined systems are tested for their applicability on more complex laboratory systems on natural material (especially batch and column experiments under near-natural conditions). The processes described by models developed from laboratory experiments are limited by the size and time constraints of such studies. Furthermore, large-scale inhomogeneities and deviation from equilibrium in the real more or less open system cannot be easily developed through investigations on the laboratory scale. In order to achieve adequate confidence that relevant processes have been regarded in models developed, the real system is also investigated with respect to for example, chemical behavior of actinide analogue trace elements in natural humic colloids and the migration behavior of humic colloids present at a real site. A schematic description of the overall approach of the project is shown in Fig. 1.

Contrary to original intentions and for reasons beyond the reach of the project partners an encompassed research site in France did not materialize and the Sellafield is not anymore a candidate site for disposal. Sellafield, however, is studied as a reference site for such geochemical conditions. Material relevant for the German "Königstein" and "Johanngeorgenstadt" uranium mining and milling sites is also used within the project. Some aspects are investigated on Boom Clay material. For above reasons, however, site-specific work in view of nuclear waste disposal focuses on the German Gorleben site.

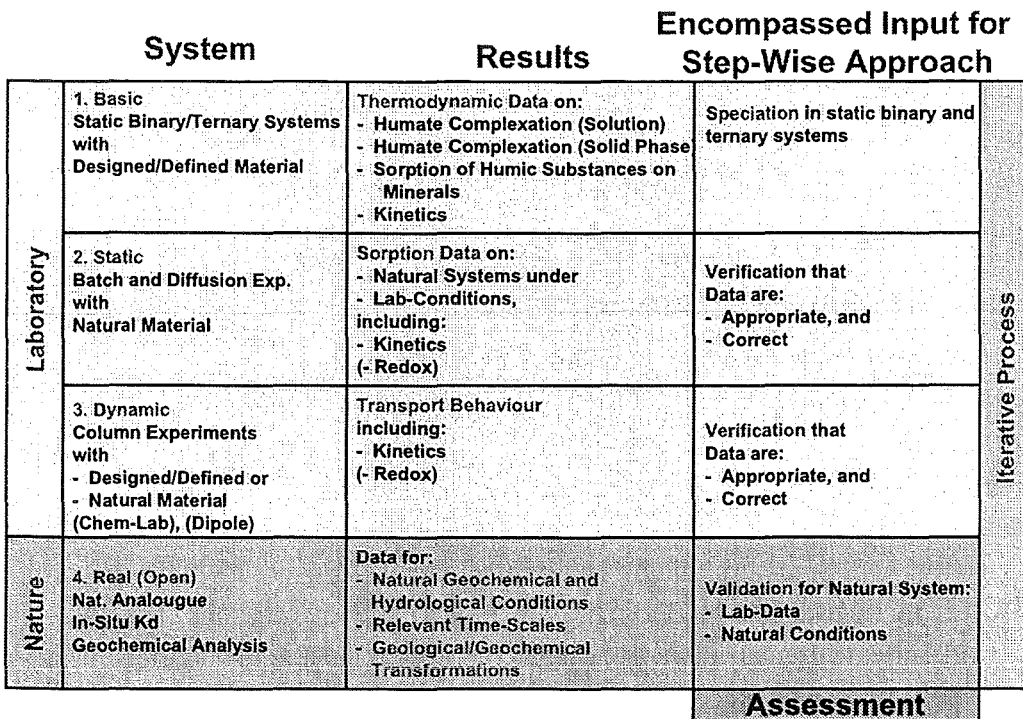
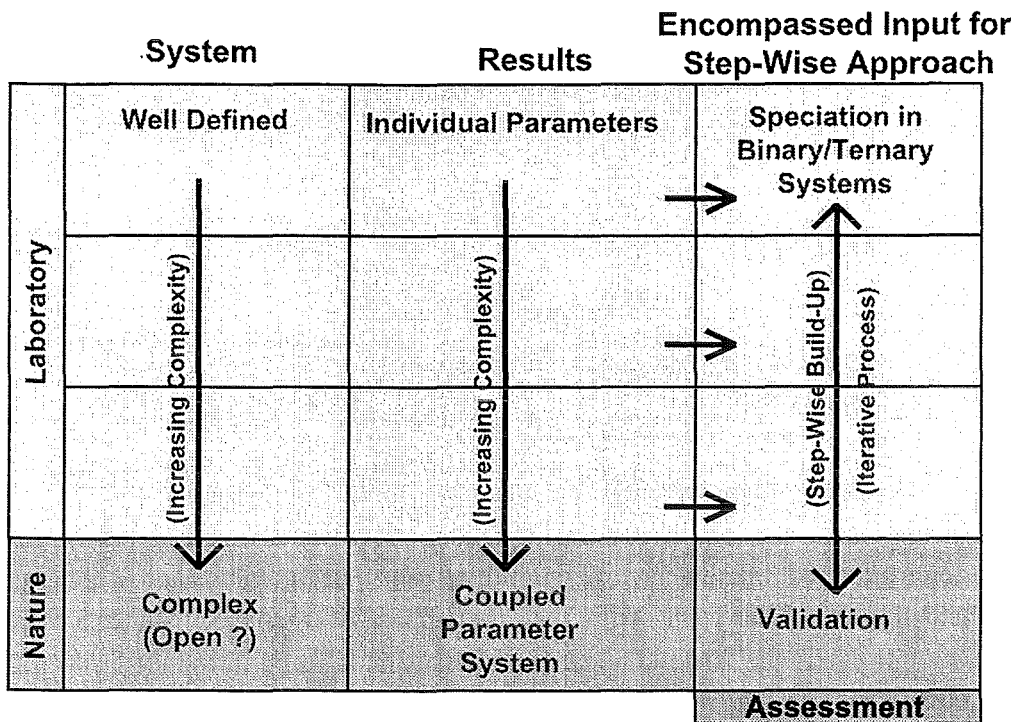


Fig. 1: Schematic description of the overall project approach

1. OBJECTIVES

The main objective of the project is to determine the influence of humic substances on the migration of radionuclides. For the long-term safety, long-lived highly radiotoxic nuclides are the most relevant. The project therefore focuses on actinide elements. In order to achieve the main objective a thorough understanding is needed for (i) the complexation of actinides with humic substances, (ii) the influence of humic substances on the sorption properties of sediments, and (iii) the mobility of actinide humic substance species in groundwater.

2. PARTNERS AND PROJECT STRUCTURE

The project has 11 partners. Three partners are associated to other contractors. The partners and their partnership is as follows:

Partner No. 1 (Coordinator): FZK/INE, D

Partner No. 2: BGS, UK

Partner No. 3: CEA-SGC, F

Partner No. 4: FZR-IfR, D

Partner No. 5: KUL, B

Partner No. 6: LBORO, UK

Partner No. 7 (Associated to Partner No. 3): CEA-LSLA, F

Partner No. 8 (Associated to Partner No. 3): GERMETRAD, F

Partner No. 9: RMC-E, UK

Partner No. 10: NERI, Dk

Partner No. 11 (Associated to Partner No. 1): GSF-IfH, D

The project is divided into five tasks with a project structure as shown in Fig. 2.

3. SUMMARY OF RESULTS

In accordance with the project time schedule work has been carried out on Task 1 to Task 4. The overall progress within individual tasks and contributions of individual partners is summarized below. Details can be found in the respective annexes.

**Project Management Structure
(Overview)**

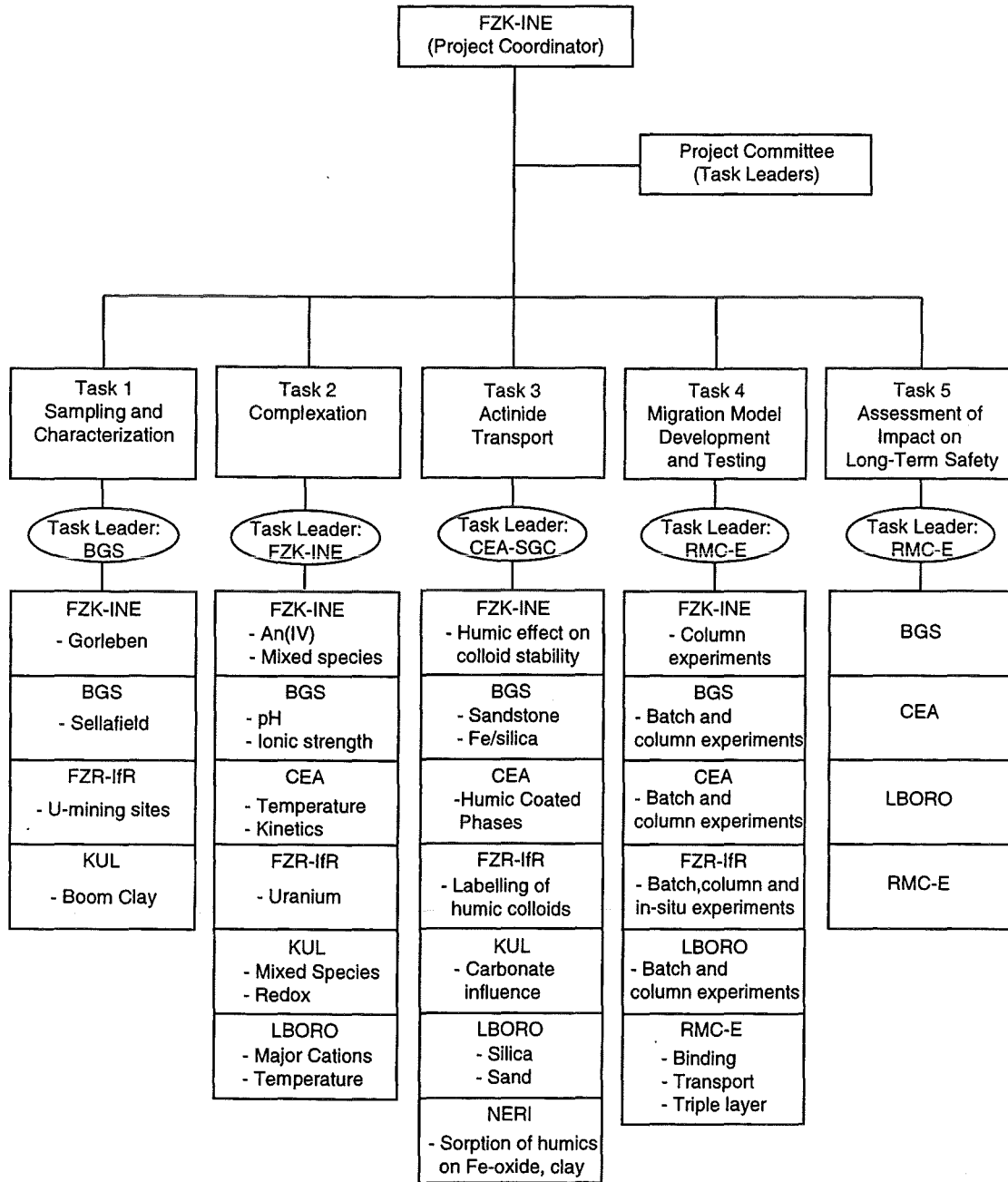


Fig. 2: Project structure

3.1 TASK 1 (Sampling and Characterization)

3.1.1 Objectives and General Achievements

The objectives of this task are to ensure appropriate sampling and characterization of relevant experimental material, ensure appropriate documentation of the sampling and characterization and thus provide the basis for trustworthy interpretation of results and inter-comparison studies between different laboratories. Natural experimental material from Gorleben (D), Sellafield and Derwent Reservoir (UK), Johanngorgenstadt (D), Königstein (D) and reference sites have been sampled and characterized. Man-made designed experimental material, such as humic acid coated silica beads and defined mineral phases have been prepared and characterized.

3.1.2 Summary of Characterization Results

Material from the Gorleben site and reference sites has been characterized and conditioned for batch and column experiments under inertgas conditions. Characterization has not only been done on the material prior to conditioning but also the influence of conditioning has been monitored. Well defined column systems with dimensions reaching up to a total length of 10 meters under defined anoxic conditions are in operation (FZK/INE and GSF/IfH).

BGS has determined the total organic carbon (TOC) concentrations in different wells at the project related Sellafield site and found that concentrations are less than 0.1 mgC/L. These results serve as input for assessment of the humic substance impact on RN-migration at this reference site. Based on the results a source was selected for isolation, purification, characterization of fulvic acid, namely "Derwent Reservoir" (Derbyshire, UK). From this source approximately 8 g fulvic acid is isolated and characterized, available as a liquid concentrate. The Derwent Reservoir fulvic acid has been characterized for elemental composition, UV/Vis spectroscopic properties, molecular weight/hydrodynamic size, inorganic impurities, proton exchange properties and uranyl ion complexation.

FZR-IfR has sampled humic and fulvic acids from the peat bog "Kranichsee" from nearby the project-related sites "Johanngorgenstadt" and "Königstein". A total of 13 g of humic acid and 10 g of fulvic acid were isolated. The most widely used internationally accepted standard procedure for the isolation of aquatic humic substances uses XAD-8 resin which is no longer commercially available. Therefore, six different resins were tested to modify the standard isolation procedure. Supelite™ DAX-8 (Supelco) was identified as a suitable replacement.

The DOC as the source material for humic and fulvic acid from "Kranichsee" was characterized by ultrafiltration using pore sizes from 100 kD to 3 kD. Isolated humic and fulvic acids were characterized by ash content, elemental composition, major inorganic components, functional group content, IR spectroscopy and Capillary Electrophoresis. The results show that the isolation and purification was successful. Considering the importance for metal ion complexation, the content and characteristics of proton-exchanging groups were determined by several methods and compared. The standard methods applied were (i) barium exchange capacity at high pH ("barium hydroxide method"); (ii) calcium exchange capacity in acetate buffered medium ("calcium acetate method"); and (iii) direct titration. Carboxylic and phenolic groups were also determined by methylation/demethylation with [^{14}C]-diazomethane. Purified Aldrich humic acid was used as a reference.

KUL has isolated in-situ Boom-Clay humic acid solution by bicarbonate extraction. Characterization of these humic acids has not yet been performed.

3.1.3 Characteristic Properties of Humic and Fulvic Acids

In Tables 1-3, elemental composition, inorganic impurities and functional group content of humic and fulvic acids is summarized. For comparison, results are also shown for EC-Coco-Club humic and fulvic acids from activities within the EC-Mirage project. Kranichsee humic and fulvic acids as well as Aldrich(FZR) humic acid have somewhat low H/C atom ratios compared to Coco reference substances and literature ranges. Aldrich(FZR) humic acid shows a relatively low O/C atom ratio. The somewhat higher O/C atom ratios of Derwent and Kranichsee fulvic acids compared to Gohy-573(Coco) fulvic acid may reflect differences in their origin. Derwent and Kranichsee materials are isolated from surface waters whereas the Gorleben material is from a deep groundwater of the Gorleben aquifer. The Kranichsee and Aldrich(FZR) humic acids in general contain higher concentrations of impurities than the other ones. The total amount of functional groups occupied by multivalent metal ions, however, is so low that no significant impact can be expected on investigations of their complexation behavior.

Results on functional group content reflect both differences in the origin of the material and differences in experimental methods applied. With exception for the higher Ba exchange capacity at high pH of Kranichsee humic acid and the corresponding high number for phenolic OH, no dramatic differences are found in the functional group contents of different humic substances measured by a given method. As expected fulvic acids show slightly higher functional group contents than humic acids.

Table 1: Elemental composition and H/C and O/C atom ratios for humic and fulvic acids. Derwent, Kranichsee and Aldrich(FZR) humic substances originate from the present project. Aldrich(Coco) and Gohy-573(Coco) are EC reference humic substances from the MIRAGE-Coco-Club and are shown for comparison. Literature value ranges are from Kim et al. 1990.

Humic Acid					
	Kranichsee	Gohy-573(Coco)	Aldrich(Coco)	Aldrich(FZR)	Literature
<u>Element</u>	<u>Weight %</u>				
C	49.9	56.3	55.2	58.7	50-60
H	3.5	4.5	4.5	3.3	4-6
N	1.8	1.7	0.3	0.8	2-6
S	0.5	1.7	2.3	4.1	0-2
O	33.4	35.8	37.6	24.8	30-35
<u>Atom ratio</u>					
H/C	0.84	0.98	0.97	0.67	0.94 ± 0.12
O/C	0.50	0.48	0.51	0.32	0.50 ± 0.03
Fulvic Acid					
	Derwent	Kranichsee	Gohy-573(Coco)	Literature	
<u>Element</u>	<u>Weight %</u>				
C	49.1	48.8	57.2	40-50	
H	4.2	2.6	4.9	4-6	
N	0.6	0.6	1.14	1-3	
S	0.3	0.5	1.44	0-2	
O	45.8	39.1	35.4	44-50	
<u>Atom ratio</u>					
H/C	1.02	0.63	1.02	1.02 ± 0.16	
O/C	0.69	0.60	0.46	0.51 ± 0.10	

Some results on characterization by hydrodynamic size/molecular weight are discussed in the annex of BGS. Ultracentrifugation and Flow-Field Flow-FFF gave remarkably similar results for the Derwent fulvic acid. The average value of ≈ 4000 Dalton is within the range expected for fulvic acids. The importance of using comparable evaluation methods is reflected in apparent differences between the present findings and previous results by Gel-Permeation-Chromatography on Gohy-573(FA/Coco) (hydrodynamic size of approximately 9000 Dalton, Kim et al. 1990). Due to differences in experimental conditions and especially calibration standards used these differences occur. This underlines that for the purpose of characterizing humic substances by hydrodynamic size/molecular weight, well defined and comparable experimental conditions need to be applied.

Table 2: Inorganic impurities (in $\mu\text{g/g}$) for humic and fulvic acids. Derwent, Kranichsee and Aldrich(FZR) humic substances originate from the present project. Aldrich(Coco) and Gohy-573(Coco) are EC reference humic substances from the MIRAGE-Coco-Club and are shown for comparison (Kim et al. 1990).

Humic Acid					
	Kranichsee	Gohy-573(Coco)	Aldrich(FZR)	Aldrich(Coco)	Aldrich(Coco) (Non-purified)
Na	1 670	19.0	226	270	75 116
K	324		36		
Ca	708	22.6	611	31.7	9 931
Mg	35	4.0	19	5.6	698
Al	149	39.3	93	35	
Si	656	68	137	15	3 333
Fe	1 018	277	863	360	12 207
Co		2.5		0.33	2.5
Ce		1.1		4.1	23.0
Eu		0.05		0.24	0.66
Th	2	7.4	1	1.53	2.0
U	4	2.2	1	0.23	0.65

Fulvic Acid			
	Derwent Reservoir.	Kranichsee	Gohy-573(Coco)
Na	36.1	10 095	2 196
K	<12	701	
Ca	<12	487	437
Mg	<24	87	44
Al	61.3	41	
Si	18.0	290	1 196
Fe	166	296	52.9
Co	2.4		0.24
Ce	0.06		0.1
Eu	<0.12		0.01
Th	0.17	n.d.	0.23
U	0.05	2	

n.d.: not detected

3.2 TASK 2 (Complexation)

3.2.1 Objectives and General Achievements

The objectives of this task is to provide relevant basic data on actinide/technetium humate complexation and the reduction of the redoxsensitive elements. The studies are conducted on laboratory systems well defined with respect physico-chemical conditions (pH, ionic strength, temperature, ..). Humate complexation studies have been conducted on U(VI), Np(V) and Eu(III), including the effect of elevated temperatures (up to 60 °C) upon the Eu(III)-humate complexation. Preparations are done for the purpose of studying mixed

hydroxo/carbonate-humate complexes of Uranium and Europium in the pH neutral and moderately alkaline range. Investigations have also been commenced to provide the basis for interpretation of Tc(VII)/Tc(IV) redox reactions in relevant systems.

3.2.2 Summary of Complexation Studies

FZK/INE has conducted complexation studies on the Np(V) humate system at pH 7 - 9 in 0.1 mol/L NaClO₄ (Marquardt and Kim, 1998). Comparison with published results give

Table 3: Content of proton exchanging functional groups in humic and fulvic acids determined by barium exchange capacity at high pH ("BaOH"), calcium exchange capacity in acetate buffered medium ("Ca-Acetate"), "Direct Titration", methylation/demethylation with [¹⁴C]-diamethane ("Radiometric") (from FZR-lfR) and fitting of pH titration curve.

Determination method	Humic Acid	Σ COOH + Phenolic OH	COOH (meq/g)	Phenolic OH
BaOH	Kranichsee(HA)	10.17 ± 0.5		
	Aldrich(HA)	7.12 ± 0.25		
	Aldrich(HA/Coco)	7.06 ± 0.67		
	Gohy-573(HA/Coco)	6.61 ± 0.27		
Ca-Acetate	Kranichsee(HA)		4.20 ± 0.17	5.97 ± 0.39 ^a
	Aldrich(HA)		4.41 ± 0.11	2.71 ± 0.34 ^a
	Aldrich(HA/Coco)		4.80 ± 0.21	2.26 ± 0.72 ^a
	Gohy-573(HA/Coco)		4.75 ± 0.29	1.86 ± 0.40 ^a
	Kranichsee(FA)		6.05 ± 0.31	
Radiometric	Kranichsee(HA)	7.75 ± 0.35	3.88 ± 0.41	3.87 ± 0.52
	Aldrich(HA)	7.4 ± 0.4	3.9 ± 0.1	3.4 ± 0.4
	Kranichsee(FA)	8.82 ± 0.48	3.98 ± 0.25	4.84 ± 0.65
Direct Titration	Kranichsee(HA)		4.83 ± 0.18	
	Aldrich(HA)		5.06 ± 0.17	
	Aldrich(HA/Coco)		5.43 ± 0.16	
	Gohy-573(HA/Coco)		5.38 ± 0.20	
	Gohy-573(FA/Coco)		5.70 ± 0.09	
	Kranichsee(FA)		5.60 ± 0.12	
	Derwent(FA) ^b	8.1	5.0	3.1

^a: Calculated from the difference between "Σ COOH + Phenolic OH" and "COOH" by BaOH and Ca-Acetate methods.

^b: Different functional group contents by fitting of the pH titration curve to NICA-Donnan continuous distribution model(cf. contribution of BGS)

important information with respect to (i) impact upon experimental results from application of different speciation methods; (ii) intercomparison of results on different humic acids; and (iii) application of different complexation models. Present and published results based upon direct spectroscopic speciation on three different humic acids result in basically indistinguishable experimental data. Application of indirect speciation by anion exchange, electrophoretic ion focusing and dialysis leads to inconsistencies. Present and published results based on direct spectroscopic speciation are successfully modeled by the Charge Neutralization Model, i.e. one complexation constant with loading capacity varying systematically with physico-chemical conditions (see Table 4). The results from three different studies agree well with each other and the minor deviations in loading capacities can be allocated to differences in experimental conditions.

Table 4: Np(V)-humate complexation results from spectroscopic speciation evaluated by the Charge Neutralization Model. Results refer to an ionic strength of 0.1 M (NaClO₄). The different humic acids (HA) are: GHA (Gorleben); AHA (Aldrich); and BHA (Bradford) (from FZK/INE).

pH	Humic Acid	LC (%)	log β (L/mol)	Reference
7.0	GHA	13	3.53 ± 0.05	FZK/INE
8.0	"	22	3.61 ± 0.07	"
9.0	"	43	3.61 ± 0.04	"
6.0	"	6.8	3.64	[Sekine]
7.0	"	9.9	3.65	"
8.0	"	14.9	3.68	"
9.0	"	30.5	3.67	"
4.5	AHA	2.8	3.43	[Rao]
6.0	"	6.9	3.45	"
7.5	"	17	3.60	"
4.5	BHA	2.8	3.84	"
6.0	"	6.9	3.58	"
7.5	"	17	3.75	"
Mean value: 3.62 ± 0.11				

BGS has studied the complexation of the uranyl ion with Derwent Reservoir fulvic acid by solvent extraction and cation exchange between pH 3.9 and 4.4. The results from the

two experimental methods used are very consistent with each other and also agree well with results from comparable experimental conditions on Drigg fulvic acid.

CEA has conducted experimental work to provide the basis for studying mixed hydroxide/carbonate-humate complexation of Uranium and Europium under pH neutral conditions. The method is based on identification of hydroxide species by fluorescence properties, including (i) position and intensity of different fluorescent transitions; (ii) fluorescence life-time of individual species; and (iii) quenching properties reflecting the local binding environment.

LBORO has investigated the complexation of Eu(III) with Aldrich humic acid and Derwent Reservoir fulvic acid at temperatures varying between 20 and 60 °C. Experiments were conducted at pH 4.5 and speciation was done by cation exchange. The results are evaluated by three different approaches, namely Schubert, Charge Neutralization Model and Scatchard. Reflecting differences in evaluation methods the number and quantity of complexation sites vary. Evaluation of experimental data by the Scatchard method result in two different types of binding with corresponding complexation capacities and complexation constants. The other evaluation methods, which inherently contain only one type of binding, nevertheless result in complexation constants with acceptable errors. Emphasis on the study is evaluation of thermodynamic data, i.e. ΔH , ΔG and ΔS , for the purpose of obtaining insight on the complexation reaction mechanism. Reflecting differences in evaluation methods thermodynamic data give somewhat different numbers from application of Schubert, CNM and Scatchard. The positive values for ΔS show that the Eu(III)-humate complexation reaction is endothermic and entropy driven.

The redox behavior of technetium has been investigated by KUL under reducing conditions (Fe(II)) in the pH neutral to slightly alkaline conditions. In the presence of Boom-Clay humic matter and reducing conditions given by Fe(II) added (redoxpotential of experiments approximately -150 to -250 mV), no reductive complexation of Tc is observed. To achieve reduction within reasonable time-scales, active mineral surfaces are required (cf. below, Task 3)

3.3 TASK 3 (Actinide Transport)

3.3.1 Objectives and General Achievements

The objectives of this task is to identify, describe and quantify relevant mechanisms influencing the actinide and technetium transport by batch and column experiments on both defined/designed and natural material. This includes not only sorption/migration of actinide elements and technetium on natural material and covalently humic acid coated silica

beads, but also for example, the sorption of humic acid on mineral surfaces and the influence of humic acid on the reduction of redoxsensitive elements on various mineral surfaces. The results show that batch and column experiments on natural material are not in equilibrium but a kinetic approach is required for a consistent description of the results. Furthermore, for redoxsensitive elements the migration behavior is mainly governed by the oxidation state.

3.3.2 Experimental Systems

Batch and column experiments have been carried out at different experimental conditions. Experimental systems used may be summarized as follows:

Humic acids: Aldrich humic acids, site-specific (Gorleben, Mol) humic acids and covalently humic acid coated silica beads. Concentration used in the experiments on site-specific material (Gorleben, Mol) are those given by the respective natural conditions;

Radionuclides: Trivalent elements (Am, Eu) and heptavalent Tc (as pertechnetate TcO_4^-);

Solid materials as column materials or as sorbent for batch experiments: Gorleben sand, Fe minerals (FeS , FeS_2 , goethite $\alpha\text{-FeOOH}$) and clay minerals (illite, kaolinite). For these different solid phases, characterization of the material itself has been carried out and also the hydraulic properties have been determined for columns used.

Physico-chemical conditions: pH and ionic composition given by the site-specific material used (Gorleben (pH 8-9) or Mol (pH~8)) or variation of pH in order to further investigate specific processes.

3.3.4 Summary of Results

The results may be summarized as follows:

<Mobility of the redox sensitive technetium>

Under relevant conditions, Tc exists in two oxidation states, namely Tc(VII) as an anion (pertechnetate TcO_4^-) and Tc(IV). The latter is relatively insoluble at $\text{pH} < 8$, predominantly present as hydrolyzed (or carbonate) species in solution (mainly $\text{TcO}(\text{OH})_2$ and $\text{TcO}(\text{OH})_3^-$). Tc(VII) is very mobile whereas the mobility of Tc(IV) depends on, amongst others, pH and possibly the interaction with humic colloids.

The behavior of Tc has been studied as a function of the nature of the sorbing phase, either iron minerals (KUL), clay minerals (KUL) or organic colloids (GERMETRAD). Ternary systems (iron minerals+organic colloids) have also been investigated (KUL). Under alkaline conditions (pH 8) and reducing conditions (presence of Fe^{2+} ions), Tc(VII) is not reduced in solution. This is also the case in the presence of humic substances. Presence of mineral surfaces containing iron (such as FeS or FeS_2) may lead to reduction of Tc followed by sorption onto these phases. The presence of illite does not induce reduction of Tc, with and without Fe^{2+} ions. In summary, Tc remains mobile unless reducing mineral phases are present. Upon reduction, Tc is expected to become immobilized except for low solubility of some complexes and it also may remain mobile through interaction with humic colloids.

In the presence of humic acids covalently bound to silica beads (GERMETRAD), the sorption of reduced Tc (in the presence of reducing agents either hydrazine or SnCl_2) is decreased when the pH increases (from pH 5 to 8). This may be due to the generation of anionic Tc species. The affinity of Tc for the HA-silica beads also depends on the reducing agent used (SnCl_2 leads to a higher retention). On both batch and column experiments kinetic effects are observed. Hence, under alkaline pH conditions (representative of those found in natural systems), reduced Tc (in the presence of a reducing agent), appears relatively mobile in the presence of humic acids fixed on silica. This confirms above discussed results.

<Mobility of Am(III)/Eu(III)>

Mobility of Am(III)/Eu(III) is investigated on site specific Gorleben material under near natural conditions, (pH 8-9, inert gas atmosphere) with varying humic colloid concentrations given by conditioning of sand with natural groundwaters with different humic colloid contents (no addition or removal of humic substances). Batch and column experiments on the same experimental material under equivalent experimental conditions show that through the formation humic colloids the portion of mobile Am(III) increases with increasing humic substance concentration. Moreover, these humic colloids migrate slightly faster than the groundwater matrix, presumably due to charge/size exclusion (FZK/INE and GSF/IfH).

The sorption of Am onto Gorleben sand is found to be kinetically controlled in the presence of humic colloids: the longer the residence time of humic colloid bound Am(III)/Eu(III) in the column, the more Am/Eu becomes sorbed onto the sand. No sorption of humic matter on the sand is observed and thus the mechanism for Am/Eu sorption does not appear to be sorption of humic colloid bound Am/Eu. The Am sorption onto the sand is not only kinetically controlled by the residence time in the column but also by the equilibration time of Am with the humic colloids prior to column injection. Hence the portion of Am that gets less available for sorption, i.e. kinetically hindered for sorption

on the sediment, increases with the equilibration time. Results from the laboratory experiments can be consistently described by an approach based on kinetically governed accessibility of Am/Eu for decomplexation of humic colloid bound Am/Eu followed by basically prompt sorption onto the sediment. To which extent observations from laboratory experiments are sufficient to describe the situation in the real system with its much longer time scales is not yet clear (FZK/INE and GSF/IfH).

This high affinity of Am (or Eu) for humic acids has also been shown through batch and column experiments with covalently humic acid coated silica beads (GERMETRAD). This affinity is slightly lower at pH 8 than at pH 5.

<Sorption of humic acid on mineral surfaces>

Organic colloids such as humic acids are sorbed onto different mineral phases such as clay minerals and in particular kaolinite (NERI). Ligand exchange mechanisms are certainly involved in the sorption processes (at pH 6). On the contrary, humic acids appears to have no significant affinity for pyrite surfaces (FeS_2) (KUL).

3.4 TASK 4 (Migration Model Development and Testing)

3.4.1 Objectives and General Achievements

The objectives of this task is to rationalize the state of understanding by establishing numerical models, test these models to ensure their applicability or identify processes still not adequately understood. A review has been conducted with respect to modeling approaches and the outcome has been summarized in a separate report/working document (RMC 1997). Following conclusions during the first project meeting, development of new models for transport modeling appears necessary. The major achievement has been to establish and test a model taking the above mentioned non-equilibrium in batch and column experiments into account.

3.4.2 Modeling based on Equilibrium Approach

RMC-E has further developed modeling based on the equilibrium approach. Modeling of static binary and ternary (actinide/humic acid/mineral surface) systems is done based on the existing PHREEQE96. In this code, the TippingV model accounts for aquatic humate complexation. Further elements has been added to this code, namely (i) colloid diffuse layer, to simulate metal ion/colloid interactions (Dzombak and Morel 1990); (ii) metal ion interaction with surface bound humic acid, through a modified version of TippingV model; and (iii) full mass balance to appropriately account for precipitation/dissolution

phase boundaries. This fully documented and tested code is named PHREEQE97. Upon testing the model was found to perform well at high pH. However, at ionic strength > 1 M, it fails due to the ionic strength correction algorithm.

Modeling of dynamic lab systems is done by combination of PHREEQE97 with a one-dimensional transport code. In the transport code, transport of the water matrix with its truly dissolved species and particles (colloids) are treated separately. The combined code is named PHAST (Phreeqe And Simple Transport). The different transport behavior of humic colloids relative to the water matrix is described via a humic colloid/mineral surface sorption isotherm (Gu et al. 1994). Testing of the model revealed that considerable effort is required to overcome prohibitively long CPU times. Application on up-flooding and peak-injection column experiments showed improvements compared to pre-existing codes, however, considerable discrepancies still exist. Upon analysis of the results, it was concluded that the basic assumption of thermodynamic equilibrium is not valid for the laboratory column experiments but kinetic effects need to be included.

3.4.3 Modeling based on Kinetic Approach

In the past, interpretation of actinide transport based on the thermodynamic equilibrium approach and filtering of humic colloids has been subject to major difficulties. These difficulties may be summarized as follows: (i) pulse injection column experiments show two different actinide fractions; one eluted slightly faster than ideal tracers and one which is not eluted within time-scales practicable for the lab experiments; (ii) batch experiments show time dependent distribution values; and (iii) combination of results from batch and column experiments on equivalent systems lead to inconsistencies. Furthermore, the fraction of the actinide ion recovered by elution with zero retention is found to vary with experimental conditions.

Evaluation of column experiments on less charged metal ions (for example, Co and Ni), i.e. ions that quantitatively elute during lab experiments, has shown less dramatic deviations between experimental results and modeling. Nevertheless, present models fail to adequately reflect the shape of the elution curves. For these reasons, both FZK/INE and RMC-E have concluded that it is necessary to include the impact of deviation from equilibrium to adequately reflect experimental results. As a very important achievement within the reporting period, application of a kinetic approach ("Kinetically Controlled Availability Model") on Am(III)/Eu(III) transport has been proven capable to overcome numerous of these difficulties (FZK/INE).

Transport experiments have shown that a number of variables influence the transport behavior of Am(III) in columns with site specific Gorleben material under anoxic condi-

tions. Such variables are the time for conditioning the americium with the groundwater and transport velocity. Both these results indicate the need for taking into account kinetic effects. Preliminary transport modeling has been performed in this direction.

The “Kinetically Controlled Availability Model“ (FZK/INE) rests on two different availability modes of humic colloid bound Am (III) for exchange with the bulk solution and consequently sorption onto the sediment. Upon addition of Am(III) to a humic colloid containing groundwater the americium is almost quantitatively humate bound within an hour. With increasing conditioning time the fraction of Am(III) transferred to the less available mode is increasing. Upon column injection the more available Am(III) is rapidly sorbed on the sediment. With increasing residence time in the column, humate bound Am(III) is progressively transferred from the less available mode to the more available mode and subsequently rapidly sorbed on the sediment. This approach leads to results consistent with the experimental observations from both batch and column experiments.

Table 5: Current state of the Humic Acid (HA) and Fulvic Acid (FA) complexation database (from RMC-E).

Element/Ion	Humic/Fulvic Acid	pH	Ionic Strength (M)
Am ³⁺	Aldrich	6.0	0.1
“	Bradford	5.0 - 6.0	0.1 - 1.0
“	Gohy-573(HA)	4.0 - 6.0	0.01 - 5.0
Cm ³⁺	“	5.0 - 6.0	0.001 - 5.0
NpO ₂ ⁺	“	6.0 - 9.0	0.1
UO ₂ ²⁺	“	4.0	0.1
“	Broubster(FA)	5.0 - 7.5	0.01 - 0.2
“	Needle's Eye(FA)	5.0 - 5.5	0.04 - 0.1
“	Drigg(FA)	3.5 - 7.0	0.005 - 0.2
Ca	Broubster(FA)	5.0 - 7.0	0.01
Co	Drigg(FA)	6.0 - 7.0	0.005 - 0.2
“	Broubster(FA)	6.0 - 7.0	0.005 - 0.2
“	Broubster(HA)	6.0 - 7.0	0.005 - 0.1
“	Needle's Eye(FA)	6.0 - 7.0	0.005 - 0.2
Ni	Needle's Eye(FA)	6.0 - 7.0	0.005 - 0.2
“	Broubster(FA)	6.0 - 7.0	0.01 - 0.2
“	Drigg(FA)	6.0 - 7.0	0.005 - 0.2

3.4.3 Joint Database on Humate Complexation

A joint database of selected humate complexation data has been established by (RMC-E) The data presently are restricted to results originating from the partners including their

previous activities. The database contains direct speciation results and thus allows modeling by different approaches and model development. The present state of the database is shown in Table 5.

4 . REFERENCES

- Dzombak, D.A.; Morel, F.M.M. (1990) "Surface Complexation Modeling: Hydrous Ferric Oxide", Wiley Interscience, John Wiley and Sons.
- Gu, B.; Schmitt, J.; Chen, Z.; Liang, L.; McCarthy, J.F. (1994) "Adsorption and Desorption of Natural Organic Matter on Iron Oxide: Mechanisms and Models", *Environmental Science and Technology*, **28**, 38.
- Kim, J.I.; Buckau, G.; Li, G.H.; Duschner, H.; Psarros, N. (1990) "Characterization of humic and fulvic acids from Gorleben groundwater", *Fresenius J. Anal. Chem.*, **338**, 245.
- Kim, J.I.; Sekine, T. (1991) "Complexation of Neptunium(V) with Humic Acid", *Radiochimica Acta*, **55**, 187.
- Lassen, P.; Carlsen, L.; Warwick, P. (1996) "The interaction between humic acids and γ - Al_2O_3 ", *Theophrastus' Contributions*, **1**, 3-17.
- Marquardt, Ch.; Kim, J.I. (1998) "Complexation of Np(V) with Humic Acid: Intercomparison of Results from Different Laboratories", *Radiochimica Acta*, accepted for publication.
- Rao, L.; Choppin, G.R. (1995) "Thermodynamic Study of the Complexation of Neptunium(V) with Humic Acid", *Radiochimica Acta*, **69**, 87.
- RMC-E (1997) "Effects of Humic Substances on the Migration of Radionuclides: Complexation and Transport of Actinides", RMC Report R97-53(E).

1st Technical Progress Report

EC Project:

**"Effects of Humic Substances on the Migration of Radionuclides:
Complexation and Transport of Actinides"**

FZK/INE Contribution to Task 1 (Sampling and Characterization)

**Sampling and Characterization of Gorleben Groundwater/Sediment
Systems for Actinide Migration Experiments**

Reporting period 1997

R. Artinger, B. Kienzler, W. Schüßler, J.I. Kim

**Forschungszentrum Karlsruhe, Institut für Nukleare Entsorgungstechnik,
P.O. Box 3640, D-76021 Karlsruhe, Germany.**

Content:

	<u>Page</u>	
1	Introduction	27
2	Objectives	27
3	Groundwaters	28
3.1	Origin of Groundwaters	28
3.2	Groundwater sampling and field analysis	28
3.3	Laboratory analysis	29
3.3.1	Inorganic composition	29
3.3.2	Dissolved organic carbon (DOC)	29
4	Sediment	31
4.1	Origin und sampling	31
4.2	Grain-size distribution	33
4.3	Composition	35
4.3.1	Mineral composition	35
4.3.2	Major inorganic components	35
4.3.3	Inorganic trace elements	36
4.3.4	Organic carbon content	36
4.4	Grain surface analysis	38
4.4.1	Specific surface (BET)	38
4.4.2	XPS (or ESCA)	38
4.4.3	Cation exchange capacity (CEC)	40
4.4.4	pH titration	41
5	References	42

1 Introduction

For a HLW disposal in a geological formation, natural barriers isolating the waste from the biosphere are the host formation and the overlaying strata. For the Gorleben site (Lower Saxony, Germany), presently under investigation for such disposal, the host rock is a Permian salt dome with an overlaying strata consisting of sedimentary rock with a complex aquifer system. The most important scenario for radionuclides moving from the repository to the biosphere is transport with groundwater. At the Gorleben site sandy sediments of high permeability are found from the surface down to the top of the salt dome (Ludwig and Schneider 1994). In this aquifer system, dissolved organic carbon (DOC) concentration up to 200 mg C/L are found (Buckau 1991). These high DOC concentrations are the result of in-situ generation in conjunction with mineralization of sedimentary organic carbon (SOC). In the Gorleben aquifer this process is favored by the combination of dissolution of sulfate from the cap-rock of the salt dome and Miocene brown coal and Pleistocene peat deposits. The DOC consists mainly of humic and fulvic acids complexed with a large number of metal ions (humic colloids). Due to their strong interaction with multivalent actinide ions, such as Am^{3+} and Cm^{3+} (Czerwinski et al. 1996), humic colloid mediated actinide transport may be cardinal importance for long-term safety of HLW disposal (Kim 1990, Maravic and Moreno 1993). For this reason, the actinide transport is thoroughly investigated in few selected well characterized Gorleben groundwater/sediment systems. This paper describes sampling and characterization of the experimental material (groundwater and sediments) used for these actinide transport investigations.

2 Objectives

At FZK/INE, the migration behavior of actinide ions is studied, amongst others, by batch and column experiments on site specific material from the Gorleben site. For adequate interpretation of the outcome of these experiments, detailed information is required on experimental material (groundwater and sediments), the set-up of experimental systems and experimental conditions. The present paper aims at providing this information for experimental material used.

3 Groundwaters

3.1 Origin of Groundwaters

The following four groundwaters from the Gorleben aquifer are sampled:

GoHy-182

GoHy-412

GoHy-532

GoHy-2277

The groundwaters origin from medium to fine-grained sandy sediments. Information on sampling and origin are summarized in Table 1.

Table 1: Sampling date and aquifer characterization of the sampled Gorleben groundwaters.

	Sampling date	Sampling date	Sediment (bulk)	Sediment type	Genesis of sediment
GoHy-182	21.05.96	70-73	medium sand	Elster	fluvioglacial?
GoHy-412	22.05.96	65-68	medium sand	Elster	fluvioglacial
GoHy-532	22.05.96	65-68	medium sand	Elster	fluvioglacial
GoHy-2227	20.05.96	128-130	medium sand	Pre-Elster	fluviatile-limnological

The groundwaters are selected in view of their highly varying DOC concentrations (1 to 80 mgC/L). This allows to study the influence of humic colloid concentration on the actinide transport behavior. Furthermore, considering the pre-dominance of groundwater-flow through highly permeable sandy sediments and the corresponding importance for the potential radionuclide migration, the groundwaters are sampled from such sediments.

3.2 Groundwater sampling and field analysis

Groundwater sampling and field analysis was carried out by Deutsche Gesellschaft zum Bau und Betrieb von Endlagern für Abfallstoffe mbH (DBE). A detailed description of sampling and field analysis is given elsewhere (Delakowitz et al. 1990). Chemical and physico-chemical parameters determined at field-sampling are summarized in Table 2.

Table 2: Chemical and physico-chemical parameters from field-analysis at groundwater sampling.

	Gorleben groundwater:			
	GoHy-182	GoHy-412	GoHy-532	GoHy-2227
Water temperature / (°C)	10.3	11.1	11.3	14.8
pH	8.1	7.7	8.9	7.7
Redoxpotential / (mV)	-87	-74	-160	-123
Electr. conductivity / (µS/cm)	144	370	950	4600
O ₂ (free) / (mg/L)	0.1	<0.1	<0.1	<0.1
CO ₂ (free) / (mg/L)	n.d.	5.2	n.d.	12.7
H ₂ S / (mg/L)	0.02	0.03	-*	-*
HCO ₃ ⁻ / (mg/L)	64.1	200.5	334.1	488.2

*: H₂S quantification not possible due to interference with the brown color of groundwater, however, smell of H₂S in both GoHy-532 and -2227.
n.d.: not detected

3.3 Laboratory analysis

3.3.1 Inorganic composition

Inorganic groundwater components are determined by ICP-AES, ICP-MS, HPIC and titration (HCO₃⁻, Cl⁻ >10 mmol/L). The results are summarized in Table 3. The salt content (Table 3), and correspondingly the ionic strength (Table 4), increases in the order:

$$\text{GoHy-182} < \text{-412} < \text{-532} < \text{-2227}.$$

3.3.2 Dissolved organic carbon (DOC)

Dissolved organic carbon is characterized with regard to concentration (TOC analyzer TOC-5000 (Shimadzu Co.)), composition (humic acids HA, fulvic acids FA, and hydrophilic acids according with the XAD-8 method) and size distribution (Filtron Co., Microsep Microconcentrators, MW cut-off 1 K to 1000 K, followed by TOC analysis of filtrates). The results show that practically all organic carbon pass through a pore-size of 0.45 µm, i.e. total organic carbon (TOC) and dissolved organic carbon (DOC) do not deviate significantly from each other. The concentration and composition of DOC is shown in Table 5.

Table 3: Inorganic composition of sampled Gorleben groundwaters.

Element/ Ion	Gorleben groundwater:							
	GoHy-182		GoHy-412		GoHy-532		GoHy-2227	
	(mg/L)	(mmol/L)	(mg/L)	(mmol/L)	(mg/L)	(mmol/L)	(mg/L)	(mmol/L)
Na	3.95	0.1717	58.54	2.5452	212.90	9.2565	932.20	40.5304
K	n.d.	n.d.	0.62	0.0159	0.99	0.0253	7.03	0.1798
Mg	1.01	0.0416	n.d.	n.d.	n.d.	n.d.	4.70	0.1934
Ca	25.94	0.6469	22.34	0.5571	1.87	0.0466	26.79	0.6681
Sr	0.05	0.0006	0.08	0.0009	0.03	0.0003	0.21	0.0024
Ba	n.d.	n.d.	0.01	0.0001	n.d.	n.d.	0.03	0.0002
Al	0.03	0.0011	n.d.	n.d.	0.02	0.0007	0.11	0.0041
Si	0.45	0.0160	0.75	0.0267	0.37	0.0132	0.62	0.0221
Fe	0.12	0.0022	0.15	0.0027	0.29	0.0052	0.33	0.0059
Mn	0.04	0.0007	0.06	0.0011	0.02	0.0004	0.03	0.0005
Ti	n.d.	n.d.	0.02	0.0004	0.10	0.0021	0.28	0.0058
B	n.d.	n.d.	n.d.	n.d.	0.17	0.0157	0.34	0.0315
Cl ⁻	9.0	0.2535	18.1	0.5099	131.7	3.7099	1195.4	33.6732
F ⁻	0.3	0.0158	0.2	0.0105	0.6	0.0316	3.9	0.2053
HCO ₃ ⁻	64.1	1.0508	200.5	3.2869	334.1	5.4770	488.2	8.0033
NO ₃ ⁻	<0.1	<0.0001	<0.1	<0.0001	<0.1	<0.0001	<0.1	<0.0001
PO ₄ ⁻	0.2	0.0021	1.7	0.0179	2.4	0.0253	3.4	0.0358
SO ₄ ⁻	2.7	0.0281	0.1	0.0010	0.5	0.0052	27.1	0.2820

n.d.: not detected

Table 4: Ionic strength (M) of sampled Gorleben groundwaters.

	Gorleben groundwater:			
	GoHy-182	GoHy-412	GoHy-532	GoHy-2227
Ionic strength	2.2 E-3	4.4 E-3	9.6 E-3	44.0 E-3

Table 5: Concentration and composition of DOC in sampled Gorleben groundwaters.

Gorleben Groundwater	DOC- (mgC/L)	HA (%)	FA (%)	Hydrophilic acids (%)
GoHy-182	1.1	16	17	67
GoHy-412	7.2	22	34	44
GoHy-532	29.9	69*	20*	11*
GoHy-2227	81.9	79	8	13

* DOC composition from (Zeh 1993), measured by ultrafiltration in combination with UV/Vis-spectroscopy.

The size distribution of the DOC is determined by ultrafiltration at different pore sizes and subsequent DOC measurement of the filtrates. Prior to their use, the ultrafilter are washed 10 times with each 3 mL highly purified Milli-Q water. This is required to remove glycerin present in the original filter to a level less than 0.5 mgC/L ultrafiltrate. The residual organic carbon contamination from the ultrafilter in combination with ≈ 0.3 mgC/L in the Milli-Q water as well as memory effects in the TOC analyzer hinders a reasonable determination of the DOC size distribution in GoHy-182. The DOC size distributions of the groundwaters GoHy-412, -532, and -2227 are illustrated in Fig. 1. As seen in this figure, the hydrodynamic size of DOC is less than 300 kDalton for these groundwaters, corresponding to a hydrodynamic diameter of less than 15 nm (Buckau 1991). The DOC size distribution also reflects the different DOC composition of the groundwaters via differences in hydrodynamic sizes of HA, FA and hydrophilic acids. The DOC fraction passing a pore size of 1000 Dalton is much higher for GoHy-412 than for GoHy-532 and -2227, reflecting a higher fraction of relatively small hydrophilic acids. GoHy-532 and 2227 with their high HA fractions (>69 %) show considerable retention of DOC at a pore-size of 50 kDalton. In contrary to this, in GoHy-412 with its low HA content (22 %), a significant retention of DOC does not occur above 3000 Dalton.

4 Sediment

4.1 Origin und sampling

A sand was selected representative for various sandy sediments at different depths in the Gorleben aquifer system. This sand from the western end of the village Gartow, a few meters north of the road in the direction of Trebel, is representative with respect to mineralogical composition and texture. The sampling place is located at a sand pit edge about 1.5 m below

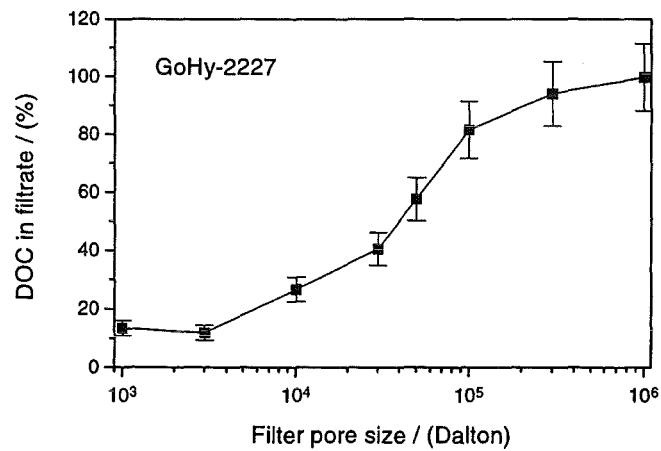
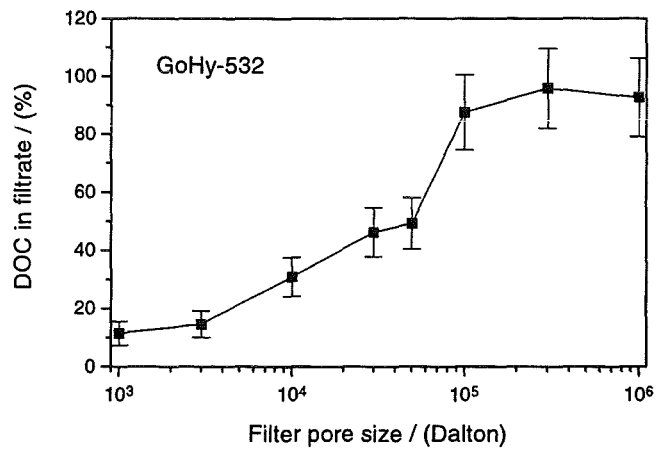
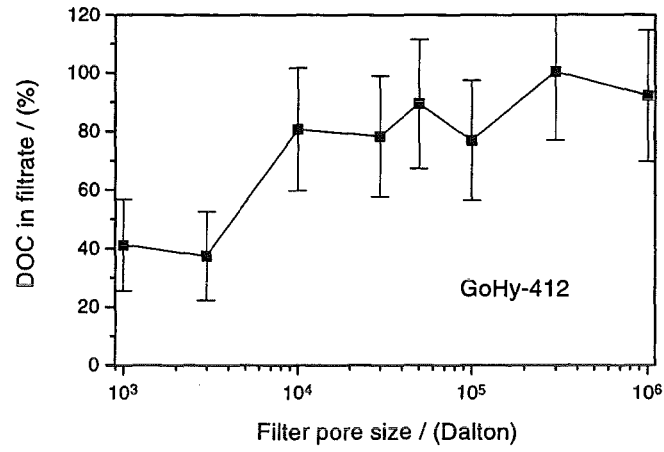


Fig. 1: Size distribution of DOC in the Gorleben groundwaters GoHy-412, -532 and -2227, determined by ultrafiltration and TOC analysis of filtrates.

ground surface covered with pine trees. The sand is in contact with air. The eolian fine to medium grained sand is related to the transition from the younger Weichsel cold age to the Holocene (≈ 20.000 to 10.000 a).

At the INE-FZK about 100 kg of the sampled sand was mixed and equally high (≈ 10 cm) distributed over a PE film. By means of a glass cylinder 20 to 30 samples were taken from arbitrary places of the whole sand layer and fit together to single sand samples of about 2 kg. By this procedure, 50 homogeneous sand samples were obtained.

4.2 Grain-size distribution

The grain-size distribution of the sampled Gorleben sand was determined by sieve analysis of the GSF Institute of Hydrology at Neuherberg and of the Institute of Environmental Geochemistry of the University of Heidelberg. The results are shown in Table 6 and illustrated in Fig. 2. The result show that it is a uniform medium grained fine sand (fS, ms). Characteristic quantities of the grain-size distribution are the grain sizes d_i ($i = 10, 50$ and 60) where “i“ % of the sand goes through a certain sieve mesh size. For the Gorleben sand, the following d_i values are obtained:

$$d_{10}=0.12 \text{ mm}$$

$$d_{50}=0.18 \text{ mm}$$

$$d_{60}=0.20 \text{ mm}$$

The ratio d_{60} to d_{10} is a measure for the degree of dissimilarity (U) of the grain size distribution, influencing the pore size and thus the pore channel cross-section and the hydraulic behavior of the sediment:

$$U = d_{60} / d_{10} = 1.7 \quad (1)$$

According to the sieve analysis, the silt fraction is about 0.2 to 0.3 % and the clay fraction <0.1 %.

Table 6: Grain-size distribution of sampled Gorleben sand (from sieve analysis of the GSF Institute of Hydrology, Neuherberg and of the Institute of Environmental Geochemistry, University of Heidelberg).

Mesh size (μm)	Fraction passing through (%)
2000	99.97
630	98.5
500	96.5
355	91.1
315	87.9
250	76.3
224	70.6
200	58.8
180	50.1
160	39.1
140	23.8
120	13.6
100	3.8
80	1.1
63	0.15
20	0.05
6.3	0.08

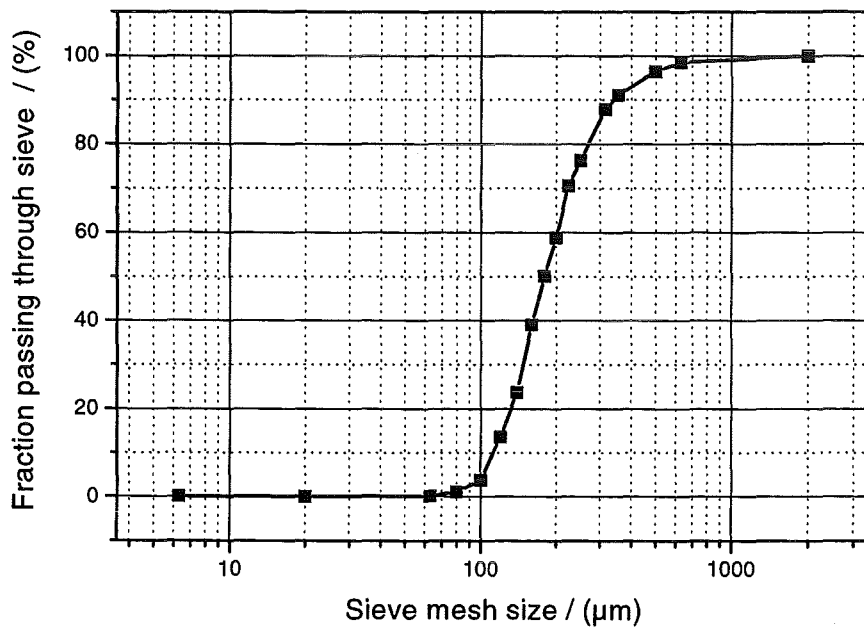


Fig 2: Cumulative curve of grain-size distribution of the sampled Gorleben sand.

4.3 Composition

4.3.1 Mineral composition

As shown in Fig. 3, X-ray diffraction analysis of the Gorleben sand reveals quartz as the dominating mineral. In addition, the alkali feldspars mikrocline and albite are identified.

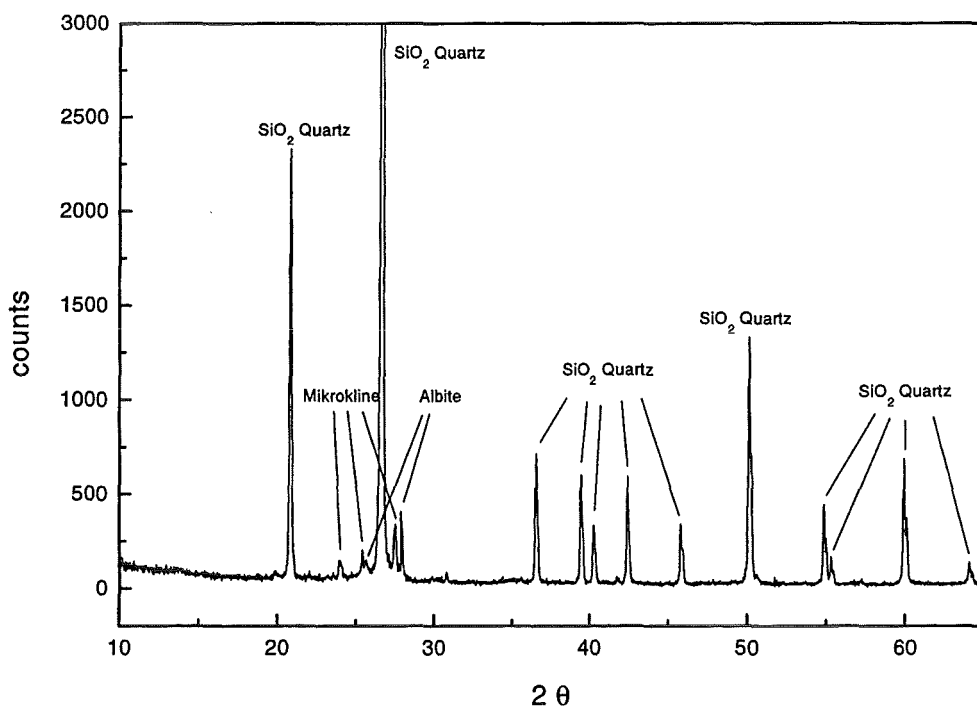


Fig. 3: X-ray diffraction spectra of the Gorleben sand.

4.3.2 Major inorganic components

The major inorganic components are determined by X-ray fluorescence spectroscopy. The analysis is performed on 8 parallel samples of the Gorleben sand. In Table 7, the results are given by the content of different oxides as mean values of the 8 measurements with an error of 1 σ . SiO₂ is found to be the dominating component (94 %). Further major components are Al₂O₃ (2.84 %), K₂O (1.09 %), Fe₂O₃ (0.48 %), and Na₂O (0.43 %). These oxides are found in feldspars like microcline and albite, also identified by X-ray diffraction (see above), as well as mica, which together with hematite may be responsible for the measured iron content. For a feldspar with a Al₂O₃ content of 20 % and a SiO₂ content of 65 % (Scheffer and Schachtschabel 1992), the

measured Al_2O_3 content of 2.8 % results in a feldspar content of 14 %. In summary, the mineral phase composition may be given as follows:

quartz:	85 %
feldspars:	10 to 15 %
others (e.g. mica, hematite)	<5 %

This result is comparable to another eolian sand consisting of 85 % quartz, 13 % feldspar and 2 % mica (Scheffer and Schachtschabel 1992).

In Table 7, results are also given for another eolian Gorleben sand used for column experiments at the Technical university of Munich (TUM) and for sand from the drilling core of the groundwater well GoHy-2227. Between both eolian sands, the contents of major components agree well. The slight deviations found may be attributed to different contributions of, for example marl and sedimentary organic carbon (SOC).

4.3.3 Inorganic trace elements

Trace elements are determined by ICP-MS (Table 7). The solid samples are dissolved in HNO_3/HF (microwave heating). In analogy to the X-ray fluorescence, analysis is made on 8 parallel samples (cf. above). The high Co concentration with its large error range is probably the result of contamination from sample preparation/analysis. Trace elements of the "TUM" and "2227" sands are determined by neutron activation analysis (NAA). In consideration of the very low concentrations and the application of different analytical methods, trace element concentrations of the three sands agree well with each other.

4.3.4 Organic carbon content

The organic carbon content of the Gorleben sand can be estimated to be <0.5 %. This is done by carbon analysis of gas released upon sample combustion. During Holocene, calcium carbonate to a large extent has been washed out from the surface near sand layers. Therefore, one can assume that the carbon content of this sand consists mainly of organic carbon. The presence of organic carbon is confirmed by black charcoal like particles with a carbon content of 55 % and an ash content of 10 %. The larger of these particles have a specific surface area (BET method) of $10 \text{ m}^2/\text{g}$. The origin of these particles is yet not clear, however, lignite particles from reworked older

Table 7: Inorganic composition of the sampled Gorleben sand together with analytic data from a Gorleben sand used for column experiments at the Technical University of Munich (TUM) as well as for Gorleben sand from the drilling core of the groundwater well GoHy-2227.

	Gorleben-sand (INE)	Gorleben-sand (TUM)	Gorleben-sand 2227
Oxide	Major and minor components (%)		
SiO ₂	94.2 ± 1.1	94.1	82.8
TiO ₂	0.16 ± 0.01	0.17	0.58
Al ₂ O ₃	2.84 ± 0.76	2.45	6.65
Fe ₂ O ₃	0.48 ± 0.12	0.42	2.44
MgO	0.09 ± 0.01	0.20	0.74
MnO	<0.05	0.09	0.01
CaO	0.13 ± 0.01	0.12	0.31
Na ₂ O	0.43 ± 0.05	0.26	0.50
K ₂ O	1.09 ± 0.12	1.02	1.34
P ₂ O ₅	<0.05	<0.05	<0.05
Weight loss on ignition		0.50	3.50
Sum	99.5 ± 0.3	99.6	98.9
Element	Trace elements (mg/kg)		
Li	2.6 ± 0.8	n.d.	n.d.
Sc	n.d.	1.14	4.8
Cr	n.d.	13.3	27
Co	(103 ± 51)	0.88	9.9
Ni	0.35 ± 0.23	n.d.	n.d.
Zn	5.7 ± 1.9	5.88	1.2
Ga	2.2 ± 0.3	n.d.	n.d.
Rb	28.4 ± 1.1	27.5	45.1
Sr	26.8 ± 0.8	<50	<50
Y	3.8 ± 0.9	n.d.	n.d.
Cs	0.11 ± 0.08	0.48	2.6
Ba	163 ± 4	184	137
La	4.0 ± 0.3	16.0	10.9
Ce	7.6 ± 0.6	14.2	23
Pr	0.91 ± 0.12	n.d.	n.d.
Nd	3.4 ± 0.2	7.0	12.0
Sm	0.61 ± 0.09	2.9	1.8
Eu	0.13 ± 0.03	0.18	0.37
Gd	0.57 ± 0.04	n.d.	n.d.
Tb	0.09 ± 0.01	0.15	0.25
Dy	0.56 ± 0.12	n.d.	n.d.
Ho	0.13 ± 0.02	n.d.	n.d.
Er	0.37 ± 0.08	n.d.	n.d.
Tm	0.07 ± 0.02	n.d.	n.d.
Yb	0.44 ± 0.07	0.81	0.88
Lu	0.08 ± 0.02	0.10	0.11
Hf	2.5 ± 0.5	6.3	2.2
Ta	0.61 ± 0.26	0.33	1.1
Tl	0.22 ± 0.08	n.d.	n.d.
Pb	4.8 ± 0.3	n.d.	n.d.
Th	1.2 ± 0.1	2.6	3.4
U	0.42 ± 0.07	1.3	1.2

n.d.: not detected

sediments appears improbable because the sampled Gorleben sand has a Pleistocene eolian origin and was not covered by glaciers in the Weichsel cold age.

4.4 Grain surface analysis

Because of the importance of the grain surface for the sorption of radionuclides, considerable emphasis has been given to this issue by application of several analytical methods, namely specific surface area (BET), XPS, cation exchange capacity (Mehlich) and pH titration.

4.4.1 Specific surface (BET)

The determination of the specific surface is performed by nitrogen gas adsorption according to Brunauer, Emmet and Teller (BET). By analysis of 6 parallel samples, a mean value of 1.1 ± 0.09 m²/g Gorleben sand was obtained.

4.4.2 XPS (or ESCA)

The surface of three grains of sand are analyzed by X-ray photoelectron spectroscopy (XPS). The information depth is in the range of a few nanometers with a relative error of 10 to 20 % for elemental composition. Fig. 5 shows a typical measured ESCA spectrum. The resulting surface compositions are summarized in Table 8. A comparison of the surface composition with the bulk composition of the sand reveals a significant enrichment of Al and Fe on the grain surface (and corresponding depletion of Si). The carbon content of the surface is about 20 % as compared to <0.5 % of the bulk (cf. above). This and the enrichment of Fe and Al on the sand surface may be an important indicator for the actinide sorption behavior. The XPS high resolution spectrum in the C1s region (cf. Fig. 5), indicate that surface bound carbon is of organic nature, not dominated by contamination from sample handling and analysis. Whether these organic compounds are humic substances or not, however, presently cannot be determined.

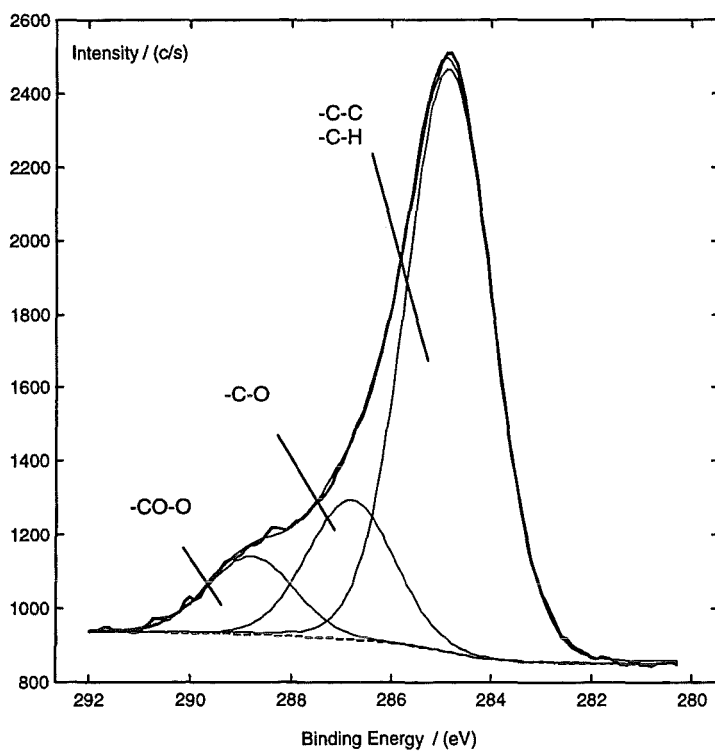
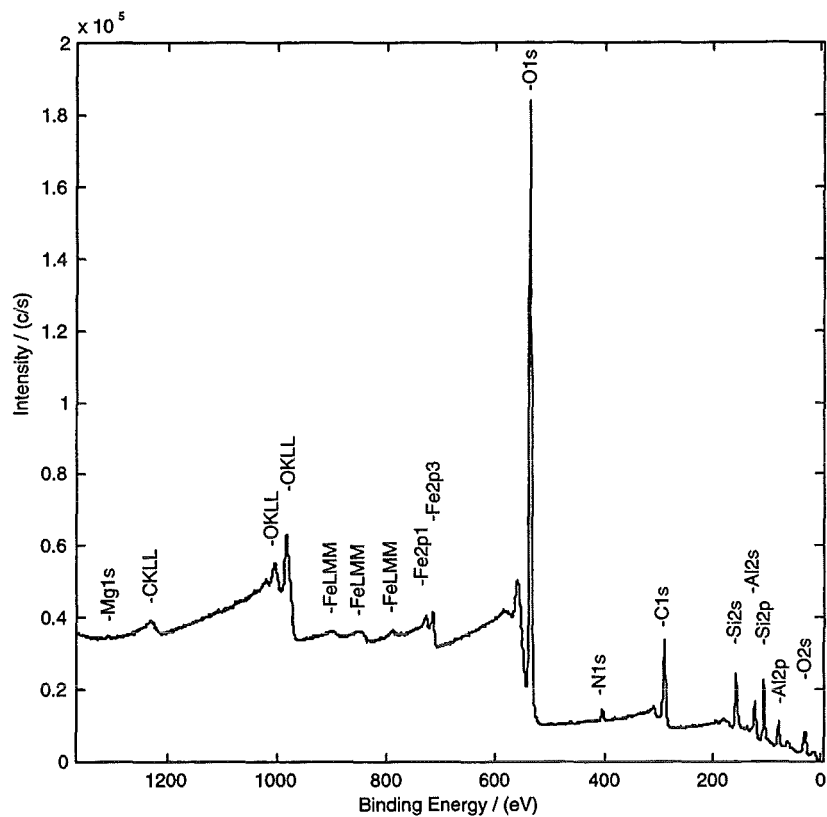


Fig. 5: Typical XPS spectrum of the Gorleben sand surface (above) with highly resolved C1s region (bottom).

Table 8: Surface composition (in atomic concentration (%)) of three grains of the Gorleben sand. For comparison, the bulk element composition determined by X-ray fluorescence spectroscopy and carbon analysis is given.

	grain 1 at.-%	grain 2 at.-%	grain 3 at.-%	average at.-%	bulk (X-ray) at.-%
Si	11.8	14.3	12.4	12.8	31.8
Al	7.0	7.0	8.3	7.4	1.1
Fe	2.4	2.8	2.7	2.6	0.1
Na	n.d.	1.2	1.1	0.8	0.3
Mg	n.d.	0.5	0.6	0.4	<0.1
K	n.d.	n.d.	n.d.	n.d.	0.5
O	56.7	55.4	55.2	55.7	66.1
C	20.1	16.5	17.5	18.0	<0.5*
N	1.5	1.5	1.4	1.5	-
Cl	n.d.	0.4	0.3	0.2	-
P	0.5	0.5	0.5	0.5	-

n.d.: not detected;

-: not detectable;

*: analyzed by carbon determination (c.f. section 4.3.4).

4.4.3 Cation exchange capacity (CEC)

The cation exchange capacity (CEC) is determined according to Mehlich. Sediment surface bound cations are exchanged for Ba ions through slow percolation with a 0.2 N barium chloride solution, buffered at pH 8.1 by triethanolamine. After a complete exchange the sorbed Ba ions are exchanged by Mg ions of a 0.2 N magnesium chloride solution. In this eluate the Ba concentration corresponds to the CEC value. In Table 9, CEC values of four sand samples are summarized to be 1.02 ± 0.02 meq/100 g. This value represents the conditions of the standard procedure and should not be uncritically extrapolated to the exchange capacity of a give cation under different experimental conditions.

Table 9: Cation exchange capacity (according to Mehlich) of the Gorleben sand.

	Sample 1	Sample 2	Sample 3	Sample 4	mean value
CEC (meq/100g)	1.002	1.033	1.036	1.009	1.02 ± 0.02

4.4.4 pH titration

Potentiometric titration data of solid phases can be used to determine the concentration of surface OH⁻ groups (SOH) as well as their surface acidity constants. This is valid on the assumption that only the amphoteric behavior of the SOH groups is responsible for the consumption of H⁺ and OH⁻ ions. Deviations are expected especially for dissolution of solid phases or ion exchange reactions, for example with clay minerals. However, as seen from the grain size analysis, the clay fraction is very small (<0.1 %). Furthermore, at the chosen pH range (from pH 3 to 8) the dissolution of the Gorleben sand minerals should not be of significant magnitude.

The surface charge Q (in mol/g) is calculated according to Eq. (2)

$$Q = \frac{(SOH_2^+) - (SO^-)}{\text{solid mass}} = \frac{c_a - c_b + (OH^-) - (H^+)}{\text{solid mass}} \frac{\text{mol/L}}{\text{g/L}} \quad (2)$$

where C_a and C_b are the added acid and base concentration in mol/L. In Fig. 6 the titration curves of the Gorleben sand at the ionic strengths of 0.1 and 0.01 M are shown as the calculated surface charge Q plotted against the measured pH value. By means of a computer code (e.g. FITEQL) the SOH concentration and acid-base constants can be determined from the titration data.

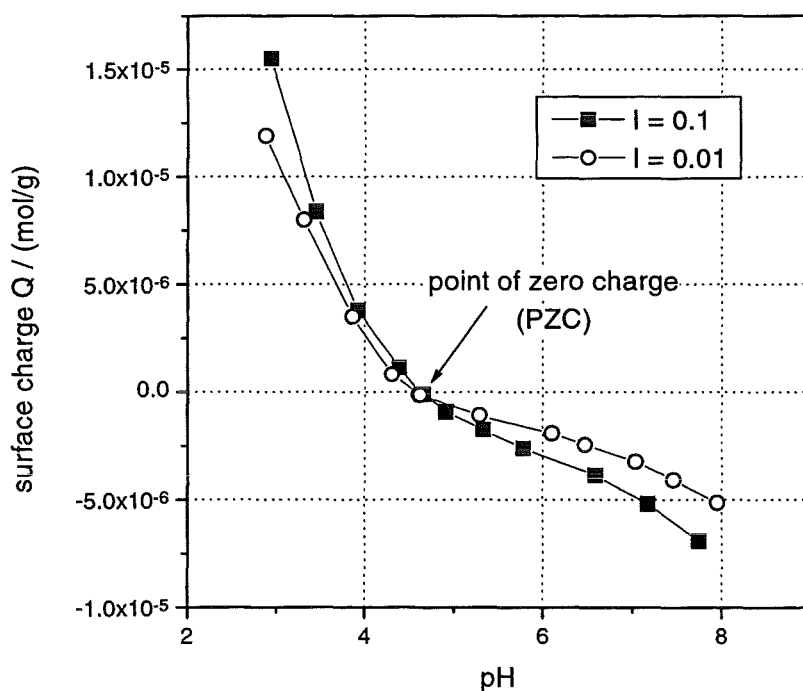


Fig. 6: Titration curve of the Gorleben sand at ionic strengths of 0.1 and 0.01 M.

The point of zero charge (PZC) is found at pH 4.6 (cf. Fig. 6). Because pure quartz has a pH_{PZC} of about two, the value of 4.6 indicates presence of considerable amounts of other proton exchanging substances. This could be organic substances or minerals, such as alkali feldspars and/or iron hydroxides like hematite, found on the quartz surface by XPS (cf. above).

5 References

- Buckau, G. (1991.) "Komplexierung von Americium(III) mit Huminstoffen in natürlichen Grundwässern", PhD Thesis. TU Munich, pp 167.
- Czerwinski, K. R., Rhee, D. S., Scherbaum, F., Buckau, G., Kim, J. I., Moulin, V., Tits, J., Laszak, I., Moulin, C., Decambox, P., De Ruty, O., Marquardt, C., Franz, C., Herrmann, G., Trautmann, N., Dierckx, A., Vancluysen, J., Maes, A., Bidoglio, G., Eliet, V. and Grenthe, I. (1996) "Effects of humic substances on the migration of radionuclides: Complexation of actinides with humic substances", Report EUR 16843 EN, European Commission, Luxembourg/Brussels.
- Delakowitz, B., Dietrich, S. and Otto, E. (1990) "Analytik von Grund- und Porenwässern im Rahmen der Huminstoff- und Migrationsuntersuchungen im Deckgebirge des geplanten Endlagerortes Gorleben", Report: RCM 00290, Technical University Munich.
- Kim, J. I. (1990) "Geochemistry of actinides and fission products in natural aquifer systems", In: CEC project MIRAGE, third summary progress. Report EUR 12858 EN, European Commission, Luxembourg/Brussels.
- Ludwig, R. and Schneider, M. (1994) "Hydrogeologische Grundlagen für Modellrechnungen - Projektgebiet Gorleben-Süd", Report: BGR 112002, Bundesanstalt für Geowissenschaften und Rohstoffe, Hannover.
- Maravic, H. v. and Moreno, J. (1993) "Migration of radionuclides in the geosphere. Proceedings of a progress meeting (work period 1991)", Report: EUR 14690 EN, European Commission, Luxembourg/Brussels.
- Scheffer and Schachtschabel (1992) "Lehrbuch der Bodenkunde", Publ. Enke, Stuttgart.
- Zeh, P. (1993) "Chemische Reaktionen von Aktiniden mit Grundwasser-Kolloiden", PhD Thesis. Technical University Munich, pp 170.

1st Technical Progress Report

EC Project:

"Effects of Humic Substances on the Migration of Radionuclides:
Complexation and Transport of Actinides"

FZK/INE Contribution to Task 2 (Complexation)

**Complexation of Np(V) with Humic Acid:
Intercomparison of Results from Different Laboratories**

Reporting period 1997

C. Marquardt, J.I. Kim

Forschungszentrum Karlsruhe, Institut für Nukleare Entsorgungstechnik,
P.O. Box 3640, D-76021 Karlsruhe, Germany.

Complexation of Np(V) with Humic Acid: Intercomparison of Results from Different Laboratories

C. Marquardt and J. I. Kim

Forschungszentrum Karlsruhe, Institut für Nukleare Entsorgungstechnik,
Postfach 3640, 76021 Karlsruhe, Germany

Neptunium / Humic acid / Complexation / Spectroscopy / Speciation

Abstract

The humate complexation of the NpO_2^+ ion has been investigated at $\text{pH} = 7 - 9$ in 0.1 M NaClO_4 with purified humic acid extracted from one of the Gorleben groundwaters in northern Germany. The experiment is conducted under Ar atmosphere in a glove box by UV-Vis spectroscopy with an optical fibre connection. The Np(V) concentration is varied from 1.08×10^{-4} to $7.28 \times 10^{-4} \text{ mol L}^{-1}$ while keeping the humic acid concentration constant at around $1 \times 10^{-3} \text{ mol L}^{-1}$. The complexation constant, which is evaluated by taking into account the loading capacity (LC) of the humic acid under investigation for the NpO_2^+ ion at each given pH, is found to be $\log \beta = 3.58 \pm 0.05$. This value is in good agreement with the result of our previous experiment with lower Np(V) concentrations and appears independent of pH and other experimental parameters. Our experimental results are compared with those from the literature, particularly with spectroscopic experiments, and the key uncertainties involved in general in the humate complexation studies are discussed.

1. Introduction

The complexation of the NpO_2^+ ion with humic acid has been investigated by various laboratories [1-5] with different experimental methods: UV-Vis spectroscopy [1-3], electrophoretic ion focusing [4], anion exchange [4], and equilibrium dialysis ligand exchange technique [5]. However, the reported complexation constants vary from $\log \beta = 2.15$ to $\log \beta = 4.9$. The variation may depend primarily on two facts: the applied speciation methods to quantify the complexed and non-complexed species are not always straightforward and the methods of evaluating the free humic acid concentration for calculation of the complexation constant are different in each of the hitherto published papers. Different

approaches to the evaluation of the free humic acid concentration give rise to significantly inconsistent results, for example, the results from the same spectroscopic speciation method applied by three different laboratories [1-3] diverge widely from $\log \beta = 2.44$ to $\log \beta = 4.6$. For the same reason, the complexation constants derived by some authors appear pH dependent [4, 5], increasing with increasing pH, and depending on the metal ion concentration as well [4]. The necessity for clarification of such inconsistencies in the reported results has prompted us to re-examine the complexation reaction. The spectroscopic method is chosen for this work, as it provides a straightforward quantification of the species involved in the reaction. The results from different laboratories are compared with one another and underlying problems are discussed.

2. Experimental

The neptunium isotope ^{237}Np is used in the present experiment. The solution made of dissolving NpO_2 in 8 M HNO_3 is passed through an anion exchange column (Dowex AG 1x8) for purification. The effluent is evaporated to dryness, fumed with addition of HClO_4 and redissolved in 0.1 M NaClO_4 . The resulting solution is maintained at about pH 3 with a Np(V) concentration of 0.05 mol L^{-1} . The oxidation state verified by spectroscopy appears quantitatively to be the NpO_2^+ ion.

The whole experiment is carried out in a glove box under Ar atmosphere. The speciation of experimental solutions is made by UV-Vis spectroscopy with an optical fibre system connected to a CARY-5E spectrometer (Varian) outside of the glove box. The light transmission efficiency is found to be about 20 % for an optical fibre of 1 mm diameter with a total length of about 30 m. The experimental concentration of Np(V) is varied from $1.08 \times 10^{-4} \text{ mol L}^{-1}$ to $7.28 \times 10^{-4} \text{ mol L}^{-1}$ in the pH range from 7 to 9 in 0.1 M NaClO_4 , whereas the humic acid concentration is maintained nearly constant at $(1.02 - 1.08) \times 10^{-3} \text{ mol L}^{-1}$. The humic acid is extracted from one of the Gorleben groundwaters (Gohy 573) and purified by a known procedure [6]. The proton exchange capacity determined under Ar atmosphere by pH titration is found to be $5.38 \pm 0.20 \text{ meq g}^{-1}$ dry weight [6]. To maintain each given pH constant, weak organic buffers are used at the concentration of $5 \times 10^{-3} \text{ mol L}^{-1}$, i.e. MES, PIPES, TRISMA and CAPSO (Sigma). The $^{237}\text{Np(V)}$ concentration is

determined by liquid scintillation spectrometry (Tri-Carb 2500 TR/AB with Ultima Gold XR Scintillator), discriminating the β -activity of its daughter nuclide ^{233}Pa . Ultrafiltration is performed by centrifugation using a cell MPS-1 from AMICON with various cut-off membrane filters.

3. Results and discussion

The spectroscopic speciation shows that the absorption peaks of the NpO_2^+ ion and its humate complex appear at 980.4 nm and 990 nm with molar absorbencies of $395 \pm 5 \text{ L mol}^{-1} \text{ cm}^{-1}$ and $230 \pm 8 \text{ L mol}^{-1} \text{ cm}^{-1}$, respectively. These values agree closely with those obtained in the previous experiment [1]. However, at pH 9, the absorption peak of the Np(V) humate is overlapped, presumably, by a Np(V) hydrolysis species (see below). After subtracting the optical baseline produced by humic acid, absorption bands of each species involved are deconvoluted, as illustrated in Fig. 1, by the program GRAMS (Galactica).

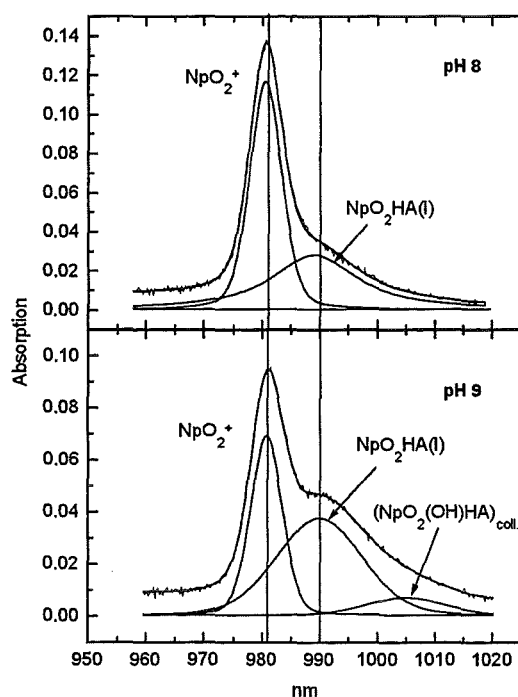


Fig. 1. Absorption spectra of Np(V) in humic acid solution at pH 8 with $[\text{Np(V)}] = 8.0 \times 10^{-5} \text{ mol L}^{-1}$ (upper part) and at pH 9 with $[\text{Np(V)}] = 1.0 \times 10^{-4} \text{ mol L}^{-1}$ (lower part), for both at $[\text{HA}]_t = 1 \times 10^{-3} \text{ eq L}^{-1}$ in 0.1 M NaClO_4 .

The operational concentration of humic acid [7] is defined by a given concentration (HA) in g L⁻¹ times the proton exchange capacity (PEC) in eq g⁻¹, which then gives mol L⁻¹ or eq L⁻¹ (denoted as C_H). As humic acid behaves similar to an ion exchanger and its functional sites can be loaded with a limited amount of the NpO₂⁺ ion at given pH, the loading capacity of humic acid (LC) [7] for Np(V) is determined at different pH by

$$LC = \frac{z[M^{z+}]_m}{C_H} \quad (1)$$

where $[M^{z+}]_m$ is the maximum concentration of the M^{z+} ion that can be loaded onto a given amount of humic acid at constant pH and ionic strength. LC varies, therefore, with pH, ionic strength and the charge of a given metal ion (z+). As a result, LC is a normalisation factor for these parameters, which results in a consistent constant for the metal ion humate complexation [7]. The complexation reaction is described by the metal ion charge neutralisation model [7] as given by



where HA(I) represents one proton exchange site. At constant ionic strength the equilibrium constant of Eq. (2) can be described by

$$\beta = \frac{[NpO_2HA(I)]}{[NpO_2^+]_f [HA(I)]_f} \quad (3)$$

where $[HA(I)]_f$ signifies the effective free humic acid concentration and is given by

$$[HA(I)]_f = [HA(I)]_t LC - [NpO_2HA(I)] \quad (4)$$

$[HA(I)]_t$ is the total humic acid concentration and LC can be determined by the relation:

$$[\text{NpO}_2^+]_f = \text{LC} \cdot F - \frac{1}{\beta} \quad (5)$$

with
$$F = \frac{[\text{NpO}_2^+]_f [\text{HA(I)}]_t}{[\text{NpO}_2\text{HA(I)}]}$$

where all data are available from experiment (Table 1). Plotting $[\text{NpO}_2^+]_f$ versus F results in a slope corresponding to LC . On the other hand, LC can also be obtained from a combination of Eqs. (3) and (4), as shown in the previous work [1], which gives a relation: $[\text{NpO}_2\text{HA(I)}]/[\text{HA(I)}]_t$ versus $[\text{Np(V)}]_t/[\text{HA(I)}]_t$, where all data are available from experiment and $[\text{Np(V)}]_t$ is the total Np(V) concentration. A numerical solution of this relation is given elsewhere [1, 7]. The two different methods for the determination of LC are illustrated in Fig. 2.

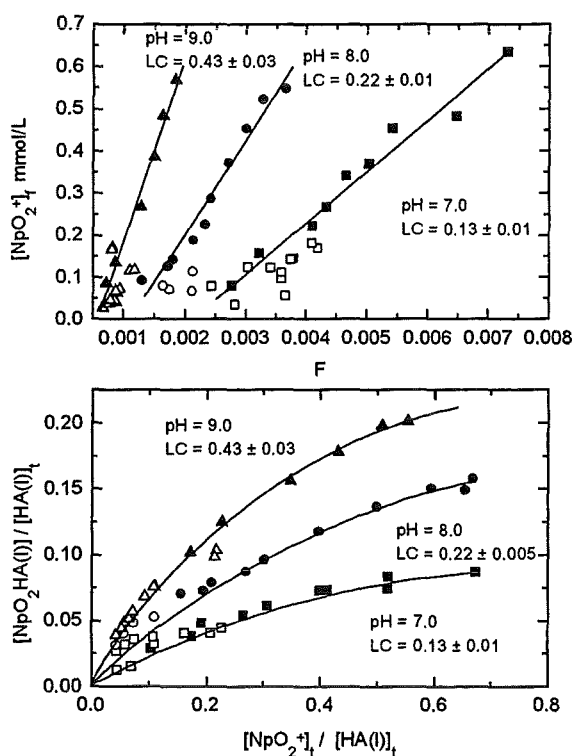


Fig. 2. Evaluation of the loading capacity (LC) of humic acid for the NpO_2^+ ion at $\text{pH} = 7 - 9$ in 0.1 M NaClO_4 according to Eq. (5) (upper part) and to Ref. 1 (lower part).

The suggested reaction of Eq. (2) is validated by plotting experimental data according to the modified Eq. (3), such that

$$\log \frac{[\text{NpO}_2\text{HA(I)}]}{[\text{NpO}_2^+]_f} = \log \beta + \log [\text{HA(I)}]_f \quad (6)$$

where $[\text{HA(I)}]_f$ is calculated by Eq.(4).

Complexation behaviour at pH 7 and pH 8

A linear regression analysis made with Eq.(6) for the experiments at pH 7 and 8 results in slopes of 1.06 ± 0.07 and 1.03 ± 0.07 , respectively. This fact infers the validity of the postulated complexation reaction of Eq. (2) and suggests no higher order complex being formed. The LC values and complexation constants are determined to be:

$$\begin{array}{llll} \text{at pH 7} & \text{LC} = 0.13 \pm 0.01 & \text{and} & \log \beta = 3.53 \pm 0.05 \\ \text{at pH 8} & \text{LC} = 0.22 \pm 0.01_5 & \text{and} & \log \beta = 3.61 \pm 0.07 \end{array}$$

The complexation constants are in good agreement with the values of the previous experiment [1], i.e. $\log \beta = 3.65 \pm 0.03$ at pH 7 and $\log \beta = 3.68 \pm 0.08$ at pH 8. A slight difference of the data at each pH is attributed to somewhat different LC values determined in the two experiments. In the previous experiment [1] the LC values are determined to be 0.099 ± 0.002 at pH 7 and 0.149 ± 0.003 at pH 8 under conditions the ratio of $[\text{NpO}_2^+]_t/[\text{HA}]_t$ being maintained up to 0.23, whereas in the present experiment this ratio is extended up to 0.67 to improve the accuracy of the LC values. However, differences of the $\log \beta$ values from the two separate experiments are found only slightly larger than the geometric sum of individual error margins, namely, $\Delta \log \beta = 0.11 \pm 0.08_5$ at pH 7 and $\Delta \log \beta = 0.12 \pm 0.10_6$ at pH 8.

Complexation behaviour at pH 9

At $\text{pH} \geq 9$, the NpO_2^+ ion becomes partially hydrolysed at $[\text{NpO}_2^+] > 10^{-4} \text{ mol L}^{-1}$, as is apparent from the known hydrolysis constants [8] and as observed in the absorption spectra given in Fig. 1 (lower part). Besides the two known absorption peaks at 980.4 nm and 990 nm for the NpO_2^+ ion and its humate complex ($\text{NpO}_2\text{HA(I)}$) a new absorption peak appears in the wavelength region at 1005 nm. Our experiments showed, that this absorption increases with increasing the Np(V) concentration. It is at first not clear whether the absorption at 1005 nm comes from the hydrolysed Np(V) species or from a neptunyl hydroxohumate complex. According to calculation of species distribution, the aquo-species of NpO_2OH is so small in concentration that it is undetectable by spectroscopy and only its solid form as $\text{NpO}_2\text{OH(s)}$ is found to prevail at excess metal ion concentrations. However, during the experiment a precipitate is not observed and hence it is assumed that the interaction of $\text{NpO}_2\text{OH(s)}$ with humic acid may take place. This interaction then prevents precipitation of $\text{NpO}_2\text{OH(s)}$ and stabilize Np(V) as a hydroxohumate complex or colloidal species in solution.

The species in question is examined by ultrafiltration at pH 10, where the hydrolysed Np(V) species becomes more abundant. As shown in Fig. 3 (upper part) the absorption spectra of the Np(V) solution in 0.1 M NaClO_4 at pH 10 taken without addition of humic acid, before and after filtration (0.45 μm), illustrate that the species showing a broad absorption with the peak maximum at 1017 nm can be filtered completely. This absorption band is then ascribed to the $\text{NpO}_2\text{OH(s)}$ suspension. The same solution, now with addition of humic acid, shows a similarly broad absorption band but with the peak maximum at 1005 nm. After ultrafiltration at 100 nm pore size, only a small amount of the unknown component can be separated, as shown in Fig. 3 (down part), and by further filtration at 30 nm pore size, the unknown species can be removed, while the NpO_2^+ ion and a small fraction of its humate complex remain in the solution. This result infers that the filterable component with a particle size larger than 30 nm is a colloid-borne Np(V) species composed presumably of hydroxohumate complexes. It is known that polynuclear hydroxo species of metal ion undergoes complexation with humic acid through dehydration process [10] but with non-stoichiometric entities.

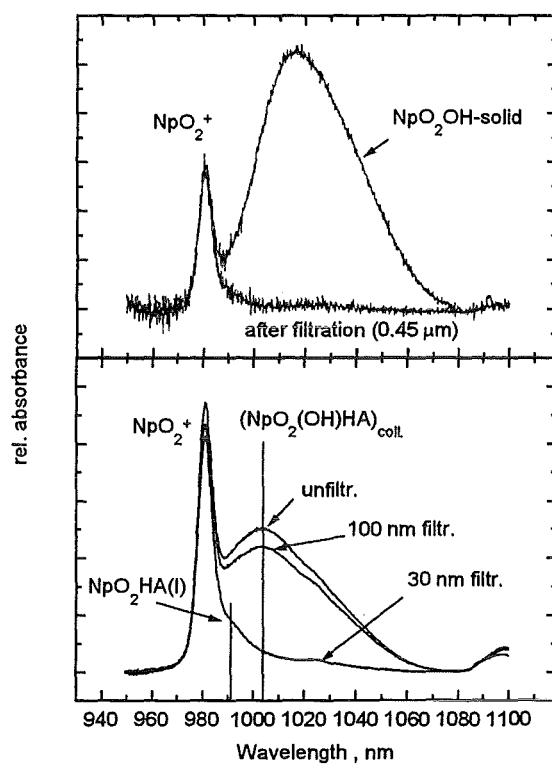


Fig. 3. Absorption spectra of Np(V) in 0.1 M NaClO₄ at pH 10 without humic acid (upper part) and with humic acid of [HA]_t = 1 × 10⁻³ eq L⁻¹ (lower part). For both [Np(V)] = 1.0 × 10⁻⁴ mol L⁻¹. Ultrafiltration at different pore sizes are indicated in the spectra.

The species concerned, as produced at pH ≥ 9, is called a colloid-borne species and assigned as (NpO₂(OH)HA)_{coll.}. Its concentration is estimated by the relation:

$$[\text{NpO}_2(\text{OH})\text{HA}]_{\text{coll.}} = [\text{NpO}_2^+]_t - [\text{NpO}_2^+]_f - [\text{NpO}_2\text{HA}(\text{I})] \quad (7)$$

[NpO₂⁺]_t is known, and [NpO₂⁺]_f and [NpO₂HA(I)] can be determined spectroscopically by subtracting the background caused by the absorption of the species (NpO₂(OH)HA)_{coll.}. The *apparent* effective humic acid concentration at pH 9 is then given by

$$[\text{HA}(\text{I})]_{\text{tLC}^*} = [\text{HA}(\text{I})]_f + [\text{NpO}_2\text{HA}(\text{I})] + [\text{NpO}_2(\text{OH})\text{HA}]_{\text{coll.}} \quad (8)$$

and the *real* effective humic acid concentration for the stoichiometric humate complexation is derived by

$$[\text{HA(I)}]_t \text{LC} = [\text{HA(I)}]_t \text{LC}^* - [\text{NpO}_2(\text{OH})\text{HA}]_{\text{coll}} \quad (9)$$

which is then introduced to Eq. (5) to calculate the LC value at pH 9. The thus corrected computation results in

$$\text{at pH 9} \quad \text{LC} = 0.43 \pm 0.03 \quad \text{and} \quad \log \beta = 3.61 \pm 0.04.$$

A linear slope of 0.99 ± 0.08 is obtained according to Eq. (6). The LC values and average complexation constants calculated for pH 7, 8 and 9 are summarised in **Table 2**. A grand average of the values at three pH is found to be

$$\log \beta = 3.58 \pm 0.05$$

for the Np(V) humate complexation. This value is slightly lower than our previous result: $\log \beta = 3.66 \pm 0.07$ [7] but they are within the overlapping range of error margins. As mentioned above the difference is mainly attributed to discrepancies in the LC values which are determined in different ranges of $[\text{NpO}_2^+]_t / [\text{HA(I)}]_t$. The present experiment covers more a wide range of $[\text{NpO}_2^+]_t / [\text{HA(I)}]_t$.

A comparison of the present results is made with the values of the previous experiment [1], as shown in **Fig. 4**, by plotting all experimental data according to Eq. (6). All data in **Fig. 4** are found to be scattered closely around the linear slope of one, suggesting that they are mutually comparable and at the same time validate the calculation of the postulated reaction of Eq. (2) by Eqs. (3) and (4). The calculated actual slope is 1.08 ± 0.02 .

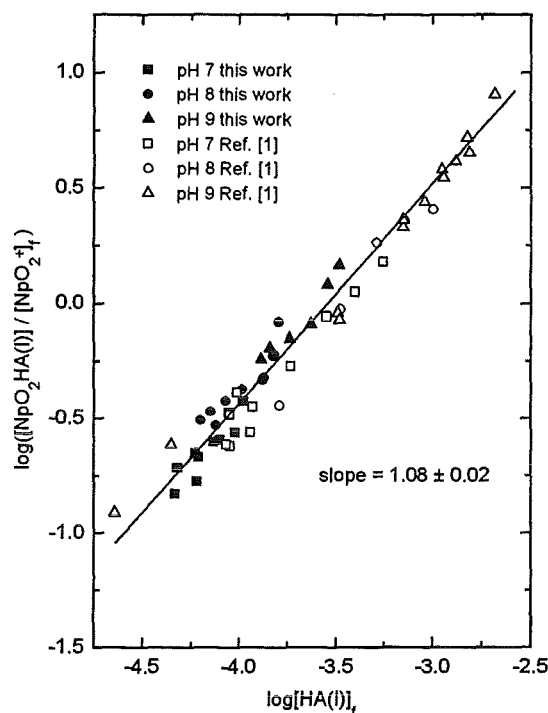


Fig. 4. Validation of the complexation of Np(V) with humic acid postulated by Eq. (6). The free humic acid concentration is evaluated by Eq. (4). The present and previous [1] experimental results are plotted together for the purpose of comparison.

Comparison of results from different laboratories

A direct intercomparison of complexation constants from different laboratories is found to be difficult, because each laboratory has used its own speciation method under different experimental conditions and also because the method applied to evaluate the free humic acid concentration differs from laboratory to laboratory. Since all published papers do not present the primary experimental data from which the complexation constants are evaluated, a reevaluation of constants for intercomparison is not directly possible. However, we have made an attempt to compare the spectroscopic results with one another, because they are resulted from the same speciation method. The intercomparison is made, first of all, among *apparent*

constants from each experiments, which are corrected neither by the loading capacity (LC) nor by the degree of proton dissociation (α). The *apparent* constant K at each given pH is calculated by

$$\log K = \log \frac{[\text{NpO}_2\text{HA(I)}]}{[\text{NpO}_2^+]_f} - \log [\text{HA(I)}]_f^* \quad (10)$$

with $[\text{HA(I)}]_f^* = [\text{HA(I)}]_f - [\text{NpO}_2\text{HA(I)}]$.

The mean values of log K from our present and pervious experiments and those of Rao and Choppin [2] are plotted in Fig. 5 as a function of pH. It becomes apparent that log K is pH

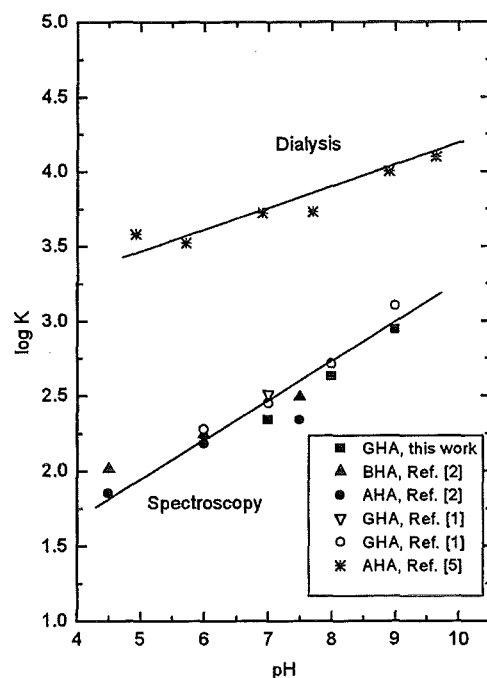


Fig. 5. The *apparent* complexation constant log K (Eq. (10)) as a function of pH for different humic acids (Aldrich humic acid, (AHA), Gorleben humic acid (GHA), Bradford humic acid (BHA)). The upper part points are from the equilibrium ligand exchange technique [5], and the lower part points are from spectroscopic experiments [1, 2] including the present experiment.

dependent. However, $\log K$ is also varying with the experimental ratio of $[\text{NpO}_2^+]_t/[\text{HA(I)}]_t$, as demonstrated in Fig. 6, at higher Np(V) concentrations. In the present experiment the total Np(V) concentration is varied from $1.08 \times 10^{-4} \text{ mol L}^{-1}$ to $7.28 \times 10^{-4} \text{ mol L}^{-1}$, whereas in the previous experiment [1] the variation of $\log K$ with the ratio of $[\text{NpO}_2^+]_t/[\text{HA(I)}]_t$ is not clearly distinguished, as the total Np(V) concentration is maintained less than $2.37 \times 10^{-4} \text{ mol L}^{-1}$. Such a variation of $\log K$ is observed in the complexation study of M(III) ($M = \text{Am}$ and Cm) with humic acid [7] also in the relatively high concentration range of M(III). The variation of $\log K$ due to the effect of the Np(V) concentration is within ± 0.14 logarithmic unit in the present experiment (see Table 1), such that the intercomparison made in Fig. 5 for all available spectroscopic results of $\log K$ can be considered as acceptable for discussion.

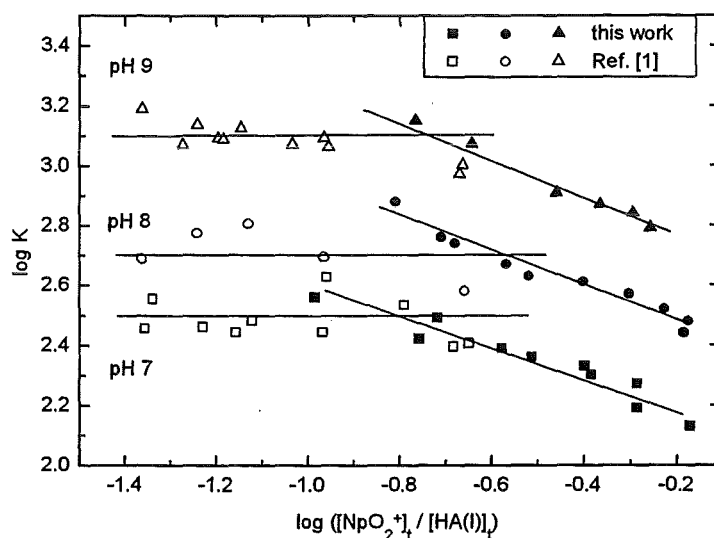


Fig. 6. Variation of $\log K$ (Eq. 10) with the total concentration ratio of $[\text{NpO}_2^+]_t$ to humic acid at different pH.

The $\log K$ values from the equilibrium dialysis ligand exchange technique (EDLE) [5] are also plotted in Fig. 5 for the purpose of comparison. They are pH dependent as well, but substantially larger than the spectroscopic results. This figure demonstrates that one of the experimental methods introduces considerable uncertainties in the determination of reaction constants. Although the same Aldrich humic acid (AHA) is used in the EDLE [5] and spectroscopic [2] experiments, the constants ($\log K$) determined by the two methods

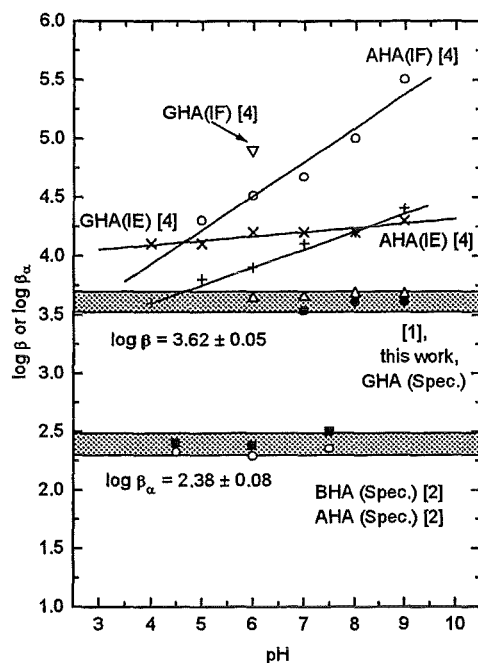


Fig. 7. Intercomparison of the humate complexation constants of Np(V) from different experiments: Spec: UV/VIS spectroscopy [1, 2], IE: ion exchange [4], IF: electrophoretic ion focusing [4] with different humic acids: Aldrich humic acid, (AHA), Gorleben humic acid (GHA), Bradford humic acid (BHA). $\log \beta$ and $\log \beta_{\alpha}$ represent the values converted by LC and α , respectively.

(Spectroscopy and EDLE) are considerably different from one another. The speciation by spectroscopy is by large straightforward and its experimental accuracy can be maintained at less than 0.1 logarithmic unit in the final results. A large discrepancy observed in the results from the two different methods is hardly ascribed to the spectroscopic method. Therefore, the observed discrepancy may be attributable to large uncertainties involved in the separation of two different organometallic complexes by the EDLE method [5]. A critical assessment of uncertainties associated with such a separation is desirable, if possible, by assisting the spectroscopic speciation.

The results of Rao and Choppin [2] are converted to the pH independent values by introducing the degree of proton dissociation (α) at each pH, namely evaluating the free humic

acid concentration: $[HA(I)]_f = [HA(I)]_t \alpha - [NpO_2HA(I)]$. The converted results are shown in Fig. 7 together with our values which are normalised by introducing the loading capacity (LC) according to Eq. (4). A grand average of the values of Rao and Choppin [2] is found to be

$$\log \beta_\alpha = 2.38 \pm 0.08$$

whereas our previous and present experiments have resulted in an average value of

$$\log \beta = 3.62 \pm 0.06$$

The difference of the two values converted either by α or by LC are significant, although the pH dependent *apparent* constants ($\log K$) are internally comparable as illustrated in Fig. 5. The experiment from Rao and Choppin shows $\alpha = 0.97$ at pH 7.5, which means that no conversion is necessary at pH > 7.5. As shown in Fig. 5 at pH > 7.5, the *apparent* constants are still increasing with pH and larger than the converted average value of $\log \beta_\alpha = 2.38$. This fact infers that a conversion by α cannot be applied at pH > 7.5 and hence does not lead to a pH independent constant in the broad pH range. However, a conversion by LC leads to a pH independent value up to higher pH.

The α value indicates the degree of proton dissociation but does not necessarily correspond to the amount of functional groups actually available for the complexation with the NpO_2^+ ion. Since humic acid is structurally cross-linked and irregular in nature, it is conceivable that the proton exchange capacity is not fully available, up to a certain pH, for the interaction with a metal ion [7], particularly with the ions of dioxo bindings or of higher charges. The LC value determined experimentally with the NpO_2^+ ion corresponds directly to the amount of functional groups of given humic acid available for the complexation at each pH. Therefore, the LC value appears to be an appropriate conversion factor as demonstrated elsewhere [7].

The results from Marquardt et al. [4], converted also by α values, are also plotted in Fig. 7 for the purpose comparison and they are found to vary with both origin of humic acid

and experimental method. These values are pH dependent even after correction by α and substantially larger than the average value from our experiments. The reason for such divergence may be borne in upon the experimental method, which does not separate properly the complexed species from the non-complexed metal ion or which influences the complexation process within a given separation procedure. The experiment with the same Aldrich humic acid (AHA) shows that the average spectroscopic value ($\log \beta_\alpha$) of Rao and Choppin [2] is substantially lower than the values (also given as $\log \beta_\alpha$) of Marquardt et al. [4], either from ion exchange (IE) or from electrophoretic ion focusing (IF) experiments. The same is true for Gorleben humic acid (GHA), i.e. the mean spectroscopic value ($\log \beta$) of our experiments is lower than the values ($\log \beta_\alpha$) of Marquardt et al. [4]. Among the values of Marquardt et al. [4], the results of the ion exchange (IE) experiment differs considerably from those of electrophoretic ion focusing (IF) experiment. Whereas their results illustrate a variation of constants ($\log \beta_\alpha$) with experimental method as well as origin of humic acid, in addition with pH, the values of Rao and Choppin ($\log \beta_\alpha$) appear consistent, being independent of pH and origin of humic acid up to pH 7.5.

As the *apparent* constants K from Rao and Choppin [2] and those from our previous [1] and present experiments are internally comparable with one another (Fig. 5), an attempt is made to convert the K values of Rao and Choppin [2] by LC to the β values. For this purpose, the ratio of β_α to K is related by the corresponding evaluation methods for the free humic acid concentration as described above, such that

$$\frac{\beta_\alpha}{K} = \frac{[\text{HA(I)}]_f^*}{[\text{HA(I)}]_f} = \frac{[\text{HA(I)}]_t - [\text{NpO}_2\text{HA(I)}]}{\alpha[\text{HA(I)}]_t - [\text{NpO}_2\text{HA(I)}]} \quad (11)$$

After rearranging Eq. (11), one obtains an experimentally available coefficient, f

$$\frac{\beta_\alpha \alpha - K}{\beta_\alpha - K} = \frac{[\text{NpO}_2\text{HA(I)}]}{[\text{HA(I)}]_t} = f \quad (12)$$

In the same manner, a related expression is obtained between the constant β converted by LC and K:

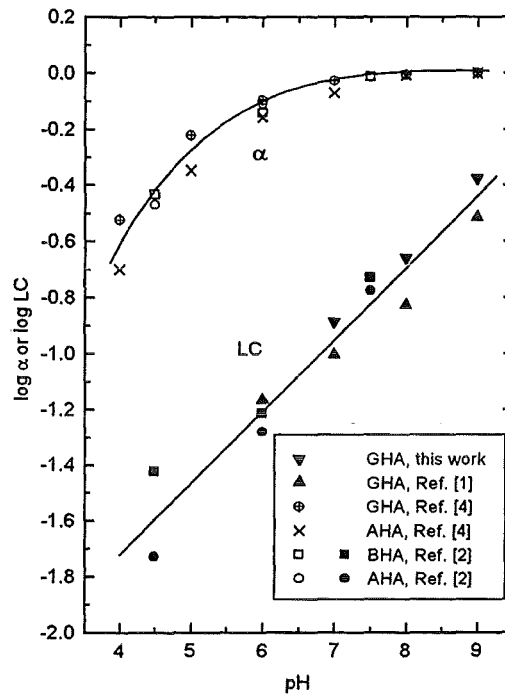


Fig. 8. Illustration of the LC and α values from different experiments [1, 2, 4] as a function of pH for different humic acids: Aldrich humic acid (AHA), Gorleben humic acid (GHA), Bradford humic acid (BHA).

$$\frac{\beta LC - K}{\beta - K} = \frac{[NpO_2HA(I)]}{[HA(I)]_t} = f \quad (13)$$

From the experimental data of Rao and Choppin [2], the f values are calculated for each given pH according to Eq. (12). With the thus obtained f values, the LC values for each experimental pH of Rao and Choppin [2] are deduced according to Eq. (13) by setting the average value of $\log \beta = 3.62$ from our experiments. They are illustrated in **Fig. 8** together with our present and previous values as a function of pH. The known α values [2, 4] are plotted in this figure for the purpose of comparison. All LC values are found to be closely scattered around a linear relationship and result in a pH correlation:

$$\log LC = (0.26 \pm 0.03) \text{ pH} - (2.72 \pm 0.02) \quad (14)$$

The linearity of LC thus obtained as a function of pH from three separate experiments suggests an internal consistency and demonstrates an indirect possibility for the intercomparison of experimental results. With the LC values deduced from Eq. (14), the complexation constants β (LC converted) are computed from the experimental data of Rao and Choppin according to

$$\beta = K \frac{1-f}{LC-f} \quad (15)$$

and the results are given in **Table 3**. A grand average value is found to be $\log \beta = 3.61 \pm 0.16$. Since this value is attended by a feedback calculation of LC by Eq. (14), its agreement with the mean value of $\log \beta = 3.62 \pm 0.05$ from our previous and present experiments is obvious. However, it is simply an additional demonstration of the internal consistency of spectroscopic results from different laboratories experimented with different humic acids (see Fig. 8).

Whereas LC is a parameter dependent on the charge of metal ion, its molecular structure, pH, ionic strength and chemical nature of given humic acid, α is dependent on pH, ionic strength and chemical nature of humic acid. As shown in Fig.8, the LC value is substantially lower than the α value at each given pH, because the dioxo neptunyl ion does not manifest, due to its charge and molecular structure, a strong affinity towards intensely cross-linked structure of humic acid. As a consequence, a conversion of the *apparent* constant K by introducing α does not result in the consistent constant β in the all pH range.

As shown in **Fig. 9**, the β values converted by LC remains consistent and hence independent of experimental conditions and origin of humic acid. For this illustration, $\log \beta$ and $\log K$ are plotted against a common denominator, $\log [\text{NpO}_2^+]_f$, for which $\log \beta$ is calculated by $[\text{HA(I)}]_f = [\text{HA(I)}]_t LC - [\text{NpO}_2\text{HA(I)}]$ and $\log K$ by $[\text{HA(I)}]_f = [\text{HA(I)}]_t - [\text{NpO}_2\text{HA(I)}]$. The results from the previous experiment with lower Np(V) concentrations [1] are well correlated with the present results. As is apparent in this figure, $\log K$ is dependent on the metal ion concentration and pH, while $\log \beta$ appears consistent and allows an intercomparison

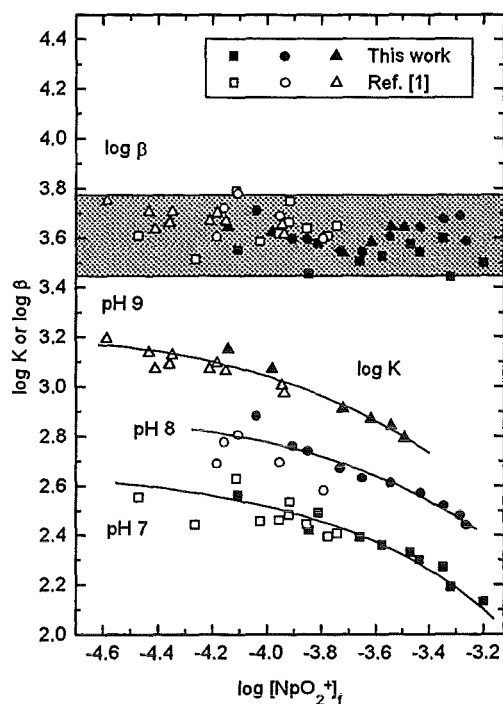


Fig. 9. Comparison of $\log \beta$ with $\log K$ (with and without conversion by LC, respectively) as a function of the free NpO_2^+ ion concentration.

of the results regardless of different experimental parameters applied and, also, of different origins of humic acid (see Ref. [7]).

Competition among different complex reactions

One of the main tasks in the present investigation is to evaluate whether or not the humate complexation of Np(V) may play an important role in the Gorleben aquifer system. For this purpose, calculation is made for the thermodynamic speciation of Np(V) under Gorleben relevant conditions. The amount of DOC in Gorleben groundwaters varies from $< 0.1 \text{ mgC L}^{-1}$ to above 100 mgC L^{-1} . On average, DOC is composed over 90% of humic and fulvic acids and thereby appears to be a relevant parameter for estimating aquatic humic substances. The thermodynamic speciation is made, as shown in Fig. 10, as a function of the humic acid

concentration. Calculation is made at pH 8, which is an average value for Gorleben groundwaters, and at two CO₂ partial pressures: P_{CO2} = 10^{-3.5} atm and 10^{-2.0} atm, which correspond to a partial pressure under normal atmosphere and an average value found in the Gorleben aquifer system, respectively. The constants for carbonate complexation and hydrolysis reactions are taken from Neck et al. [8, 9].

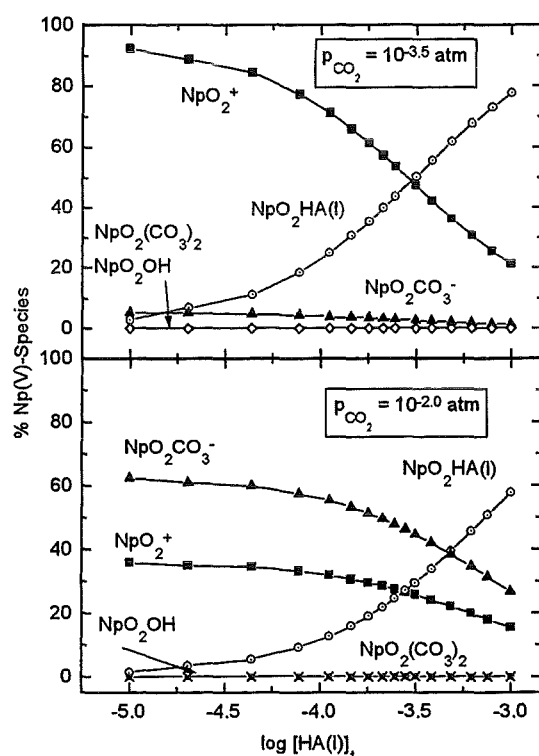


Fig. 10. Speciation of Np(V) at pH 8 as a function of the humic acid concentration at $p_{\text{CO}_2} = 10^{-3.5}$ atm (upper part) and $p_{\text{CO}_2} = 10^{-2}$ atm (lower part).

It is apparent in Fig. 10 that hydrolysis is found to be negligible at pH 8. Under atmospheric conditions the humate complexation becomes predominant in the humic acid concentration range of $> 3 \times 10^{-5}$ eq L⁻¹, whereas at $P_{\text{CO}_2} = 10^{-2.0}$ atm the carbonate complexation appears dominant and the humate complexation plays a minor role but becomes important with increasing the humic acid concentration and dominant at a humic acid concentration larger than 2×10^{-4} eq L⁻¹. The speciation shows that only reaction competitive

to the Np(V) humate complexation is the carbonate complexation in Gorleben groundwaters. According to the calculated results shown in Fig. 10, the humate complexation of Np(V) may play an important role only in Gorleben groundwaters with relatively high humic acid concentrations. However, another important reaction to be considered is a reduction process of Np(V) to Np(IV) by interaction with humic acid, which will be dealt with in another occasion.

Literature

- [1] Kim, J.I., Sekine, T., Complexation of Neptunium(V) with Humic Acid, *Radiochim. Acta* **55**, 187 (1991).
- [2] Rao, L., Choppin, G.R., Thermodynamic Study of the Complexation of Neptunium (V) with Humic Acid, *Radiochim. Acta*, **69**, 87 (1995).
- [3] Moulin, V., Moulin, C., Fate of Actinides in the Presence of Humic Substances under Conditions relevant to Nuclear Waste Disposal, *Appl. Geochem.* **10**, 573 (1995).
- [4] Marquardt, C., Herrmann, G., Trautmann, N., Complexation of Neptunium (V) with Humic Acids at Very Low Metal Concentrations, *Radiochim. Acta* **73**, 119 (1996).
- [5] Glaus, M.A., Hummel, W., Van Loon, L.R., PSI-Report, Labor für Entsorgung, TM-44-94-04 (1994).
- [6] Kim, J.I., Buckau, G., Li, G.H., Duschner, H., Psarros, N.Z., Characterization of Humic and Fulvic Acids from Gorleben Groundwaters, *Anal. Chem.* **338**, 245 (1986).
- [7] Kim, J.I., Czerwinski, K.R., Complexation of Metal Ions with Humic Acid: Metal Ion Charge Neutralization Model, *Radiochim. Acta* **73**, 5 (1996).
- [8] Neck, V., Kim, J.I., Kanellakopoulos, B., Solubility and Hydrolysis Behaviour of Neptunium (V), *Radiochim. Acta* **56**, 25 (1992).
- [9] Neck, V., Runde, W., Kim, J.I., Kanellakopoulos, B., Solid-Liquid Equilibrium Reactions of Neptunium(V) in Carbonate Solution at Different Ionic Strength, *Radiochim. Acta* **65**, 29 (1994).
- [10] Kim, J.I., Chemical Behaviour of Transuranium Elements in Natural Aquatic Systems, in "Handbook on the Physics and Chemistry of the Actinides", Freedman, A.J. and Keller, C., Eds., Vol. 4, Elsevier Science Publ., Amsterdam (1986) Chap. 8.

Table 1: Analytical data and concentrations of different Np(V)- species in the Np(V)-complexation study by absorption spectroscopy at pH 7, 8 and 9, in 0.1 M NaClO₄ under 100 % argon atmosphere.

[HA(I)] _t eq L ⁻¹ x 10 ⁻³	[Np(V)] _t mol L ⁻¹ x 10 ⁻⁴	[NpHA(I)] mol L ⁻¹ x 10 ⁻⁴	[Np(V)] _f mol L ⁻¹ x 10 ⁻⁴	[Np(OH)HA] _{coll} mol L ⁻¹ x 10 ⁻⁴	log K	log β
pH 7						
1.04	1.08	0.295	0.787	-	2.56	3.55
1.04	1.82	0.391	1.43	-	2.42	3.45
1.08	2.07	0.518	1.55	-	2.49	3.58
1.04	2.76	0.557	2.20	-	2.39	3.50
1.08	3.32	0.661	2.66	-	2.36	3.52
1.04	4.16	0.757	3.40	-	2.33	3.57
1.08	4.47	0.788	3.68	-	2.30	3.54
1.04	5.41	0.868	4.53	-	2.27	3.60
1.08	5.61	0.801	4.81	-	2.19	3.44
1.08	7.28	0.934	6.34	-	2.13	3.50
mean value					2.34 ± 0.13	3.53 ± 0.05
pH 8						
1.08	1.68	0.761	0.921	-	2.88	3.71
1.02	1.99	0.740	1.25	-	2.76	3.60
1.08	2.26	0.849	1.42	-	2.74	3.59
1.02	2.76	0.889	1.87	-	2.67	3.55
1.08	3.27	1.04	2.24	-	2.63	3.54
1.02	4.06	1.20	2.86	-	2.61	3.60
1.02	5.10	1.39	3.71	-	2.57	3.64
1.02	6.06	1.53	4.53	-	2.52	3.67
1.02	6.82	1.61	5.21	-	2.48	3.69
1.08	7.07	1.61	5.47	-	2.44	3.58
mean value					2.63 ± 0.14	3.61 ± 0.07
pH 9						
1.05	1.94	1.05	0.724	0.166	3.15	3.64
1.05	2.68	1.26	1.05	0.37	3.07	3.62
1.05	4.06	1.54	1.90	0.62	2.91	3.54
1.05	5.10	1.69	2.42	0.99	2.87	3.58
1.05	5.95	1.83	2.88	1.24	2.84	3.64
1.05	6.43	1.83	3.22	1.38	2.79	3.64
mean value					2.94 ± 0.14	3.61 ± 0.04

Table 2. Loading capacities and stability constants for the neptunium(V) humate complexation at ionic strength 0.1 M.

pH	loading capacity LC	stability constant log β	n (slope)
7.0	0.13 ± 0.01	3.53 ± 0.05	1.06 ± 0.07
8.0	0.22 ± 0.015	3.61 ± 0.07	1.03 ± 0.07
9.0	0.43 ± 0.03	3.61 ± 0.04	0.99 ± 0.08
	mean value	3.58 ± 0.05	

Table 3: Conversion of the α -corrected complexation stability constants β_α of the Np(V)-humate complexation (from Rao and Choppin [2]) into the LC-corrected complexation constants β as described in the text.

pH	log K	α	log β_α	f	LC from Eq.(14)	log β
AHA						
4.5	1.85	0.34	2.32	0.00175	0.0282	3.43
6.0	2.18	0.78	2.29	0.01677	0.0692	3.45
7.5	2.34	0.97	2.35	0.1213	0.1698	3.60
BHA						
4.5	2.01	0.37	2.44	0.001346	0.0282	3.84
6.0	2.24	0.72	2.38	0.02019	0.0692	3.58
7.5	2.49	0.97	2.50	0.1214	0.1698	3.75
					mean value	3.61 ± 0.16

1st Technical Progress Report

EC Project:

"Effects of Humic Substances on the Migration of Radionuclides:
Complexation and Transport of Actinides"

FZK/INE Contribution to Task 3 (Actinide Transport)

**Effects of Humic Substances on the ²⁴¹Am Migration in a Sandy
Aquifer: Batch and Column Experiments with Gorleben
Groundwater/Sediment Systems**

Reporting period 1997

R. Artinger, B. Kienzler, W. Schüßler, J.I. Kim

Forschungszentrum Karlsruhe, Institut für Nukleare Entsorgungstechnik,
P.O. Box 3640, D-76021 Karlsruhe, Germany.

Abstract

Migration experiments are performed to study the influence of aquatic humic substances on the transport behavior of Am(III). Four groundwaters with different humic substance concentrations (TOC: 1 to 80 mg/L) are sampled together with Pleistocene aeolian quartz sand from the Gorleben site. Sand, groundwaters and humic substances are characterized by different analytical methods (e.g. ICP-MS, X-ray diffraction, X-ray fluorescence analysis, ultrafiltration). The sand is equilibrated with the 4 groundwaters under inert gas atmosphere with 1 % CO₂ for a period of at least three months. As confirmed by ultrafiltration the size distribution of humic colloids remains unchanged during equilibration. The hydraulic properties of sand columns are characterized with tritiated water as inert tracer. Column and batch experiments are carried out with the 4 groundwaters as a function of the reaction period and flow velocity. In addition, the influence of the equilibration period of Am with groundwater is investigated prior to the injection into a column. The results reveal that an increasing humic substance concentration reduce the Am sorption onto sand and enhance the transport as colloid-borne Am species. The migration of the mobile fraction of colloid-associated Am is slightly faster than the groundwater flow velocity. Furthermore, the migration behavior of Am is found to depend on kinetically controlled interaction of humic colloid-bound Am with the sand surface. The application of the laboratory data to natural conditions is discussed. The results are found applicable for the assessment of a humic colloid facilitated radionuclide migration in natural aquifers.

1. Introduction

Natural barriers isolating radioactive wastes from the biosphere are the host formation and the overlaying strata. In the case of the Gorleben site (Lower Saxony, Germany), which is under investigation as a possible nuclear waste repository, the strata covers a Permian salt

dome, which consists of sedimentary rocks having a distinguished aquifer system. A possible transport of radionuclides would occur by groundwater moving in geologic formations of high permeability. At the Gorleben site sandy sediments of high permeability are found from the surface down to the top of the salt dome (Ludwig and Schneider, 1994). Due to local Miocene brown coal and Pleistocene peat deposits, dissolved organic carbon (DOC) in groundwater is found to be locally up to 200 mg C/L (Buckau, 1991). In these groundwaters, DOC consists mainly of colloidal fulvic and humic acids, which, in general, strongly absorb multivalent radionuclides, like actinides Am^{3+} and Cm^{3+} (Czerwinski et al., 1996). Therefore, aquatic humic substances are of cardinal importance for radionuclide migration through colloid facilitated transport (Kim, 1990, Maravic and Moreno, 1993).

Laboratory procedures to assess the migration behavior of radionuclides in geological formations of high permeability are batch and column experiments (Meier et al., 1994, Kim et al., 1994, Klotz and Lazik, 1995). Batch experiments suggest a significant retardation of the humic colloid-associated actinides, although high humic colloid concentrations reduce the actinide sorption onto mineral surfaces (Kim et al., 1995). Contrary to this, column experiments with natural sand sediment and groundwater rich in humic colloids show a certain fraction of multivalent actinides as fast as the conservative tracer, indicating no significant interaction between humic colloid-borne actinides and sediment (Kim et al., 1994). The possible explanation for the different results of batch and column experiments is the kinetic of actinide-humic colloid interactions. The kinetic effects and the question whether or not actinides are reversibly bound to humic colloids plays a fundamental role for the migration of actinides in the geosphere (Smith and Degueldre, 1993).

The present study focuses on the influence of aquatic colloidal humic substances on the migration behavior of Am(III) in Gorleben specific groundwater/sand systems. Investigations are carried out by batch and columns experiments, varying the humic substance concentration

as well as the reaction period. The aim of this work is to appraise the humic colloid facilitated radionuclide migration in the geosphere.

2. Experimental

Samples

Four different groundwater with varying DOC and humic colloid concentrations are sampled from the Gorleben aquifer on 20-22 May 1996, indicated as GoHy-182, -412, -532, and -2227 (cf. Table 1). All sampled groundwaters are in contact with sandy sediments of different stratifications. DOC is characterized for its concentration and composition (fulvic, humic, and hydrophilic acids) by acid-base treatment and isolation with XAD-8 resin.

As a solid phase a Pleistocene aeolian quartz sand is sampled from the near aquifer surface. According to X-ray fluorescence and X-ray diffraction analysis the uniform fine sand ($d_{10} = 0.12$ mm and $d_{50} = 0.18$ mm, $U = 1.7$) consists of about 85 % quartz, 10 to 15 % feldspars and <5 % of other minerals as e.g. mica and others. Organic material is found to be <0.5 %. The grain size analysis shows that silt part is about 0.25 % and clay <0.1 %. In agreement with this composition a cation exchange capacity of the sand is characterized to be 1.0 meq/100 g (according to Mehlich), a surface area is 1.1 m²/g (BET; nitrogen sorption), and a point of zero charge at pH 4.6.

²⁴¹Am spiked solutions

Aliquots of an ²⁴¹Am stock solution of about 10⁻⁴ mol/L in 0.1 M perchloric acid are allowed to react with different groundwaters, depending on experiment for 5 minutes to several weeks. In batch experiments the equilibration continues at least for a period of one week. The Am concentration in spiked groundwaters is typically 2·10⁻⁶ mol/L. At this concentration Am is found to be quantitatively sorbed on humic colloids. However, the

Table 1: Depth below ground, stratification, fundamental physico-chemical properties of sampled Gorleben groundwaters and DOC characteristics.

Groundwater	Depth (m)	Stratification	pH	Eh (mV)	Conductivity (μ S/cm)	Σ cations (meq/L)	Σ anions (meq/L)	DOC (mg/L)	FA (%)	HA (%)	Hydrophilic acids (%)
GoHy-182	70-73	Elster	8.1	-90	144	1.56	1.38	1.1	17	16	67
GoHy-412	65-68	Elster	7.7	-70	370	3.69	3.86	7.2	34	22	44
GoHy-532	65-68	Elster	8.9	-160	950	9.45	9.30	29.9	20*	69*	11*
GoHy-2227	128-130	Pre-Elster	7.7	-120	4600	42.59	42.55	81.9	8	79	13

* estimated by UV/Vis spectroscopy (Zeh, 1993) and ultrafiltration

Table 2: Physical parameters, major ion- and DOC concentrations of equilibrated groundwaters.

Groundwater	pH	Eh (mV)	Na (mmol/L)	K (mmol/L)	Mg (mmol/L)	Ca (mmol/L)	Fe (mmol/L)	Cl (mmol/L)	HCO ₃ (mmol/L)	DOC (mmol/L)
GoHy-182	6.3	-180	0.194	<0.013	0.039	0.256	0.076	0.299	0.700	6.4
GoHy-412	6.8	-220	2.773	<0.013	0.051	0.144	0.059	0.515	2.661	17.1
GoHy-532	7.1	-220	9.538	<0.013	0.002	0.026	0.057	3.868	5.271	49.1
GoHy-2227	7.5	-250	42.778	0.166	0.122	0.227	0.041	36.140	7.850	102.7

groundwater GoHy-182 with the lowest humic substance concentration (cf. Table 1), ultrafiltration indicates a fraction of about 20 % Am which is not colloid-associated but probably present as the first carbonato complex of Am(III).

Procedures

Batch and column experiments are performed under anaerobic conditions (Ar + 1 % CO₂) in a glove box. During the reaction period, all experiments are kept in the dark to minimize any degradation of humic substances and to avoid alga growth.

Batch experiments are performed with a liquid/solid ratio of 10 mL groundwater to 2.5 g sand (V/m = 4 mL/g) and Am concentrations in the range of 10⁻¹⁰ to 10⁻⁷ mol/L. The sand is packed in columns and groundwater is pumped in circle for a period of two months for equilibration. Afterwards, the sand is dried and mixed with groundwaters in 20 mL PE vial and further equilibrated for over a week. After adding the groundwater spiked with ²⁴¹Am, the vials are agitated by hand to obtain contact between both phases. For reaction periods over one day the samples are shaken each day.

Flow through column experiments are performed using separate columns (500 mm long, and 50 mm in diameter) for each groundwater/sand system. Pre-columns (250 mm long, and 50 mm in diameter) are used as filter to remove possibly generated larger particles and to pre-equilibrate the groundwater. Columns are tightly packed with sand (Klotz 1991) and equilibrated with groundwaters over a period of at least three months. The experimental set-up is shown in Fig. 1. Tritiated water HTO is used as a conservative tracer to determine the hydraulic properties of columns (cf. Table 3). The breakthrough curves of HTO and Am are measured using flow through monitors for β- and γ-radiation and additionally by single fraction analysis. The ²⁴¹Am concentrations in eluate fractions and batch experiments are determined by liquid scintillation counting.

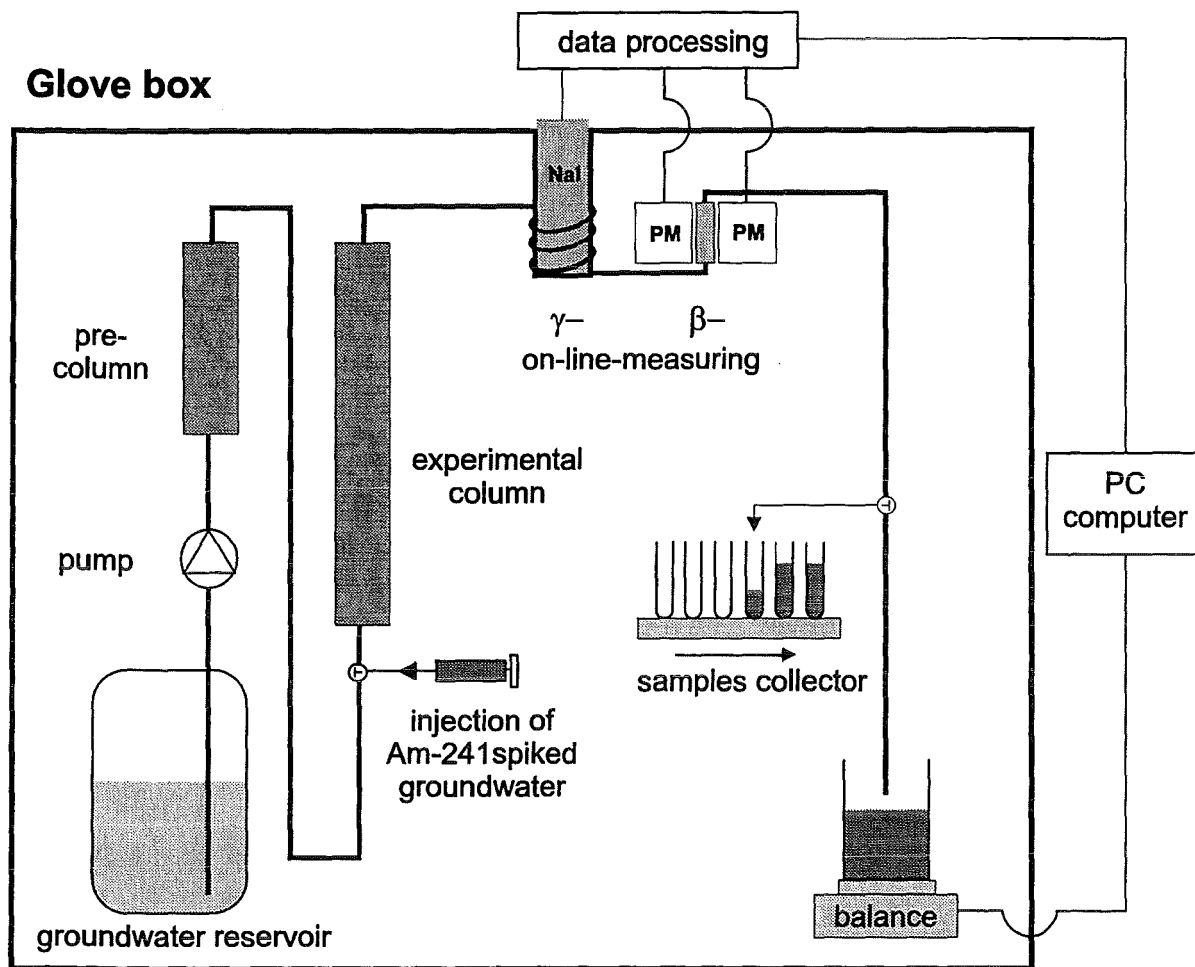


Fig. 1: Experimental setup for column experiments

3. Results and discussion

3.1. Groundwater/sediment equilibration

Before and after equilibration, the chemical composition of groundwater, DOC concentration and its size distribution are determined. The analytical data of the four equilibrated groundwaters are shown in Table 2. Equilibration under the CO_2 partial pressure of 1 % makes the groundwater pH shifted to a lower value compared to the initial condition. Fe concentrations are increased by dissolution of Fe(III) from the sand surface through its reduction to Fe(II). DOC concentrations are enhanced as well by the equilibration process mainly due to a pH dependent dissolution of organic material from the sand (cf. Tables 1 and

Table 3: Results from ^{241}Am column experiments and hydraulic properties of used columns determined by HTO*.

Groundwater / experiment number	Darcy velocity v_D (m/day)	Pore water flow velocity v (m/day)	Effective porosity ϵ	Longitudinal dispersion coefficient D_L ($10^{-5} \text{ cm}^2/\text{s}$)	^{241}Am / ground- water equili- bration time (days)	^{241}Am concentration in injected solution (mol/L)	pH	Recovery R (%)	Retardation factor R_f (± 0.01)
GoHy-2227 / 1	0.251	0.763	0.329	3.08	0.04	$1.9 \cdot 10^{-6}$	7.4	1.9 ± 0.2	0.95
GoHy-2227 / 2	0.252	0.767	0.329	3.03	7	$1.9 \cdot 10^{-6}$	7.4	22.6 ± 1.1	0.95
GoHy-2227 / 3	0.255	0.776	0.329	3.31	36	$1.9 \cdot 10^{-6}$	7.5	35.4 ± 1.8	0.96
GoHy-532 / 1	2.246	6.812	0.330	19.8	20	$1.9 \cdot 10^{-6}$	7.5	34.0 ± 1.7	0.95
GoHy-532 / 2	0.268	0.812	0.330	1.96	10	$1.9 \cdot 10^{-6}$	7.1	19.6 ± 1.0	0.96
GoHy-532 / 3	0.021	0.063	0.330	0.17	40	$1.9 \cdot 10^{-6}$	7.3	6.5 ± 0.3	0.97
GoHy-412 / 1	0.262	0.787	0.333	3.06	41	$1.5 \cdot 10^{-6}$	6.9	1.6 ± 0.2	0.98
GoHy-412 / 2	0.270	0.819	0.330	3.24	26	$1.7 \cdot 10^{-7}$	6.8	2.3 ± 0.8	0.99
GoHy-182 / 1	0.273	0.823	0.332	2.71	7	$1.8 \cdot 10^{-6}$	6.1	0.1 ± 0.2	0.98

* For each groundwater a separate column is used.

2). However, the size distribution of humic colloids is unchanged as determined by ultrafiltration. In summary, the equilibration procedure results in some particular differences with respect to the original groundwater composition. The changes are observed to be within the natural variation of Gorleben groundwaters and therefore from these changes no drastic consequences for the humic colloid-borne actinide migration should be expected.

3.2. Batch experiments

The sorption behavior of ^{241}Am on the Gorleben sand is described by the sorption coefficient R_s , which is calculated by

$$R_s = \frac{c_0 - c}{c} \frac{V}{m} \quad (\text{mL} / \text{g}) \quad (1)$$

where c_0 is the initial Am concentration (Bq/mL), c the Am concentration in solution after a given reaction period, V the groundwater volume (mL) and m the sand mass (g). The Am concentration in solution represents the fraction passing a $0.45 \mu\text{m}$ filter.

Sorption progresses are shown in Fig. 2 for the four different groundwaters (initial ^{241}Am concentration $5 \cdot 10^{-8} \text{ mol/L}$). The equilibrium state for the Am sorption onto the Gorleben sand is not reached up to 100 days for all groundwaters. The results demonstrate the problems of the comparison between batch and column experiments and indicate that kinetic effects must be taken into account. Therefore, a comparable reaction period for both methods is necessary. A strong influence on the Am sorption is exerted by the humic colloid concentration. The higher the humic colloid concentration in groundwater, the lower is the sorption coefficient R_s . This behavior is also found in earlier studies (Ticknor et al., 1996, Labonne et al., 1992, Buckau, 1991). Fig. 3 shows the time dependent Am sorption for GoHy-2227 at the initial concentration range of $2 \cdot 10^{-7}$ to $2 \cdot 10^{-10} \text{ mol/L}$. The sorption behavior of Am is found to be independent of the initial Am concentration up to 46 d. However, after a reaction period of 100 days, a decrease of the sorption is observed at lower initial Am concentrations $< 5 \cdot 10^{-9}$

mol/L. This phenomenon is also found for other groundwater/sand systems. A plausible explanation for this behavior is not available at the moment. Only a few studies are known for investigating kinetically controlled sorption isotherms (e.g. Rabung, 1997). A substantial influence of the groundwater pH on the Am sorption behavior is not expected, because in the pH range between 6 to 7.5 the sorption of Am(III), and its homologue Eu(III), onto different minerals (silica, haematite, etc.) is found to be largely constant in the presence of humic substances (Fairhurst et al., 1995, Moulin and Stammose, 1989). This fact may be also valid to the column experiment.

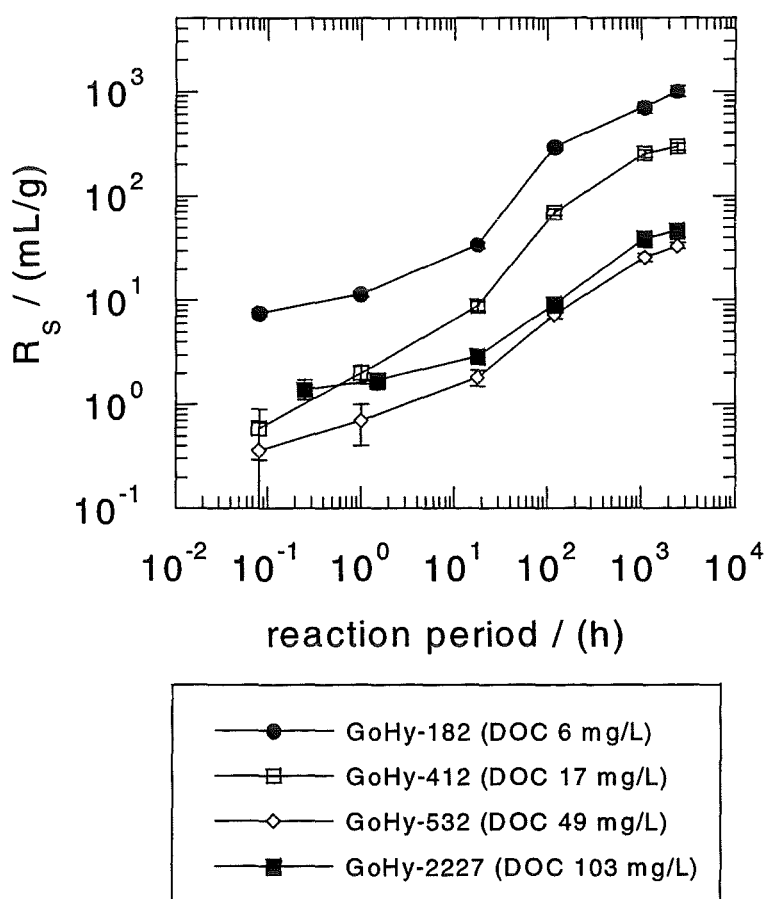


Fig. 2: Kinetic sorption data from batch experiments in dependence on DOC concentration at an initial Am concentration of $5 \cdot 10^{-8}$ mol/L.

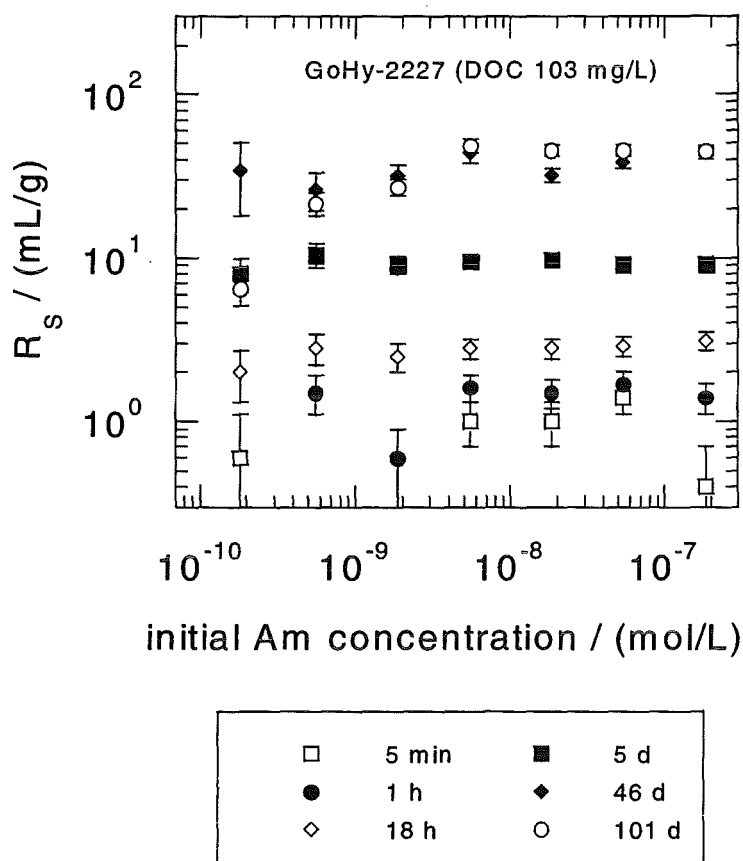


Fig. 3: Kinetic sorption data from batch experiments for GoHy-2227 (DOC 103 mg/L) in dependence on the initial Am concentration.

3.3. Column experiments

Hydraulic properties

During the equilibration phase and the Am migration experiment, the hydraulic properties, effective porosity and dispersion coefficient, are determined for each column. The Darcy velocity of groundwater pumped through the columns is varied from 0.02 m/d up to more than 2 m/d. The hydraulic data obtained are summarized in Table 3. The effective porosity ϵ , which is determined by the mean pore water flow velocity v of the conservative HTO tracer, appears to be on average of about 33 % and remains constant during the equilibration and experimental period. Among different columns, no variation in the effective porosity is

observed. For this reason a stable grain structure in the columns can be concluded. The measured hydrodynamic longitudinal dispersion coefficients D_L varies from 10^{-6} to 10^{-4} cm²/s depending on the pore water flow velocity. The column Peclet number calculated by Eq. (2) varies from 2000 at a pore water flow velocity of 0.06 m/d up to 2400 at 6.8 m/d (column length $L = 50$ cm).

$$Pe^* = \frac{vL}{D_L} \quad (2)$$

Based on such a small change in the column Peclet number for a variation of the flow velocity over two orders of magnitude, it can be concluded that the dispersion is dominated by transport and not by diffusion (Appelo and Postma, 1996, Bürgisser et al., 1993).

Influence of DOC concentration

The influence of DOC and humic colloid concentration is investigated by injecting 1 mL of the four equilibrated Gorleben groundwaters (DOC: 6 to 100 mg C/L) spiked with ²⁴¹Am. A constant size distribution of Am-bound humic colloids is observed in the groundwaters GoHy-532 and -2227. The size spectrum in GoHy-412 and -182 is significantly changed to larger particles, which can be attributed to a higher loading of Am(III) on the humic colloids.

The migration characteristics of Am(III) (retardation / recovery) are depicted in Fig. 4. The ²⁴¹Am concentration in the eluate is normalized to the injected ²⁴¹Am concentration and plotted as a function of ratio of eluted volume to pore volume of the column (V/V_p). In different groundwaters, different fractions of ²⁴¹Am are transported but with the nearly same retardation factor $R_f = 0.95$ to 0.99 , which suggests that ²⁴¹Am migrates slightly faster than water. The observed migration behavior is attributed to the association of Am with humic colloids, which moves faster due to size exclusion. This process explains also the enhanced Am transport in the case of GoHy-2227 and GoHy-532 compared to GoHy-412 and -182,

because aquatic humic colloids of the former two have larger hydrodynamic size (Artinger et al., 1997). Ultrafiltration of the eluate confirms the humic colloid-borne transport of ^{241}Am . The recovery R of ^{241}Am , related to an eluted volume of about 15 pore volumes, increases up to $R = 20\%$ with increasing DOC content in groundwater. The enhanced Am recovery with increasing the humic colloid concentration is also reported in earlier studies with comparable groundwater/sand systems (Kim et al., 1995).

In conclusion, the increase of eluted ^{241}Am with increasing DOC supports the stabilization of Am(III) in solution by aquatic humic colloids, which suppresses the interaction of Am with the sand surface.

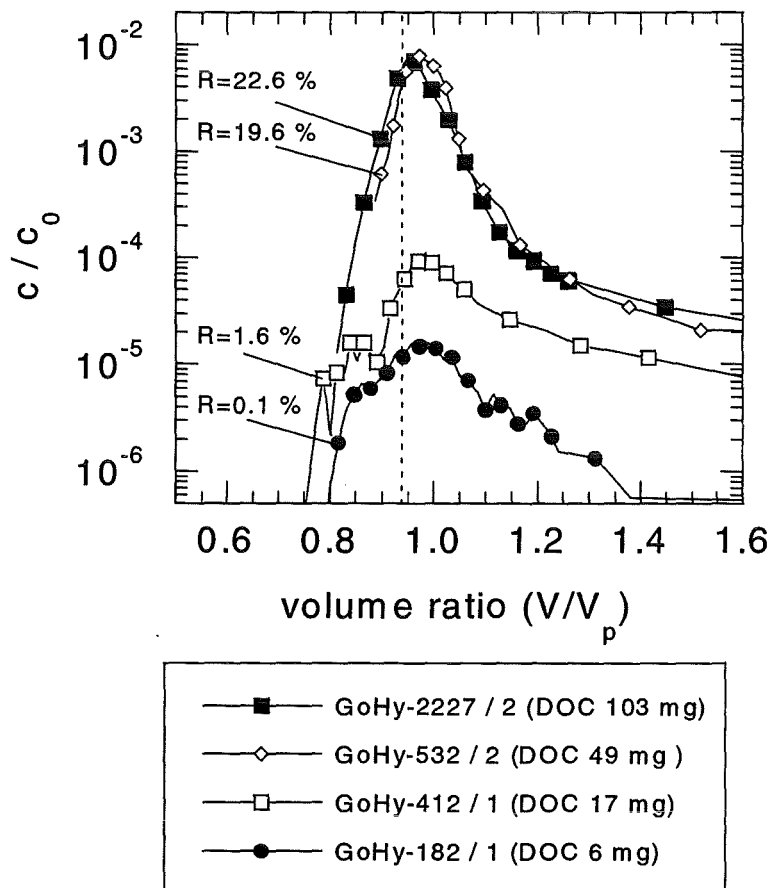


Fig. 4: ^{241}Am breakthrough curves and recoveries R in dependence on the DOC concentration in groundwater. The recoveries are related to an eluted groundwater volume of about 15 effective pore volumes.

Kinetic effects

As shown in Fig. 2 batch experiments reveal significant kinetic effects of the ^{241}Am sorption onto sand in the presence of humic colloids. The kinetic effects on the migration of humic colloid-borne ^{241}Am through sand are studied by the following experiments: (i) the variation of the groundwater flow velocity and residence time of humic colloid-borne ^{241}Am in a given column and (ii) the variation of the equilibration period of Am with groundwater before injection into the column. The results are shown in Figs. 5 and 6, which illustrate the Am breakthrough curves.

Varying the groundwater flow velocity about two orders of magnitude (0.06 to 7 m/d), an increase of the ^{241}Am recovery from 6 to 34 % is obtained (Fig. 5). This tendency has been also found for Eu in a comparable groundwater/sand system (Kim et al., 1994). That means, the longer the residence time of the humic colloid-borne Am in a column, the higher is the amount of Am sorbed onto the sand. This is consistent with the results obtained from the batch experiments, which reveals in principle the same kinetic effect. The varying Am/groundwater equilibration time within a period of 10 to 40 days seems to have a minor influence on the recovery within this period, because no correlation is observed. The dominant dependence of the Am recovery on the groundwater flow velocity may be explained by time-dependent turn over of Am from humic colloids onto sand surface. The observation that humic colloids are not significantly sorbed onto sand during the equilibration period of several months supports the fact, that the Am fraction retained on sand (94 to 64 %) is not sorbed as humic colloid-complex. The retardation factor of the mobile fraction of humic colloid-borne Am varies for groundwater GoHy-532 from 0.95 to 0.97, indicating no significant influence of the groundwater flow velocity.

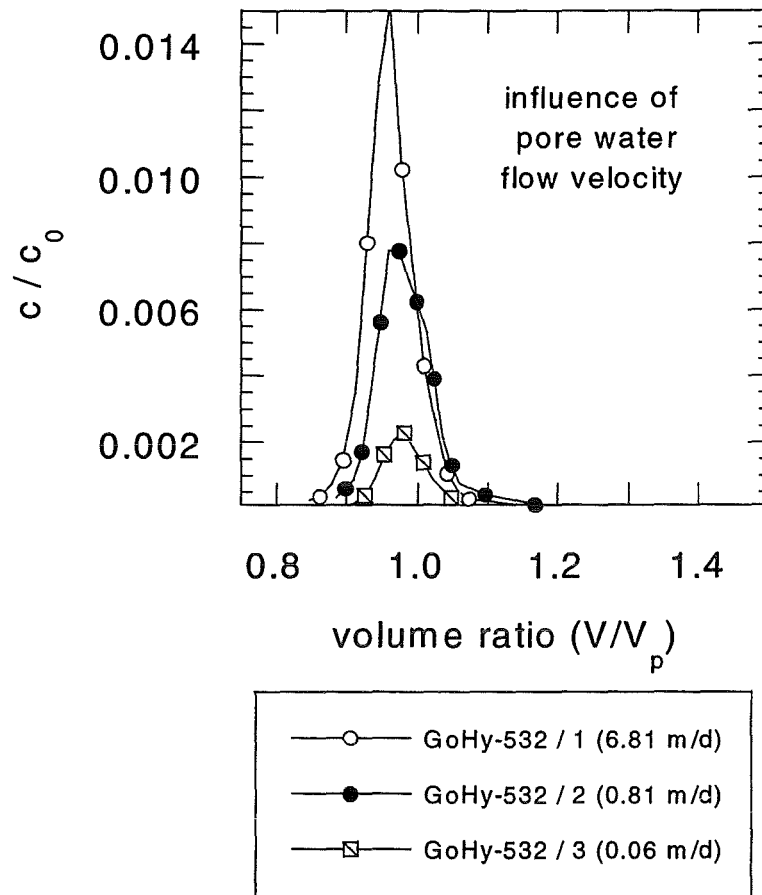


Fig. 5: ^{241}Am breakthrough curves in dependence on pore water velocity.

The sorption of the humic colloid-borne Am onto sand is not only kinetically controlled by the residence time in column but also by the equilibration period of Am with aquatic humic colloids in solution. As shown in Fig. 6 the Am recovery for GoHy-2227 increases at the same groundwater flow velocity ($v = 0.8 \text{ m/d}$) with increasing the equilibration time. After a equilibration period of about 5 minutes, only 2 % of the injected ^{241}Am is recovered with a R_f value of 0.95, although it is determined that Am is quantitatively sorbed onto humic colloids before injection. Contrary to this, at an equilibration period of 36 days the Am recovery increases up to 35 %. This fact suggests that Am is more strongly bound to humic colloids with increasing the equilibration time. Consequently, Am becomes less available for

the surface complexation onto sand during the migration period in column. The phenomenon of a time-dependent strong binding of a trivalent metal ion with humic colloids is also found by Rao et al., 1994, who studied the interaction of Eu(III) with humic acid using cation exchange columns.

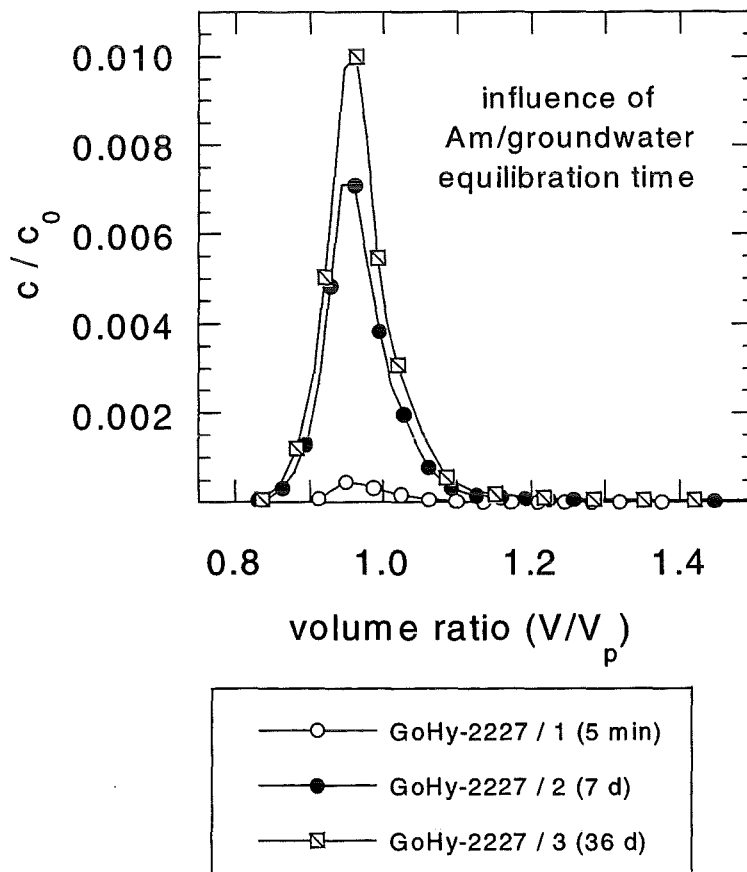


Fig. 6: ^{241}Am breakthrough curves in dependence on equilibration period of ^{241}Am with groundwater before injection into column.

In summary, the column experiments indicate within the period of the investigation a reversible binding of Am onto the mobile humic colloids. For this reason, an increased Am sorption onto sand with an advancing migration front of Am-bound humic colloids in an uncontaminated aquifer is expected. However, the present column experiments do not provide

any information on the fate of the Am fraction retained in column, which has to be studied separately.

3.4. Significance of experimental results for the natural aquifer

Every effort is made to perform the column experiments close to natural conditions. However, the question arises to what extent the obtained data can be applied to the natural aquifer. Therefore, a short assessment of critical experimental parameter is given.

The sandy sediment used should be conservative with regard to a humic colloid-borne actinide transport in the Gorleben aquifer, since sand have a high permeability and relatively low tendency to sorb humic substances (Fairhurst et al., 1995) at given groundwater pH. The properties of the equilibrated groundwaters, pH, redox potential, inorganic composition as well as the humic colloid concentration and size distribution, are comparable with natural conditions in the Gorleben aquifer. The hydraulic properties of the columns and the chosen groundwater flow velocities do not indicate significant deviations from natural conditions, since the lowest experimental Darcy velocity of 0.02 m/d is also found in the Gorleben aquifer (BGR, 1991). However, considerable uncertainties are involved in the formation of the humic colloid-borne Am in our experiments which cannot be extrapolated to natural conditions. Little known is which way (e.g. Am in form of Am^{3+} or as inorganic subcolloids) Am forms complexes with humic colloids under natural conditions and how strong the effect of a long natural reaction period on the stability of such complex is. The latter questions are key to the validation of the present experimental results, namely their applicability to natural conditions.

4. Summary and conclusions

The results from the batch and column experiments with Am(III) reveal that groundwaters rich in aquatic humic substances reduce its sorption onto sand and enhance the transport of

mobile humic colloid-borne Am in sandy sediments. The fraction of mobile humic colloid-borne Am is slightly faster than the groundwater flow velocity. The interaction of humic colloid-associated Am with sand is kinetically controlled, which makes the direct comparison of batch and column experiments difficult and indicates why differences can be found in the literature. In migration experiments of Am the kinetic effect for the association as well as for the dissociation of Am onto and from humic colloids is significant and indicates a reversible binding. Such kinetic effects strongly influence the migration behavior of humic colloid-borne Am and have to be taken into account in transport/speciation codes based on a thermodynamical database and for modeling of colloid-facilitated actinide migration. Although every effort is made to perform the column experiments close to natural conditions, the validation of the Am migration experiments appears to be difficult, since little is known about the Am-humic colloid binding processes in natural aquifer systems.

REFERENCES

- Appelo, C. A. J. and Postma, D., 1996. *Geochemistry, groundwater and pollution*. Balkema, Rotterdam.
- Artinger, R., Buckau, G., Geyer, S., Wolf, M., Fritz, P. and Kim, J. I., 1997. Characterization of aquatic humic substances isolated from groundwater: The influence of admixing from sedimentary organic carbon (SOC). Submitted to publication.
- BGR, 1991. *Übertägige geowissenschaftliche Erkundung des Standortes Gorleben*. Report 108880, Bundesanstalt für Geowissenschaften und Rohstoffe, Hannover.
- Buckau, G., 1991. *Komplexierung von Americium(III) mit Huminstoffen in natürlichen Grundwässern*. PhD Thesis. TU Munich, Munich. pp 167.

- Bürgisser, C. S., Cernik, M., Borkovec, M. and Sticher, H., 1993. Determination of nonlinear adsorption isotherms from column experiments: an alternative to batch studies. *Environ. Sci. Technol.*, 27: 943-948.
- Czerwinski, K. R., Rhee, D. S., Scherbaum, F., Buckau, G., Kim, J. I., Moulin, V., Tits, J., Laszak, I., Moulin, C., Decambox, P., De Ruty, O., Marquardt, C., Franz, C., Herrmann, G., Trautmann, N., Dierckx, A., Vancluysen, J., Maes, A., Bidoglio, G., Eliet, V. and Grenthe, I., 1996. Effects of humic substances on the migration of radionuclides: Complexation of actinides with humic substances. Report EUR 16843 EN, European Commission, Luxembourg/Brussels.
- Fairhurst, J., Warwick, P. and Richardson, S., 1995. The effect of pH on Europium-mineral interactions in the presence of humic acid. *Radiochimica Acta*, 69: 103-111.
- Kim, J. I., 1990. Geochemistry of actinides and fission products in natural aquifer systems. In: CEC project MIRAGE, third summary progress. Report EUR 12858 EN, European Commission, Luxembourg/Brussels.
- Kim, J. I., Delakowitz, B., Zeh, P., Klotz, D. and Lazik, D., 1994. A column experiment for the study of colloidal radionuclide migration in Gorleben aquifer systems. *Radiochim. Acta*, 66/67: 165-171.
- Kim, J. I., Zeh, P., Runde, W., Mauser, C., Pashalidis, I., Kornprobst, B. and Stöwer, C., 1995. Nuklidmigration (Tc-99, Np-237, Pu-238, Am-241) im Deckgebirge und Salzstock des geplanten Endlagerortes Gorleben. Report RCM 01495, Institut für Radiochemie, Technical University of Munich, Munich.
- Klotz, D. and Lazik, D., 1995. Transport von ^{152}Eu -Kolloiden in einem System Feinsand/huminstoffhaltiges Wasser. *Isotopes Environ. Health Stud.*, 31: 61-75.

- Labonne, N., Moulin, V. and Stammose, D., 1992. Actinide sorption onto silica in the presence of humic substances: proposal of retention mechanisms. *Mat. Res. Soc. Symp. Proc.*, 257.
- Ludwig, R. and Schneider, M., 1994. Hydrogeologische Grundlagen für Modellrechnungen - Projektgebiet Gorleben-Süd. Report 112002, Bundesanstalt für Geowissenschaften und Rohstoffe, Hannover.
- Maravic, H. v. and Moreno, J., 1993. Migration of radionuclides in the geosphere. Proceedings of a progress meeting (work period 1991). Report EUR 14690 EN, European Commission, Luxembourg/Brussels.
- Meier, H., Zimmerhackl, E., Zeitler, G. and Menge, P., 1994. Parameter studies of radionuclide sorption in site-specific sediment/groundwater systems. *Radiochim. Acta*, 66/67: 277-284.
- Moulin, V. and Stammose, D., 1989. Effect of humic substances on americium (III) retention onto silica. *Mat. Res. Symp. Proc.*, 127: 723-727.
- Rabung, T., 1997. Einfluß von Huminstoffen auf die Europium(III)-Sorption an Hämatit. PhD Thesis. Universität des Saarlandes, Saarbrücken. pp 203.
- Rao, L., Choppin, G. R. and Clark, S. B., 1994. A study of metal-humate interactions using cation exchange. *Radiochim. Acta*, 66/67: 141-147.
- Smith, P. A. and Degueldre, C., 1993. Colloid-facilitated transport of radionuclides through fractured media. *J. Contam. Hydrol.*, 13: 143-166.
- Ticknor, K. V., Vilks, P. and Vandergraaf, T. T., 1996. The effect of fulvic acid on the sorption of actinides and fission products on granite and selected minerals. *Appl. Geochem.*, 11: 555-565.
- Zeh, P., 1993. Chemische Reaktionen von Aktiniden mit Grundwasser-Kolloiden. PhD Thesis. TU Munich, Munich. pp 170.

1st Technical Progress Report

EC Project:

"Effects of Humic Substances on the Migration of Radionuclides:
Complexation and Transport of Actinides"

FZK/INE Contribution to Task 4(I) (Migration Model Development)

**Modeling of Humic Colloid Mediated Transport of Americium (III)
by a Kinetic Approach**

Reporting period 1997

W. Schüßler, R. Artinger, B. Kienzler, J.I. Kim

Forschungszentrum Karlsruhe, Institut für Nukleare Entsorgungstechnik,
P.O. Box 3640, D-76021 Karlsruhe, Germany.

Abstract

A kinetic approach is described to the modeling of humic colloid mediated transport of Am(III). For the modeling, experimental results are used from batch and column experiments under inert gas atmosphere (argon + 1% CO₂) on Gorleben groundwater/sediment systems with very different humic colloid concentrations (Artinger et al. 1998, and see FZK/INE contribution to task 1). Previous attempts to model the outcome of such experiments systems based on thermodynamic equilibrium have not been satisfactory. In this paper it is shown that the experimental results are successfully modeled by introduction of kinetic effects. One important feature of the "kinetically controlled availability model" (KCAM) is two different kinetically distinguished modes of humic colloid bound Am(III). Modeling results in a consistent description for both batch and column experiments on four different Gorleben sand/sediment systems.

Keywords: Americium; Colloid; Humic; Modeling; Transport

1. Introduction

The Gorleben site (Lower Saxony, Germany) is presently under investigation for disposal of HLW. In this aquifer system, dissolved organic carbon (DOC) concentrations as high as 200 mg/L are found (Buckau 1991). This DOC consists mainly of colloidal humic and fulvic acids, strongly binding multivalent actinide ions (Czerwinski et al. 1996). For assessment of the migration of radionuclides in this aquifer system, and consequently its potential impact on the long-term safety of HLW disposal, the high concentrations of humic colloids are of cardinal importance.

Laboratory investigations on humate mediated actinide transport has been conducted by both column and batch experiments (e.g. Zeh 1993, Randall et al. 1994, Klotz 1995). Major difficulty in interpretation of the results from batch experiments is the lack of identification of unambiguous equilibrium. For column experiments the major difficulty is that no retention is found for a varying fraction of the actinide ion and that no elution is observed for the residual amount. Attempts to model these results by means of thermodynamic equilibrium or sorption coefficients in combination with filtering of humic colloids have not been successful. For column experiments with Ca in a humic rich groundwater, a minor peak with no retention is observed and the major part of Ca is eluted with a retention factor (R_f) of approximately 8 (Klotz and Lang 1996). The experimental results from multivalent actinide ions and the divalent Ca ion can be brought to a common pattern, namely bimodal elution: (1) a humic colloid

bound fraction eluted with no retention and (2) the residual fraction eluted with a measurable delay (Ca) or with such a delay that it is not experimentally observed (multivalent actinide ions). The reason for the bimodal elution behavior, with the ratio between these two elution fractions varying with experimental conditions, can be allocated to kinetic effects.

2. Experimental

Below a short overview of experimental material and conditions is given. A detailed description can be found in (Artinger et al 1998 and FZK/INE contribution to task 1). Handling of experimental material/systems and performance of experiments is done under inert-gas conditions (Ar + 1 % CO₂).

Four Gorleben groundwaters with different humic colloid concentrations (between 1 and 80 mg/L DOC) and a near surface eolian Pleistocene quartz sand are used. Prior to experiments the sand/groundwater systems are conditioned for approximately 3 months. The DOC concentrations change with conditioning and subsequently are found to be between 6 and 103 mgC/L.

Aliquots of Am(III) stock solution (10^{-4} mol/L) are added to portions of the different groundwaters and left for 5 minutes to several weeks prior to use in batch and column experiments. Am concentration in spiked groundwaters is typically $2 \cdot 10^{-6}$ mol/L. Am is quantitatively (> 95 %) sorbed on humic colloids in spiked groundwater solutions, with exception for the groundwater with the lowest humic substance concentration (about 80 % Am sorbed on humic colloids).

Hydraulic properties of the columns were determined from breakthrough curves for tritium as an ideal tracer. In batch experiments, Am starting concentrations ranged from 10^{-10} to 10^{-7} mol/L and in column experiments Am concentrations in injected pulses were typically $2 \cdot 10^{-6}$ mol/L. The elution behavior of tritium and Am(III) was measured by flow-through monitoring and by liquid scintillation counting of sampled fractions.

3. Results and Discussion

3.1. Batch experiments

Fig. 1 shows the time dependency of the Am(III) sorption coefficient R_s for the four groundwater systems. Two important observations are made:

- (1) Strong influence of humic substance concentration (DOC). The sorption coefficient is about 1 to 2 orders of magnitude lower in the system with 103 mgC/L compared to the system with 6 mgC/L.
- (2) After 100 days equilibrium is still not obtained. The sorption coefficient R_s continuously increases with the reaction time with a difference of about two orders of magnitude between 5 minutes and 100 days.

The first observation underlines the importance of humic colloids for the sorption behavior of Am(III). From the second observation it becomes evident that kinetic effects need to be regarded for adequate description of the Am(III) sorption behavior.

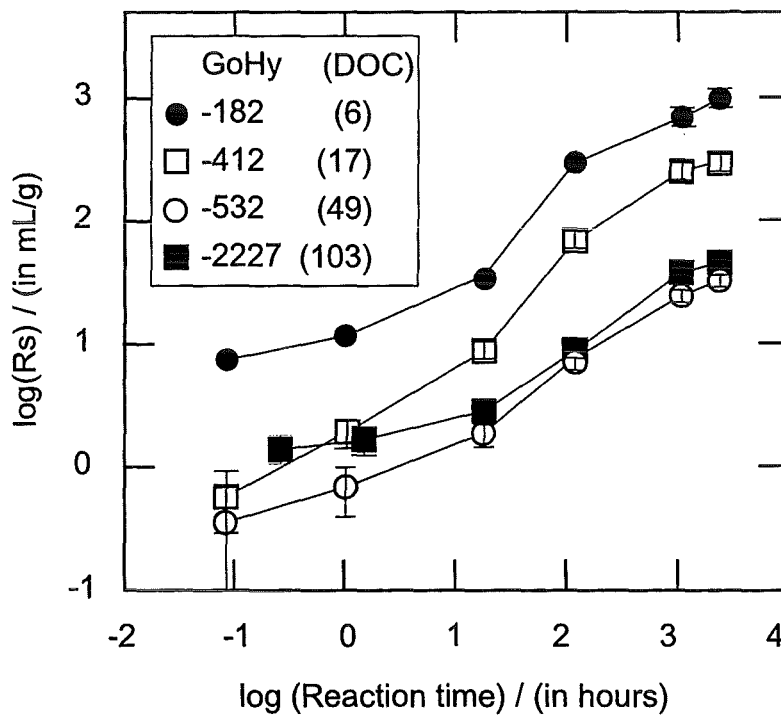


Fig 1: Batch experiments with Am(III) in Gorleben systems of different DOC concentrations: The influence of reaction time on the sorption coefficient R_s . The initial Am concentration is $5 \cdot 10^{-8}$ mol/L.

3.2. Column experiments

In Fig. 2, Am(III) breakthrough curves are shown for different groundwater flow-velocities. The lowest flow-velocity (0.06 m/d, i.e. a darcy velocity of ~ 8 m/a) is in the range of darcy velocities found at the Gorleben site (0.4 to 45 m/a (BfS 1990)). With increasing flow-velocity, recovery of Am(III) at breakthrough becomes higher. Fig. 3 shows the effect of equilibration

time (i.e. the contact time between spiking groundwater with Am(III) and the column peak injection) on the breakthrough of Am(III). The longer the equilibration time, the lower the recovery. These observation could be attributed to:

- (1) Filtering of Am-bearing colloids.
- (2) Sorption/exchange of Am-bearing colloids with sediment bound humic matter.
- (3) Dissociation of colloid bound Am followed by sorption onto the sediment.

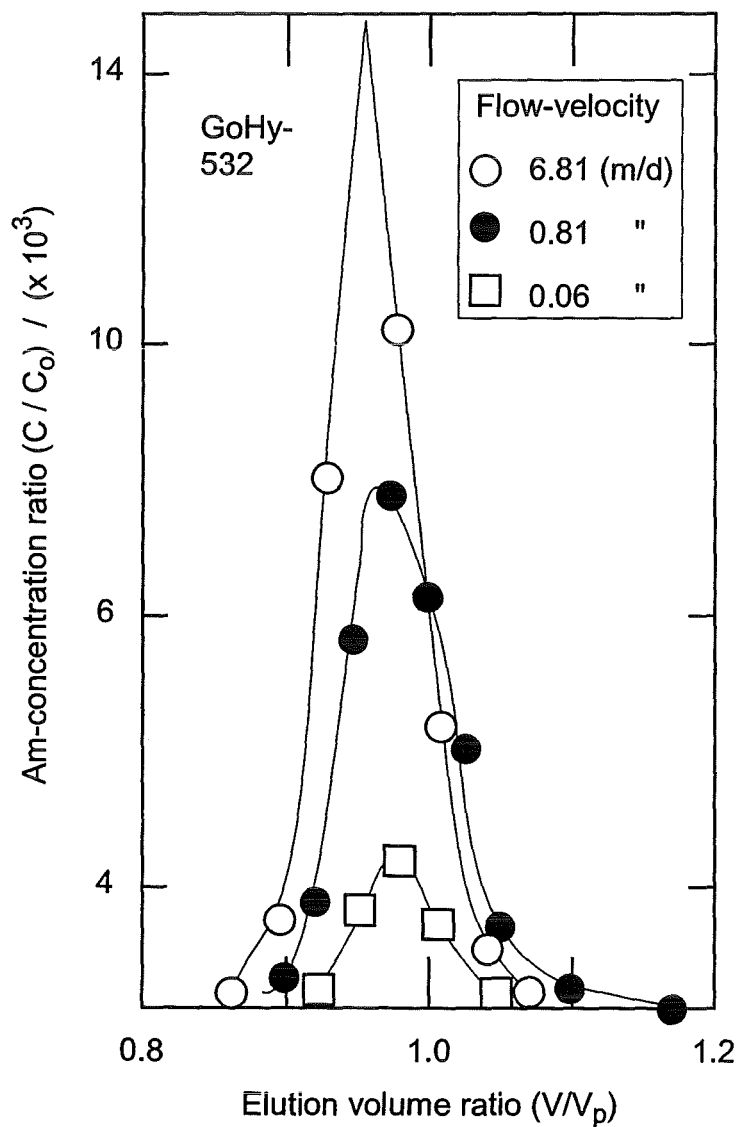


Fig. 2: Column experiments with Am(III) in the GoHy-532 system: The influence of groundwater flow velocity on Am(III) breakthrough.

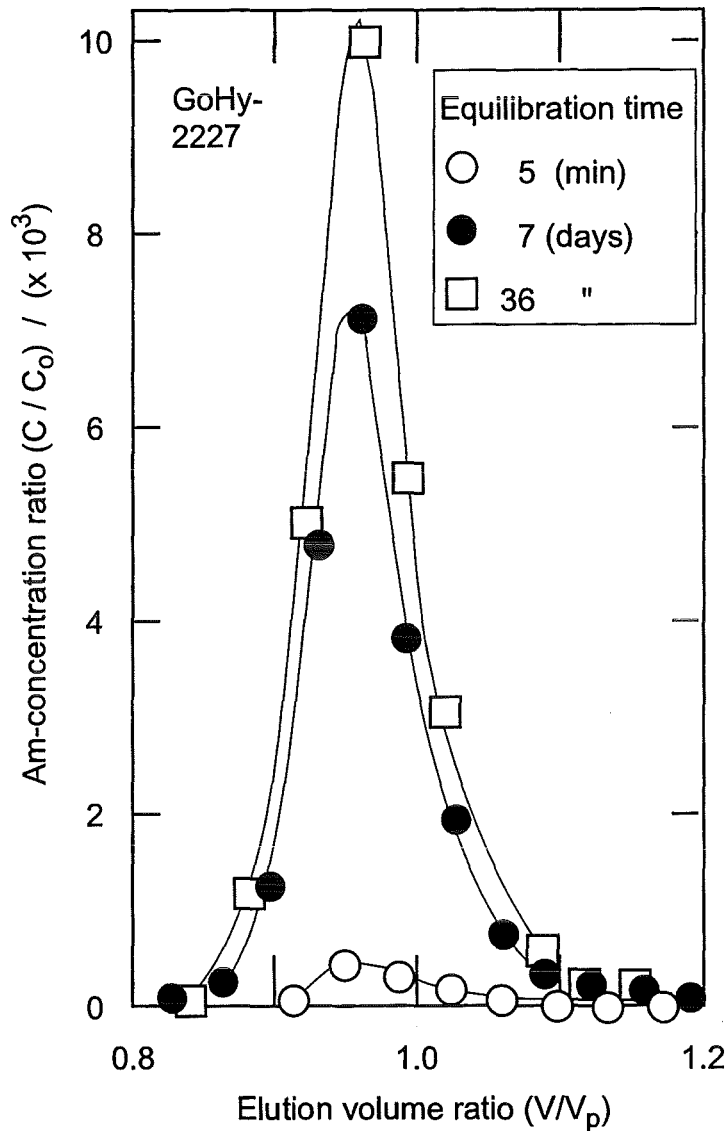


Fig. 3: Column experiments with Am(III) in the GoHy 2227 system: The influence on Am(III) breakthrough of equilibration time between Am(III) and groundwater prior to pulse injection.

Taking into account additional ultrafiltration experiments, showing no variation in the size distribution of Am-bearing colloids, filtering of colloids appears to be of low importance. Sandy sediments show relatively low tendency to sorb humic substances in this pH range (Fairhurst 1995), and thus sorption/exchange of Am-colloids as the responsible mechanism appears unlikely. Kinetically controlled dissociation of Am(III) from humic colloids followed by sorption on sediment, however, is in agreement with all above experimental observations. Consequently, this approach is tested for its applicability.

4. Modeling

The key step in the model described below is the kinetically controlled dissociation of Am(III) from humic colloids into groundwater solution, governing its availability for sorption on the sediment. For this reason the model is called: Kinetically Controlled Availability Model (KCAM).

4.1 Model description

Fig. 4 shows features of and processes regarded in the KCAM model. The following Am(III) species are taken into consideration: the free Am^{3+} ion (Am^{3+}); Am sorbed onto the sediment (Am_{sed}); and humic colloid bound Am. The humic colloid bound Am is divided into two different binding modes: "fast" (Am_f) and "slow" (Am_s), related to association/dissociation kinetics. For the slow binding mode, Am dissociation occurs via transformation to the fast mode. Thus, the concept regards six single reactions with corresponding rate constants (k_i , see Fig. 4). The corresponding single reaction rates (j_i) are assumed to be of first order with respect to concentrations of reacting Am-species (Am_x):

$$j_i = -k_i [\text{Am}_x]$$

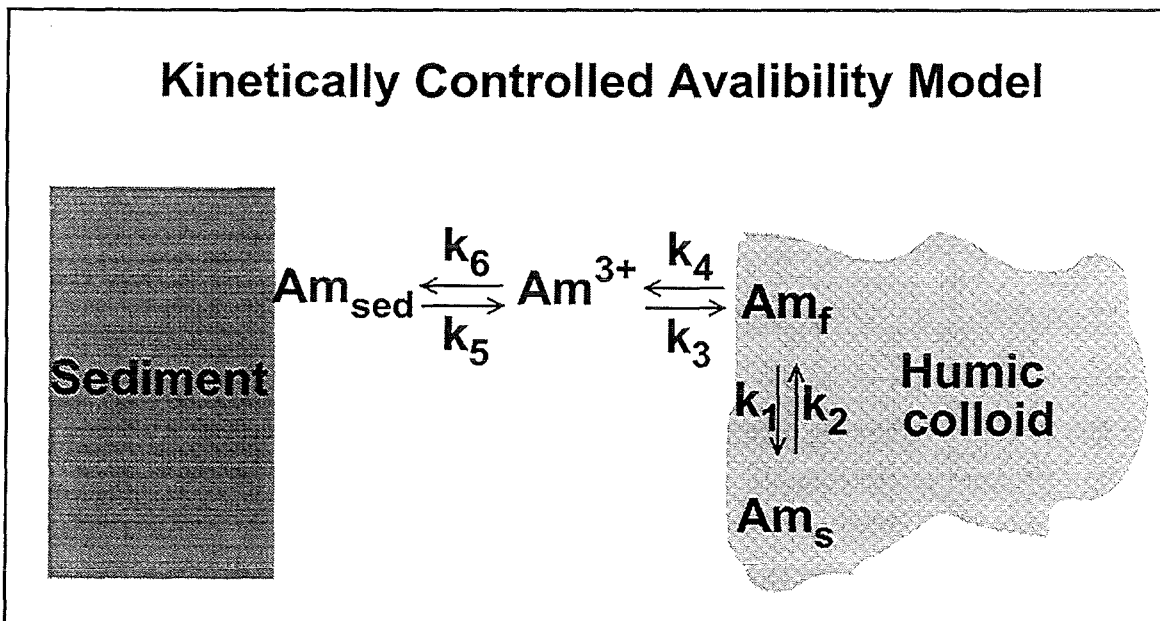


Fig. 4: Concept of the Kinetically Controlled Availability Model (KCAM) (for details see text).

4.2 Model parameters

The rate constants k_1 , k_2 , k_4 and k_5 are fitted to a set of batch and column experiments of the GoHy-2227 system. Batch experiments included reflect different reaction times (shown in Fig. 1). Column experiments included reflect different equilibration times of Am(III) with groundwater prior to column pulse injection (shown in Fig. 3). The two rate constants k_3 and k_6 are calculated from equilibrium distribution data, i.e. k_3 from Am(III)-humate complexation data and k_6 from batch R_s values. They are found to be so high compared to the other four rate constants that they can be neglected. From the two types of experiments one common set of rate constants is derived. This means that batch and column experiments are brought together to one consistent description. The following set of rate constants is obtained:

k_1	k_2	k_4	k_5
$5.9 \times 10^{-7} \text{ sec}^{-1}$	$1.1 \times 10^{-6} \text{ sec}^{-1}$	$9.3 \times 10^{-5} \text{ sec}^{-1}$	$1.1 \times 10^{-5} \text{ sec}^{-1}$

and for comparison the time constants $\tau_i (= 1/k_i)$

τ_1	τ_2	τ_4	τ_5
470 h	250 h	3 h	25 h

For below model testing this set of preliminary rate constants is used.

4.3 Modeling testing

In Table 1, experimental and calculated values are shown for the Am(III) recovery from column experiments under various conditions on groundwater systems with different DOC concentrations. The good agreement for the results on the GoHy-2227 system merely reflects the use of this system for establishing the parameter set used. To account for different humic colloid concentrations in the other three systems, a linear scaling factor of DOC is introduced. The agreement between experimental and calculated data for these other three systems are in remarkably good agreement.

Table 1: Comparison of experimental data and prediction from KCAM modeling for the recovery of Am(III) in column experiments.

Variables:	Groundwater systems:								
	GoHy-2227			GoHy-532			GoHy-412		GoHy-182
	Eq. time* (cf. Fig. 3)			Flow-velocity (cf. Fig. 2)			Eq. time* (26 and 41 d)		
	Recovery (%)								
Experimental	1.9	22.6	35.4	6.5	34.0	19.6	2.3	1.6	0.1
Predicted	1.5	18.4	28.9	6.8	31.1	10.3	4.5	4.6	1.1

*: equilibration time of Am(III) with groundwater prior to column pulse injection

Summary and Conclusions

The presented model (Kinetically Controlled Availability Model) is developed to adequately describe actinide sorption and transport in laboratory batch and column experiments. It is an empirical approach based on the kinetics of important reactions. Model parameters are determined by fitting to experimental data. Differences in humic acid concentration are accounted for by a linear scaling factor of DOC. The result is an adequate and consistent description of both column and batch experiments under various conditions and verifies the predominant impact of humic colloids on the chemical behavior of actinide ions in groundwater. The approach appears to be a major achievement compared to previous attempts applying equilibrium approaches in combination with filtering of colloids.

It should be noted that the present model development is based on experimental data from static and dynamic laboratory systems with an experimental time scale from about minutes up to some thousands of hours. The model appears to adequately describe processes that can be observed within such time-scales. Other much slower processes that may be relevant for the real system, however, cannot be observed and quantified for inclusion into the model. Therefore, application for predictions in the real system requires critical validation.

References

- BfS (1990) "Fortschreibung des zusammenfassenden Zwischenberichts über bisherige Ergebnisse der Standortuntersuchung Gorleben vom Mai 1983", Report: BfS ET-2/90, Bundesamt für Strahlenschutz (BfS), Salzgitter.
- Artinger R.; Kienzler B.; Schüßler W.; Kim J.I. (1998) "Effects of humic substances on the ^{241}Am migration in a sandy aquifer: Column experiments with Gorleben groundwater/sediment systems", submitted to J. Contam. Hydrol.
- Buckau G. (1991) "Komplexierung von Americium(III) mit Huminstoffen in natürlichen Grundwässern", PhD Thesis, FU Berlin, Berlin, 167 pp.
- Czerwinski K.R. et al. (1996) "Effects of humic substances on the migration of radionuclides: Complexation of actinides with humic substances", Report: EUR 16843 EN, European Commission, Luxembourg/Brussels
- Fairhurst J; Warwick P.; Richardson S. (1995) "The Effect of pH on Eurium-Mineral Interactions in the Presece of Humic Acid", Radiochim. Acta, **69**, 103-111.
- Klotz, D. (1995) "Transport von ^{152}Eu -Kolloiden in einem System Feinsand/huminstoffhaltiges Wasser", Report: GSF 20/94, Institute of Hydrology, GSF-National Research Center for Environment and Health, Neuherberg.
- Klotz D.; Lang H. (1996) "Experimentelle Untersuchungen zur Radionuklidmigration im Deckgebirge des geplanten Endlagers Gorleben, Untersuchungsprogramm V.", Report: GSF 22/95, Institute of Hydrology, GSF-National Research Center for Environment and Health, Neuherberg.
- Randall A.; Warwick P.; Lassen P.; Carlsen L.; Grindrod P. (1994) "Transport of Europium and Iodine through Sand Columns in the Presence of Humic Acids", Radiochim. Acta, **66/67**, 363-368.
- Zeh P. (1993) "Chemische Reaktionen von Aktiniden mit Grundwasser-Kolloiden". PhD Thesis, TU Munich, Munich, 170 pp.

1st Technical Progress Report

EC Project:

"Effects of Humic Substances on the Migration of Radionuclides:
Complexation and Transport of Actinides"

BGS Contribution to Task 1 (Characterization)

Extraction, Purification and Characterization of Fulvic Acid

Reporting period 1997

JJW Higgo, JR Davies, B Smith and C Milne

British Geological Survey
GB-Nottingham NG 12 5GG
United Kingdom.

EXTRACTION, PURIFICATION AND CHARACTERISATION OF FULVIC ACID

JJW Higgs, JR Davis, B. Smith, and C. Milne

British Geological Survey,

Abstract

The aim of this project was to extract and purify gram quantities of fulvic acid for distribution to the group members. Ideally the material should have come from groundwater in the Sellafield repository area but the total organic carbon content of water samples taken from boreholes in the area was found to be between 0.03 and 0.05 ppm. In order to extract sufficient fulvic for distribution to group members it would, therefore, be necessary to process more than 100 000 litres of groundwater. This was considered impractical and instead fulvic acid was extracted from four thousand litres of water taken from the Derwent Reservoir (Derbyshire, UK) using DEAE-cellulose. Several stages of purification included anion exchange on Amberlite XAD-8 resin and cation exchange on Amberlite AG50W-X8. The final purified fulvic acid concentrate, volume 1300 ml, contained 4.1 g/l TOC (total fulvic acid \approx 11 g). It was characterised in terms of elemental analysis, molecular weight, proton-binding properties, UV absorbance. Uranium binding measurements were also made for comparison with previous work.

1. INTRODUCTION

Naturally occurring organic matter in groundwater is a complex mixture of humic substances, hydrophilic acids, carbohydrates, carboxylic acids, amino acids, hydrocarbons and other simple compounds. The majority of all groundwaters have concentrations of dissolved organic carbon (DOC) below 2 mg/l except under exceptional conditions e.g. groundwaters associated with coal deposits or in oil-shale regions (Thurman, 1985). Leenheer *et al* (1974) surveyed a range of aquifers and reported median DOC concentrations of 0.7 mg/l for sandstone, limestone and sand gravel aquifers and 0.5 mg/l for crystalline rock. Vilks and Bachinski (1996) in a survey of DOC concentrations in groundwaters from granitic fractures in the Canadian Shield found concentrations averaging 0.8 ± 0.1 mg/l in horizontal fractures in the upper 500 m and 2.3 ± 0.8 mg/l for deeper saline waters. The dissolved organic carbon consisted mainly of hydrophilic neutral compounds and hydrophobic acids (including fulvic acid and humic acid) and hydrophilic acids. Of these the most important from the point of view of actinide complexation are probably the humic and fulvic acids. Groundwaters being studied in the current CEC programme include Fanny-Augères water which is taken from a depth of 280 m in a gallery of a granitic uranium mine and contains 2 mg/l TOC (Moulin *et al*, 1991), groundwaters from the Königstein uranium mine which contains between 0.5 and 0.7 mg/l DOC (Schmeide *et al.*, this volume) and groundwaters from the Gorleben repository area. The DOC content of the latter ranges from 0.1 mg/l to nearly 100 mg/l (Kim *et al.*, 1987)

Humic material in groundwater is typically more aliphatic in character and lower in molecular

weight than humic substances extracted from soils and, in deep groundwaters, is likely to be dominated by fulvic acids (as larger humic molecules are filtered out, degraded or sorbed).

Initially it was proposed to extract humic material from deep ground waters from the proposed repository area at Sellafield and samples were taken from a number of boreholes in the area. The DOC concentrations ranged between 0.03 and 0.05 mg/l which meant that in order to extract sufficient fulvic for distribution to group members it would be necessary to process more than 100 000 litres of groundwater. This was considered impractical and it was decided to extract the humic material from Derwent Reservoir¹ in Derbyshire. Four thousand litres of this water were processed and a total of 8.3 grams of purified fulvic acid were obtained. Only fulvic acid was purified for use in future work because this is likely to be the main organic complexing agent in deep groundwaters and humic material from other sources is already being studied by group members.

After purification the fulvic acid was characterised in terms of elemental analysis, molecular weight, proton-binding properties and UV absorbance. Uranium binding measurements were made for comparison with previous work. In order to make characterisation as complete as possible our partners in this project provided expertise and equipment where this was lacking at the BGS. This material is now available for use by all group members for fundamental and inter-comparison work.

¹Howden, Derwent and Ladybower reservoirs form a network of interlinking water supply reservoirs in the High Peak area of the Derbyshire Peak District. They are located 13 km west of Sheffield, the approximate locations of their centres being; Howden Reservoir - 1(45'W, 53(26'N (NGR: 417 393), Derwent Reservoir - 1(45'W, 53(25'N (NGR: 417 391), Ladybower Reservoir - 1(43'W, 53(23'N (NGR: 419 387). The reservoirs were formed by damming the River Derwent in three places, thereby flooding the Upper Derwent Valley along 9km of it's length. The damming also flooded the lower portions of the valleys of two tributaries of the River Derwent. Howden reservoir extends 1.5 km upstream from the Derwent into the River Westend valley and Ladybower reservoir extends 4 km upstream from the Derwent into the River Ashop valley. Howden reservoir has an area of about 1km² and a catchment of approximately 38 km². The outflow from Howden drains southwards, directly into Derwent reservoir which has an area of approximately 0.75 km². In addition to the supply from Howden a catchment area of approximately 12.5 km² also flows into Derwent Reservoir. Derwent again drains southwards into Ladybower reservoir which has an additional catchment of approximately 70.5 km², the area of Ladybower reservoir is approximately 2.5 km². The reservoir network drains southwards via the river Derwent and has a combined catchment area of approximately 121 km². The rocks of the upland catchment area are exclusively of the Millstone Grit Series, these are mostly coarse, thickly-bedded sandstones with interbedded shale and mudstone beds.

2. ISOLATION AND PURIFICATION

Humic and fulvic acids are usually extracted from water using either DEAE-cellulose or Amberlite XAD-8 resin. DEAE-cellulose is a weak anion-exchange resin, which has the advantage of being able to remove humic substances from water by anion exchange without the need for sample acidification. XAD-8 is a cross-linked polymeric methacrylate ester that can remove humic substances from groundwater acidified to pH \approx 2 by hydrophobic interactions. Because of the large volumes involved, DEAE-cellulose was used for the initial extraction from the groundwater with XAD-8 being used in a second purification stage.

2.1 Extraction from the water

3.31 kg of Whatman Express-Ion D (supplied pre-swollen and 'defined') was dispersed in tap water. This was packed into a 20 cm diameter Pharmacia Biotech BPG™ 200 column. After settling the bed height was 16.8 cm. The column was installed in-line into the water treatment system via 3/4" Philmac style fittings. This water was extracted directly from the Derwent reservoir after filtration through a drum screen. The experimental set up is illustrated in Figures 2.1 and 2.2. Figure 2.3 is a flow diagram showing all the extraction and purification steps. Include Figure 2.3 are figures showing the TOC recoveries at each stage.

The system was pumped constantly for a total of 41.17 hours and a total of 4044 litres (763 column volumes) were passed through the column at a mean flow-rate of 1.64 l/min. A full analysis of the inlet water and of the final eluate was made. In addition, the pH, conductivity and TOC of the inlet and outlet water were monitored during the extraction. Tables 2.1 and 2.2 give the analytical data.

The TOC content of the eluate was below detection limit throughout the extraction and pumping was stopped as soon as breakthrough occurred (at about 4000 l). pH and conductivity changes during the extraction were small.

The only metals that showed a significant decrease in concentration after passage through the column were aluminium and iron (Table 2.2). This was to be expected since they both form strong complexes with humic and fulvic acids.

Table 2.1 Monitoring of inlet and outlet water during passage through DEAE-cellulose column

	Inlet	Outlet 1 to 2000 l	Outlet 2000 to 4000 l	Final eluate 4040 to 4044 l
pH	5.8-7.6	7.5-9.4	6.6-7.4	6.6
Conductivity, μSv/cm	72-102	76-173	42-92	92
TOC mg/l	4.2-5.2	<1.0	<1.0	1.2

Table 2.2 Composition of water before and after passage through DEAE-cellulose column.
All concentrations in mg/l

	Inlet	Outlet after 4000 l		Inlet	Outlet after 4000 l
Ca	5.29	5.20	Si	2.64	2.46
Mg	3.30	3.00	Mn	0.007	0.008
Na	5.91	5.71	Fe	0.08	0.03
K	0.9	<0.5	Al	0.1	0.04
Cl	8.92	8.75	Ni	<0.1	<0.1
SO4	13.4	13.1	Cu	<0.01	<0.01
NO3	3.25	3.29	Zn	0.02	0.02
NO2	<0.02	<0.02	Cr	<0.01	<0.01
TOC	4.77	1.19	Cd	<0.01	<0.01
TIC	1.39	1.01	Pb	<0.1	<0.1
Sr	0.02	0.02	B	<0.05	<0.05
Ba	0.02	0.02			

Philmac System integrated
in-line to reservoir systems

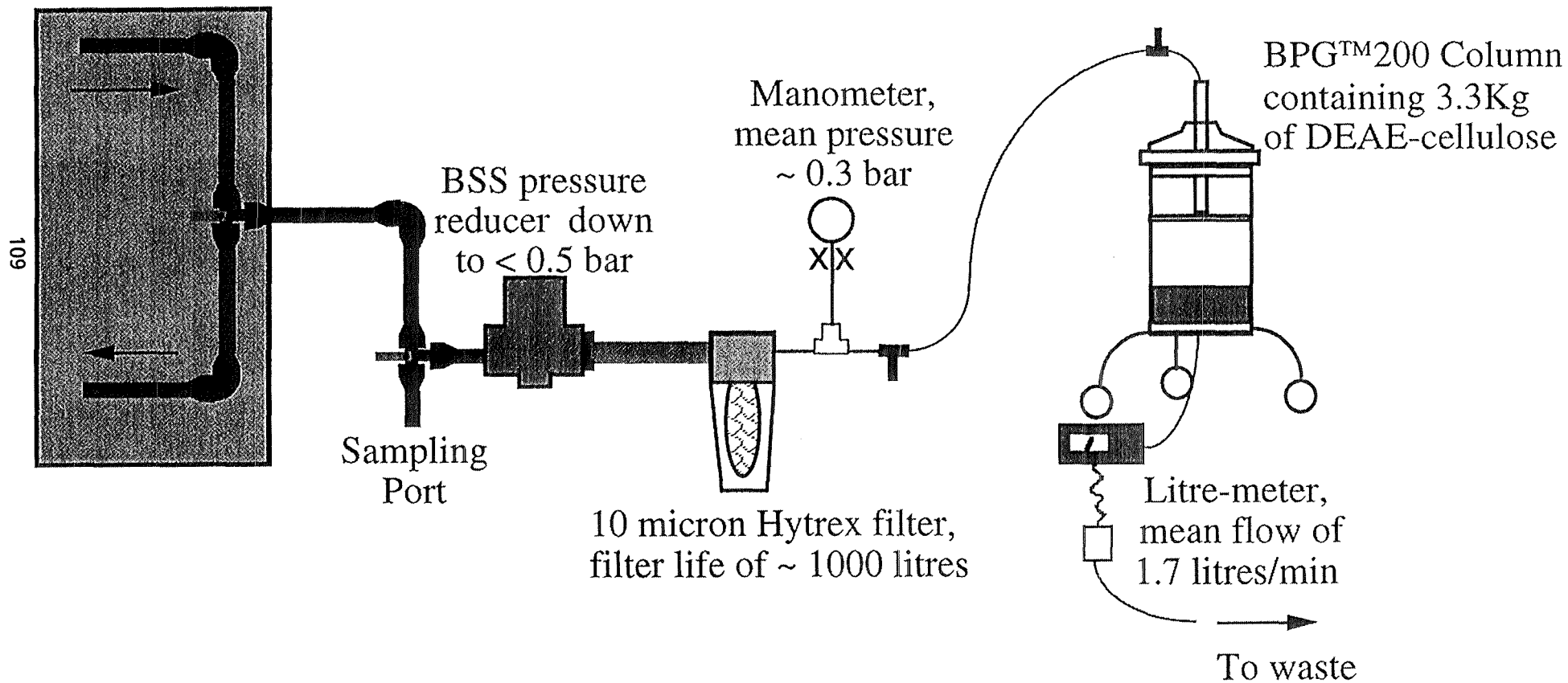


Figure 2.1 Field Extraction Apparatus

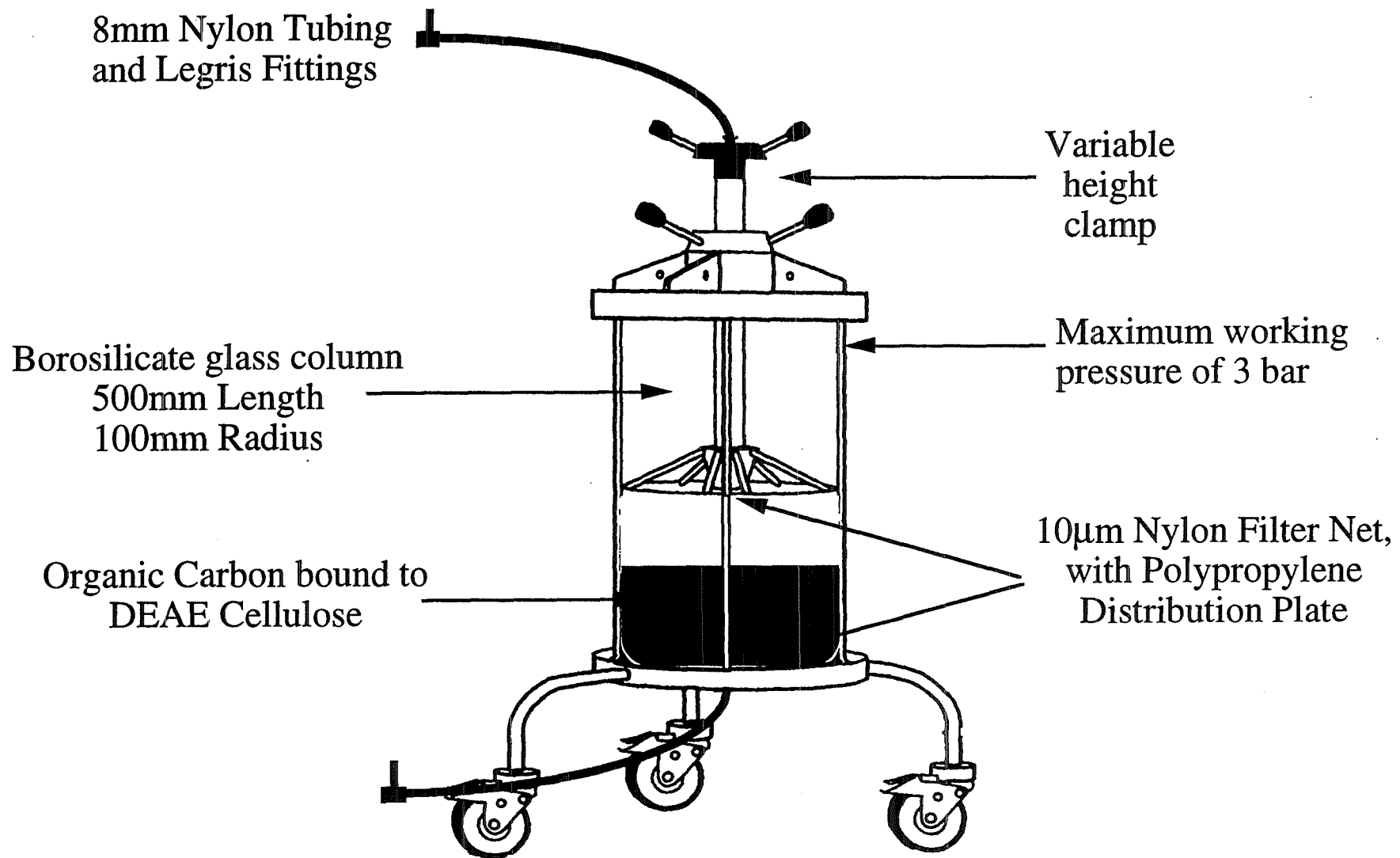
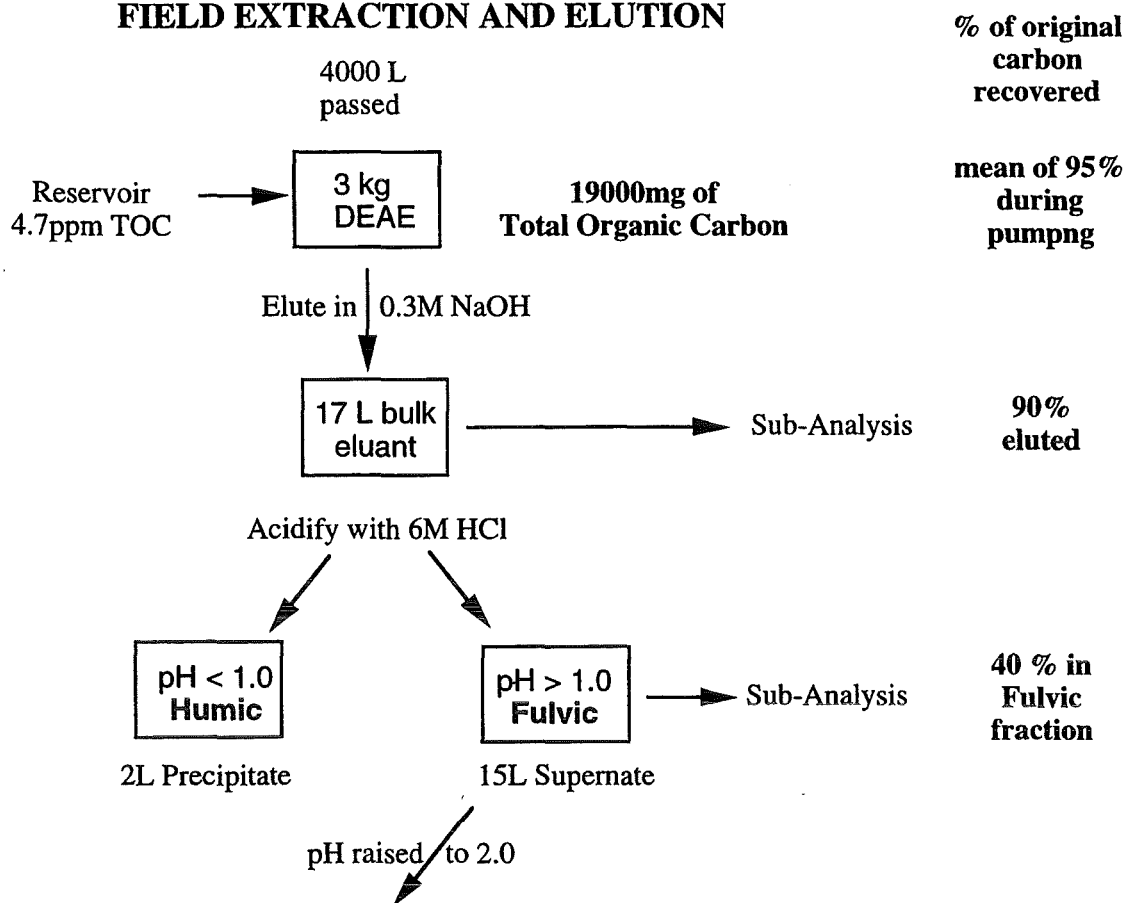


Figure 2.2 BPG™ 200 Column containing DEAE Cellulose

FIELD EXTRACTION AND ELUTION



LABORATORY PURIFICATION

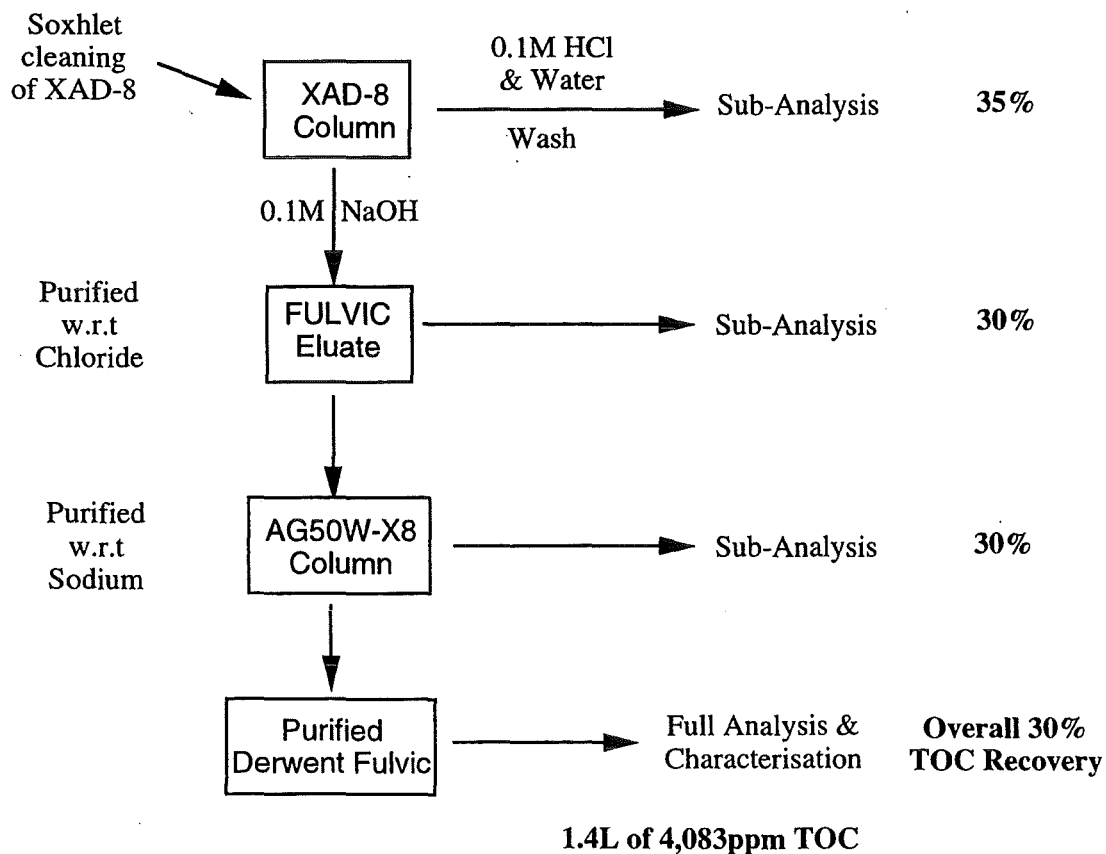


Figure 2.3 Flow chart to summarise purification procedure

2.2 Elution from DEAE-cellulose column

The humic material was eluted from the column with 0.3M NaOH (prepared with deoxygenated water) at a flow rate of 180 ml/min. The effluent was collected in 800 ml fractions of dark brown liquid and a final 4.7 l of straw coloured effluent. Immediately after elution the pH of each fraction was lowered to ≤ 6 with oxygen-free 6M HCl. The most concentrated fractions were bulked into a 25 l container and the pH lowered to about one in order to precipitate out the humic acid. The solutions were allowed to settle overnight in the dark at 4° C. They were then centrifuged in 250 ml portions at 4° C. This produced 15 l of fulvic acid solution and 2 l of humic slurry. All samples were stored in the dark at 4° C.

2.3 Purification of the fulvic solution

The pH of the fulvic solution was lowered to 2.0 and it was then passed through a 30 x 2.5 cm column of XAD-8 resin². The column was then washed with three column volumes of 0.1M HCl followed by water. When the coloured band began to move the fulvic acid was eluted, in the reverse direction to loading, with 0.1M NaOH. About 1500 ml of a dark fulvic-acid solution was collected.

This solution was now passed through a 1.25 x 30 cm column of AG50W-X8 (100-200#) resin (hydrogen form) at 2.1 ml/min in order to remove sodium and other cations in solution. 1380 ml of fully purified Derwent Fulvic solution was obtained.

3. CHARACTERISATION OF HUMIC MATERIALS

After purification the fulvic acid was analysed for CH& N content and impurities. It was also characterised in terms of molecular weight, proton-binding properties and UV-spectra.

3.1 Elemental Analysis

Carbon hydrogen and oxygen were determined on freeze dried material using a Perkin Elmer Elemental Analyzer model 2400 CHN. The analysis is based on high temperature decomposition of the fulvic acid which converts the elements of interest to gaseous molecules.

² The resin had been cleaned extensively by first washing in 0.1 M NaOH and then extracting in a 2 litre Soxhlet extractor with acetone followed by acetonitrile and finally methanol. It was then washed with high purity water until it was free of methanol (Thurman, 1981, Vilkes, 1996)

The gases are separated by selective sorption and detected by thermal conductivity. Total sulphur was determined on the aqueous solution by inductively coupled optical emission spectrometry (ICP-OES) and sulphate by ion chromatography (DIONEX™). The sulphur content of the fulvic acid was assumed to be the difference between the total sulphur and the sulphur in the sulphate in solution. The results are given in Table 3.1

Table 3.1: Elemental Analysis of purified fulvic acid

	Wt % on freeze-dried material		Wt % on freeze-dried material
Carbon	49.06	Nitrogen	0.6
Hydrogen	4.18	Sulphur	0.32

3.2 Trace Impurities

The solution containing the purified material was analysed for cations by inductively-coupled plasma techniques (optical emission spectrometry ICP-OES) and mass spectrometry (ICP-MS) and for anions by ion chromatography (DIONEX™). Table 3.2 shows the composition of the purified materials. Iron and aluminium were the most difficult metals to remove and traces of lanthanides and uranium remained in all samples. However, the purity of these materials compared favourably with literature values and it appears to be difficult to achieve greater purity without risking structural damage to the humic materials. The total number of sites occupied by these impurities is less than 2% of the total proton capacity. Since these impurities probably occupy the strongest binding sites it is possible that experiments with trace metals give slightly low values for binding constants.

Table 3.2 Impurities in Derwent Reservoir fulvic acid

	Conc in Soln. mg/l (ppm)	Conc. in FA mg/Kg (ppm)		Conc in Soln. µg/l (ppb)	Conc. in FA mg/Kg (ppm)
Na	0.3	36.1	Rb	<1	<0.12
K	<0.1	<12	Sr	<1	<0.12
Ca	<0.1	<12	Y	0.33	0.04
Mg	<0.2	<24	Ba	<2	<0.2
Al	0.51	61.3	La	0.19	0.02
Si	0.15	18.0	Ce	0.5	0.06
Fe	1.54	168	Pr	0.14	0.02
Cr	0.24	28.8	Nd	0.62	0.07
Mo	0.08	9.6	Sm	0.2	0.02
Co	<0.02	<2.4	Eu	<0.1	<0.12
Ni	<0.1	<12	Tb	<0.1	<0.12
Mn	<0.001	<0.12	Gd	0.21	0.03
B	0.07	8.4	Dy	0.17	0.02
S	30.3	3190*	Ho	<0.1	<0.12
Cl	46.3		Er	<0.1	<0.12
SO₄	11.4		Tm	<0.1	<0.12
NO₃	<5		Yb	<0.1	<0.12
NO₂	<2		Lu	<0.1	<0.12
			Th	1.4	0.17
			U	0.4	0.05

* Corrected for S in SO₄

3.3 Molecular Weights

The weight average molecular weight of the fulvic sample was determined by two different laboratories using two different methods. Manchester University used analytical U.V. scanning ultracentrifugation and Forschungszentrum Karlsruhe used flow-field flow fractionation (Flow-FFF). A description of the two methods and the results obtained follows.

3.3.1 U.V. Scanning Ultracentrifugation (Dr N. Bryan (Manchester University))

U.V. scanning ultracentrifugation makes use of the fact that large molecules in solution will tend to sediment in the high centrifugal field of an ultracentrifuge. The samples are spun in cells with quartz windows, which allow the behaviour of the humic sample to be monitored *via* their strong absorption of ultraviolet light.

The two centrifugation methods commonly used for the determination of the molecular weights of humic substances are the Archibald and equilibrium methods. In the case of higher molecular weight samples, the equilibrium method suffers from inaccuracies, which derive from the fact that heavy molecules can fall to the bottom of the centrifuge column and hence are 'lost' from the analysis. However, the Archibald method is far more prone to errors. Since the sample analysed here is a fulvic acid, and would hence be expected to have a relatively low molecular weight, the equilibrium method was selected. However, for each analysis, the amount of the sample which remained in the column was carefully monitored to ensure that the determined molecular weight would be representative of the whole sample.

Theory

The weight average molecular weight of the sample is determined by examining the gradient and concentration profile of the humic sample in the column at equilibrium. The average molecular weight of material at any point in the column can be determined from,

$$\bar{M}_w(r) = \frac{2RT}{(1-\bar{v}_2\rho)\omega^2} \cdot \frac{(d \ln c)}{d(r^2)}$$

where ω is the rotational velocity, ρ is the density of the sample solution, \bar{v}_2 is the partial specific volume, c is the concentration of the sample, r is the radial velocity, T is the absolute temperature, and R is the universal gas constant. By integrating over all of the material in a scan, the average molecular weight of the material in the column can be determined.

Experimental

Measurements were made with a Beckman X.L.A. UV-scanning ultracentrifuge and a 4-hole titanium rotor. The machine has a built in UV-scanning unit, which can make measurements in an optical density range of 0 to 2 across the entire ultraviolet and visible region of the spectrum. On this occasion, all absorbances were recorded at 280 nm. The sample was diluted in PBS buffer (density 1.019 g/cm³) to give an optical density of approximately 0.45. The main purpose of the P.B.S. buffer is to increase the concentration of dissolved solids in the sample

solution. This reduces the possibility of convective mixing during the experiment, which prevents the sample attaining equilibrium in the centrifuge column. Measurements were made using short-column multiple sample cells, with a total column length of approximately 3 mm per sample. The samples were spun for a period of several hours at a pre-equilibration speed of 3 000 rpm, before being accelerated to an equilibrium speed of 20 000 rpm. An initial scan was taken to determine the amount of the sample present in the column at the start of the experiment. The samples were left until the columns achieved a state of equilibrium, which took one to two days. The columns were scanned regularly, and successive scans compared to ascertain when equilibrium had been achieved. All scans were recorded as lists of O.D. versus radial distance directly onto the hard disk of an IBM-PC, which also controlled the centrifuge during the experiments. The scans were analysed and the weight-average molecular weights calculated using an in-house fortran program.

Results

Five separate measurements were made on the sample. The values obtained are given in Table 3.3.

Table 3.3 Measured Molecular weights

Run number	Determined weight-average molecular weight	Percentage of sample remaining in the scan
1	3954	97.9
2	4086	98.5
3	3993	98.4
4	3858	97.5
5	3884	93.4

Taking these values, the mean average molecular weight of sample is:

$$3955 (\sigma = 90)$$

In all of the scans, the vast majority of the sample material remained in the column. Therefore, this value is representative of the whole of the sample.

In comment on the results, the average molecular weight of the sample is higher than might usually be expected for a fulvic acid sample, although it is much lighter than one would expect for a humic acid sample. The sample also showed significant polydispersity, with significant

amounts of material over the mass range 2000 - 5000.

3.3.2 Flow-Field Flow Fractionation (Flow-FFF) (Ngo Manh Thang and H. Geckeis, Forschungszentrum Karlsruhe, Institut für Nukleare Entsorgungstechnik)

Method

The Flow-FFF method was developed by Giddings (1988) and Beckett *et al.* (1987, 1988). Colloids are introduced into a flow of eluent passing a flat open channel of small thickness. The separation of colloids with respect to their hydrodynamic radius is achieved by application of a force field rectangular to the sample flow. In case of Flow-FFF this force field is realized by a fluid cross-flow, driving sample constituents towards a membrane. During a relaxation period, where the channel flow is stopped, particles form a cloud at a certain position in the channel corresponding to an equilibrium between cross flow and back diffusion forces. Separation is achieved by switching on the channel flow, which transports the sample components towards the detector cell (UV/VIS detector), while cross flow is still active.

Experimental Conditions

Channel void volume (V_0): 1.21 ml (determined by injection of NaN_3)

Channel thickness (w): 0.0218 cm (given by the purchaser)

Dead volume : 0.1 ml

Eluent: 0.01M NaClO_4 + 0.01% Tween (non-ionic surfactant) + 0.02% NaN_3 , pH 7

Channel flow: 1 ml/min

Cross flow (V_c): 5 ml/min, Equilibration period 0.48 min.

Sample volume: 20 μl

Calibration

The system was calibrated with standardised poly(styrene sulphonate) sodium salt (PSS). (Table 3.4 and Figure 3.1)

Table 3.4 FFF Calibration using poly(styrene sulphonate)

PSS Standard, M_p /Dalton	Retention volume (peak max V_r)/ml
3 800	2.74
6 710	2.84
8 000	3.64
16 900	4.32
31 500	6.11
46 400	7.38

Diffusion coefficients are calculated using the relationship

$$D = \frac{V_c w^2}{6V_r - 2V_0}$$

Where V_c = cross flow (ml/min),

w = channel thickness,

V_0 : Void volume: 1.21 ml

Linear correlation yields the equation for the calculation of M:

$$\log D = A + B \cdot \log M$$

with

$$A = -2.1123 \quad 0.1859$$

$$B = -0.4533 \quad 0.0449$$

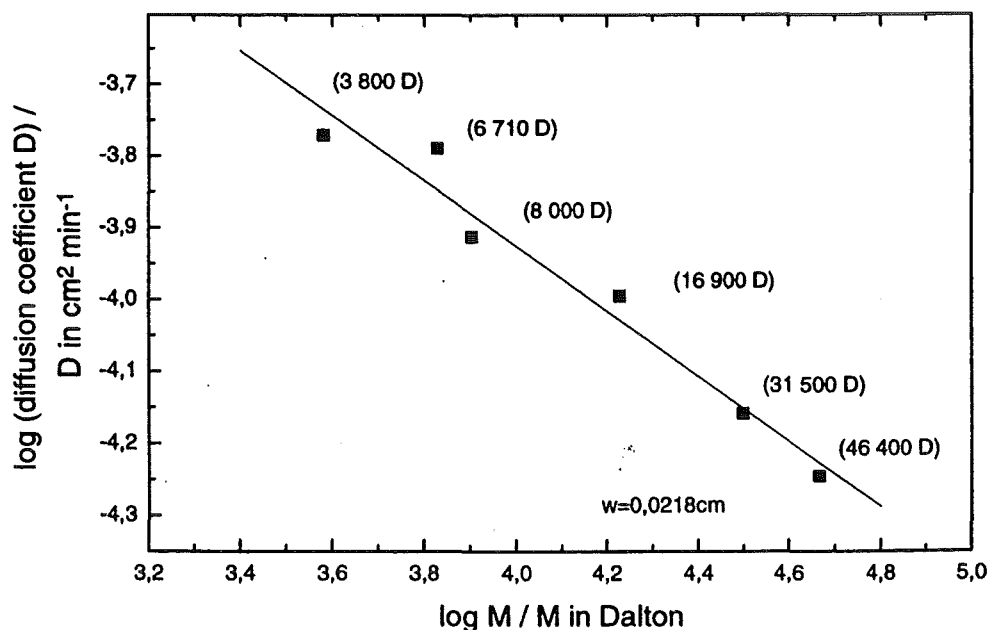


Figure 3.1 Calibration curve obtained with Flow-FFF for standardised poly(styrene) sulfonate sodium salt

Sample Analysis

The sample fractogram was recorded three times and from the peak maximum an average value for the molecular weight at peak maximum was calculated to be

$$M_p = 2.217 \pm 0.007 \text{ kDalton.}$$

Taking into account the error of calibration a relative error of 23.1 % is found, which makes clear that the uncertainty of the calibration dominates the error of the result for the molecular weight.

Fig. 3.2 shows the results for M_p and the corresponding number and weight averaged molecular weights (M_n , M_w).

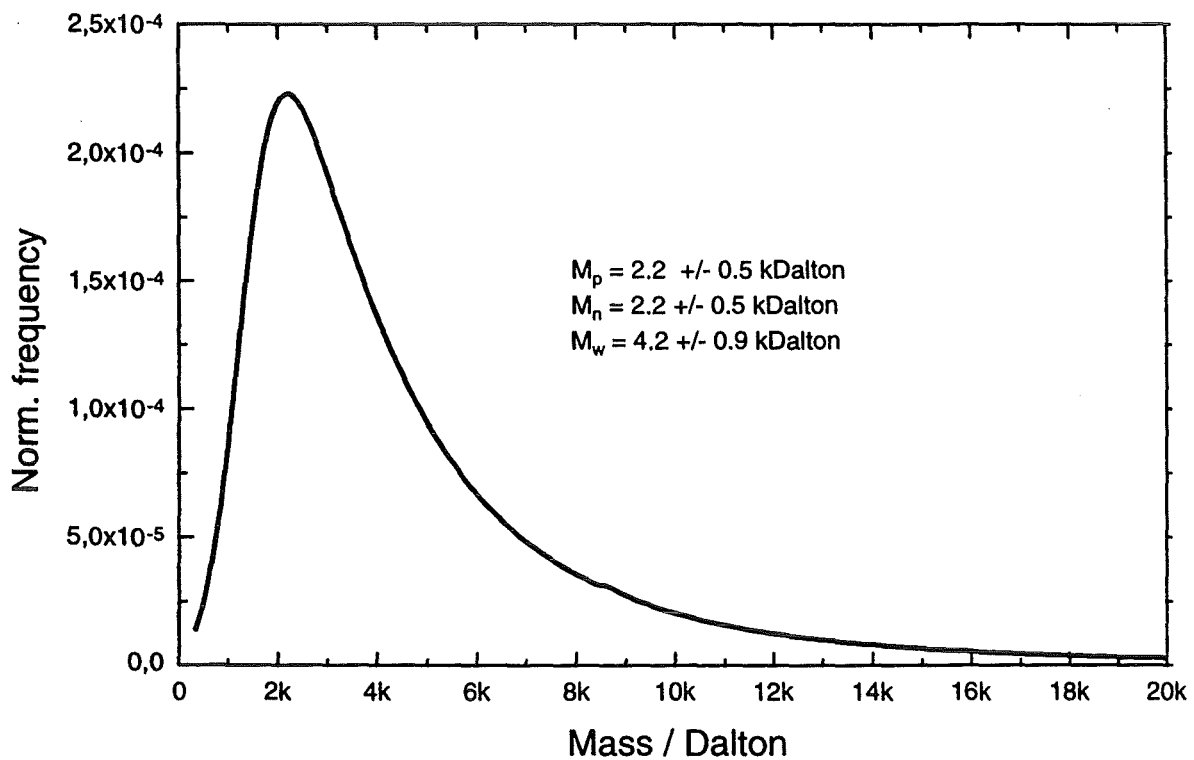


Figure 3.2 Fractogram of Derwent fulvic acid sample

3.4 Proton Binding (C.Milne, BGS Wallingford)

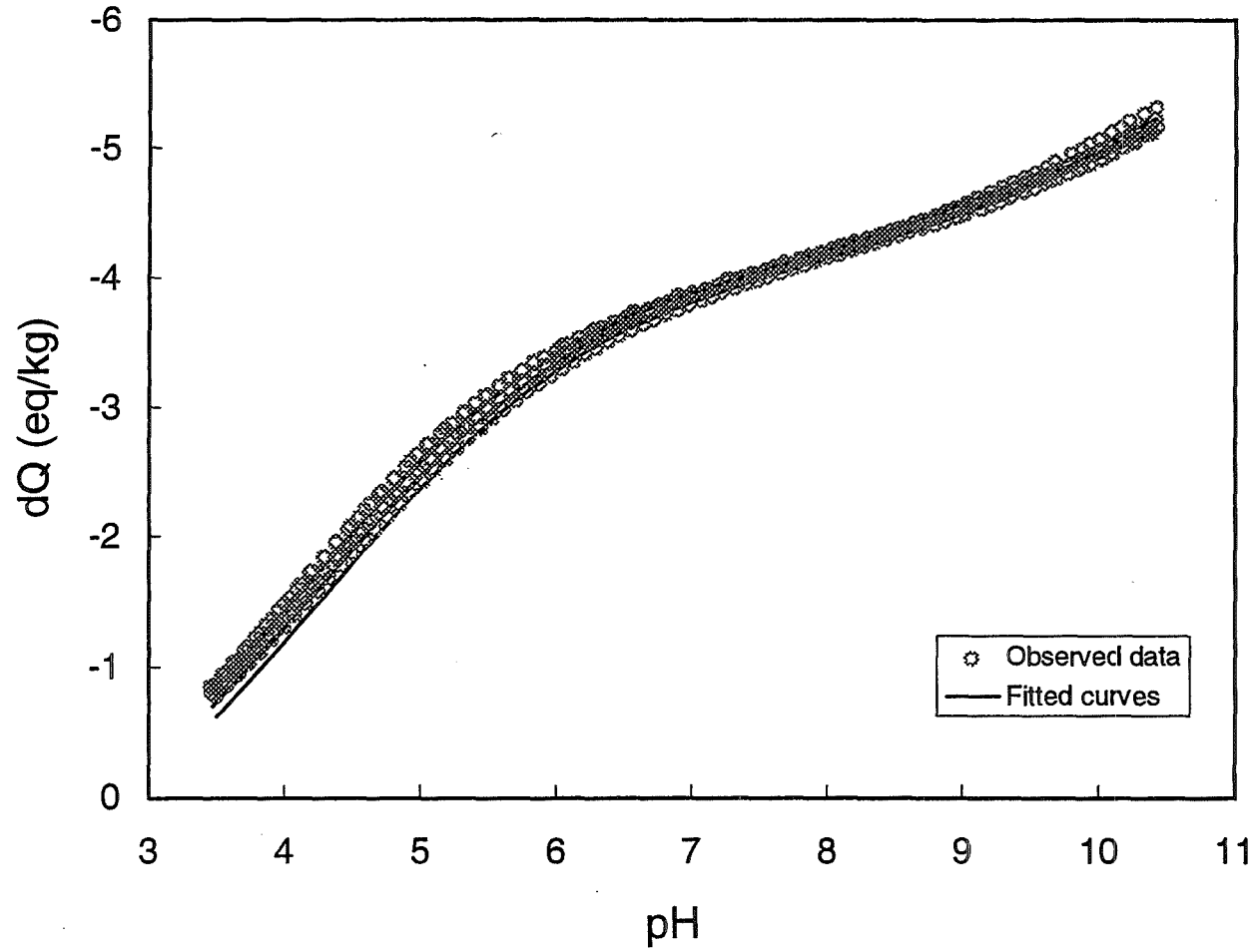
Proton binding was measured using a PC-controlled programmable titration system developed at BGS Wallingford and consisting of Dosimat burettes (Metrohm) and a Microlink pH4 module and interface (Biodata). Three burettes were used, containing KOH, HNO₃ and KNO₃ respectively (all approx 0.1 M). To titrate, a sample of fulvic acid was diluted with deionized water to give an initial solution which contained no added salt and with a moderately high fulvic acid concentration (1.6 mg/ml). The titrator was programmed to perform four complete titration cycles, at ionic strengths nominally 0.003, 0.01, 0.03 and 0.1 M. To achieve this, at the beginning of each cycle, the programme calculates the existing ionic strength of the solution from the known previous additions of acid, base or salt and calculates the additional dose of neutral salt required to obtain the required ionic strength. The solution is then titrated with base to pH approx 11 and back with acid to pH approx 3. The ionic strength is then recalculated, adjusted and the next titration cycle executed.

During experiments on the Derwent Fulvic Acid data points were recorded at approx 0.1 pH intervals, with the titrator adjusting the size of acid or base doses in order to maintain constant pH increments. Electrode drift was monitored following each addition, for a minimum of 2 minutes and until the pH drift was less than 0.001 pH/min (at regions of low buffer capacity, up to 20 minutes). Separate pH and reference half cells were used, with a saturated calomel reference fitted with a continuously refreshed double-junction electrolyte bridge (0.1 M KNO₃). The reaction vessel was thermostatted at 25° ± 0.1°C and was continuously purged with a trickle flow of O₂- and CO₂-free N₂. The complete four-cycle titration took 72 hours.

3.4.1 Results

Raw experimental titration volumes were corrected for the volume of reagents required to titrate the background neutral electrolyte solution yielding data for the change in charge of the fulvic acid, dQ (eq/kg), as a function of pH. At pH<3.5 and pH>10.5 the volume of titrant required to titrate the electrolyte becomes large compared to that used to titrate the FA. Therefore at these pH values the uncertainty in the charging curve is correspondingly large and the data are not used. The corrected curves showed that the charging behaviour during the first leg of the titration, titrating with base from the natural acidity of the fulvic acid to pH 10, was significantly different to that observed in all subsequent legs. A similar difference has been observed previously with other humic material (e.g. Milne *et al*, 1995)

Figure 3.3. NICA-Donnan fit to DFA proton data. Model parameters derived from combination of acid and base curves. Three curves in order of increasing (i.e. more negative) dQ , represent ionic strengths of approx 0.01, 0.029 and 0.097 M respectively.



and it is possible that the effect is due to conformational changes in the fulvic acid as it relaxes after being stored as a very high concentration suspension. In subsequent legs the titration curves were extremely similar and reproducible: the sets of acid or base titrations at increasing ionic strength each generated sets of curves with very consistent shape, but shifted progressively on the Q/dQ axis as the ionic strength increased. The curves did not cross within each set although there was a very small residual hysteresis pattern distinguishable between the acid and base titrations sets. After discarding the first, different, curve the set of three base titration curves at ionic strengths approximately 0.01, 0.029 and 0.097 M are shown in Figure 3.3.

The overall form of the titration curve is typical for a fulvic acid. It shows a smooth progressive titration, without clearly defined strong acid pK values and with proton dissociation continuing from below pH 3 to above pH 10.5. The 'hip' in the curve where the gradient changes at around pH 6.5 (slightly steeper at pH<6.5) is indication that the site-density of acid carboxylic-type groups with pK in the acid region is higher than the density of phenolic- and other similar types of groups with pK at the alkaline end of the scale. Overall the curve is remarkably congruent with titration curves which have been recorded for some other fulvic acids (Christensen *et al*, 1998).

The data were modelled by applying a non-linear least squares optimization fit to the NICA-Donnan model of ion-binding by humic materials (Kinniburgh *et al*, 1996). Because of the difficulty in interpreting the minor hysteresis between the acid and base titration data the model was fitted to both datasets simultaneously. The best fit results for the model were then:

$$b = 0.80 \pm 0.01$$

$$Q_{\text{init}} = 1.15 \pm 0.5 \text{ eq/kg}$$

$$Q_{\text{max1}} = 5.0 \pm 0.2 \text{ eq/kg}$$

$$Q_{\text{max2}} = 3.1 \pm 0.5 \text{ eq/kg}$$

$$\log K_{\text{H1}} = 3.15 \pm 0.2$$

$$\log K_{\text{H2}} = 9.5 \pm 1.5$$

$$m_{\text{H1}} = 0.50 \pm 0.02$$

$$m_{\text{H2}} = 0.30 \pm 0.05$$

$$R^2 = 0.9987$$

$$\text{RMSE} = 0.046 \text{ eq/kg}$$

As can be seen from the figure and the R^2 coefficient the quality of the fit is very good. The model fits the form of the curves well, and reproduces the size of the ionic strength dependence of the data well. The observed hysteresis is sufficiently small that the consequent distortion of the model fit is also small.

The greatest difficulty in obtaining a good model fit derives from the charging behaviour of the Derwent fulvic acid at high pH. As the charge on the fulvic acid is still increasing steadily at the highest pH available in the titration window and shows no clear inflection to an asymptote, it is extremely difficult to extrapolate the curve to the fully-deprotonated limit at which maximum negative charge will occur. This, therefore, makes it difficult to estimate reliably the total number of available binding sites. If the model parameters are allowed to vary unconstrained during optimization there can be a tendency for the model to infer the existence of a physically unreasonable number of high pK sites in order to obtain a numerically optimum fit. Therefore it is necessary to constrain the fit to the second, high pK distribution, by a combination of previous experience and ensuring that the fitted values are physically reasonable. In this case it proved most effective to set the modal for the second distribution to $\log pK_{H2} = 9.5$. This value is consistent with studies of previous fulvic acids, and a simple sensitivity analysis indicated that the goodness-of-fit was fairly insensitive to variation of $\log pK_{H2}$ within a ± 1.5 eq/kg range. The effect of any such variation is that if the modal value is allowed to go to higher pH then the model predicts the existence of more sites with very high pK_a , beyond the experimentally observable range; the fit to the data within the observable window remains almost unchanged.

The model indicates that the number of binding sites in the first (carboxylic, K_{H1} or K_A) distribution is 5.0 eq/kg (exactly the same as for Model V) and that the total number of binding sites available is 8.1 eq/kg. The value of $Q_{init} = 1.15 \pm 0.5$ eq/kg shows how many sites can be expected to be deprotonated at pH lower than the pH3.5 at which the data begins, and allows the dQ scale to be converted to true absolute charge of the fulvic ($Q = dQ + 1.15$). Experimental observation of the initial pH of the untitrated fulvic acid is consistent with this model projection, although the logarithmic nature of the pH scale can introduce moderately large uncertainty into the experimental figure.

The data were also fitted in order to obtain Model V parameters (Tipping *et al.*, 1990) A first fit to the same data gives the parameters:-
 $nCOOH = 4.99e-3$ typical (average is $4.8e-3$)

pKA = 3.10 slightly lower than average (3.3)

pKB = 7.82 slightly lower than average

DpKA = 3.22 typical

DpKB = 4.65 typical

P = - 50.8 low (average is c115)

The fit is averagely good - rmsd in Z = 0.12 meq/g

Thus the final fitted parameters provide a model descriptions which are in good agreement. The raw titration data are available on disk for those members who wish to interpret it for use in a specific model.

3.5 Uranium Complexation

Uranium stability constants were determined using two versions of Schubert's competition method in which a metal in a solution containing complexing ligands is contacted with an ion exchanger. The metal will distribute itself between the ion exchanger and the complexing ligand in such a way as to simultaneously satisfy the distribution constant of the resin and the stability constant of the complex. The data may be analysed using the following equation

$$\log \left(\frac{D_0}{D} - 1 \right) = \log \beta + i \log [L]$$

where D_0 is the distribution ratio in the absence of complexing ligand

D is the distribution ratio in the presence of complexing ligand

i is the number of moles of ligand reacting per mole of metal

$[L]$ is the concentration of ligand

so that if $n = 1$

$$\log \left(\frac{D_0}{D} - 1 \right) = \log \beta + \log [L]$$

Experimental

The ion exchange method has been described in detail elsewhere (Higgo *et al*, 1992 & 1993). The solvent extraction method was similar to that used by Nash & Choppin (1980). Thus, 5.0 ml portions of aqueous solutions containing fulvic acid and U²³³ in 0.01M NaCl at pH 4.0 were shaken with an equal volume of 10⁻⁵ M HDEP in toluene for 24 hours. The phases were then separated and 1 ml portions counted in a liquid scintillation counter. Fulvic acid concentrations ranged from 2 to 15 mg/l. The uranium concentration was approx 3 x 10⁻⁷ M/l. In the absence of fulvic acid phase (D₀ measurements) separation was good and both phases could be counted but in the presence of fulvic acid a band was formed at the interface. It was assumed that this contained uranium fulvate. Only the organic phase was, therefore, counted and the activity of the aqueous phase obtained by difference. At pH 4.0 sorption to the walls of the centrifuge tube was low and recoveries in the D₀ experiments were close to 100%. However at pH 6.0 these recoveries were low and it was impossible to estimate D. For this reason only results at pH 4 are reported. The two methods gave similar results and the values obtained were of the same order as those obtained previously on fulvic acids extracted from Drigg and Broubster groundwaters (higgo *et al*, 1992 & 1993) and to values reported in the literature (Czerwinski *et al.*, 1994). It appears, therefore, that complexation (of uranium) behaviour of the Derwent Water fulvic acid is similar to that of other fulvic acids studied in the past.

Table 3.5 Derwent Water Fulvic acid - Uranium stability constants

	M.Wt Dalton	pH	Ionic strength M/l NaCl	Log beta l/g	Log beta l/mole	Method
Drigg GW	1800	3.7	0.01	1.8	5.0	Ion exchange
Drigg GW	1800	4.7	0.01	2.7	6.0	Ion exchange
Drigg GW	1800	5.0	0.01	2.4	5.6	Ion exchange
Derwent Reservoir	4000	3.9	0.01	2.9	6.5	Solvent Extraction
Derwent Reservoir	4000	4.3	0.01	2.8	6.4	Solvent Extraction
Derwent Reservoir	4000	4.1	0.01	2.6	6.2	Solvent Extraction
Derwent Reservoir	4000	4.4	0.03	2.9	6.5	Ion exchange

4. SUMMARY AND CONCLUSIONS

Fulvic acid has been extracted from four thousand litres of water taken from the Derwent Reservoir (Derbyshire, UK) using DEAE-cellulose. Several stages of purification included anion exchange on Amberlite XAD-8 resin and cation exchange on Amberlite AG50W-X8. The final purified fulvic acid concentrate, volume 1300 ml, contained 4.1 g/l TOC (total fulvic acid \approx 11 g). It was characterised in terms of elemental analysis, molecular weight, proton-binding properties, UV absorbance and uranium binding properties. This material is now available for use by all members of the group for experimental studies.

5. ACKNOWLEDGEMENTS

This work was funded by the Commission of the European Communities and the United Kingdom Environment Agency. The results will be used in the formulation of Government Policy but do not necessarily represent that policy.

The help of several members of the consortium are gratefully acknowledged. In particular the work of the following is much appreciated

Dr N. Bryan (Manchester University) for measuring the molecular weight of the fulvic acid by ultracentrifugation (Section 3.3.1)

Dr Ngo Manh Thang and Dr H. Geckeis (Forschungszentrum Karlsruhe, Institut für Nukleare Entsorgungstechnik) for measuring the molecular weight of the fulvic acid by flow-field fractionation (Section 3.3.2)

C. Milne (BGS Wallingford) for carrying out the proton exchange studies

Dr P. Warwick (Loughborough University) for measuring the CHN content of the fulvic acid (Section 3.2)

Dr. E. Tipping (Institute of Freshwater Ecology) for carrying out Model-V modelling

Dr M. Cave and other members of the BGS Analytical Geochemistry group for analysing the groundwaters and the fulvic acid for cations and anions.

5. REFERENCES

Czerwinski, K., Buckau, G., Scherbaum, F. and J.I. Kim (1994). "Complexation of the uranyl ion with aquatic humic acid." *Radiochimica Acta*, **65**: 111-119.

Christensen, J.B., Tipping, E., Kinniburgh, D.G. Gron, C. and Christensen, T.H. (1998)

“Proton binding by groundwater fulvic acid”s of different age,origin and structure modelled with the Model V and NICA-Donnan Model. Submitted to *Environmental Science and Technology*.

Higgo, J. J.W., Kinniburgh, D., Smith, B. and E. Tipping. (1992). “Complexation of Co^{2+} , Ni^{2+} , UO_2^{2+} and Ca^{2+} by humic substances in groundwaters. *Radiochimica Acta* , 61: 91-103.

Higgo, J J W, Davis,J. *et al.* (1992). Comparative study of humic and fulvic substances in groundwaters: 3. Metal complexation with humic substances. British Geological Survey Technical Report No. WE/92/12

Kim, J. I., Buckau, G. and Zhuang, W. (1987). “Humic colloid generation of transuranic elements in groundwater and their migration behaviour.” *Materials Research Society Symposium*, 84: 747-756.

Kinniburgh, D.G., Milne, C.J., Benedetti, M.F., Pinheiro, J.P., Filius, J, Koopal, L.K. and van Riemsdijk, W.H. (1996) Metal-ion binding by humic acid: application of the NICA-Donnan model. *Environmental Science and Technology*. 30, 1687-1698

Leenheer, J. A., Malcolm,R.L., Mckinley I. and P.W.Eccles, (1974). “Occurrence of dissolved organic carbon in selected groundwater samples in the United States.” *US Geological Survey Journal of Research*, 2: 361-369.

Milne,C.J., Kinniburgh, D.G., de Wit, J.C.M., van Riemsdijk,W.H. and Koopal, L.K. (1995) Analysis of proton binding by a peat humic acids using a simple electrostatic model. *Geochimica et Cosmochimica Acta*, 59, 1101-1112.

Moulin, V., A. Billon, Theyssier, M. And Dellis, Th. (1991). Study of the interactions between organic matter and transuranic elements. CEC Report EUR 13651

Nash, K. L. and G. R. Choppin (1980). “Interaction of Humic and fulvic Acids with Th(IV) .” *J. Inorg. Nucl. Chem*, 42: 1045-1050.

Tipping, E., Reddy, M.M., and Hurley, M.A. (1990), “Modelling electrostatic and heterogeneity effects on proton dissociation from humic substances. *Environmental Science and Technology*, 24 , 1700-1705.

Thurman, E. M. and R. L. Malcolm (1981). "Preparative Isolation of Aquatic Humic Substances." *Environmental Science and Technology*, **15**(4): 463-466.

Thurman, E. M. (1985). *Organic Geochemistry of Natural Waters*. Martinus Nijhoff / Dr W. Junk Publishers.

Vilks, P. and D. B. Bachinski (1996). "Characterisation of organics in Whiteshell Research Area groundwater and the implications for radionuclide transport." *Applied Geochemistry*, **11**: 387-402.

1st Technical Report

EC Project

**"EFFECTS OF HUMIC SUBSTANCES ON THE MIGRATION OF RADIONUCLIDES:
COMPLEXATION AND TRANSPORT OF ACTINIDES"**

CEA Contribution to Task 2

***URANIUM INORGANIC SPECIATION DETERMINED BY
TIME-RESOLVED LASER-INDUCED FLUORESCENCE***

Reporting period 1997

Ivan LASZAK, Valérie MOULIN, Christophe MOULIN*, Patrick MAUCHIEN*

CEA, CE-Saclay, Fuel Cycle Division, DESD/SESD

91191 Gif-sur-Yvette, FRANCE

**CEA, CE-Saclay, Fuel Cycle Division, DPE/SPEA*

91191 Gif-sur-Yvette, FRANCE

ABSTRACT^a

Time-Resolved Laser-Induced Fluorescence is used as a method for direct uranium speciation at low level. By varying pH and uranium concentration in the absence of carbonate ions and at fixed ionic strength, it is possible together with free uranyl UO_2^{2+} , to identify spectrally and temporally, all the uranium-hydroxo complexes namely UO_2OH^+ , $\text{UO}_2(\text{OH})_2$, $\text{UO}_2(\text{OH})_3^-$, $(\text{UO}_2)_2(\text{OH})_2^{2+}$, $(\text{UO}_2)_3(\text{OH})_5^+$, $(\text{UO}_2)_3(\text{OH})_7^-$. This identification is very important for further investigations in the framework of complexation with humic substances

INTRODUCTION

Direct uranium speciation in solution, *i.e.* determination of the different chemical species present, is of great importance in the framework of nuclear waste disposal studies (Choppin, 1985; Buffle, 1988; Moulin and Ouzounian, 1991). Among ligands present in groundwaters which could complex radionuclides are found hydroxide, carbonate ions and also organic matters such as humic and fulvic acids. In the case of uranium (particularly U(VI)), this radionuclide possesses a very complex inorganic and organic chemistry, and for example, more than twelve complexes from hydroxo to carbonate complexes as well as polynuclear have already been reported.

Uranium speciation requires a very sensitive method allowing to work at low concentrations that are orders of magnitude below the solubility limit and moreover, representative of the concentrations possibly encountered in the case of a leakage from the radwaste disposal. This also requires a very selective method that is capable of clearly identifying directly in solution the different complexes without prior separation which would modify the equilibrium of the medium under investigation.

Time-Resolved Laser-Induced Fluorescence (TRLIF) is a very sensitive and selective method for uranium (as uranyl ion UO_2^{2+}) ultratrace analysis in the different fields of the nuclear, environment and medical (Zook *et al.*, 1981; Young *et al.*, 1984; Berthoud *et al.*, 1988; Fujimori *et al.*, 1988; Moulin *et al.*, 1990; Brina and Miller, 1992; Moulin *et al.*, 1991a; Deniau *et al.*, 1993; Moulin *et al.* 1996), and is knowing a growing interest for complexation and speciation

^a This report is one part of a publication accepted in Applied Spectroscopy (1998)

studies. Briefly, this technique is based on laser excitation followed by temporal resolution of the fluorescence signal. Sensitivity reached for uranium is down to 10^{-12} M in the case of analysis (with the help of appropriate complexing reagent) and down to 10^{-9} M in the case of complexing and speciation studies (the composition of the medium being fixed by real conditions). The other great advantage of TRLIF is its triple resolution:

- i) excitation resolution by the proper choice of the laser wavelength (N_2 , tripled or quadrupled Nd-YAG, dye, ...),
- ii) emission fluorescence which gives characteristics spectra of the fluorescent cation (free or complexed) and
- iii) fluorescence lifetime characteristic of its environment (complexation, quenching).

These two latter data provide useful informations on the chemical species present in solution as well as for complexation studies. For example, this technique used as a "fluorescent titration method" has allowed the determination of complex formation at low level between trivalent elements (such as europium, dysprosium and curium) and humic acids (Dobbs *et al.*, 1989; Bidoglio *et al.*, 1991; Moulin *et al.*, 1991b, Kim *et al.*, 1991; Moulin *et al.*, 1992). *Through the knowledge of U(VI) inorganic speciation (such as hydrolysis and carbonate complexation) by TRLIF (identification of the different chemical species, spectrally and temporally), the study of the possible formation of mixed or ternary complexes with humic substances (M-OH/CO₃-humic acids) can be investigated.*

Several studies (Deschaux and Marcantonatos, 1979; Graca *et al.*, 1984; Azenha *et al.*, 1991; Meinrath *et al.*, 1993; Couston *et al.*, 1995; Kato *et al.*, 1994; Eliet *et al.*, 1995; Moulin *et al.*, 1996) exist on the speciation of uranium but very few at low level. This TRLIF study is specially devoted to the spectral and temporal characterization of uranium hydroxo-complexes as well as carbonato complexes by working at different pH and uranium concentrations and to compare them when existing to published data.

EXPERIMENTAL

Apparatus *Time-resolved laser-induced fluorescence.*

A Nd-YAG laser (Model minilite, Continuum) operating at 266 nm (quadrupled) or 355 nm (tripled) and delivering about 2.5 mJ of energy in a 4 ns pulse with a repetition rate of 20 Hz is used as the excitation source. The laser output energy is monitored by a laser power meter (Scientech). The beam is directed into a 4 ml quartz cell. The laser beam is directed into the cell of the spectrofluorometer "FLUO 2001" (Dilor, France) by a quartz lens. The radiation coming from the cell is focused on the entrance slit of the polychromator. Taking into account dispersion of the

holographic grating used in the polychromator, measurement range extends to approximately 200 nm into the visible spectrum with a resolution of 1 nm. The detection is performed by an intensified photodiodes (1024) array cooled by Peltier effect (-25°C) and positioned at the polychromator exit. Recording of spectra is performed by integration of the pulsed light signal given by the intensifier. The integration time adjustable from 1 to 99 s allows for variation in detection sensitivity. Logic circuits, synchronized with the laser shot, allow the intensifier to be active with determined time delay (from 0.1 to 999 μ s) and during a determined aperture time (from 0.5 to 999 μ s). The whole system is controlled by a microcomputer.

Fluorescence measurement procedure. All fluorescence measurements are performed at 20 °C. For carbonate free experiments, all solutions used are directly prepared in a specially equipped gloves box with nitrogen gas recirculation. Solutions are further degazed with nitrogen for several hours prior to experiments. The pH of the solution in the cell is measured with a conventional pH meter (Model PHN 81, Tacussel) equipped with a subminiature combined electrode (Model MIXC710).

For each identification, uranium concentration, pH, ionic strength and controlled atmosphere (with or without air) are perfectly fixed and controlled. From a spectroscopic point of view, various gate delay and duration are used to certify the presence of only one complex by the measurement of a single fluorescence lifetime and spectrum.

Fluorescence spectra are analyzed using the deconvolution software GRAMS 386[®]. All peaks are described using mixed Gaussian-Lorentzian profile (the apparatus function was previously recorded using a mercury lamp). Fluorescence lifetime measurements are made by varying the temporal delay and gatewidth depending on the complex studied.

Materials. Standard solutions of uranium (VI) in sodium perchlorate (NaClO₄ 0.1M) are obtained from suitable dilution of a solution prepared by dissolution of high purity metal with concentrated perchloric acid (Merck). Due to the hazardous properties of perchloric acid, this reaction is performed in a hood with absolutely no grease on vessels. Uranium concentration of the initial standard solution is measured by mass spectrometry. Perchloric acid and sodium hydroxide (Merck) are used for pH adjustment. The ionic strength is fixed by the sodium perchlorate concentration at 0.1M for all the experiments. All chemicals used are reagent grade and Millipore water is used throughout the procedure.

RESULTS AND DISCUSSION

For speciation studies under representative natural conditions, several requirements have to be fulfilled:

- the method has to be the less intrusive in order not to modify the system (as chromatographic techniques which can perturb the various equilibria due to the use of stationary phases),
- the method has to be very sensitive since under natural conditions, uranium will be present at very low concentrations, and finally
- the method should give specific informations on the complexes present in solution.

Time-Resolved Laser-Induced Fluorescence (TRLIF) meets these different requirements, since it is directly applicable in solution and processes associated (excitation and fluorescence) with the technique involve only photons of low energy. TRLIF first developed for uranium ultratrace analysis as a sensitivity close to 10^{-12} M in appropriate complexing media (Moulin *et al.*, 1990) such as phosphoric acid that enhances the uranium fluorescence properties. This very low limit of detection (< ng/l) allows to work at concentration down to 10^{-9} M for speciation studies where the medium under investigation must not be modified. Moreover, TRLIF can identify soluble complexes present in solution by its capability to give spectral (peaks position, broadening characterized by the full width at half maximum (FWHM)) and temporal (lifetime) informations.

Lifetime measurement characterizes the environment of the fluorescent species and can be used for the determination of water molecules surrounding the fluorescent species as well as for the determination of quenching constants using the Stern-Volmer equation (Romanovskaya *et al.*, 1980; Moriyasu *et al.*, 1977; Bünzli and Choppin, 1989, Nikitin *et al.*, 1978). However, especially for uranium, large discrepancies on quenching constants are observed between published data. Most of the time, these differences arise from uncontrolled chemistry in terms of pH, ionic strength, presence of carbonates or initial chemistry *i.e.* using compounds that contain unwanted reagents. In this particular study, special cares are taken in terms of chemistry (initial dissolution, reagents, ionic strength, pH). Therefore, as explained in the experimental part, uranium metal and not uranium nitrate is used as the starting material. Hence, TRLIF as a very sensitive method for uranium studies can also be strongly affected by the presence of unwanted complexing reagents such as nitrate (Moulin *et al.*, 1996), carbonate or non controlled physico-chemical parameters such as ionic strength, pH, temperature.

Figure 1 presents the very complex speciation diagram of uranium at 4.10^{-6} M at atmospheric pressure based on the complexing constants of the Organisation for Economic Cooperation and Development - Nuclear Energy Agency (O.E.C.D. - N.E.A) thermodynamical

data bank (Grenthe *et al.*, 1992) and Lemire and Tremaine (Lemire and Tremaine, 1980) for $\text{UO}_2(\text{OH})_2$. As can be seen aside free uranyl (UO_2^{2+}), nine complexes are present, six uranium-hydroxo complexes, namely UO_2OH^+ , $(\text{UO}_2)_2(\text{OH})_2^{2+}$, $(\text{UO}_2)_3(\text{OH})_5^+$, $\text{UO}_2(\text{OH})_2$, $(\text{UO}_2)_3(\text{OH})_7^-$, $\text{UO}_2(\text{OH})_3^-$ (at this uranium concentration $(\text{UO}_2)_3(\text{OH})_4^{2+}$ can be neglected) and three uranium-carbonato complexes, namely UO_2CO_3 , $\text{UO}_2(\text{CO}_3)_2^{2-}$, $\text{UO}_2(\text{CO}_3)_3^{4-}$.

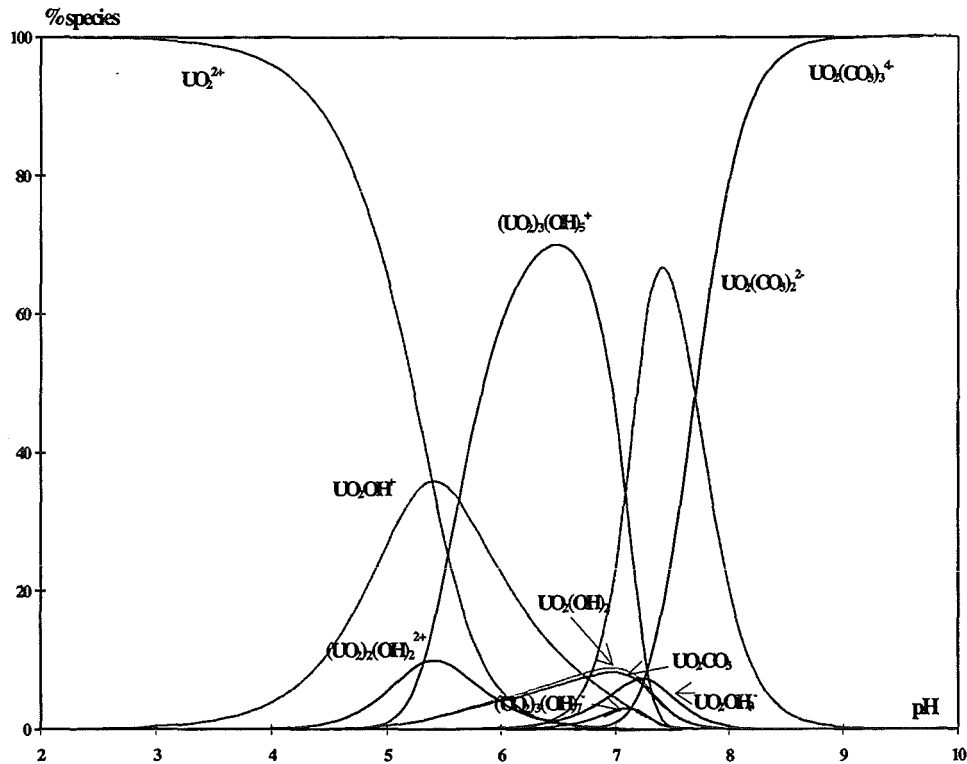


Figure 1 : Uranium speciation diagram (from O.E.C.D.³⁰ and³¹) at 4.10^{-6}M , $I\ 0.1$, P_{CO_2} atm. $\log\beta\text{UO}_2\text{OH}^+ : -5.2$, $\log\beta\text{UO}_2(\text{OH})_2 : 11.9^{31}$, $\log\beta\text{UO}_2(\text{OH})_3^- : -19.2$, $\log\beta(\text{UO}_2)_2(\text{OH})_2^{2+} : -5.62$, $\log\beta(\text{UO}_2)_3(\text{OH})_5^+ : -15.55$, $\log\beta(\text{UO}_2)_3(\text{OH})_7^- : -31$, $\log\beta\text{UO}_2\text{CO}_3 : 9.68$, $\log\beta\text{UO}_2(\text{CO}_3)_2^{2-} : 16.94$, $\log\beta\text{UO}_2(\text{CO}_3)_3^{4-} : 21.6$.

The strategy is first to simplify this diagram, by working in air free gloves-box (*i.e.* free from carbonate) then to work at different uranium concentrations to favour specific complexes. Uranium speciation calculations have thus been performed at four different uranium concentrations, namely : 4.10^{-5}M , 4.10^{-6}M , 4.10^{-7}M and 4.10^{-8}M in order to determine the chemical conditions ($[\text{U}]$ and pH) of interest for the identification studies.

- at 4.10^{-5}M (pH of interest: 6.5, 8.5 ; figure 2a) seven different uranium hydroxo complexes are present, which do not simplify the speciation diagram but that will be used to identify the polynuclear species ($(\text{UO}_2)_3(\text{OH})_5^+$, $(\text{UO}_2)_3(\text{OH})_7^-$).

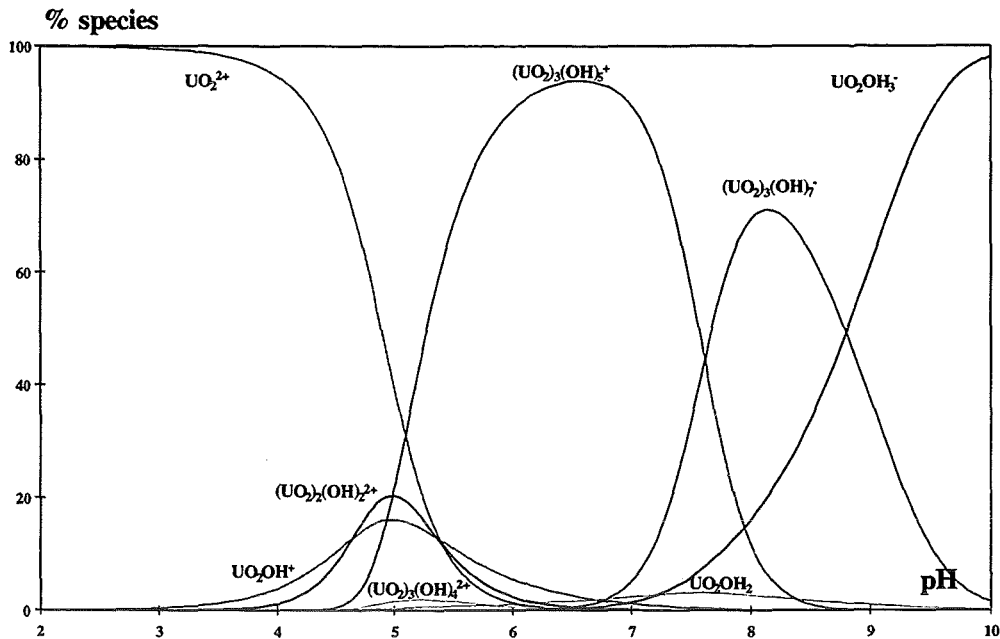


Figure 2a : Uranium speciation diagram (from Grenthe *et al.*, 1992 and Lemire and Tremaine, 1980) at 4.10^{-5} M, $I = 0.1$, $P_{CO_2} = 0$.

- at 4.10^{-6} M (pH of interest: 6.8, 8.4 and 9.5 ; figure 2b) compared to figure 1, only six uranium hydroxo complexes are present and their percentages are not the same as at 4.10^{-5} M.

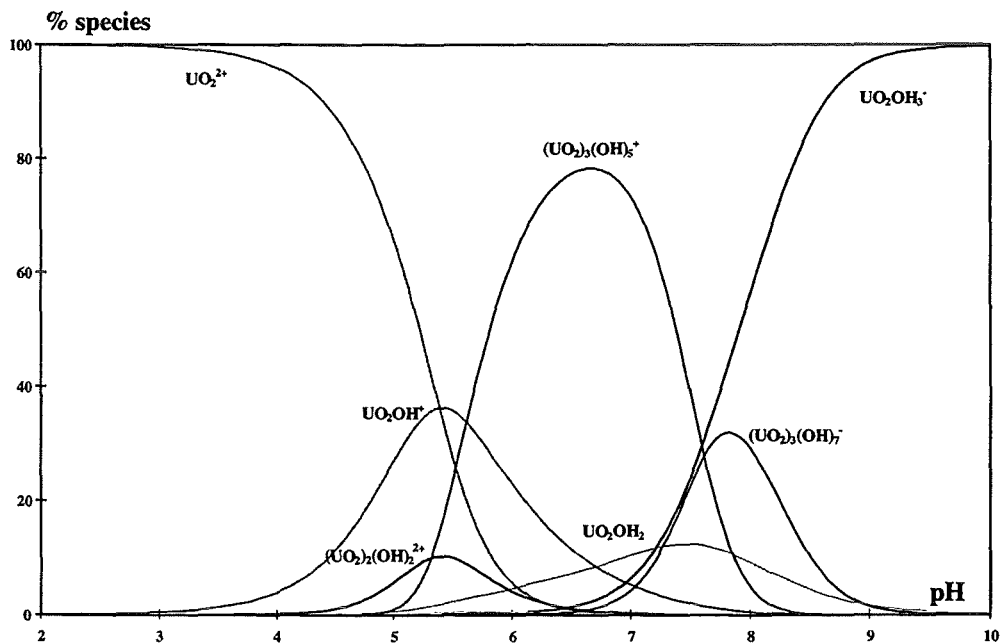


Figure 2b : Uranium speciation diagram (from Grenthe *et al.*, 1992 and Lemire and Tremaine, 1980) at 4.10^{-6} M, $I = 0.1$, $P_{CO_2} = 0$.

- At 4.10^{-7} M (pH of interest: 4, 8.4 and 9.8 ; figure 2c), six uranium hydroxo complexes are still present again with different percentage compared to 4.10^{-6} M, especially among the polynuclear species where $(UO_2)_2(OH)_2^{2+}$ and $(UO_2)_3(OH)_7^-$ are present at very low concentration.

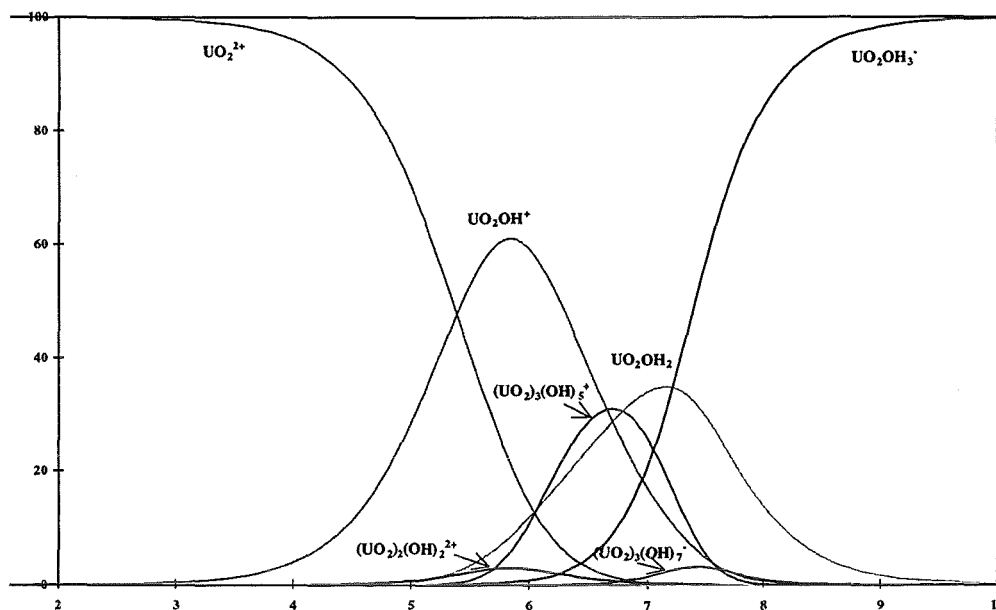


Figure 2c : Uranium speciation diagram (from Grenthe *et al.*, 1992 and Lemire and Tremaine, 1980) at $4.10^{-7}M$.

$I=0.1, P_{CO_2} = 0$.

- Concerning $4.10^{-8}M$ (pH of interest: 4.8, 7 and 9.8 ; figure 2d), this particular concentration is very interesting, since all polynuclear species have disappeared and only three uranium-hydroxo complexes are present, namely UO_2OH^+ , $UO_2(OH)_2$ and $UO_2(OH)_3^-$. It should be pointed out that further lowering of the uranium concentration does not simplify anymore the speciation diagram.

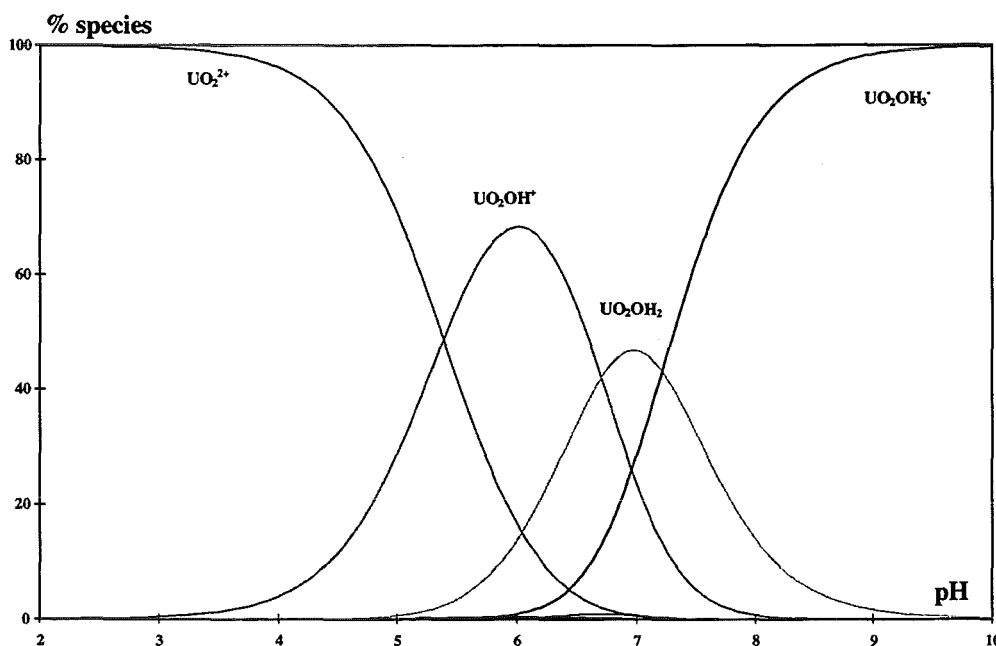


Figure 2d : Uranium speciation diagram (from Grenthe *et al.*, 1992 and Lemire and Tremaine, 1980) at $4.10^{-8}M$.

$I=0.1, P_{CO_2} = 0$.

With these different figures, it can be seen that by, using various uranium concentrations and by selecting appropriate pH, it is possible to chemically favour uranium complexes among others for fluorescence studies. The first one, easy to identify and already well known, is UO_2^{2+} . Figure 3 presents the uranyl fluorescence spectrum at pH 2 with the six characteristics peaks located around 470, 488, 509, 533, 559 and 585 nm together with the convoluted spectrum obtained from peak deconvolutions and the residual (difference between experimental and convoluted spectrum). These different emission lines come from transitions of the excited state at 21270 cm^{-1} to the groundstate (470 nm) and mainly from the excited state at 20502 cm^{-1} to groundstates at 0, 855, 1710, 2565 and 3420 cm^{-1} (488, 509, 533, 559 and 585 nm) (Bell and Biggers, 1968). The four main peaks (488, 509, 533 and 559 nm) have average full width at mid height (FWMH) of around 13 nm. Fluorescence lifetime is around $2 \mu\text{s}$ with general agreement in the literature, values varying between 1 to $2 \mu\text{s}$. UO_2^{2+} , free uranyl is taken as a reference in terms of spectroscopic scale since it is very likely that all the other species will present a bathochromic shift due to complexation and a broadening due to the addition of new vibrational modes.

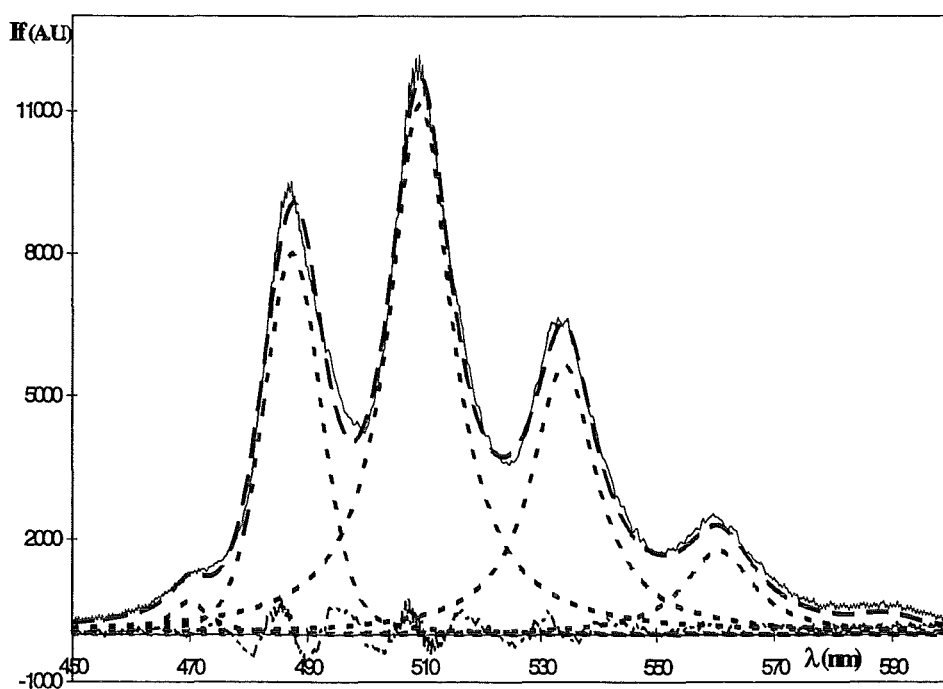


Figure 3 : UO_2^{2+} (free uranyl) fluorescence spectrum (—) together with convoluted spectrum (— —) (obtained from single peaks (- -)) and residual (— . . —). $[\text{U}] 4.10^{-6}\text{M}$, $I = 0.1$, pH 1. Time delay $0.5 \mu\text{s}$, aperture time $1 \mu\text{s}$, integration time 1s, number of accumulations 30.

The next step is to identify $\text{UO}_2(\text{OH})_3^-$ by performing experiments at the other side of the pH scale (see figures at different U concentrations) and to strongly chemically favour this complex. Figure 4 presents the uranium fluorescence spectrum obtained at pH 10 ($[\text{U}] 4.10^{-8}\text{M}$) attributed to $\text{UO}_2(\text{OH})_3^-$, experiments are also carried out at different concentrations (4.10^{-7}M , 4.10^{-6}M) and at higher pH (pH 11). In all cases, this spectrum is confirmed with four main wavelengths at 499, 519, 543, 567 nm corresponding to a shift of around 11 nm compared to UO_2^{2+} . Furthermore, the average FWHM for $\text{UO}_2(\text{OH})_3^-$ is around 23 nm. Fluorescence lifetime for $\text{UO}_2(\text{OH})_3^-$ is evaluated around 0.8 μs .

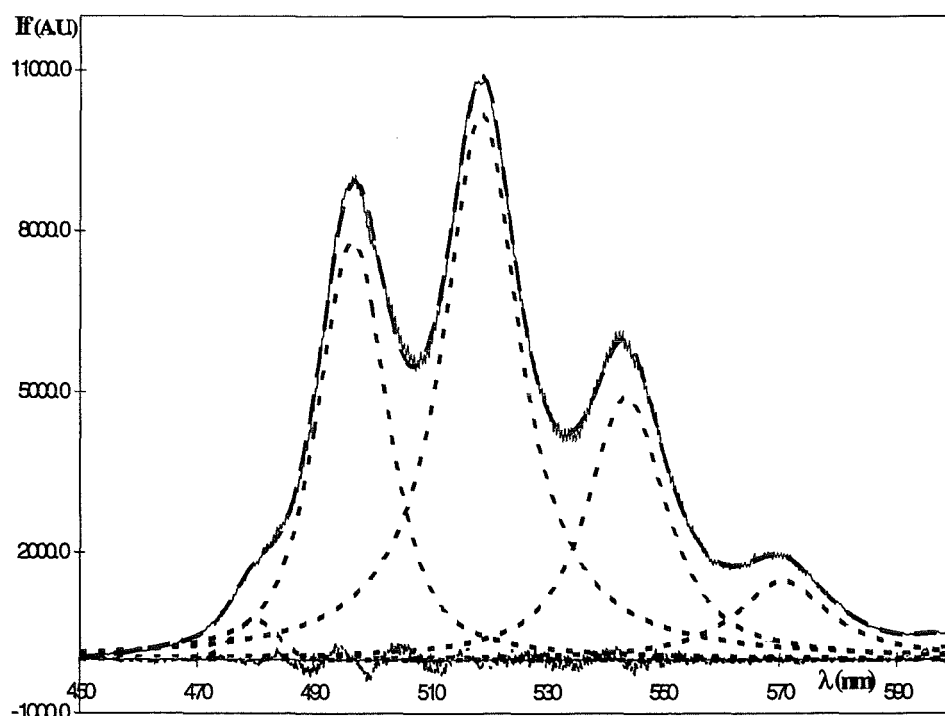


Figure 4 : $\text{UO}_2(\text{OH})_3^-$ fluorescence spectrum (—) together with convoluted spectrum (— —) (obtained from single peaks (- -)) and residual (— . . —). $[\text{U}] 4.10^{-7}\text{M}$, $I = 0.1$, pH 10. Time delay 1.5 μs , aperture time 0.7 μs , integration time 1s, number of accumulations 30.

Recent work (Moulin *et al.*, 1995) at 4.10^{-7}M and 4.10^{-8}M (see figures 2c and 2d) between pH 3 and 4 has allowed to identify the first uranium hydroxo complex using time resolution. Figure 5 presents the fluorescence spectrum of UO_2OH^+ obtained at pH 4. The four main peaks are located at 497, 519, 544 and 570 nm (shift of 9 nm relative to free uranyl) and the average FWHM is around 16 nm. Fluorescence lifetime observed for UO_2OH^+ is much longer than for free uranyl or $\text{UO}_2(\text{OH})_3^-$, namely 80 μs .

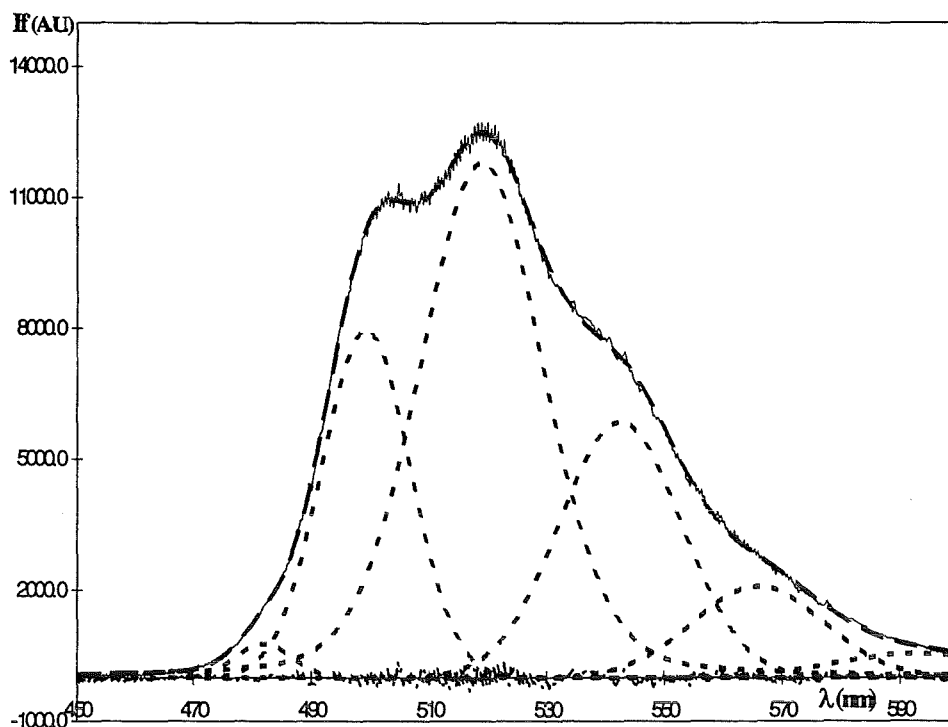


Figure 5 : UO_2OH^+ fluorescence spectrum (—) together with convoluted spectrum (— · —) (obtained from single peaks (- -)) and residual (— · · —). 4.10^{-8}M , $I = 0.1$, $\text{pH } 4$. Time delay $10 \mu\text{s}$, aperture time $100 \mu\text{s}$, integration time 1s , number of accumulations 30.

The next step is to identify $\text{UO}_2(\text{OH})_2$ (see figure at $[\text{U}] = 40 \text{ nM}$), but this time, there is the presence of two other species (UO_2OH^+ and $\text{UO}_2(\text{OH})_3^-$). The latter one, as previously mentioned, has a very short lifetime ($0.8 \mu\text{s}$) and is likely to be eliminated by time resolution, on the contrary the former one has a very long lifetime and it is necessary to work at pH high enough to limit its concentration. It has been decided to work at uranium concentration of 4.10^{-7}M with pH close to 8.5 and at uranium concentration of 4.10^{-8}M with pH close to 7 (see figures 2c and 2d) with different gates set at least $10 \mu\text{s}$ after the laser pulse in order to eliminate spectroscopically the influence of $\text{UO}_2(\text{OH})_3^-$. However, whatever the delay (or width) of the gate, it is not possible to directly obtain a single fluorescence spectrum. Hence, lifetime estimated for $\text{UO}_2(\text{OH})_2$ is around 10 to $20 \mu\text{s}$ which is shorter than UO_2OH^+ ($80 \mu\text{s}$) Therefore, in this particular case, spectrum deconvolution is necessary and by doing so, it is possible to characterize the fluorescence spectrum of $\text{UO}_2(\text{OH})_2$ with four main peaks located at 488, 508, 534 and 558 nm and an average FWHM around 21 nm. It should also be noted that fluorescence wavelengths obtained for $\text{UO}_2(\text{OH})_2$ are very close to the one of free uranyl.

The next step is to identify, the polynuclear species such as $(\text{UO}_2)_2(\text{OH})_2^{2+}$, $(\text{UO}_2)_3(\text{OH})_5^+$, $(\text{UO}_2)_3(\text{OH})_7^-$. Hence, even if these species are only present at high uranium concentrations (except for $(\text{UO}_2)_3(\text{OH})_5^+$) likely not to be representative of those encountered near a waste nuclear disposal, spectroscopic characterization is important both for comparison purposes and fluorescence data bank improvement. For $(\text{UO}_2)_3(\text{OH})_7^-$ identification, the uranium concentration is fixed to 4.10^{-6}M (see figure) and more specially to 4.10^{-5}M (see figure 2a) with pH between 8 and 9 in order to eliminate $\text{UO}_2(\text{OH})_2$ in terms of concentration. Figure 6 presents the fluorescence spectrum of $(\text{UO}_2)_3(\text{OH})_7^-$ with main fluorescence wavelengths located at 503, 523, 547 and 574 nm with a very large average FWHM of 24 nm. Moreover, the lifetime observed is around 230 μs and has allowed easy time resolution elimination of $\text{UO}_2(\text{OH})_3^-$ ($\tau = 0.8 \mu\text{s}$). It should be noted that this lifetime is very long, since it is even longer than the one obtained for uranium ultratrace analysis in phosphoric acid (200 μs) (Moulin *et al.*, 1990).

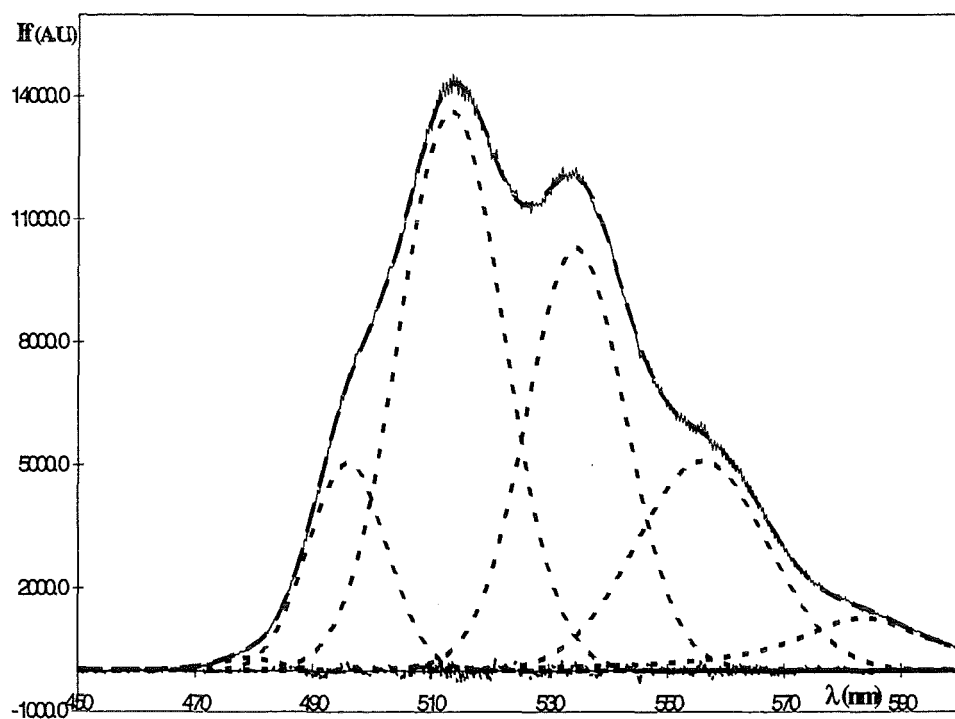


Figure 6 : $(\text{UO}_2)_3(\text{OH})_7^-$ fluorescence spectrum (—) together with convoluted spectrum (---) (obtained from single peaks (- -)) and residual (- . -). $[\text{U}] 4.10^{-5}\text{M}$, $I=0.1$, $\text{pH } 8.9$. Time delay 250 μs , aperture time 250 μs , integration time 5 s, number of accumulations 30.

For the observation of $(\text{UO}_2)_3(\text{OH})_5^+$, the concentration used is 4.10^{-5}M at pH 6.6 (see figure 2a). Figure 7 presents the fluorescence spectrum of $(\text{UO}_2)_3(\text{OH})_5^+$ with main fluorescence wavelengths at 496, 514, 535 and 556 nm with an average FWHM of 20 nm. The lifetime observed for this complex is around 23 μs .

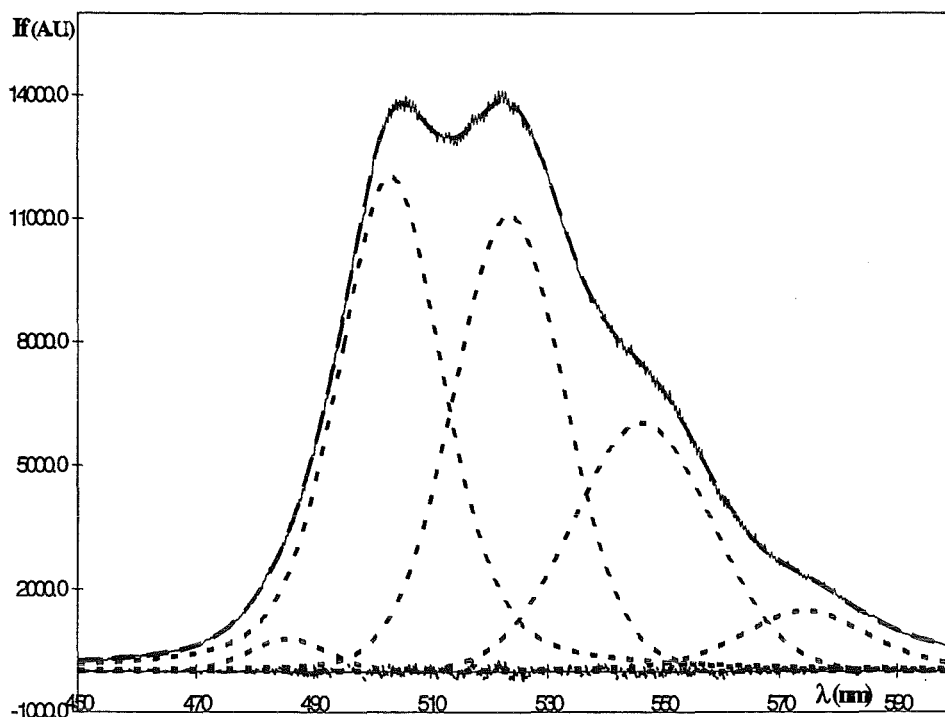


Figure 7 : $(\text{UO}_2)_3(\text{OH})_5^+$ fluorescence spectrum (—) together with convoluted spectrum (— —) (obtained from single peaks (- -)) and residual (— . . —). $[\text{U}] 4.10^{-5}\text{M}$, $I = 0.1$, $\text{pH } 6.6$. Time delay $10 \mu\text{s}$, aperture time $80 \mu\text{s}$, integration time 1s , number of accumulations 30.

Finally, for $(\text{UO}_2)_2(\text{OH})_2^{2+}$ identification, three different uranium concentrations are used 2.10^{-4}M , 4.10^{-4}M and 8.10^{-4}M and working close to $\text{pH } 4$. Hence, it is necessary to work at very high uranium concentration to favour $(\text{UO}_2)_2(\text{OH})_2^{2+}$ relatively to UO_2OH^+ as one begins to see it on figure 2b and 2a where increasing the uranium concentration clearly favour the former one. For example, at 8.10^{-4}M , the concentration of $(\text{UO}_2)_2(\text{OH})_2^{2+}$ is five times the one of UO_2OH^+ . Nevertheless, the main problem encountered here is the presence in all cases of UO_2OH^+ that has a rather long lifetime of $80 \mu\text{s}$. By performing experiments at these different concentrations, it is possible to drastically vary, the ratio of the first uranium hydroxo complex and the uranium hydroxo dimer and by doing so, it is possible to observe by spectral deconvolution that $(\text{UO}_2)_2(\text{OH})_2^{2+}$ had a similar spectrum than UO_2OH^+ *i.e.* 497, 519, 542, and 570 nm with an average FWHM of 18 nm. The lifetime observed for this complex is around $9 \mu\text{s}$. It should be noted that, as expected, all these different polynuclear complexes ($(\text{UO}_2)_3(\text{OH})_7^-$, $(\text{UO}_2)_3(\text{OH})_5^+$, $(\text{UO}_2)_2(\text{OH})_2^{2+}$) present broader spectra than the mononuclear complexes due to the presence of more vibrational modes for the former ones.

Concerning the **carbonato complexes**, experiments have shown that they are not fluorescent.

Table I sums-up precisely the different spectroscopic data obtained in this study (main fluorescence wavelengths, full width at mid height for each main peak and lifetime) as well as a comparison with literature data. It should be noted that it exists a rather good agreement in terms of fluorescence wavelengths for free uranyl, the first hydroxo complex and the dimer $((\text{UO}_2)_2(\text{OH})_2^{2+})$.

Table I : Spectroscopic data (fluorescence wavelengths, full width at mid height, lifetime) on uranium hydroxo complexes and comparison with literature data.

Species	Fluorescence wavelengths ^a (nm)	FWMH ^b (nm)	Lifetime (μs)
UO_2^{2+} ^c	470-488-509-533-559-588	12-13-13-14	2 ± 0.1
d	489-510-535-560	-	1.7
e	488-509-534-560	-	0.9
UO_2OH^+ ^f	480-497-519-544-570-598	14-16-16-19	80 ± 5
d	496-518-542-566	-	32.8
$\text{UO}_2(\text{OH})_2$ ^c	488-508-534-558	19-21-21-23	10 - 20
d	-	-	3.2
$\text{UO}_2(\text{OH})_3$ ^{-c}	482-499-519-543-567-594	18-24-24-27	0.8 ± 0.1
d	506-524-555-568	-	0.4
$(\text{UO}_2)_2(\text{OH})_2^{2+}$ ^c	480-497-519-542-570-598	14-18-17-20	9 ± 1
d	498-518-544	-	9.5
e	499-519-542-566	-	2.9
$(\text{UO}_2)_3(\text{OH})_5$ ^{+c}	479-496-514-535-556-584	16-20-20-25	23 ± 3
d	515-536	-	6.6
e	500-516-533-554	-	7
$(\text{UO}_2)_3(\text{OH})_7$ ^{-c}	503-523-547-574	21-23-25-26	230 ± 20
d	-	-	10

a) In dark, main fluorescence wavelengths, b) FWMH for main fluorescence wavelengths,

c) this work, d) see Eliet *et al.* 1995 e) see Kato *et al.* 1994 f) see Moulin *et al.* 1995.

The major interest in using powerful deconvolution software is the capability to first precisely determine peak positions especially in the case of very broad spectra such as for the uranium tri hydroxo and polynuclear species where main transitions interfere with one another and lead to spectroscopic shifts of the global fluorescence spectrum. Secondly, the wavelength gaps observed between each peaks (corresponding to energy gaps between the different ground state levels) of each fluorescent species are constants and equal (within ± 2 nm) to 17, 20, 24, 25 and 28 nm corresponding respectively to the energy gaps of the ground state as previously mentioned. This speciation study shows also that hydrolysis of uranium leads to the stabilization of the excited state at 20502 cm^{-1} (which leads to a bathochromic shift) with no (or little) modification of the different ground states. It is also interesting to note that if, as previously mentioned, free uranyl is taken as a reference, the fluorescence peaks gradually shift (except for $\text{UO}_2(\text{OH})_2$) as a function of hydrolysis or complexation starting at 488 nm (first main fluorescent peak) for UO_2^{2+} , continuing at 499 nm for $\text{UO}_2(\text{OH})_3^-$ and finishing at 503 nm for $(\text{UO}_2)_3(\text{OH})_7^-$. The same trend is observed for the full width at mid height from 13 nm to 24 nm since with complexation of the uranyl ion, more vibrational modes are present which contribute to a broadening of the fluorescence spectrum.

Concerning the lifetimes, except for free uranyl and the dimer, the data obtained are very different and always smaller in the literature. These differences are likely to be due as said previously to quenching or complexing effects (presence of unwanted inorganic or organic constituents in the initial solution preparation or in reagents used), temperature effects (since uranium fluorescence is very sensitive to temperature variation) or differences in chemical conditions (ionic strength, buffer, ...). Anyhow, a longer lifetime (with single exponential decay) is likely to be representative of the real lifetime of the species in solution.

Concerning the evolution of the lifetime with the degree of hydrolysis, no clear trend is observed. On the contrary, for polymer species, the lifetime increases as a function of the complexity of the molecule, that can be eventually linked to the diminution of water molecules as a function of the steric hindrance of the complex.

In this particular study, only two selectivity criteria of TRLIF *i.e.* emission and temporal selectivity have been used since most measurements are performed with a fixed excitation wavelength (266 nm). By using various excitation wavelengths, it is possible to favour one complex over another, since every complex possess a specific excitation spectrum. Hence, this feature has been recently observed for $(\text{UO}_2)_3(\text{OH})_5^+$ where fluorescence intensity is five times more important with excitation at 355 nm than at 266 nm (with the same laser energy and operating conditions). On the contrary, fluorescence intensity for UO_2^{2+} and UO_2OH^+ are respectively ten and forty times less important with excitation at 355 nm than at 266 nm. This

excitation selectivity feature could be used together with emission and temporal selectivity when dealing with very complex solutions.

Works in this direction are under progress as well as the study of interactions between these different complexes and humic acids.

CONCLUSION

Time-Resolved Laser-Induced Fluorescence (TRLIF) has been successfully used for the spectroscopic characterization of the different uranium hydroxo complexes. By using very well characterized chemical conditions (uranium concentration, pH, ionic strength, atmospheric partial pressure) and using whenever possible time-resolution and then spectral deconvolution, the obtaining of precise fluorescence spectra and lifetimes for these different complexes proved to be feasible.

ACKNOWLEDGEMENTS

We would like to thank Dr P. Reiller for realizing the uranium speciation program.

REFERENCES

- Azenha M.E.D.G., H.D Burrows, S.J. Formosinho, M.G.M Miguel, A.P. Daramayan, and I.V. Khudyakov, *J. Lumines.* **48/49**, 522 (1991).
- Bell J.Y., and R.E. Bigers, *J. Mol. Spectrosc.* **25**, 312 (1968).
- Berthoud T., P. Decambox, B. Kirsch, P. Mauchien, and C. Moulin, *Anal. Chem.* **60**, 1296 (1988).
- Bidoglio G., N. Omenetto, and P. Robouch, *Radiochim. Acta* **52/53**, 57 (1991).
- Brina R., and A.G. Miller, *Anal. Chem.* **64**, 1413 (1992).
- Buffle J., *Complexation reactions in aquatic systems* (Wiley and Son, Eds), New-York, 1988.
- Bünzli J.C.G., and G.R. Choppin, *Lanthanide probes in life chemical and earth sciences*. Elsevier. Amsterdam, Oxford, New-York, Tokyo (1989).
- Choppin G.R., and B. Allard, *Handbook on the Physics and Chemistry of the Actinides* (A.J. Freeman, C. Keller Eds), Amsterdam (1985), Vol. 3, Chap 11.
- Couston L., D. Pouyat, C. Moulin, and P. Decambox, *Appl. Spectro.* **49**, (1995).
- Deniau H., P. Decambox, P. Mauchien, and C. Moulin, *Radiochim. Acta* **61**, 23 (1993).
- Deschaux M., and M. D. Marcantonatos, *Chem. Phys. Lett.* **63**, 283 (1979).
- Dobbs J.C., W. Susetyo, F.E. Knight, M.A. Castles, L.A. Carreira, and L.V. Azarraga, *Anal. Chem.* **61**, 483 (1989).

- Eliet V., G. Bidoglio, N. Omenetto, L. Parma, and I. Grenthe, *J. Chem. Soc. Farad. Trans* **91**, 275, 2285(1995).
- Fujimori H., T. Matsui, and K. Suzuki, *J. Nuclear Sci and Techno.* **25**, 798 (1988).
- Graca M., S.J. Formosinho, A.C. Cardoso, and H.D. Burrows, *Faraday Trans I* **80**, 1735 (1984).
- Grenthe I., J. Fuger, J.M. Konings, R. J. Lemire, A.B. Muller, C. Nguyen Trung, H. Wanner, *Chemical Thermodynamics of Uranium*, NEA-TDB, O.E.C.D. Nuclear Energy Agency Data Bank, North Holland, Amsterdam (1992).
- Kato Y., G. Meinrath, T. Kimura, and Z. Yoshida, *Radiochim. Acta* **64**, 107 (1994).
- Kim J.I., H. Wimmer, and R. Klenze, *Radiochim. Acta* **54**, 35 (1991).
- Lemire R.J., and P.R. Tremaine, *J. Chem. Eng. Data* **25**, 361 (1980).
- Meinrath G., Y. Kato, and Z.J. Yoshida, *Radio. Nucl. Chem.* **174**, 299 (1993).
- Moriyasu M., Y. Yokoyama, and S.J. Ykeda, *Inorg. Nucl. Chim.* **39**, 2205 (1977).
- Moulin C., C. Beaucaire, P. Decambox, and P. Mauchien, *Anal. Chim. Acta*, **238**, 291 (1990).
- Moulin C., P. Decambox, and L. Trecani, *Anal. Chim. Acta* **321**, 121 (1996).
- Moulin C., P. Decambox, and P. Mauchien, *Appl. Spectro.* **45**, 116 (1991).
- Moulin C., P. Decambox, and P. Mauchien, V. Moulin, and M. Theyssier, *Radiochim. Acta* **52/53**, 119 (1991).
- Moulin C., P. Decambox, P. Mauchien, L. Couston and D. Pouyat, *Anal. Chem.* **68**, 3204 (1996).
- Moulin C., P. Decambox, V. Moulin, J.G. Decaillon, *Anal. Chem.* **67**, 348 (1995).
- Moulin V., and G. Ouzounian, *Appl. Geochem.* **1**, 179 (1992).
- Moulin V., J. Tits, C. Moulin, P. Decambox, P. Mauchien, and O. de Ruty, *Radiochim. Acta* **58/59**, 121 (1992).
- Nikitin Y.E., Y.I. Murinov, D.D. Fonichev, G.S. Parshin, and V.P. Kazakov, *Radiokhimiya* **20**, 244 (1978).
- Romanovskaya G.I., V.I. Pogonin, and A.K. Chibisov, *Zhurnal Analiticheskoi Khimii* **35**, 70 (1980).
- Young J.E., and P. T. Deason, *Anal. Chem. Sym. Ser.* **19**, 7 (1984).
- Zook A., L.H. Collins, and C.E. Pietri, *Mikrochim. Acta II* 457 (1981).

1st Technical Report

EC Project

**"EFFECTS OF HUMIC SUBSTANCES ON THE MIGRATION OF RADIONUCLIDES:
COMPLEXATION AND TRANSPORT OF ACTINIDES"**

GERMETRAD Contribution to Task 3

MOBILITY OF Am, Eu AND Tc IN THE PRESENCE OF HUMIC ACIDS

Reporting period 1997

Christelle FLEURY, Jacques PIERI, Françoise GOUDARD, Jean-Pierre DURAND

***GERMETRAD
2 Rue de la Houssinière 44072 NANTES, FRANCE***

INTRODUCTION

The impact of the radionuclides on the environment is the subject of intensive studies to determine their toxicity. The speciation forms of the radionuclides have to be known ; their mobility in the biosphere can be assessed in this way.

The supports able to increase or decrease the mobility of these toxic elements are of different types : inorganic (rock matrix, oxides) or organic (humic substances). The latter are recognized for their great affinity towards some radionuclides, i.e. actinides, Kim *et al.* (1989).

The present work will try to estimate the sorption rate of three radionuclides (americium, europium and technetium) by humic acids.

Actinides (Am) and lanthanides (Eu) have a similar behaviour towards organic matter ; on the other hand, comparatively, few studies have been undertaken on technetium.

This radionuclide is released in the environment as highly mobile pertechnetate TcO_4^- ; its biological availability is very high and the assessment of radiation dose to man has to be determined. However, when reducing conditions prevail in the soils, the geochemical mobility is in fact much lower than was originally suspected.

The aim of this work is to try to assess the behaviour of Tc in oxic and anoxic conditions in order to establish the mobility of Tc in the presence of humic acids. The study is based on two methodologies : a static one (in batch) and a dynamic one (in column), where different parameters can be investigated : length of the incubation, flow rate, amount of humic acid, oxidation state of Tc.

EXPERIMENTAL PROCEDURE

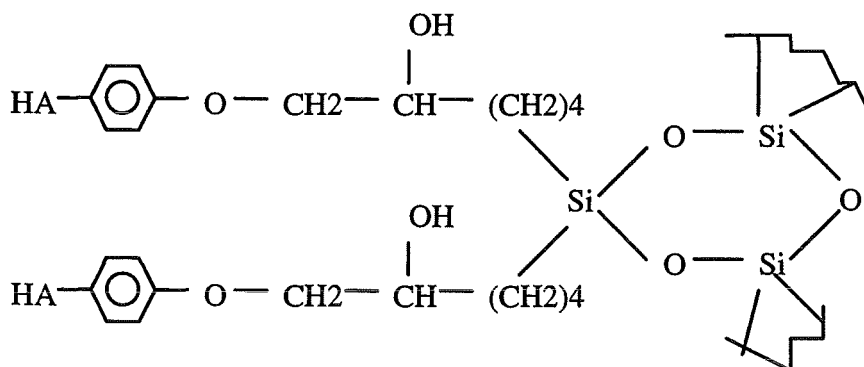
In order to investigate the retention of actinides (Am-241) and lanthanides (Eu-152) by humic substances, column experiments were carried out and also static experiments in the case of europium.

Two series of experiments were performed to determine the behaviour of technetium-99 towards humic acids :

- ◆ a series of batch experiments
- ◆ a series of dynamic experiments (in column).

Material

The "humic acid gel" was created at the laboratory ; it is made of porous silica beads on which was humic acid (Aldrich) covalently bound :



The features of the Sorbsil silica are :

BET surface area : 320m²/g

Pore volume : 1.75mL/g

SiO₂ 99.5% min.

The proton exchange capacity (PEC) of the gel was investigated by Czerwinski *et al.* ; the gel was composed by 2.23mg HA/g silica and the PEC=2.54 10⁻²meq/g.

In the present experiments, the humic acid content is 18mg per gram of silica ; the PEC should be increased proportionnaly.

The radionuclides used were :

- ◆ Am-241 (in HNO₃) and Eu-152 (in HCl) supplied by CEA are detected by gamma counting (Cobra II Packard)
- ◆ Tc-99 (NH₄TcO₄) supplied by Amersham is determined by a liquid scintillation analyser (Tri-Carb Packard).

Americium was firstly used and was then replaced by europium, considered as an analogue to the actinides.

The initial experiments (with Am and Eu) were conducted with phosphate buffer, but it was demonstrated that it was very complexant towards actinides ; thus, it has been replaced by sodium perchlorate. The NaClO₄ has no buffering capacity but it is inert towards the radionuclides.

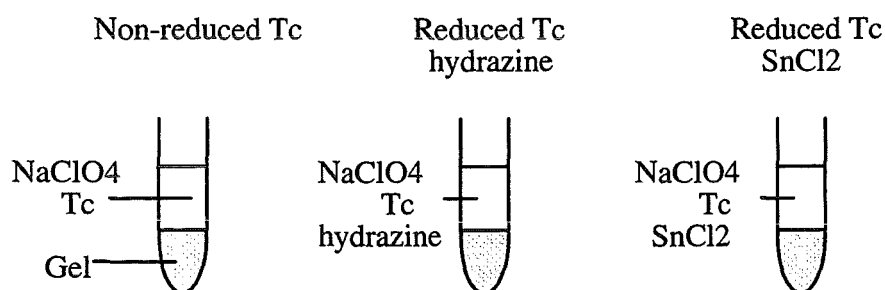
Procedure

♦ *Batch experiments*

For the europium study, a constant amount of "HA-silica gel" has been incubated and shaken overnight with increasing amounts of Eu in phosphate buffer. The samples were centrifuged and the supernatants and pellets were analysed for γ -activity.

In the case of Tc-99, 50mg of "HA-silica gel" were incubated with the radionuclide in the presence or not of a reducing agent (hydrazine or stannous chloride SnCl_2).

Three sorts of tests were investigated :



- The humic acids were first incubated with the reducing agent (1 hour) in NaClO_4 50mM (degassed and saturated with nitrogen) ; the pH was adjusted at 5 or 8.

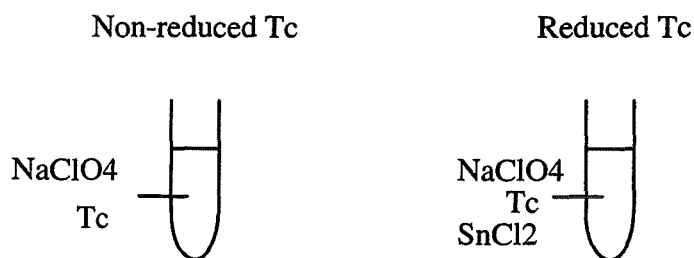
- Tc, in NaClO_4 at the required pH, was then added to the gel. The solution and the tube were saturated with nitrogen. The samples were incubated and shaken 5 or 30 hours at room temperature.

- The tubes were then centrifuged 15 minutes at 4000tr/min.

The advantage of the binding of the humic acids to the silica is the size of the particle. They sediment at very low centrifugal field and it is very easy to separate the HA from the solution.

- The supernatants were removed and analysed by scintillation counting. The pellets were resuspended in NaClO_4 and counted too.

Two standards, without humic acids, were done in parallel :



The standards were incubated, shaken, centrifuged and counted the same way as the tests.

♦ *Column experiments*

Small columns containing 0.7g of HA-silica gel (12.6mg HA approx.) were equilibrated overnight with the chosen eluent.

For the study of Am and Eu, a phosphate buffer was used at pH from 6 to 8 and at different flow rates (4.5, 11 and 19 mL/h)

In the case of technetium, two types of solutions were used to equilibrate the HA-silica gel :

- ♦ a non-reducing medium containing NaClO_4 50mM only, degased and saturated with nitrogen, at the required pH,
- ♦ a reducing medium containing NaClO_4 50mM and hydrazine or SnCl_2 .

Several combinations of these experimental conditions were used to study the influence of the oxydation state :

HA-silica gel	Technetium
Non-reduced	Non-reduced
Non-reduced	Reduced (hydrazine)
Non-reduced	Reduced (SnCl_2)
Reduced (SnCl_2)	Reduced (SnCl_2)

- The radionuclide was incubated 3 to 4 hours with the reducing agent and NaClO_4 at the required pH before injecting. All the solutions were degased and saturated with nitrogen to prevent re-oxidation.

- The flow rate was relatively low (5 mL/h) because the affinity of Tc for HA is smaller than that of the actinides.

- After the injection, Tc is eluted with NaClO_4 . Approximately 10mL are collected and an aliquot is taken for the scintillation counting. The humic acid gel is resuspended in NaClO_4 and an aliquot is counted.

RESULTS

Americium and europium

♦ *Column experiments*

The retention rate of Am and Eu by the humic acid-silica gel is represented in the figures 1 and 2.

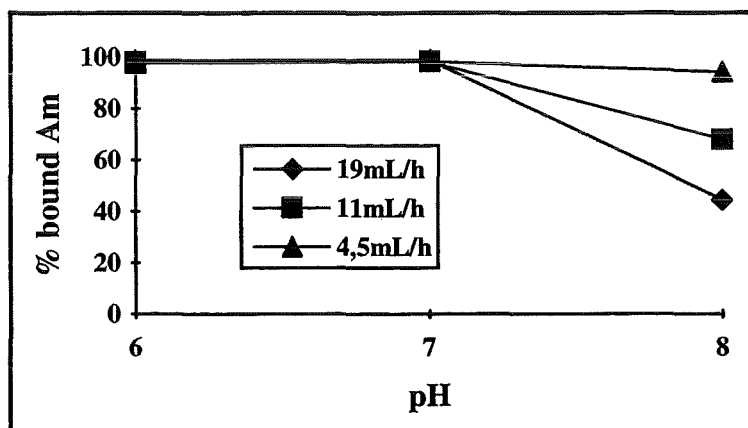


Fig 1 : Retention of Am-241 by HA-silica gel.

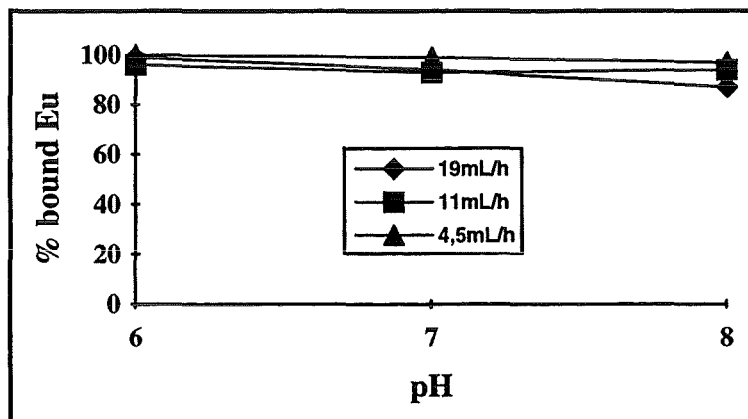


Fig 2 : Retention of Eu-152 by HA-silica gel.

♦ *Batch experiments*

These are the results of one experiment (Fig 3).

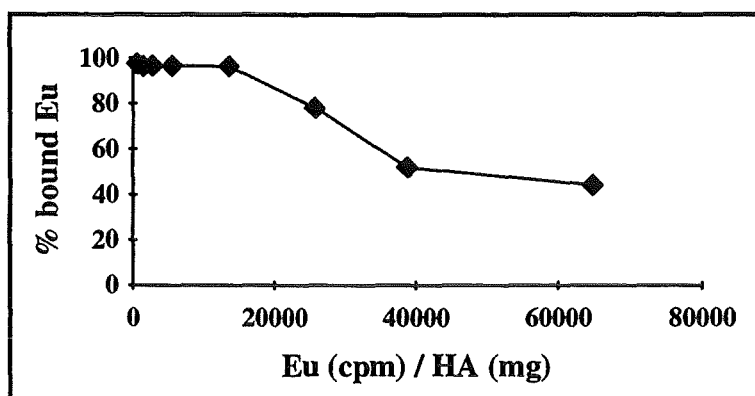


Fig 3 : Retention of Eu by HA-silica gel in static conditions.

Technetium

♦ *Column experiments*

The results are expressed in the table 1 and the figure 4.

	HA-silica gel not reduced (HA-NR)			HA-silica gel reduced (HA R)
	Tc not reduced (Tc NR)	Tc reduced by hydrazine (Tc R hydr)	Tc reduced by SnCl ₂ (Tc R SnCl ₂)	Tc reduced by SnCl ₂ (Tc R SnCl ₂)
pH 5	0	4	21	94
pH 8	0	3.4	8.3	38.7

Table 1 : % Tc bound to HA-silica gel in dynamic conditions.

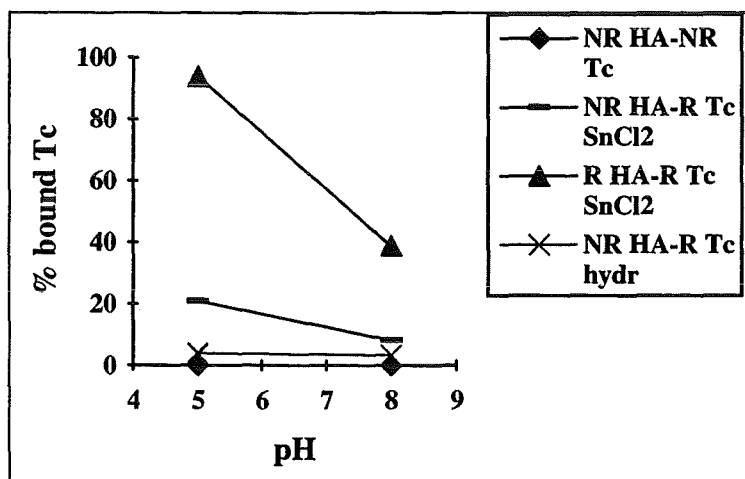


Fig 4 : Retention of Tc on HA-silica gel in dynamic conditions.

♦ *Batch experiments*

The obtained results are summarised in table 2 and represented in figure 5

% Tc bound to non-reduced HA-silica gel				
Incubation	pH	NR Tc	R Tc-SnCl ₂	R Tc hydrazine
5 hours	5	7.4	99.4	27.9
5 hours	8	9.4	9.9	14
30 hours	5	7.8	89.9	28.1
30 hours	8	9.1	9.5	18.8

Table 2 : Retention of Tc on HA-silica gel in static conditions.

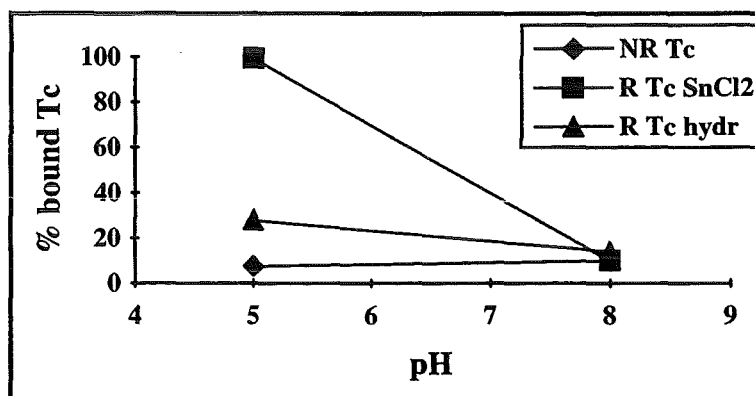


Fig 5 : Retention of Tc on HA-silica gel in static conditions.

DISCUSSION

Americium and europium

♦ *Column experiments*

The retention was dependent on the pH and the flow rate.

The sorption rate at pH 6 and 7 was quite total, reflecting a great affinity between the radionuclides and the humic acids. Similar results were observed in number of works (Bertha and Choppin (1978), Torres and Choppin (1984), Caceci (1985)).

The influence of the flow rate was not significative at pH6 and 7 because Am and Eu are very reactive towards humic acids. The speciation forms were positively charged while the humic

acids were negative : the affinity was at its maximum and the sorption was very quick (Moulin *et al.* (1992)).

At pH 8, carbonated forms of radionuclides appear ; they are less positively charged and even negative. At lower flow rate, the affinity was great enough to allow radionuclides to bind to the humic acids but as the flow rate was increased, the amount of bound radionuclides decreased, especially in the case of americium.

♦ *Batch experiments*

These were carried out to estimate, in the future, the binding constant between Eu and the humic acid coated silica beads.

Increasing ratios of Eu to HA-silica gel were used to try to saturate the binding sites of the biopolymer.

The figure 3 showed that the sorption of Eu decreased as the ratio Eu/HA increased, but a plateau was attained at approximately 45% of Eu bound to the HA silica gel.

The binding capacity of this gel is very important and higher ratios Eu/HA have to be used to decrease the sorption rate of europium.

Technetium

♦ *Non-reduced Tc*

Under oxic conditions, Tc is present as pertechnetate TcO_4^- in the environment. TcO_4^- is very mobile and available for plants, before reducing progressively in TcO_2 which is hydrolysed in $TcO(OH)_2$, insoluble.

In batch experiments, a sorption of 7 to 9% of Tc was observed in oxic conditions (fig 5). Two hypothesis can be put forward : either a part of TcO_4^- was reduced (by humic acids or the oxygen of the medium) and sorbed onto the humic acids, or TcO_4^- was directly bound to the HA. The highly polar groups of the humate fraction may indeed be expected to play a role in Tc retention but "pertechnetate would not be expected to sorb in major quantities on the largely anionic colloids in natural water or soils" (Wildung *et al.*, 1979).

In dynamic conditions (fig 4), Tc was entirely eluted with NaClO_4 without any sorption onto the humic acids. The flow rate was however relatively low, but it was still too fast to allow humic acids to eventually reduce the pertechnetate ion..

♦ *Reduced Tc*

Hydrazine

Whatever the conditions were, static or dynamic, the retention of hydrazine-reduced Tc was not very important, except at pH 5 (batch, fig 5) where the sorption rate was increased to 30%. This influence of pH was already noticed by Stalmans *et al.* (1986), Wildung *et al.* (1979). In dynamic system, the sorption of Tc was weaker (fig 4). But nevertheless, hydrazine was recognized as a good reducing agent (Fowler *et al.* (1981), Masson *et al.* (1981)). Further experiments will be carried out to confirm this result.

Stannous chloride

The sorption of Tc on humic acids in batch experiments was very important at pH 5 (Table 2). The reduction of TcO_4^- in $\text{TcO}(\text{OH})_2$ has a great impact on its behaviour. This fact was also remarked by Stalmans (1986).

Doubts were expressed about the physicochemical form of the technetium ; as $\text{TcO}(\text{OH})_2$, it is insoluble and seems to sorb onto the walls of the vessels (tube, column, pipes). This phenomenon has been noticed with the two standards realized without HA. The whole amount of non-reduced Tc, after centrifugation, was in solution whereas the amount of reduced Tc was not entirely recovered after counting. The technetium certainly sorbed onto the walls or precipitated (because it was insoluble) and sedimented during centrifugation.

In the presence of the humic acids, if $\text{TcO}(\text{OH})_2$ sedimented, the pellet would contain both HA and Tc ; the radionuclide would not be sorbed onto the gel, but just "co-sedimented".

At pH 8, however, the sorption was much weaker. Since Sn^{2+} were found to reduce TcO_4^- over the pH range from 0 to 14 (Stalmans, 1986), at pH 5 or 8 the same speciation forms were encountered. Insoluble reduced Tc was then able to stay in solution during centrifugation.

Concerning the kinetics of adsorption, the results were very similar for both lengths of incubation (5 or 30 hours), this is the reason why the results obtained with 30 hours of incubation were not represented on the figure 5. Equilibrium was more quickly attained than in a previous work (Stalmans, 1986).

Column experiments gave the same order of results (Table1, fig 4). At pH 5, the strong retention of Tc by the gel could represent a great affinity of $TcO(OH)_2$ for HA or could show the presence of colloids too large to flow through the gel. Once again, the results at pH 8 evidenced that the sorption of reduced Tc depends on the pH.

There was however a larger amount of Tc sorbed onto the gel in dynamic than in static conditions ; this difference could be due to the amount of binding sites which is much greater in the columns than in the tubes of the batch experiments.

CONCLUSION

The results obtained in this study confirmed the great affinity of the humic substances towards transuranic elements. The retention rate is in fact very near to 100% in dynamic conditions, except when the flow rate is too fast and the pH too alkaline.

In batch experiments, it is very difficult for Eu to saturate all the available sites ; the amount of radionuclides should be increased.

The disadvantage of this kind of study was that americium and europium sorbed to the walls of the tubes and the columns and this supplementary sites could compete with those of the humic acids.

This problem was encountered with Tc too, but only at the reduced state. But as pertechnetate, it always stays in solution, and it does not even bind to the humic acids. On the other hand, under reducing conditions, the amount of Tc sorbed to the walls increases, but $TcO(OH)_2$ is also more reactive towards the binding sites of the humic acids, especially when these are reduced. In this case, a total retention of Tc can be observed. These reducing conditions can be found in roc matrix pores in which anoxic atmosphere is present due to the absence of oxygen (used by the microbiological activity).

These results will be followed by other experiments in other conditions (pH, ionic strength) to complete the knowledge concerning the sorption of Am, Eu and Tc by the "humic acid gel".

REFERENCES

- BERTHA E.L., and CHOPPIN G.R.** (1978). Interaction of humic and fulvic acids with Eu(III) and Am(III). *J. Inorg. Nucl. Chem.*, 40, 655-658.
- CACECI M.S.** (1985). The interaction of humic acid with europium(III). Complexation strength as a function of load and pH. *Radiochimica Acta* 39, 51-56.
- CZERWINSKI K.R., CEREFICE G.S., BUCKAU G., KIM J.I., MILCENT M.C., FLEURY C., and PIERI J.** Sorption of europium to humic acid based resin : the role of humic coating in sorption. Submitted to Environmental Science and Technology.
- FOWLER S.W., BENAYOUN G., PARSI P., ESSA M.W.A., and SHULTE E.H.** (1981). Experimental studies on the bioavailability of technetium in selected marine organisms. *In : Impact of radionuclide releases into the marine environment*, 319-339. Vienna : IAEA.
- KIM J.I., BUCKAU G., BRYANT E., AND KLENZE R.** (1989). Complexation of americium(III) with humic acid. *Radiochimica Acta*, 48, 135-143.
- MASSON M., APROSI G., LANIECE A., GUEGUENIAT P., and BELOT Y.** (1981). Approches expérimentales de l'étude des transferts du technetium à des sédiments et à des espèces marines benthiques. *In : Impact of radionuclide releases into the marine environment*, 341-359. Vienna : IAEA.
- MOULIN V., TITS J., and OUZOUNIAN G.** (1992). Actinide speciation in the presence of humic substances in natural water conditions. *Radiochimica Acta* 58/59, 179-190.
- STALMANS M.** (1986). The behaviour of technetium in the environment. Physicochemical aspects. *Thesis*, University of Leuven, Belgium.
- STALMANS M., MAES A., and CREMERS A.** (1986). Role of organic matter as a geochemical sink for technetium in soils and sediments. *In : Technetium in the environment*, Desmet G. and Myttenaere C. Ed. 91-113.
- TORRES R.A., and CHOPPIN G.R.** (1984). Europium(III) and americium(III) stability constants with humic acid. *Radiochimica Acta*, 35, 143-148.
- WILDUNG R.E., McFADDEN K.M., and GARLAND T.R.** (1979). Technetium sources and behavior in the environment. *J. Envir. Qual.*, 8, N°2, 156-161.

1st Technical Progress Report

EC Project:

**"Effects of Humic Substances on the Migration of Radionuclides:
Complexation and Transport of Actinides"**

Project No.: FI4W-CT96-0027

FZR/IFR Contribution to Task 1 (Sampling and Characterization)

**Isolation and Characterization of Aquatic Humic Substances
from the Bog "Kleiner Kranichsee"**

Reporting period 1997

K. Schmeide, H. Zänker, K.H. Heise, H. Nitsche

Forschungszentrum Rossendorf e. V.
Institute of Radiochemistry
P.O. Box 510119
01314 Dresden
Germany

CONTENTS

	<u>Page</u>
Abstract	165
1 Introduction	167
2 Testing of Different Resins for Isolating Aquatic Humic Substances	168
3 Water-sampling Sites	173
3.1 Johanngeorgenstadt Area	173
3.2 Königstein Area	173
4 Characterization of Colloid Particles in the Kranichsee Bog Water	175
5 Preparation of Reference and Site-Specific Humic Substances	181
5.1 Reference Humic Acid	183
5.2 Isolation and Purification of Site-Specific Humic Substances	183
6 Characterization of the Isolated Humic Substances	185
6.1 Ash and Moisture Content	185
6.2 Elemental Composition	186
6.3 Major Inorganic Components	187
6.4 Functional Groups	188
6.5 Capillary Zone Electrophoresis	190
6.6 IR Spectroscopy	191
7 References	194

Abstract

Surface water has been studied from the mountain bog 'Kleiner Kranichsee'. This bog is situated in the Johanngeorgenstadt area (Saxony/Germany) close to an abandoned uranium mine and mine tailing piles. The bog water contains about 130 mg/L of organics (primarily humic and fulvic acid).

First, bog water colloids were determined for their particle size and size distribution using photon correlation spectroscopy (PCS) and scanning electron microscopy (SEM) in combination with size fractionation by filtration. Second, about 400 L of the bog water were processed in order to isolate aquatic humic substances. Supelite™ DAX-8 (Supelco) was used as adsorption resin. The humic material was separated into humic and fulvic acids. A total of 14 g of humic acid and 10 g of fulvic acid were isolated. The humic substances were characterized in terms of their elemental composition, functional properties including proton exchange capacity, charge/size ratios and spectroscopic characteristics. The results were compared with data of a commercial humic acid from Aldrich.

1 Introduction

This report summarizes the contribution of the Institute of Radiochemistry, Forschungszentrum Rossendorf to the EC study "Effects of Humic Substances on the Migration of Radionuclides: Complexation and Transport of Actinides" (FI4W-CT96-0027) during the reporting period.

The objective of this part of the project was the collection and characterization of aquatic humic substances (humic and fulvic acids) in selected abandoned Saxonian uranium mines. Because the project-related sites 'Johanngeorgenstadt' and 'Königstein' have relatively low concentrations of aquatic humic and fulvic acids, samples were taken from the nearby peat bog 'Kleiner Kranichsee'.

For the investigations, we applied the following methods:

- (i) photon correlation spectroscopy, scanning electron microscopy and filtration for colloid-chemical characterizations,
- (ii) isolation of humic substances from the Johanngeorgenstadt site by adsorption onto DAX-8 type resin,
- (iii) elemental analysis, calcium acetate exchange (determination of carboxylic groups), radiometric determination of functional groups (carboxylic and phenolic OH groups), direct titration (proton exchange capacity), thermoanalysis, atomic absorption spectrometry, inductively coupled plasma mass spectrometry, capillary zone electrophoresis, and IR spectroscopy for the characterization of the isolated humic substances.

Humic substances are generally present in natural aquifer systems at different concentration ranges. They are known for their high complexation affinities for metal ions (Brachmann, 1997; Glaus et al., 1997; Nash and Choppin, 1980; Pompe et al., 1996). The interactions between humic substances and metal ions can increase or retard the migration of metal ions in the geosphere. For actinides, which could be released from waste repositories, the quantification of these interactions is especially important. The investigation of the influence of humic substances on the radionuclide migration allows an assessment of their impact on the long-term safety of radioactive waste repository sites and on abandoned uranium mines such as the ones in Saxony and Thuringia.

2 Testing of Different Resins for Isolating Aquatic Humic Substances

In order to conduct site-specific studies on uranium-humic acid interaction, it is necessary to isolate dissolved humic substances from ground or surface water of uranium mining sites. Because the on-site waters usually only contain low concentrations of humic material, it is necessary to use highly efficient isolation methods.

The adsorption of humic substances onto macroporous resins is a practicable method for isolating humic substances from surface and ground water. Amberlite XAD-8 was widely used to separate aquatic humic substances (Aiken et al., 1985). This resin is no longer commercially available. Therefore, several potential replacement resins were tested for their capacity to sorb humic material. The adsorption capacity and the elution efficiency of the following six different pre-cleaned resins was determined:

EP 61 (Chemiekombinat Bitterfeld), Lewatit 1062, Lewatit 1064, Lewatit 1066 (all from Bayer AG, Leverkusen), Supelite™ DAX-8 (Supelco, Bellefonte, PA), and Amberlite XAD-8 (Merck, Darmstadt).

All resins are non-ionic macroporous copolymers that vary in composition and physical properties as shown in Table 1.

Table 1: Composition and features of different adsorption resins

Resin	Polymer Matrix	Average Pore Size [nm]	Specific Surface Area [m ² /g]	Specific Pore Volume [cm ³ /g]	Particle -size Range [mm]	Bulk Density (± 5%) [g/L]
EP 61 ^a	Ethylvinylbenzene-divinylbenzene	20	600		0.5-1.0	
Lewatit 1062 ^b	Styrene-divinylbenzene	10-50	500-600	1.2	0.4-1.0	650-700
Lewatit 1064 ^b	Styrene-divinylbenzene	5-10	670	1.2	0.4-1.0	650-800
Lewatit 1066 ^b	Styrene-divinylbenzene	5-10	700	0.5	0.3-1.2	650-800
Amberlite XAD-8 ^c	Acrylic ester	25	140	0.82	0.3-0.9	
Supelite DAX-8 ^d	Acrylic ester	22.5	160	0.79		

^a Product information from VEB Chemiekombinat Bitterfeld (liquidated).

^b Product information from Bayer AG, Leverkusen.

^c (Aiken et al., 1985)

^d Product information from Supelco, Bellefonte, PA.

Commercial humic acid (HA) from Aldrich was used to test the resins. It was purified by a combination of repeated precipitation, washing and dialysis according to Kim and Buckau (1988). Test solutions containing 4.5 mg HA/L at pH 2 were passed through glass columns

that were filled with equal volumes (10 mL) of the resins. The average flow rate was 0.28 mL/min. The column eluate was collected as small-volume fractions (≈ 20 mL) and the ultraviolet absorption of all fractions was monitored at 360 nm. The loading of the resin was stopped after the HA had broken through and the light absorption of the fractions became nearly constant. The resin was washed with 0.1 M HCl to displace the residual HA solution. Then the HA was eluted with 0.1 M NaOH. This elution solution desorbed the HA and thus, the HA concentration in the column eluate increased rapidly. The small-volume middle fraction that contained the highly concentrated HA solution is termed 'center cut'. After the 'center cut', the HA concentration in the column eluate gradually decreased.

In order to determine the amount of adsorbed humic acid and its recovery, the ultraviolet absorption of all fractions at 360 nm was compared with the absorption of the HA standard solution at the same wavelength and pH.

As examples, the combination of the breakthrough curve (loading process) and the elution (unloading process) are shown in Figures 1 and 2 for DAX-8 and Lewatit 1066, respectively.

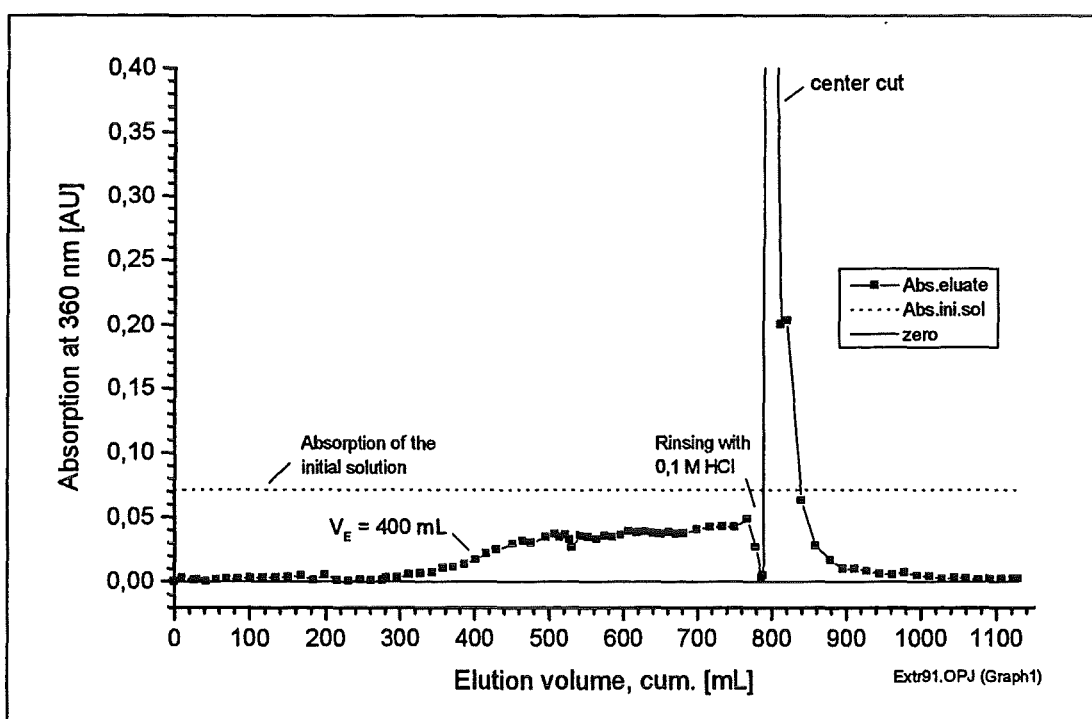


Fig. 1: Elution curve of a column containing DAX-8
(4,5 mg HA/L, pH = 2,0, average flow rate: 0,26 mL/min)

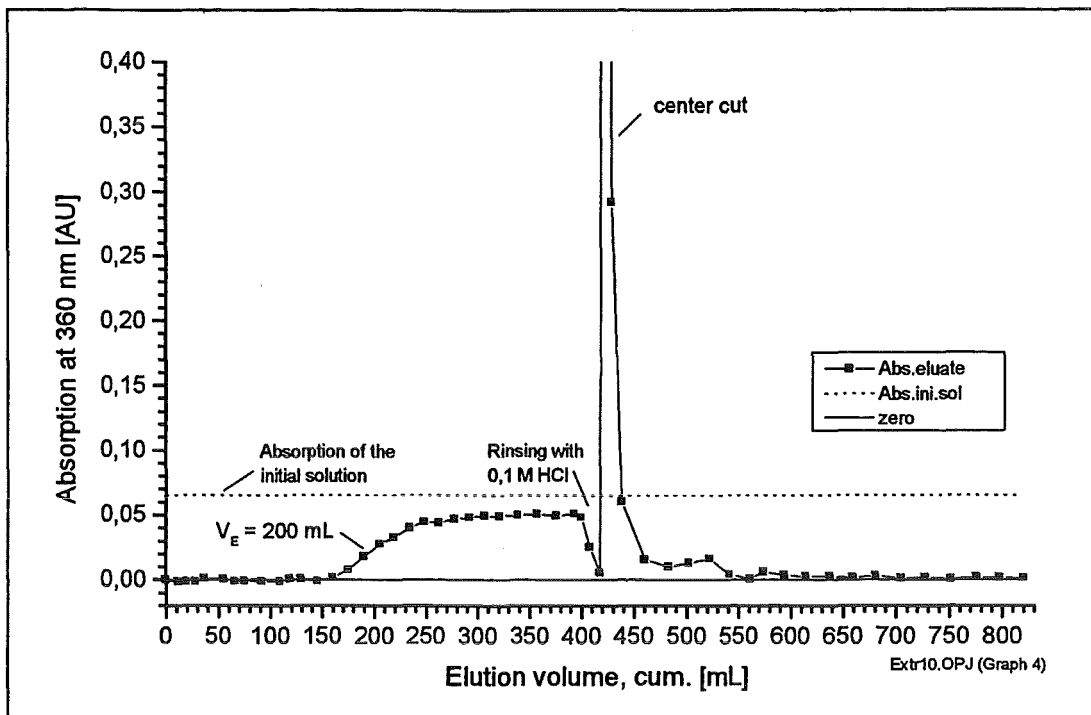


Fig. 2: Elution curve of a column containing Lewatit 1066
(4,5 mg HA/L, pH = 2,0, average flow rate: 0,30 mL/min)

In order to determine the resins' adsorption capacity, the breakthrough curves were analyzed until the breakthrough point V_E (V_E corresponds to the inflection point of the curves). At V_E the column is near saturation so that large particles break through while smaller ones are further adsorbed. This is indicated by the fact that the light absorption of the HA standard solution is not yet reached even after adding much more HA solution (equilibrium state). This causes an undesired fractionation of HA particles. For the different resins the following characteristic data were determined: i) the breakthrough volume V_E , ii) the part of the added HA that was adsorbed until V_E , and iii) the part of the added HA that could not be adsorbed until V_E .

Furthermore, the elution efficiency of the resins was determined by means of the elution curves. The recovery of the HA was analyzed in relation to the amount of HA that was totally adsorbed during the entire loading process. Moreover, the HA concentration in the first 25 mL of column effluent during the elution (~center cut) was calculated. This is a measure of the resins' ability to concentrate diluted HA solutions.

Results:

The results of the adsorption experiments are listed in Table 2 and are discussed below.

- EP 61: The HA particles are almost completely adsorbed before the breakthrough point V_E , but both V_E and the adsorption capacity are very low (62 ml and 0.25 mg, respectively). Corresponding to this, the resin shows the lowest ability to concentrate HA.
($C_{HA} = 0.37$ mg HA/25 mL)

Table 2: Results of the adsorption experiments

No.	Resin	UV-Absorption at 360 nm								
		Solutions totally added 4.5 mg/L HA 0.1 M HCl 0.1 M NaOH	Average flow rate [mL/min]	Breakthrough volume V_E [mL]	HA not adsorbed until V_E [mg]	HA adsorbed until V_E (loading process) [mg]	HA adsorbed until V_E (loading process) [%]	Elution of the HA adsorbed (in relation to total loading process) [mg]	Elution of the HA adsorbed (in relation to total loading process) [%]	C_{HA} in the first 25 mL during the unloading process [mg/25mL]
6	EP 61	200 mL HA-Sol. 15 mL HCl 200 mL NaOH	0.27	62	0.02	0.25	92.3	0.4	82	0.37
8	Lewatit 1062	430 mL HA-Sol. 15 mL HCl 160 mL NaOH	0.29	100	0.03	0.4	92.1	1.05	72.2	0.87
4	Lewatit 1064	310 mL HA-Sol. 15 mL HCl 200 mL NaOH	0.25	177	0.06	0.72	91.8	0.84	76.3	0.71
7	Lewatit 1064	320 mL HA-Sol. 15 mL HCl 250 mL NaOH	0.30	174	0.03	0.73	94.5	0.84	76.3	0.83
10	Lewatit 1066	390 mL HA-Sol. 15 mL HCl 415 mL NaOH	0.30	200	0.006	1.08	100.7	0.69	54.3	0.65
5	XAD-8	460 mL HA-Sol. 15 mL HCl 200 mL NaOH	0.27/0.39	354	0.09	1.5	94.4	1.96	104.3	1.84
9	DAX-8	760 mL HA-Sol. 15 mL HCl 360 mL NaOH	0.26	400	0.02	1.76	99.0	2.19	80.6	1.97

- Lewatit 1062: The adsorption capacity is only slightly higher (until V_E only 0.4 mg of the HA are adsorbed).
- Lewatit 1066: The resin adsorbs a higher amount of humic acid (1.1 mg) and its fractionation tendency until V_E is very low. That means, the HA added to the resin is completely adsorbed.
- XAD-8: This resin shows a high adsorption capacity; until V_E 1.5 mg of HA are adsorbed (twice as much as for Lewatit 1064). The adsorbed HA is completely recovered by eluting the column with NaOH. The concentration in the 'center cut' is 1.84 mg HA/25 mL.
- DAX-8: DAX-8 is the most efficient resin of all tested resins for the removal of humic acid from water. It adsorbs 1.8 mg of HA until V_E which means that 99 % of the added humic acids are adsorbed. The recovery, being 81 %, is somewhat lower than the recovery with XAD-8. In contrast to XAD-8, the sorbent DAX-8 was a new and unused resin. We assume that a certain fraction of the HA particles is retained in the pores of the resin. A higher elution efficiency is expected for DAX-8 if further adsorption and desorption cycles are performed.

Furthermore, DAX-8 enables one to collect a highly concentrated 'center cut' - a concentration of 1.97 mg HA/25 mL is achieved.

Conclusion:

The sequence of resin adsorption capacity was determined as:

DAX-8 > XAD-8 > Lewatit 1066 > Lewatit 1064 > Lewatit 1062 > EP 61.

This demonstrates that high specific surface areas, as shown by the Lewatit resins and EP 61 (500-700 m²/g compared to 140-160 m²/g of XAD-8 and DAX-8 - see Table 1), do not necessarily result in high sorption.

Furthermore, XAD-8 and DAX-8 (resins with aliphatic polymer matrices) can be more efficiently eluted than resins of aromatic polymer matrices (Lewatit resins and EP 61). They are very efficient for isolating aquatic humic acids.

EP 61 and Lewatit 1062 are inefficient for isolating HA. Lewatit 1064 and 1066 can possibly be used as sorbents for HA because of their somewhat higher adsorption capacities.

DAX-8 was shown to be an excellent sorbent for humic acid. The adsorption efficiency of Supelite™ DAX-8 (Supelco) is nearly identical to that of Amberlite XAD-8.

3 Water-sampling Sites

3.1 Johanngeorgenstadt Area

Several abandoned uranium mines and many uranium mine tailing piles are located within the Johanngeorgenstadt area (Saxony/Germany). Investigations of seepage and ground waters of different uranium mines in this area showed that these waters have low concentrations of humic material and higher concentrations of anthropogenic substances, such as lubricants, tar oils, grease, motor fuel, acids, etc. Because of the potential co-isolation of these anthropogenics, it is difficult to isolate from these waters a sufficient quantity of humic material with satisfactory quality within a reasonable experimental time.

Interestingly, in the Johanngeorgenstadt area are also different bogs surrounding the mines whose surface waters have a higher DOC (dissolved organic carbon) because of higher biomass and more intense biological activities. The sphagnum bog 'Kleiner Kranichsee' is a nature reserve and consequently predominantly free from local influences of contamination (industry, agriculture).

The bog at the Kranichsee site is located elevated in relation to the mine and mine tailing piles. Thus, there is the potential possibility that the bog water can come in contact with the uranium mine and therefore, the increase of the humic concentration in the mining water is a conceivable scenario. It is reasonable to assume that the humic substances, isolated from the bog water, may become representative for those at the uranium mines. Therefore, we investigated bog water from the 'Kleiner Kranichsee'. About 400 L surface water were taken from the bog and processed to isolate humic substances. A detailed characterization of the bog water will be given in paragraph 4.

Furthermore, we are planning to isolate humic material from uranium mining sites and mine tailing piles at Johanngeorgenstadt, and to compare the humic materials from all sites with each other.

3.2 Königstein Area

The Königstein uranium mine is located in the upper Elbe valley in Saxony about 20 km south of Dresden. It was operated until 1990. The geological formation of the Königstein uranium mine consists mainly of sandstone sediments that contain very fine pores.

Conventional underground mining operations commenced in 1967. Since 1984 the production of uranium was accomplished by in-situ leaching of the uranium-rich sandstone with diluted sulfuric acid. After closing the uranium mine, remediation was started by flooding it with water from different groundwater aquifers. Groundwater analyses showed that the content of total organic material (TOC) is very low. The TOC lies between 0.5 and 0.7 mg/L (Jenk, 1995). The specific conductivity was found to be between 5.5 and 0.09 mS/cm.

The water in the sediment pores has a TOC <5 mg/L (Jenk, 1995; Seeliger and Schreyer, 1997). This TOC is mainly caused by organic impurities (toluene, benzene, nitrotoluene) of the technical grade sulfuric acid which was used for the leaching process. A residue of 20,000 tons sulfuric acid remained in the mine. The current pH value of the flood water is between 2.6 and 3. That means, that the extremely low amount of humic acid that may be present in the mine is expected to occur mostly as insoluble and possibly colloidal material.

Like in the Johanngeorgenstadt area, surface waters that are to be regarded as potential sources of humics for the uranium mine were investigated for their content of humics.

Ten water samples were characterized for their pH values, specific conductivities, DOCs, TOCs, anion and cation contents. The analyses showed DOC concentrations between 0.1 and 1.8 mg/L coming from humic substances. Taking into consideration the distance between the sampling sites and the uranium mine, the humics found in the surface waters should not affect the migration of uranium in the mine. Therefore, we did not isolate humics from these ten sampling sites. Nevertheless, humic substances are certain to be formed in the mine by wood degradation products. Large amounts of wood were used to reinforce and shore up the mine shafts. The degradation products may be eventually converted in part to humic substances. As the mine continues to be flooded the pH value increases and the humic acids become soluble and thus available to complex U(VI). We are currently studying this effect.

4 Characterization of Colloid Particles in the Kranichsee Bog Water

Humic and inorganic colloids were studied in the surface water from the mountain bog 'Kleiner Kranichsee'. The objective was to record the original colloid-chemical state of a humic-rich natural water before the addition of complexing actinide ions in the next step of the experiment. The following methods were used: filtration, ultrafiltration, photon correlation spectroscopy (PCS), scanning electron microscopy (SEM), analysis of total organic carbon (TOC), UV-Vis spectrometry (UV-Vis), inductively coupled plasma mass spectrometry (ICP-MS), atomic absorption spectrometry (AAS), and ion chromatograph (IC). The water was transparent but had a brown color. Humic acid and fulvic acid were the prevailing organic constituents of the solution. The chemical analysis of the water gave the following results:

Na	0.610	mg/L	Sulphate	5.0	mg/L
Mg	0.231	mg/L	Nitrate	<1	mg/L
Al	0.477	mg/L	Carbonate	4.1	mg/L
Si	0.133	mg/L	Chloride	1.2	mg/L
K	0.480	mg/L	Phosphate	<2	mg/L
Ca	0.940	mg/L	Nitrite	<1	mg/L
Fe	0.990	mg/L	Fluoride	<1	mg/L
Mn	0.096	mg/L	Conductivity	77.6	mS/cm
Zn	0.057	mg/L	TOC	65	mg/L
As	0.007	mg/L	pH	3.7	
Sr	0.006	mg/L			
Ba	0.012	mg/L			
Pb	0.012	mg/L			

We studied the colloids by a combination of the above-mentioned methods. PCS allows in-situ measurements on the original water and on the filtrates. The results can be compared with SEM micrographs of the filter cakes. The fractions of organic matter passing through the filters can be determined by TOC analysis and by UV-Vis spectrometry. Inorganic constituents in the filtrates and on the filters were analyzed by ICP-MS. Information on the colloids was derived by a juxtaposition of the results from all these methods.

Figure 3 shows the filtration scheme according to which the bog water was separated into particle size fractions for the PCS measurements.

The scattered light intensities (count rates of the PCS photomultiplier) are given in Figure 4. This Figure shows that the scattered light intensity decreases strongly if filters of pore sizes of ≤ 100 nm are used. It is, on the other hand, not much influenced when using filters of ≥ 400 nm in pore size.

Figure 5 shows the deconvolutions of the autocorrelation functions obtained for the first four filtrates (the autocorrelation functions are not given here). The method of deconvolution was CONTIN (Schurtenberger and Newman, 1993; Stock and Ray, 1985). The figure demonstrates that filtration leads to the appearance of progressively smaller particles with decreasing filter pore size. This is due to the unmasking of the small particles by the removal of the larger ones. PCS was not applicable because of poor count statistics for the raw sample and the last two filtrates. If one wants to assess the inventory of the submicron particles in the original bog water, one has to take into consideration the results of all the filtrates investigated. It follows that the size of the particles in the bog water detectable by PCS lies between 20 and 300 nm.

SEM micrographs of the particles removed from the solution by a 50 nm Nuclepore filter are shown in Figures 6 through 8 (prefiltration of the water through a 5 µm filter). Agglomerates consisting of 'building units' of 50 to 300 nm were found on the filter membrane. Occasionally, the 'building units' were also found as isolated particles (Figure 7). Thus, the filtration/SEM results confirm our PCS results. On the other hand, it follows from the PCS results that most of the agglomerates on the filter membranes are formed during filtration, i. e., that the 'building units' essentially move freely in the water prior to their filtration. The particles detected by PCS and SEM include both organic and inorganic components. Note, however, that these particles represent only a minor mass fraction of the organics and inorganics in the water (< 30 %). Most of the solution constituents were able to pass through the Nuclepore filters.

Finer particles such as the unagglomerated humic molecules should be characterized by different methods. Ultrafiltration (UF), field-flow fractionation (FFF) or size exclusion chromatography (SEC) are potentially suited for measuring such small particles. We applied ultrafiltration with the aid of Centricon type concentrators equipped with YM membranes (Amicon GmbH, Witten, Germany). Figure 9 shows the filtration scheme. A prefiltration through a 5 µm Nuclepore filter was carried out and the ultrafiltrations were done in parallel. Both the filtrates and the retentates were investigated by UV-Vis spectrometry (calibrated against TOC analysis). The results are given in Figure 10. Decreasing amounts of humic material were passing through the ultrafilters with decreasing molecular weight cut-off. The sums of the filtrate and the retentate concentrations show that the recovery of the ultrafiltration procedure is reasonable (the poorest recovery was found for the 30 kD ultrafilter). From the differences between the filtrate concentrations an estimation of the fractions of humic substance in five molecular weight ranges can be made. These fractions are:

>100 kD	(about > 5 nm)	30,2 %
30 to 100 kD	(about 2 to 5 nm)	26,1 %
10 to 30 kD	(about 1.5 to 2 nm)	11,6 %
3 to 10 kD	(about 1.2 to 1.5 nm)	14,5 %
<3 kD	(about < 1.2 nm)	17,6 %

Filtration can be relatively susceptible to artifacts. Concentration polarization in the diffusion layer above the filter membrane can lead to so-called 'self-coagulation' and, thus, to the removal of particles much smaller than the filter pore size (Buffle and Leppard, 1995; Klein and Nießner, 1997). Even if agglomeration does not play a role, one has to consider that the humic molecules do not have a rigid conformation but are flexible and their shapes depend on the solution conditions such as ionic strength, pH value, and humic concentration (Burba et al., 1995; Swift, 1989). Thus, the molecular weight determined by ultrafiltration is dependent on the ambient conditions and is rather an 'apparent molecular weight' than a real one (which shows a further systematic error since ultrafilters are calibrated with substances very different from humic substances).

We made one (very rough) test to check the influence of the solution conditions on the molecular weight distribution of the system. Therefore, we repeated the filtration according to Scheme 2 (Fig. 9) but used now a sample of the bog water that had been diluted by a factor of 10 prior to the filtration. This manipulation decreased the humic concentration and the ionic strength by a factor of 10 and increased the pH value from 3.7 to 4.5. The results are shown in Figure 11. It can be seen from this figure that the recovery decreased somewhat which was to be expected. Recovery problems are more probable for low concentrations since the influence of adsorption onto the filter membranes will increase if concentration is decreased. The recovery, however, is still reasonable also for the diluted raw sample. The change of solution conditions did not dramatically influence the molecular weight distribution, i. e., the percentages given above are still valid in spite of the dilution. Thus, the molecular weights found by our ultrafiltration experiments should not be influenced too much by filtration artifacts. Nevertheless, our molecular weights are relatively high when compared with results for humic acid molecular weights by other researchers (Beckett, 1989; Klein and Nießner, 1997; Reid, et al., 1990; Schimpf and Petteys, 1997). We are therefore still cautious about our ultrafiltration results. Definite conclusions should not be drawn before the ultrafiltration results can be compared with results of a second method of measuring molecular weights. FFF will be in hand at Rossendorf in 1998.

After having determined the original colloid-chemistry of the bog water we intend to add in a next step varying concentrations of uranyl ions to the water. This will elucidate the influence of uranyl complexation of the humic substances on the colloids. Conclusions on the colloid-facilitated uranium transport in humic-rich natural waters can be drawn from such interrelations.

Scheme 1

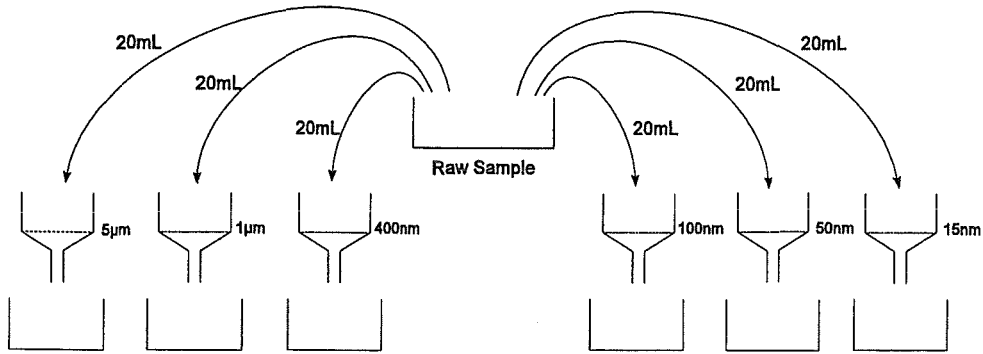


Fig. 3. Scheme 1 of filtration. Application of Nuclepore filters of varying filter pore size.

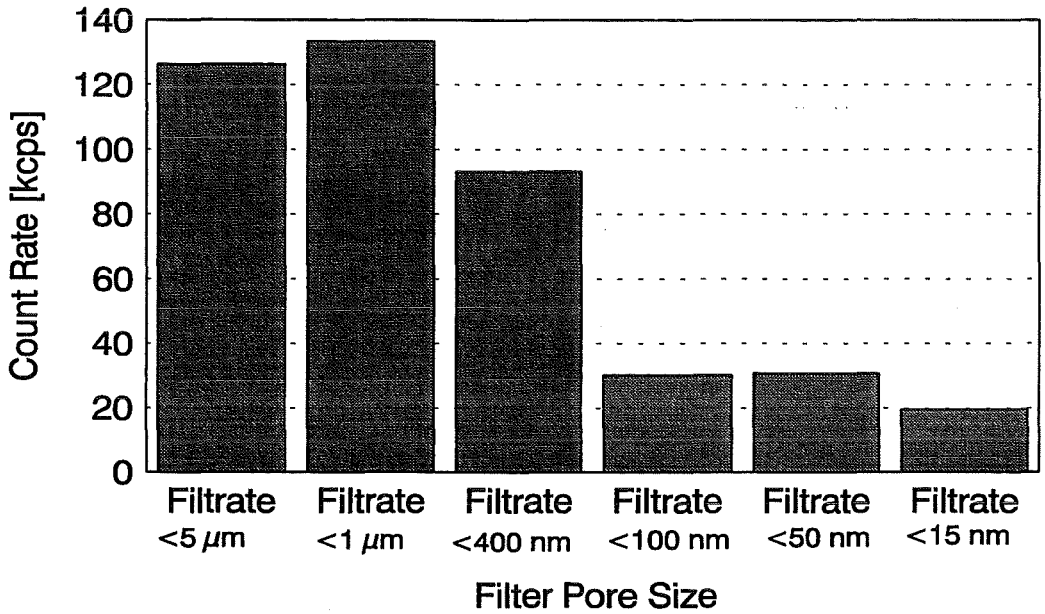
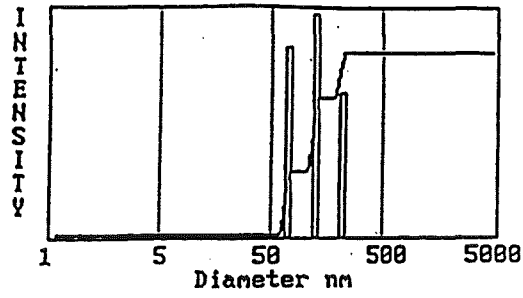
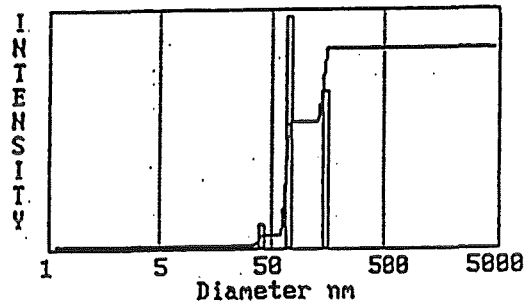


Fig. 4. Photomultiplier count rates of the filtrates obtained from the filtration through Nuclepore filters according to Scheme 1 (Fig. 3.)

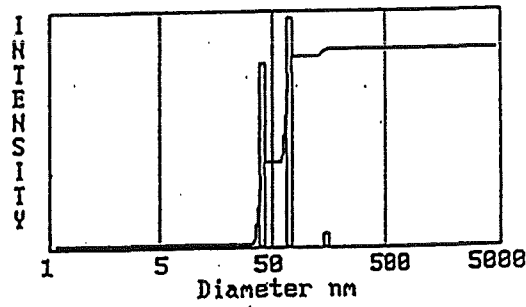
<5 μm



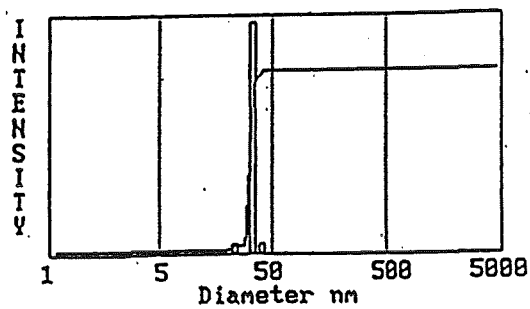
<1 μm



<400 nm



<100 nm



Summary: particle size 20...300 nm

Fig. 5. Particle size distribution according to PCS after filtration through a 5 μm filter, a 1 μm filter, a 400 nm filter, and a 100 nm filter (Nuclepore filters). Deconvolution of the autocorrelation functions by CONTIN.



Fig. 6. SEM micrograph of the filter cake on a 50 nm Nuclepore filter. Prefiltration through a 5 μm Filter.

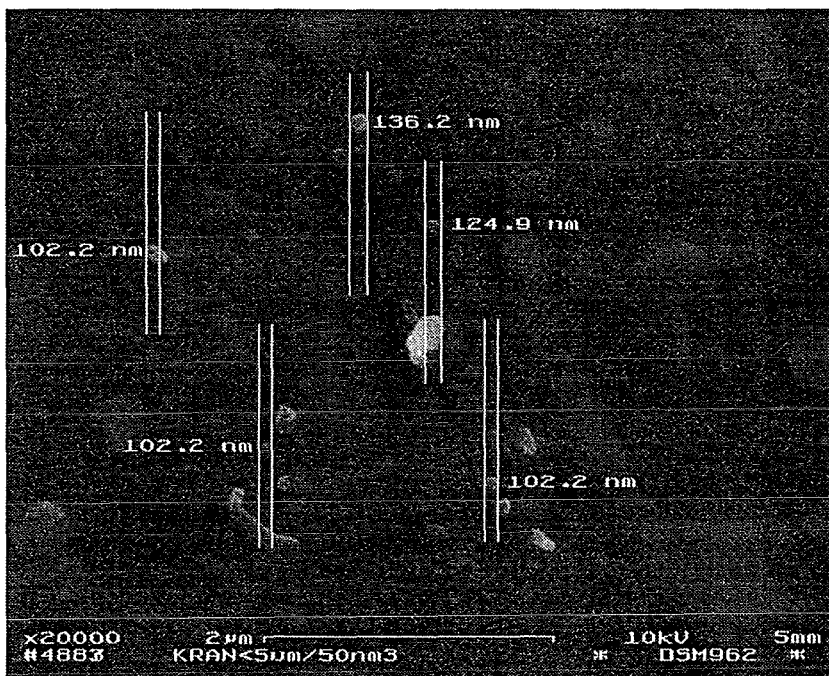


Fig. 7. SEM micrograph of the filter cake on a 50 nm Nuclepore filter. Prefiltration through a 5 μm Filter.

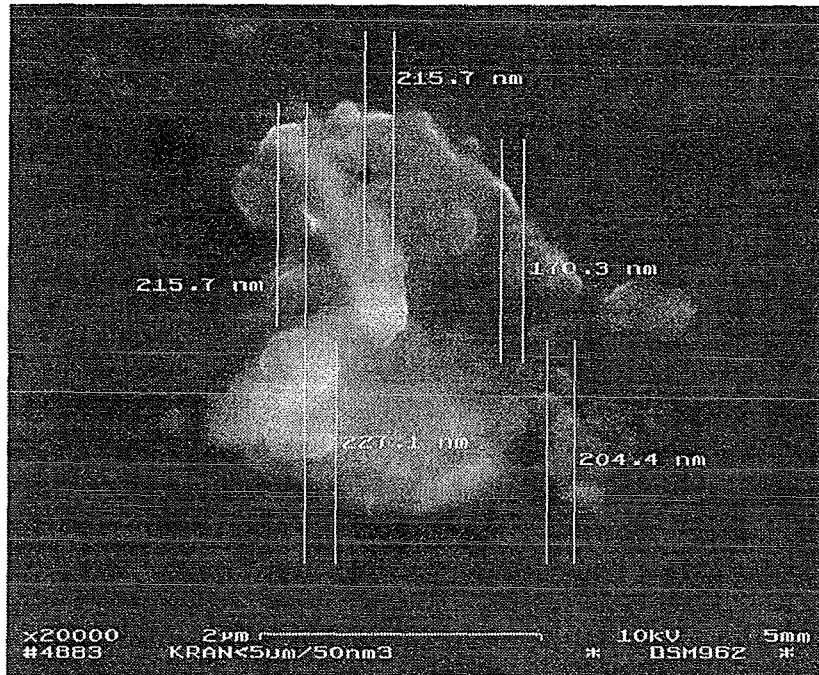


Fig. 8. SEM micrograph of the filter cake on a 50 nm Nuclepore filter. Prefiltration through a 5 μ m filter.

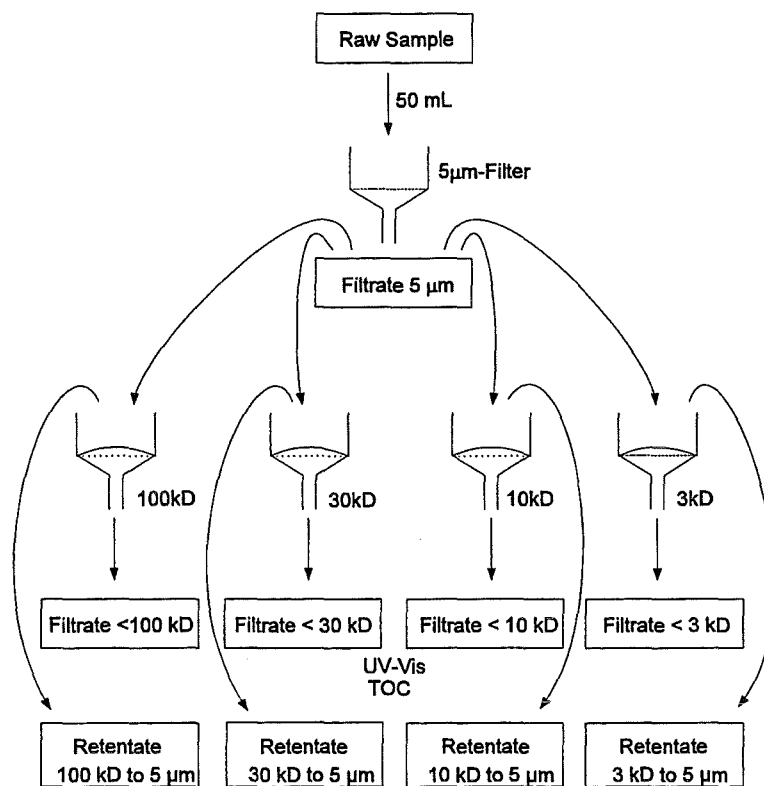


Fig. 9. Scheme 2 of filtration. Application of a 5 μ m Nuclepore filter and of Centricon type Amicon ultrafilters of varying molecular weight cut-off.

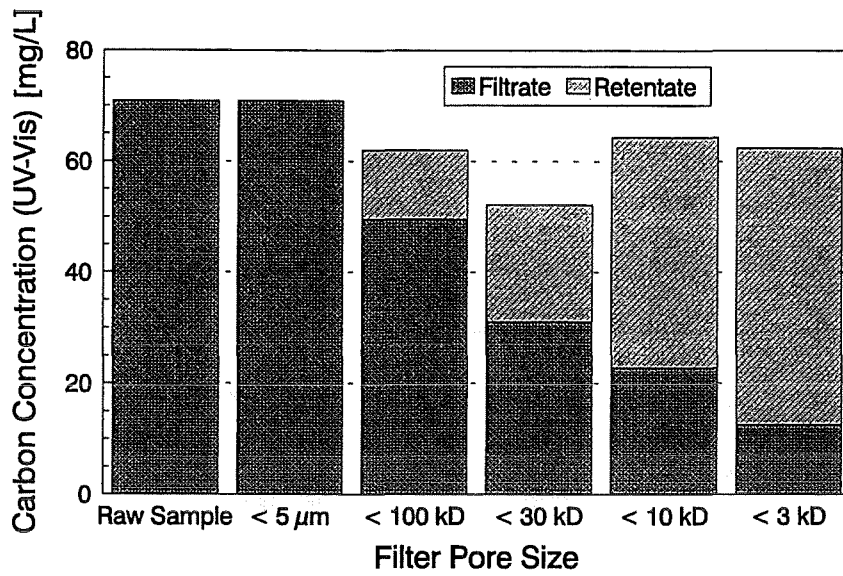


Fig. 10. Carbon concentration in the sample fractions obtained from the filtration/ultrafiltrations according to Scheme 2 (Fig. 9.).

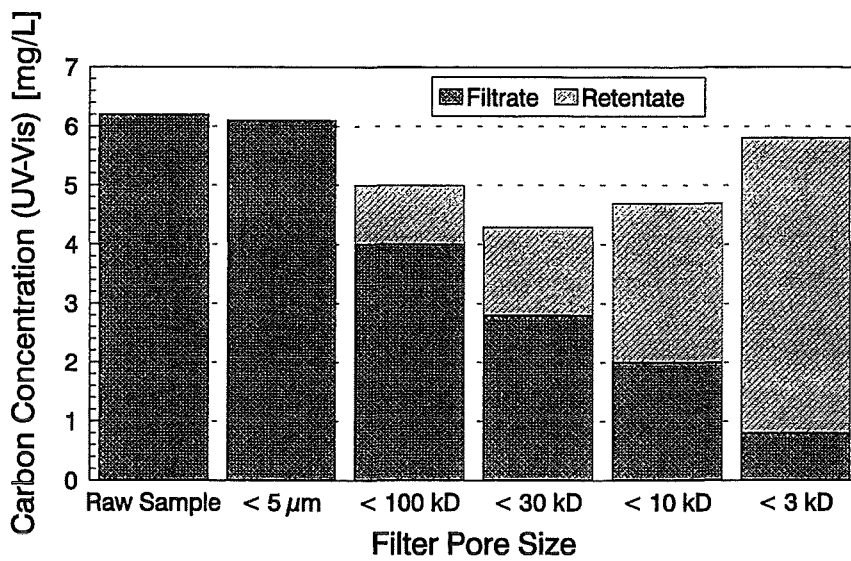


Fig. 11. Carbon concentration in the sample fractions obtained from the filtration/ultrafiltrations according to Scheme 2 (Fig. 9.). Filtration of the moor water after dilution by a factor of 10.

5 Preparation of Reference and Site-Specific Humic Substances

5.1 Reference Humic Acid

The commercial Na-salt of Aldrich humic acid (Aldrich, Steinheim, Germany) was used as a reference substance. It was purified according to Kim and Buckau (1988) and transferred into the H-form. For the purification, humic acid was dissolved in 0.1 M NaOH and 0.01 M NaF and stirred for 46 h. Then, the solution was centrifuged. The supernatant was acidified with HCl to pH 1. The humic acid precipitate was washed with 0.1 M HCl, centrifuged, suspended in water and again centrifuged. This procedure was repeated three times and then, the humic acid was lyophilized.

5.2 Isolation and Purification of Site-Specific Humic Substances

The resins Supelite™ DAX-8 (acrylic ester polymer; Supelco, Bellefonte) and Lewatit 1066 (styrene-divinylbenzene copolymer; Bayer AG, Leverkusen) were pre-cleaned by washing with 0.1 M NaOH and by subsequent Soxhlet extraction with methanol. The resins were stored in Milli-Q-water until needed. After the resins were packed into the columns, they were rinsed with 0.1 M HCl.

The applied isolation method was a modification of that described by Thurman and Malcolm (1981). This method is suitable to isolate aquatic humic substances and to separate them from potential organic impurities and from the majority of accompanying inorganic impurities. A scheme of the applied isolation and purification procedure is shown in Figure 12.

The original water samples were pressure filtered using cellulose acetate filter (450 nm) to remove particulate matter. The samples were then acidified to pH 2 with concentrated HCl and passed through a series of two columns, one containing Supelite DAX-8 resin (2.5 L), and the second containing Lewatit 1066 resin (250 mL) at a flow-rate of about 500 mL/h. The column with Lewatit 1066 resin was used to secure complete adsorption of humics, because of its very low fractionation tendency until the breakthrough point V_E (see paragraph 2). The complete adsorption of humics was checked by monitoring the UV absorbance at 254 nm. After breakthrough of humic material, the loading process was stopped and the columns were eluted with 6 L 0.1 M NaOH to produce a range of fractions. The low concentrated humic material fractions were kept for further reconcentration on a smaller DAX-8 column. The high concentrated fractions were unified and acidified to pH 1.0 with concentrated HCl to precipitate the humic acid. After storing the concentrate at 4 °C for 24 h, the humic and fulvic acids were separated by centrifugation (at 4000 rpm for 20 min). The humic acid precipitate was washed with 0.1 M HCl and again centrifuged. This procedure was repeated three times. Then, the residue was suspended in Milli-Q-water and dialyzed (Spectra Por CE, exclusion limit MWCO < 1000) against deionised water for about 8 days. The resulting humic acid suspension was lyophilized.

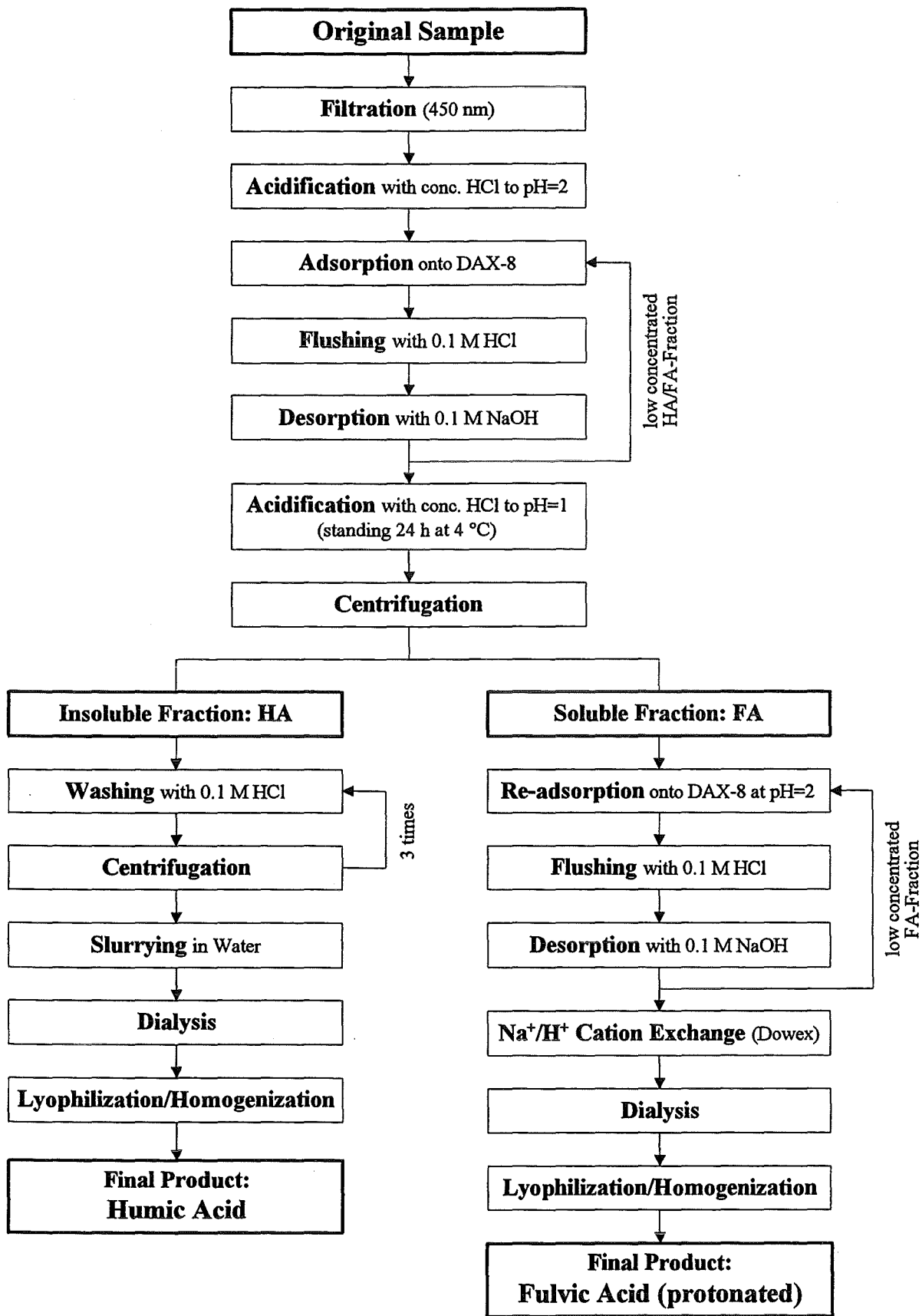


Fig. 12: Isolation and purification of aquatic humic and fulvic acids from the bog 'Kleiner Kranichsee'

The supernatant from centrifugation (fulvic acid fraction) was re-adsorbed onto a DAX-8 column. The loaded resin was rinsed with 0.1 M HCl (2-3 x column volume). Then, the fulvic acid was eluted with 0.1 M NaOH and the eluate was passed through a strong cation exchange resin in the H⁺-form (Dowex 50 WX 8) to remove the Na⁺-ion. The final solution of fulvic acid was dialyzed and lyophilized.

Finally, the humic and fulvic acid fractions were individually homogenized and stored in glass vials in a desiccator to avoid moisture absorption. The yields were 14 g Kranichsee humic acid and 10 g Kranichsee fulvic acid.

6 Characterization of the Isolated Humic Substances

The isolated humic acid (HA) and fulvic acid (FA) from the mountain bog 'Kleiner Kranichsee' near Johannegeorgenstadt were characterized by different analytical methods. The commercially available purified natural HA from Aldrich (Steinheim, Germany) was used for comparison.

6.1 Ash and Moisture Content

Thermoanalysis was used to determine the ash and moisture contents of humic substances (TG/DTA thermoanalyzer STA 92, Setaram, Lyon, France). The results are given in Table 3.

Table 3: Moisture and ash content in Kranichsee humic substances and Aldrich HA determined by thermoanalysis

Sample	Kranichsee HA	Kranichsee FA	Aldrich HA ^a
Moisture content [%] (up to 110°C)	7.8 ± 0.7	6.4 ± 0.8	7.95 ± 0.7
Ash content [%] (up to 800°C)	3.1 ± 0.9 ^b	2.0 ± 0.5	0.5 ± 0.3

^a Aldrich humic acid, purified according to Kim and Buckau (1988).

^b The oxidation residue is of brown color, similar to Fe₂O₃.

The ash content is an indication of total inorganic content of the humic material. The oxidation residue of Kranichsee HA is of brown color, similar to Fe₂O₃.

6.2 Elemental Composition

Carbon, hydrogen, nitrogen and sulfur were analyzed by an elemental analyzer (Model CHNS-932, Leco, St. Joseph, MI, USA). The elemental composition of the humic substances is normalized to a ash- and moisture-free basis (100 % organic components). The oxygen content is calculated from the difference to 100 %.

The elemental compositions of the humic substances are shown in Table 4. The Kranichsee humic substances have a similar carbon and sulfur content. The hydrogen and especially the nitrogen content of the Kranichsee FA are lower than those of Kranichsee HA. A lower nitrogen content of fulvic acids compared to that of corresponding humic acids is also reported in the literature (Aiken et al., 1985, pp.70, 191, 199; Rhee, 1992).

The Kranichsee FA has a higher oxygen content than the Kranichsee HA and thus, a higher O/C atomic ratio. These values are typical of those compiled in the literature (Stevenson, 1982; Kim et al., 1995).

The Aldrich HA has a somewhat different elemental composition than the Kranichsee humic substances which can be attributed to its different origin.

Table 4 also shows that the elemental compositions of the analyzed humic substances are similar to the average elemental compositions of humic substances given in the literature.

Table 4: Elemental composition of Kranichsee HA and FA in comparison with Aldrich HA and with literature data

Element ^a [%]	Kranichsee HA	Aldrich HA	Literature ^d HA	Kranichsee FA	Literature ^d FA
C	49.9 ± 0.3	58.7 ± 0.6	50 - 60	48.8 ± 0.06	40 - 50
H ^b	3.5 ± 0.4	3.3 ± 0.1	4 - 6	2.6 ± 0.1	4 - 6
N	1.8 ± 0.1	0.8 ± 0.1	2 - 6	0.6 ± 0.005	1 - 3
S	0.5 ± 0.01	4.1 ± 0.03	0 - 2	0.5 ± 0.02	0 - 2
O ^c	33.4 ± 0.3	24.8 ± 0.6	30 - 35	39.1 ± 0.1	44 - 50
H/C	0.84	0.67	0.94 ± 0.12	0.63	1.02 ± 0.11
O/C	0.50	0.32	0.50 ± 0.03	0.60	0.51 ± 0.10

^a Calculated on a ash- and moisture-free basis (100 % organic components).

^b Corrected for water content of samples.

^c Calculated as difference to 100 %.

^d according to Stevenson (1982)

6.3 Major Inorganic Components

The humic substances were analyzed for Na, K, Ca, Fe and Mg by atomic absorption spectrometry (AAS) and for Al, Si, Ti, Cr, Zn, Th, U, Na, Mg, K, Ca and Fe by inductively coupled plasma mass spectrometry (ICP-MS). The anions of the Kranichsee fulvic acid were determined by ion-chromatography.

The low concentrations of inorganic components, listed in Table 5, show that the Kranichsee humic substances could be satisfactorily purified.

Table 5: Major inorganic components of Kranichsee HA and FA and Aldrich HA determined by ICP-MS, AAS-F and ion-chromatography

Element	Kranichsee HA [ppm]	Kranichsee FA [ppm]	Aldrich HA ^a [ppm]	Kranichsee HA [meq/g]	Kranichsee FA [meq/g]	Aldrich HA ^a [meq/g]
Na	1670 ± 20	10095 ± 268	226 ± 14	7.26E-02	4.39E-01	9.83E-03
Mg	35 ± 12	87 ± 2	19 ± 3	2.89E-03	7.16E-03	1.56E-03
Al	149 ± 21	41 ± 11	93 ± 18	1.66E-02	4.56E-03	1.03E-02
K	324 ± 40	701 ± 28	36 ± 15	8.28E-03	1.79E-02	9.21E-04
Ca	708 ± 367	487 ± 130	611 ± 124	3.53E-02	2.43E-02	3.05E-02
Cr	9 ± 1	7 ± 0.5	32 ± 0.5	4.97E-04	4.04E-04	1.85E-03
Fe	1018 ± 30	296 ± 20	863 ± 40	5.47E-02	1.59E-02	4.64E-02
Zn	16 ± 4	40 ± 27	n.d.	4.80E-04	1.22E-03	0
Th	2 ± 0.2	n.d.	1 ± 0.1	3.71E-05	0	1.72E-05
U	4 ± 0.3	2 ± 0.3	1 ± 0.2	9.13E-05	5.04E-05	2.52E-05
Cl ⁻		< 500			1.41E-02	
SO ₄ ²⁻		290			1.81E-02	
HPO ₄ ²⁻		< 50			2.60E-03	
HCO ₃ ⁻		1210			7.93E-02	
NO ₃ ⁻		< 20			1.61E-03	
NO ₂ ⁻		< 10			6.52E-04	
SiO ₃ ²⁻	1780 ± 467	786 ± 131	372 ± 61	9.36E-02	4.13E-02	1.96E-02
TiO ₃ ²⁻	113 ± 1	10 ± 3	79 ± 11	4.71E-03	4.17E-04	3.30E-03
Σcations [meq/g]				1.92E-01	5.11E-01	1.01E-01
Σanions [meq/g]					1.58E-01	

n.d.: not detectable

n.m.: not measured

^a Aldrich humic acid, purified according to Kim and Buckau (1988).

The Kranichsee FA shows a somewhat higher concentration of inorganic impurities ($\Sigma\text{cations} = 0.51 \text{ meq/g}$) compared to the Kranichsee HA ($\Sigma\text{cations} = 0.19 \text{ meq/g}$). The difference between $\Sigma\text{cations}$ and Σanions of the FA amounts to 0.35 meq/g . That means, if the proton exchange capacity of the FA is 5.6 meq/g then approximately 6.3 % of the sites are occupied by cations. For Kranichsee HA, Fe is in addition to Na a major inorganic component. From this one can conduct that Fe interacts very strongly with the HA. The Fe content of the Kranichsee FA is lower.

6.4 Functional Groups

The proton exchange capacity was determined by different methods. They are:

- Barium hydroxide method: The total proton exchange capacity (as sum of carboxylic and phenolic groups) was determined as the barium exchange capacity in alkaline medium ($\text{pH} > 13$). (Schnitzer and Khan, 1972; Aiken et al., 1985)
- Calcium acetate method: The number of carboxylic groups were determined as the calcium exchange capacity in neutral medium (Schnitzer and Khan, 1972; Aiken et al., 1985).
- The phenolic groups, as a measure of weak acidic groups, were calculated from the difference between the total acidity and the carboxylic group content.
- Direct titration: The content of proton exchanging functional groups that are deprotonated at neutral pH values were determined by direct titration (Aiken et al., 1985). The values are between the carboxylic group capacities determined by the calcium acetate method and the total proton exchange capacities. It is assumed that mainly the carboxylic groups and a small part of phenolic groups (acidic OH groups) are determined by this method.
- Radiometric method: The carboxylic, phenolic OH and ester groups were also determined radiometrically by methylation with $[^{14}\text{C}]$ -diazomethane according to the scheme shown in Figure 13 (Bubner and Heise, 1994).

The results of the different methods are summarized in Table 6.

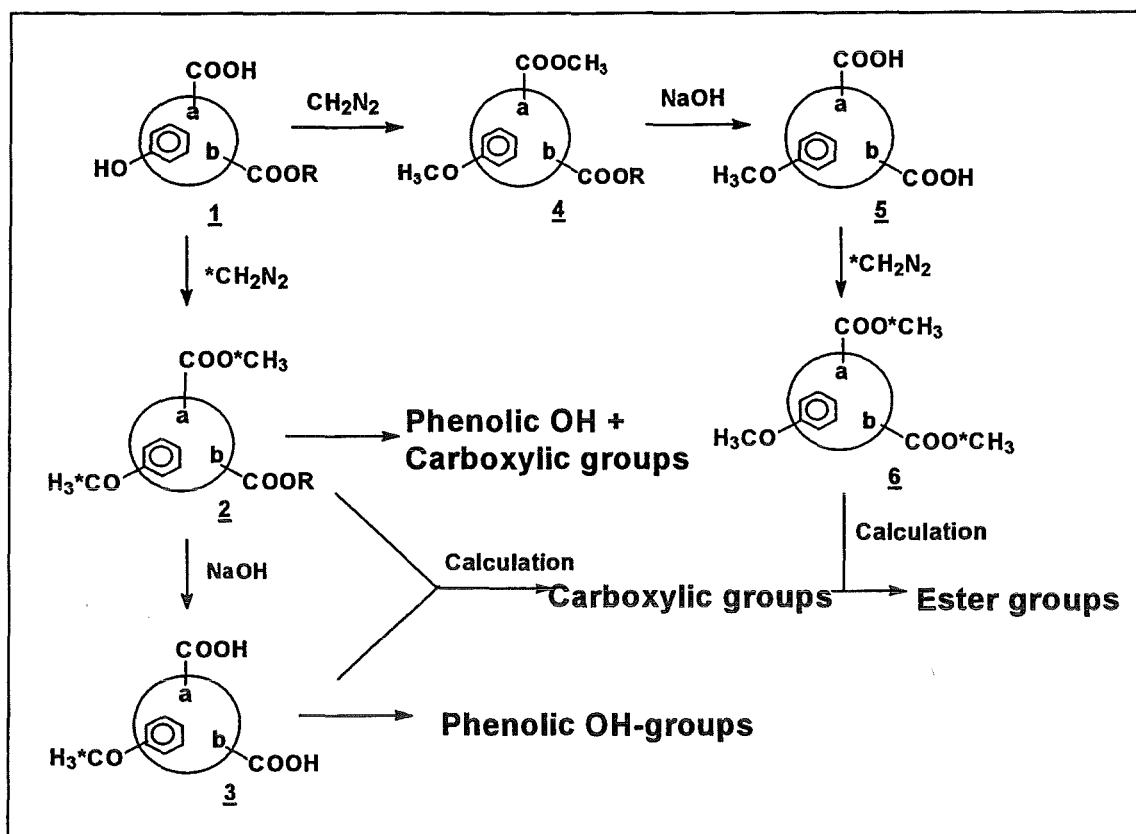


Fig. 13: Determination of functional groups of humic substances by methylation with [¹⁴C]diazomethane (*C = ¹⁴C) (Bubner and Heise, 1994)

Table 6: Functional groups of Kranichsee HA and FA in comparison with Aldrich HA

Functional group [meq/g]		COOH + phenolic OH	COOH	Phenolic OH
Barium hydroxide method	Kranichsee HA	10.17 ± 0.5	-	-
	Kranichsee FA	-	-	-
	Aldrich HA	7.12 ± 0.25	-	-
Calcium acetate method	Kranichsee HA	-	4.20 ± 0.17	5.97 ± 0.39 ^a
	Kranichsee FA	-	6.05 ± 0.31	-
	Aldrich HA	-	4.41 ± 0.11	2.71 ± 0.34 ^a
Radiometric method	Kranichsee HA	7.75 ± 0.35	3.88 ± 0.41	3.87 ± 0.52
	Kranichsee FA	8.82 ± 0.48	3.98 ± 0.25	4.84 ± 0.65
	Aldrich HA	7.4 ± 0.4	3.9 ± 0.1	3.4 ± 0.4
Direct titration	Kranichsee HA		4.83 ± 0.18	
	Kranichsee FA		5.60 ± 0.12	
	Aldrich HA		5.06 ± 0.17	

^a Calculated from the difference of total acidity (barium hydroxide method) and carboxylic group content (calcium acetate method).

According to the radiometric analysis, the total acidity and the carboxylic group content of the Kranichsee FA are only slightly higher than those of the Kranichsee HA. However, the carboxylic group content of the Kranichsee FA determined by Ca-exchange (6.05 meq/g) is much higher than the carboxylic group content determined radiometrically (3.98 meq/g). Furthermore, it is even higher than the proton exchange capacity determined by direct titration (5.6 meq/g). We assume that the carboxylic group content of the FA determined by Ca-exchange is too high. One reason could be an incomplete filtration of FA during the calcium acetate method because it may contain acidic OH groups (Stevenson, 1982) or other acidic protons that could influence the titration result.

The Aldrich humic acid contains more COOH and fewer phenolic OH groups than the Kranichsee HA.

6.5 Capillary Zone Electrophoresis

The investigations of the Kranichsee HA and FA and of the Aldrich HA as well, were performed by capillary zone electrophoresis in three different buffers:

1. 40 mM Na₂HPO₄, 20 mM H₃BO₃, pH 7.86
2. 0.4 % H₃BO₃, 0.3 % Na₂B₄O₇, pH 8.62
3. 3 mM KH₂PO₄, 6 mM Na₂B₄O₇, pH 8.96

Fig. 14 shows the electropherograms of the humic substances in buffer no. 1.

The peak shapes of the different humic substances are similar but there are differences in their migration time and in their UV absorption. The larger migration time of the Kranichsee FA compared to that of Kranichsee HA is caused by its smaller molecular size and its somewhat higher number of dissociated functional groups. This confirms the results of the functional group determination (see paragraph 6.4). That means, the longer migration time of Kranichsee FA is caused by its higher charge-to-size ratio. Furthermore, the FA shows a slightly higher UV absorption.

Aldrich HA exhibits both a higher migration time and a higher UV absorption intensity than the Kranichsee HA. This can also be attributed to a higher charge-to-size ratio. Presuming that both HA's have comparable molecular masses, a different amount of charge carriers must exist. According to the calcium acetate and the radiometric method, the COOH-content of Aldrich HA is higher than that of Kranichsee HA. Thus, the longer migration time of the Aldrich HA is caused by a larger amount of charge carriers. The higher UV absorption intensity could be caused by a greater number of UV-active groups (chromophores, such as conjugated double bonds, aromatic rings, phenolic functional groups).

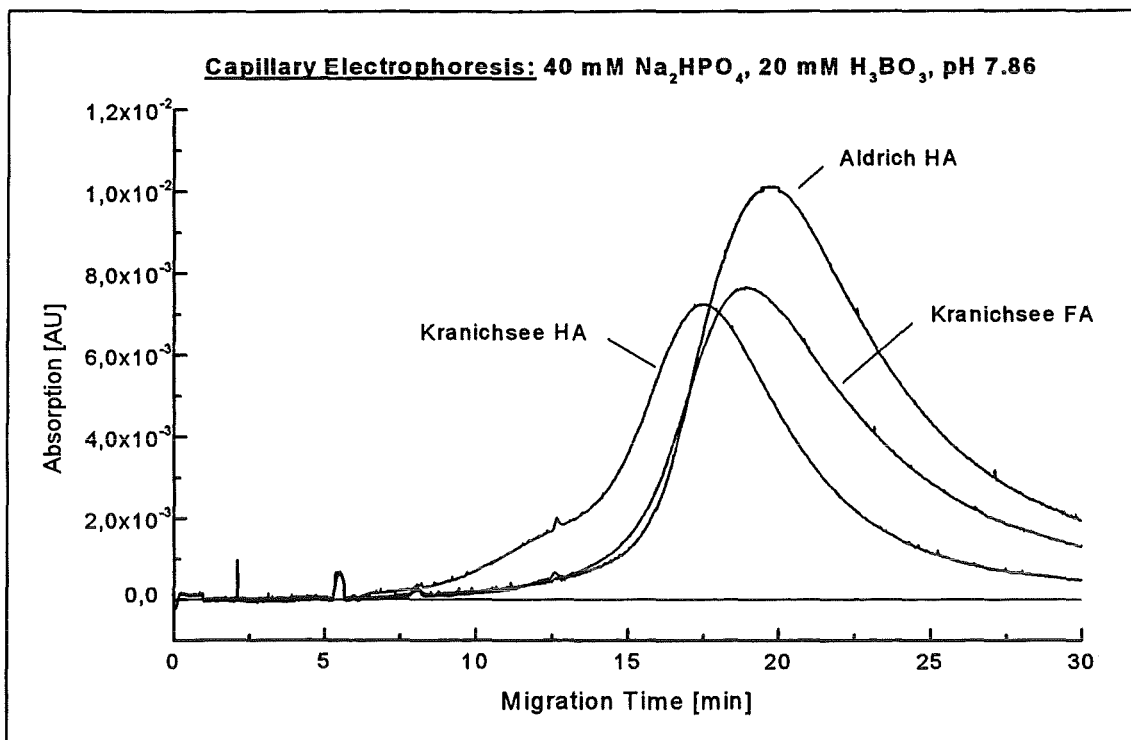


Fig. 14: Electropherograms of Kranichsee HA and FA compared to Aldrich HA. Separation conditions: buffer 40 mM Na₂HPO₄, 20 mM H₃BO₃, pH 7.86; temperature 30 °C; separation voltage 15 kV, I: 84 μA; detection 214 nm; 15 s injection; fused silica capillary, 57 cm total length, 50 cm effective length, 75 μm internal diameter; Model P/ACE 2050 Beckman Instruments, Palo Alto, CA, USA.

6.6 IR Spectroscopy

IR spectroscopy of humic substances provides information on functional groups, especially on oxygen containing groups. The IR spectra of Kranichsee HA and FA and Aldrich HA as well are shown in Figure 15. These spectra are similar to typical IR spectra of humic and fulvic acids published in the literature (Schnitzer and Khan, 1972). In addition to characteristic absorption bands that are common to all three spectra, differences in the absorption intensity of some bands exist:

- The intensity of the broad band centered at about 3410 cm⁻¹ (O-H stretching vibrations) is stronger for the Kranichsee HA and FA than for the Aldrich HA. This is due to the higher phenolic content of the Kranichsee humic substances compared to Aldrich HA and confirms the result of the functional group determination (paragraph 6.4).

- The higher intensity of the absorption bands in the 2960-2850 cm^{-1} region corresponds to a higher content of aliphatic C-H bonds (Aldrich HA > Kranichsee HA \geq Kranichsee FA).
- All three IR spectra show two sharp absorption bands near 1720 cm^{-1} (C=O stretching of COOH and ketones) and 1620 cm^{-1} (aromatic C=C and H bonded C=O). There are minor differences between the intensities of the 1720 cm^{-1} band and the 1620 cm^{-1} band. The 1720 cm^{-1} band has a slightly higher relative intensity compared to the band at 1620 cm^{-1} for the Kranichsee FA than for the Kranichsee HA, indicating a somewhat higher COOH content for the FA.
- The small band at 1510 cm^{-1} , present in the spectra of the Kranichsee HA and even smaller in the spectra of the Kranichsee FA, can be assigned to aromatic C=C double bonds.
- The very broad band in the 1280-1200 cm^{-1} region (C-O stretch and OH deformation of COOH) decreases in the following sequence:
Aldrich HA > Kranichsee FA \sim Kranichsee HA.
This band again can be attributed to the content of carboxylic groups and would not appear for the salt from the humic substances (Kim and Buckau, 1988).

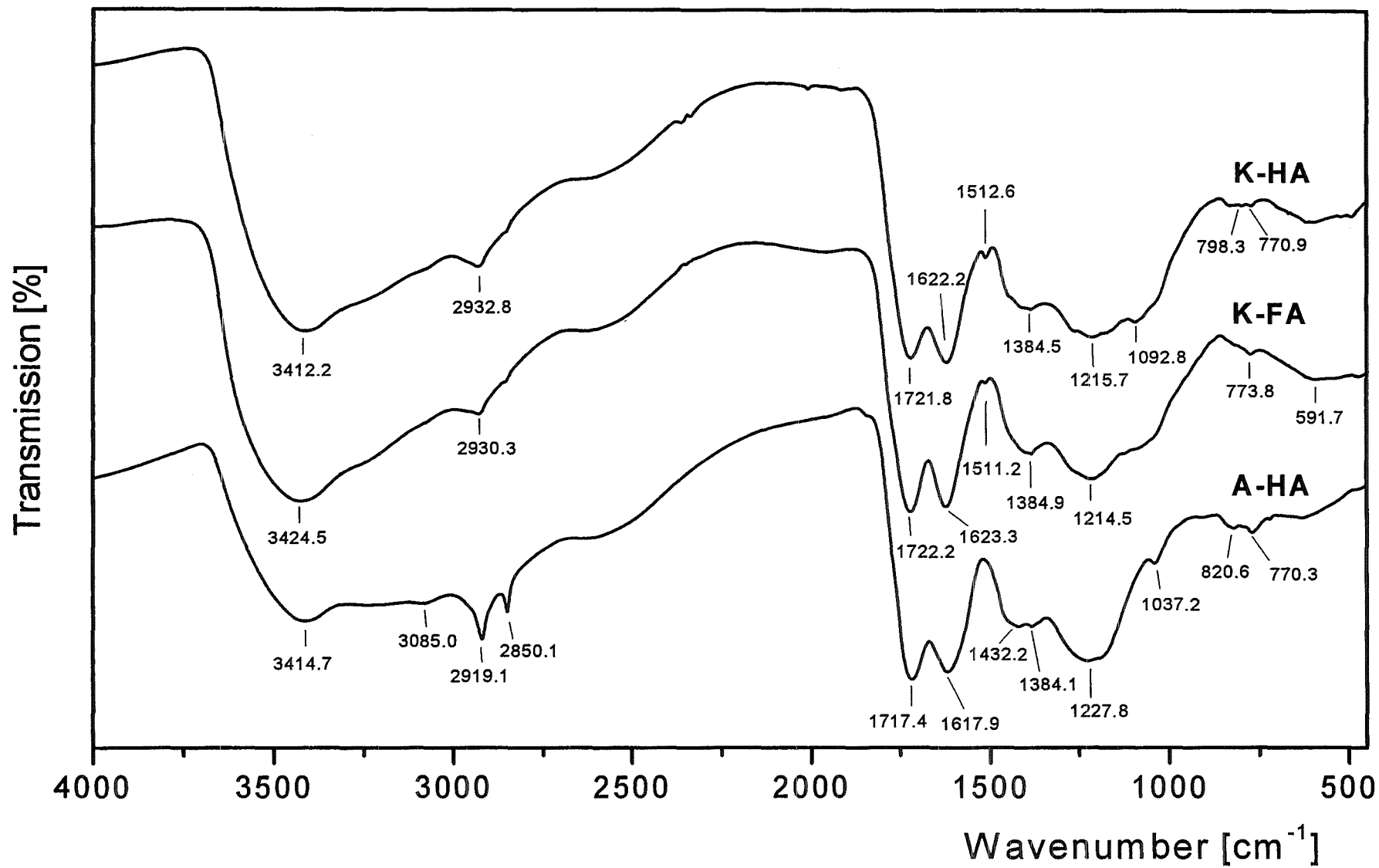


Fig. 15: IR spectra of Kranichsee HA (K-HA) and Kranichsee FA (K-FA) compared to Aldrich HA (A-HA)

7 References

- Aiken, G.R., McKnight, D.M., Wershaw, R.L., and MacCarthy, P. (1985) *Humic Substances in Soil, Sediment, and Water-Geochemistry, Isolation, and Characterization*. John Wiley & Sons, New York.
- Beckett, R., Bigelow, J.C., Zhang, J., and Giddings, J. C. (1989) Analysis of Humic Substances Using Flow Field-Fractionation. In *Influence of Aquatic Humic Substances on Fate and Treatment of Pollutants* (ed. P. MacCarthy and I. H. Suffet), ACS Advances in Chemistry Series 219, Chapter 5, ACS, Washington DC.
- Brachmann, A. (1997) Zeitaufgelöste laserinduzierte Fluoreszenzspektroskopie zur Charakterisierung der Wechselwirkung des Uranylions mit Huminsäuren sowie Carboxylatliganden zur Simulation der Huminsäurefunktionalität. Dissertation, TU Dresden.
- Bubner, M. and Heise, K.H. (1994) Characterization of Humic Acids. II. Characterization by Radioreagent-Derivatization with [¹⁴C]Diazomethane. In *Annual Report 1993*, Forschungszentrum Rossendorf, Institute of Radiochemistry, FZR 43, 22-24.
- Buffle, J. and Leppard, G.G. (1995) Characterization of Aquatic Colloids and Macromolecules. 2. Key Role of Physical Structures on Analytical Results. *Environ. Sci. Technol.* 29, 2176-2184.
- Burba, P., Shkinev, V. Spivakov, and B. Ya (1995) On-line fractionation and characterization of aquatic humic substances by means of sequential-stage ultrafiltration. *Fresenius J. Anal. Chem.* 351, 74-82.
- Glaus, M.A., Hummel, W., Van Loon, L.R. (1997) Experimental Determination and Modelling of Trace Metal - Humate Interactions: A Pragmatic Approach for Applications in Groundwater. *PSI Report 97-13*, Paul Scherrer Institute, Villigen, Switzerland.
- Jenk, U. (1995) Untersuchungen zu den chemischen und geochemischen Verhältnissen in der Uranlagerstätte Königstein nach Einstellung der Urangewinnung durch schwefelsaure Untertagelaugung. Dissertation, TU Bergakademie Freiberg.
- Kim, J.I., Artinger, R., Buckau, G., Kardinal, Ch., Geyer, S., Wolf, M., Halder, H., and Fritz, P. (1995) Grundwasserdatierung mittels ¹⁴C-Bestimmungen an gelösten Humin- und Fulvinsäuren. In *Abschlußbericht - RCM 00895*, TU München, Institut für Radiochemie, 86-92.
- Kim, J.I. and Buckau, G. (1988) Characterization of Reference and Site Specific Humic Acids. In *RCM-Report 02188*, TU München, Institute of Radiochemistry.
- Kim, J.I. and Czerwinski, K.R. (1996) Complexation of Metal Ions with Humic Acids: Metal Ion Charge Neutralization Model. *Radiochim. Acta* 73, 5.
- Klein, T. and Nießner, R. (1997) Characterization of Heavy Metal Containing Seepage Water Colloids by Flow FFF, Ultrafiltration, ELISA and AAS. *Microchim. Acta*, in press.
- Nash, K.L. and Choppin, G.R. (1980) Interaction of Humic and Fulvic Acids with Th(IV). *Inorg. Nucl. Chem.* 42, 1045.
- Pompe, S., Bubner, M., Denecke, M.A., Reich, T., Brachmann, A., Geipel, G., Nicoletti, R., Heise, K.H., and Nitsche, H. (1996) A Comparison of Natural Humic Acids with Synthetic Humic Acid Model Substances: Characterization and Interaction with Uranium(VI). *Radiochim. Acta* 74, 135-140.
- Reid, P. M., Wilkinson, A. E., Tipping, E., and Jones M. N. (1990) Determination of molecular weights of humic substances by analytical (UV scanning) ultracentrifugation. *Geochim. Cosmochim. Acta* 54, 131-138.
- Rhee, D.S. (1992) Komplexierungsverhalten der Huminstoffe mit dreiwertigen Aktinoiden in aquatischen Systemen, Dissertation, TU München.

Schimpf, M. E. and Petteys, M. P. (1997) Characterization of humic materials by flow field-flow fractionation. *Colloids Surfaces A: Physicochem. Eng. Aspects* **120**, 87-100.

Schnitzer, M., Khan, S.U. (1972) *Humic substances in the environment*. (A.D. McLaren, ed.), Marcel Dekker, Inc., New York.

Schurtenberger, P. and Newman, M.E. (1993) Characterization of Biological and Environmental Particles Using Static and Dynamic Light Scattering. In *Environmental Particles, IUPAC Series on Environmental Analytical and Physical Chemistry*, (ed. J. Buffle and H. P. van Leeuwen), Volume 2, pp. 37-116. Lewis Publishers.

Seeliger, D. and Schreyer, J. (1997) Optimierung von konventionellen Verfahren zur Behandlung von Flutungswässern am Beispiel der Lagerstätte Königstein. In *Tagungsbeitrag zum Wismut '97 Workshop: Wasserbehandlung und Rückstandentsorgung - konventionelle und innovative Lösungen*, Chemnitz, 24. bis 26. September 1997.

Stevenson, F.J. (1982) *Humus Chemistry, Genesis, Composition, Reactions*. John Wiley & Sons, New York.

Stock, R. S. and Ray, W. H. (1985) Interpretation of Photon Correlation Spectroscopy Data: A Comparison of Analysis Methods. *J. Polym. Sci.: Polym. Phys. Ed.* **23**, 1393-1447.

Swift, R. S. (1989) Molecular Weight, Size, Shape, and Charge Characteristics of Humic Substances: Some Basic Considerations. In *Humic Substances II. In Search of Structure* (ed. Hayes, M. H. B. et al.) p. 449-465. John Wiley & Sons.

Thurman, E.M. and Malcolm, R.L. (1981) Preparative Isolation of Aquatic Humic Substances. *Environ. Sci. Technol.* **15**, 463-466.



FACULTEIT LANDBOUWKUNDIGE EN TOEGEPASTE
BIOLOGISCHE WETENSCHAPPEN
DEPARTEMENT INTERFASECHEMIE
LABORATORIUM VOOR COLLOIDCHEMIE
KARDINAAL MERCIERLAAN 92
B-3001 HEVERLEE



KATHOLIEKE
UNIVERSITEIT
LEUVEN

Reduction of Technetium in Solution: Influence of Ferrous Iron, Mineral Phases and Organic Matter

A. Maes*, L. Capon

**Technical Progress Report for the
EC contract F14W-CT96-0027:**

**Effects of humic substances on the migration of radionuclides: complexation
and transport of actinides**

(Reporting Period 1997)

*** E-Mail: André Maes@agr.kuleuven.ac.be.**

1. Experimental Setup

All experiments were carried out at ambient temperature (22 °C) in a controlled atmosphere glovebox flushed with a mixture of N₂ (95 %) and H₂ (5 %) to minimize the intrusion of oxygen into the reaction vessels. The box atmosphere was circulated over a catalytic converter (Pt) in order to remove excessive oxygen. By this, the mean concentration of O₂ in the glovebox throughout the experiments was around 2 ppm. All chemicals used were of analytical grade and the water used was deionized, filtered by a Water Purification System (Milli-Q) and finally boiled out to obtain oxygen-free water. ⁹⁹Tc was purchased from Amersham in 0.1 M NH₄OH aqueous solution. TcO₄⁻ solutions of about 5 × 10⁻⁶ M in NaClO₄ (10⁻² M) and NaHCO₃ (2 × 10⁻² M) were prepared by diluting aliquots of a stock solution. FeS was purchased from Cerac TM Incorporations, whereas pyrite and illite were obtained from a minerals shop. The organic matter used was obtained by extracting 5 times a Boom clay sample using 10⁻² M NaHCO₃ (S/L = 1/5). After each extraction step, the sample was centrifuged for 45 minutes at 12000 rpm. The extract was filtered and one more time centrifuged.

Experiments were conducted in polypropylene vials which were shaken head over head to ensure good mixing. After certain periods of time the reaction vials were centrifuged for half an hour at 18000 rpm and afterwards analyzed.

The centrifuged samples were analyzed for ⁹⁹Tc in a Packard Liquid Scintillation Analyzer using Ultima Gold Liquid Scintillation Cocktail (Packard).

The pH measurements were made by a Portatest 655 and a WTW SenTix 50 glass electrode, and the redox potentials were monitored by a combined redox Toledo Mettler P14805-DXK-S8/120 electrode connected to the Portatest 655.

Total Fe(II)-concentration in solution was determined by a colorimetric method at 508 nm using o-phenantroline and sodiumacetate.

The presence of reduced Tc(IV) in solutions was determined by extracting an aliquot of the solution three times with equal volumes of chloroform containing 0.001 mol dm⁻³ tetraphenyl arsonium chloride.

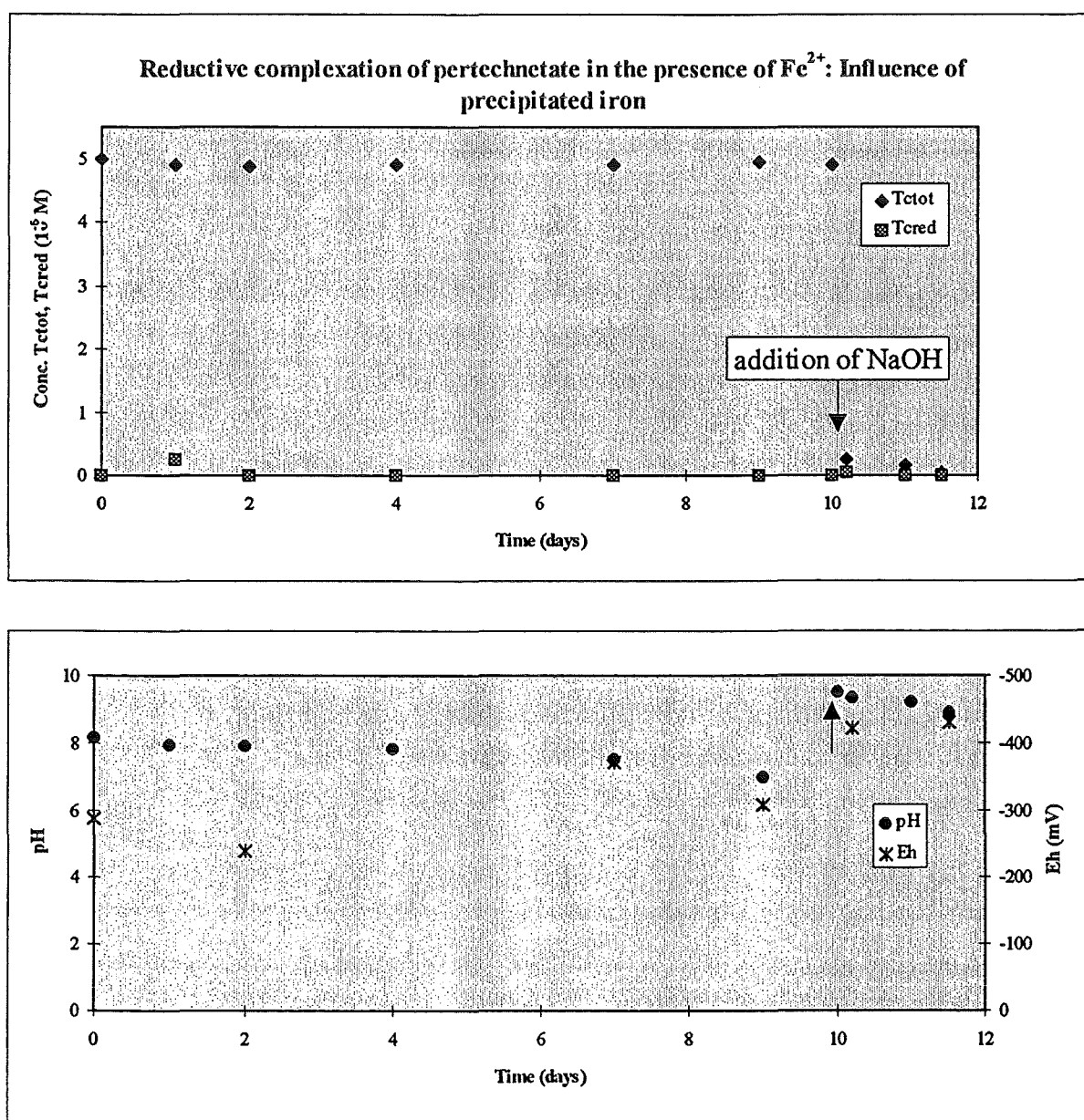
Separation of the TcO₄⁻/Tc-humic fraction was determined by gel exclusion chromatography. This was carried out by eluting a 1 ml sample over a glass column (30 x 1 cm), filled with a Superdex 30 Prep Grade gel (Pharmacia Biotech). The eluent was a boiled out, saline NaCl solution (0.15 M containing 0.002 % NaN₃). The U.V.-absorbance (at 254 nm) was measured continuously and the collected fractions were β-monitored radiometrically for their Tc-levels.

2. Behaviour of Tc in aqueous solution in the presence of Fe^{2+} and humic compounds

2.1. Reductive complexation of pertechnetate in the presence of Fe^{2+} : influence of precipitated iron

Under reducing conditions, $\text{Tc}_{(\text{VII})}$ may precipitate as $\text{Tc}_{(\text{IV})}$. Therefore, the removal of Tc, added as pertechnetate ($^{99}\text{TcO}_4^-$) in aqueous solutions under reducing conditions was measured.

Experimental data are shown in figure 1 where $[\text{Tc}]$, pH, Eh and $[\text{Fe}_{(\text{II})}]$ are plotted vs time.



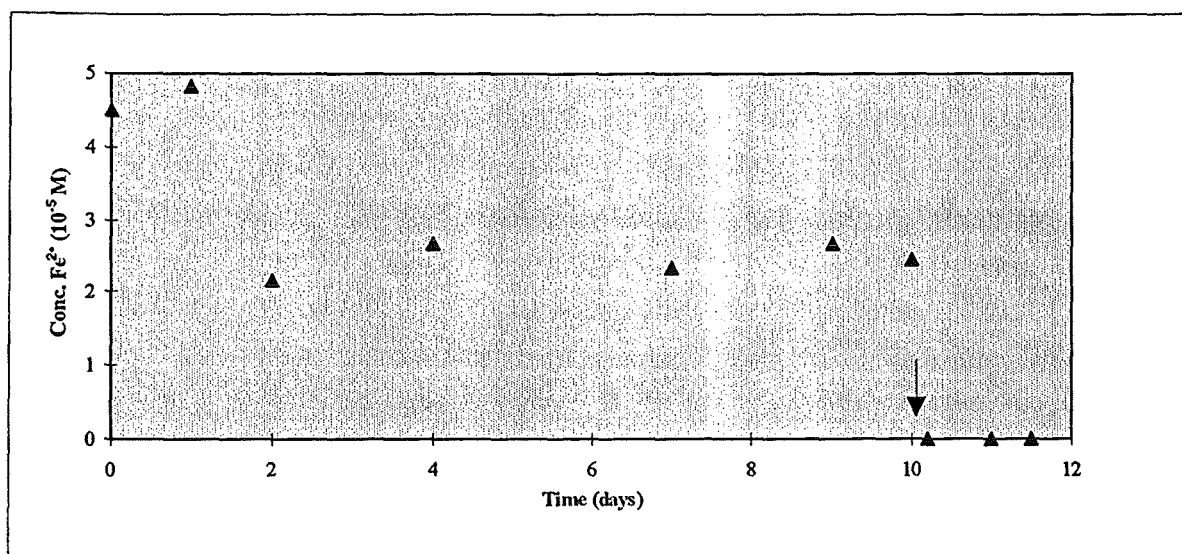
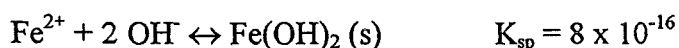


Figure 1: Reductive complexation of pertechnetate in the presence of Fe²⁺: influence of precipitated iron (the arrow marks the addition of NaOH).

Experiments were conducted in neutral to slightly alkaline solutions in the presence of free Fe(II), added as FeCl₂. At different time intervals, the redox state was determined. Redox potential values (-240 to -310 mV vs H₂) were always below those necessary for TcO₄⁻ reduction. The initial Fe(II)-concentration (4.5 × 10⁻⁵ M) decreased within a few days to approximately 2.5 × 10⁻⁵ M. The decrease in Fe(II)-concentration was concurrent with a slight decrease in pH. The Fe(II)-concentration was, following the initial decrease, found to be stable for at least 1 week. It was observed that no reduction of Tc(VII) occurred within 10 days. Upon increasing the pH to 9 by adding NaOH, 99 % of the initial technetium concentration disappeared from the solution within 5 hours. The Fe(II)-concentration in solution decreased to undetectable values (i.e. < 10⁻⁶ M).

These data can be explained as follows. Fe(II) in solution is not reacting, or at least very slowly, with the pertechnetate anion. Upon the addition of NaOH, Fe(II) was precipitated as Fe(OH)₂ (however not seen) according to:



The disappearance of TcO₄⁻ from solution is most probably caused by reactions with the 'active' precipitate Fe(OH)₂. This can be explained by a higher electron density of Fe(II)-containing precipitates compared with Fe(II)-solutions. The addition of ferrous-containing minerals or precipitates is sufficient to drive the redoxpotential to lower values, as noticed on figure 1 (Eh upto -431 mV).

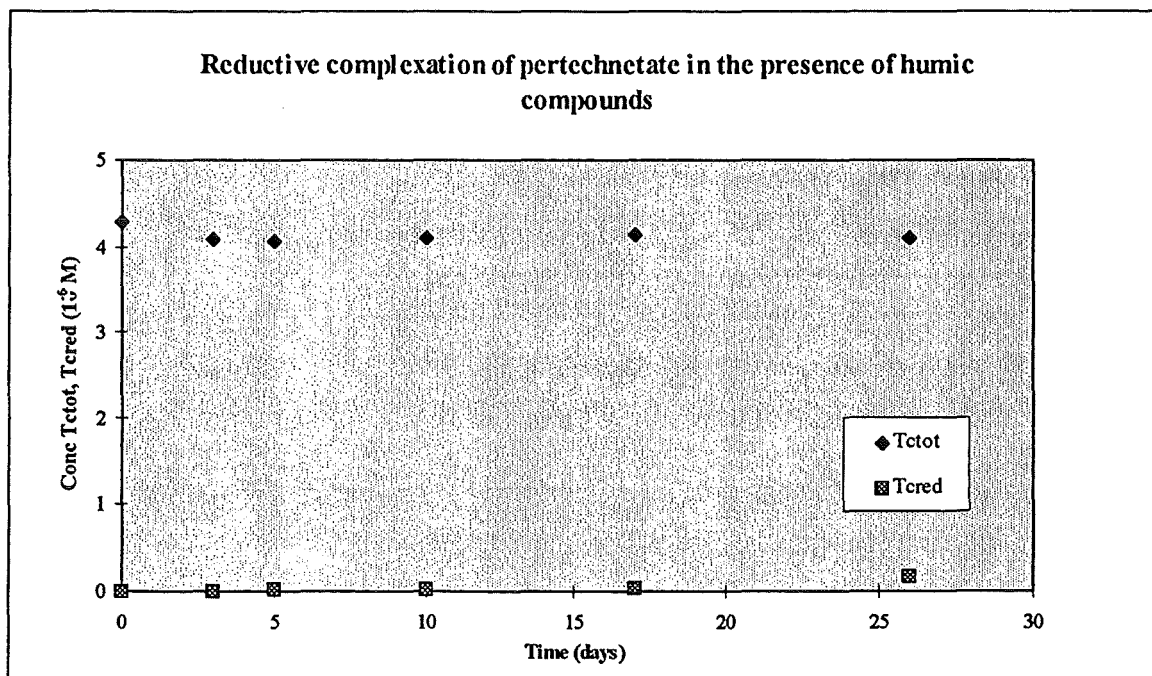
A plausible mechanism for the disappearance of Tc from the solution is sorption of TcO_4^- on the $\text{Fe}(\text{OH})_2$ precipitate followed by a reduction of TcO_4^- to $\text{TcO}_2 \cdot n\text{H}_2\text{O}$.

The fact that during the whole experiment no significant amounts of reduced Tc were measured in solution supports this hypothesis.

2.2. Reductive complexation of pertechnetate in the presence of humic substances

To study the complexation of Tc with organic matter, experiments were conducted with organic matter solutions both in the presence and absence of Fe^{2+} as a major cation. The organic matter (humic acid) used was extracted from Boom clay. In order to decarbonate the humic extract, HCl was added until pH 4 and the solution was stirred overnight until all CO_2 was volatilized. The pH was brought to its initial value (8.6) by adding NaOH, before pertechnetate was added ($[\text{TcO}_4^-] = 4.3 \times 10^{-6} \text{ M}$; $[\text{O.M.}] = 165 \text{ ppm}$). The initial concentration of the free Fe^{2+} was 10^{-4} M . At different time intervals, the redox state was determined.

Experimental data shown in figures 2 and 3 correspond to two independent identical experiments except for the absence and presence of Fe^{2+} .



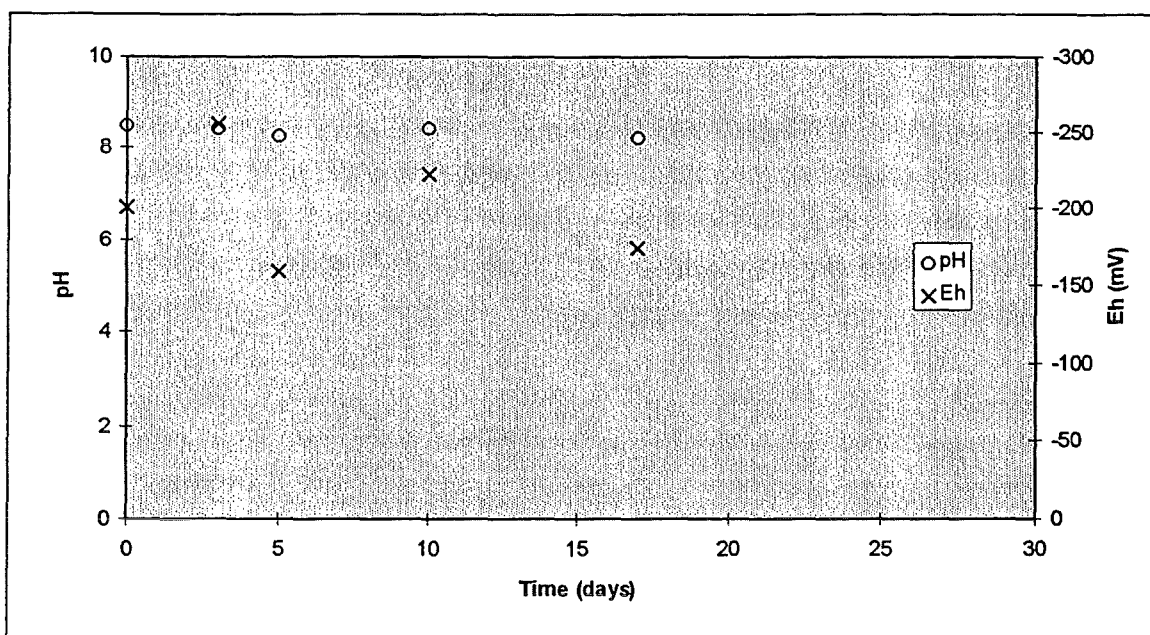
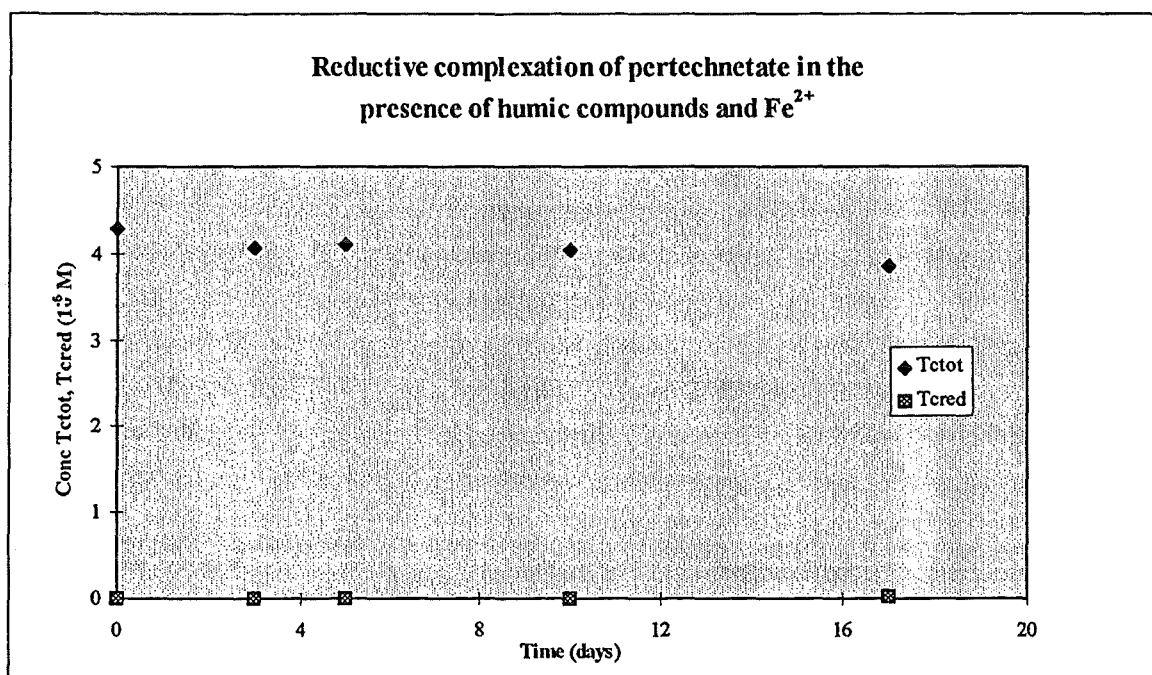


Figure 2: Reductive complexation of pertechnetate in the presence of humic compounds

No reduction could be obtained in both experiments. TcO_4^- levels, which were chromatographically monitored over a period of three weeks, remained unchanged, in spite of the fact that the redoxpotential values (-150 to -250 mV) were well below those necessary for reduction of TcO_4^- . Although ferrous iron may be present in the systems studied here, its e^- donor capacity is strongly impeded. No reductive complexation could be generated in the studied humic substance solutions.



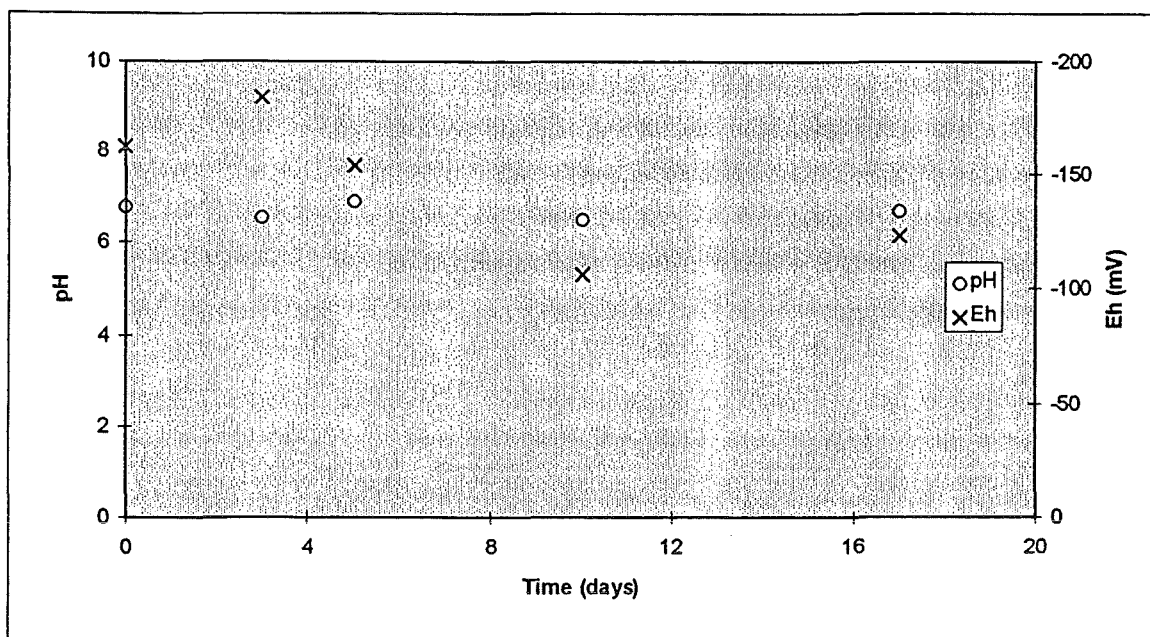


Figure 3: Reductive complexation of pertechnetate in the presence of humic compounds and Fe^{2+}

2.3. Conclusions

Although in both series of experiments favourable Eh-pH conditions were obtained, no removal of pertechnetate was observed, even in the presence of ferrous iron. These results show that reducing conditions alone are not sufficient for the reduction of TcO_4^- and that other factors, such as the presence of surfaces, play a significant role in the Tc reduction process.

3. Behaviour of Tc in aqueous solution in the presence of Fe-containing minerals and clay minerals

Experiments were conducted in neutral to slightly alkaline solutions in the presence of different Fe(II)-containing minerals. The polypropylene vials containing $100 (\pm 2)$ mg of the mineral (FeS, pyrite) and different volumes of the pertechnetate solutions were turned slowly head over head to ensure good mixing. After certain periods of time the minerals and solutions were separated by centrifugation at 18000 rpm for half an hour before being analyzed. Different experiments were carried out with each mixture. Experiments with the pertechnetate solution alone were also made to check for adsorption onto the container wall.

3.1. Influence of Fe-containing minerals on the behaviour of technetium

3.1.1. Sorption/precipitation of pertechnetate in the presence of FeS

In a first series of experiments FeS (100 mesh) was used as Fe-containing mineral.

Different amounts of ^{99}Tc radiolabelled pertechnetate solutions were added to the vials to obtain solid/liquid ratios of 1/100, 1/150 and 1/200 g/ml.

Within 2 days all Tc was removed from solution for all examined solid/liquid ratios. During those 2 days the pH dropped from 8.9 to 8, whereas the redoxpotential remained stable at values around -250 mV. No reduced Tc ($< 10^{-8}\text{M}$) was present in solution which indicates that all Tc was sorbed on the mineral surface. The data from this experiment are shown in $[\text{Tc}_{(\text{tot})}]$ and pH vs time plots for the different solid/liquid ratios in figure 4.

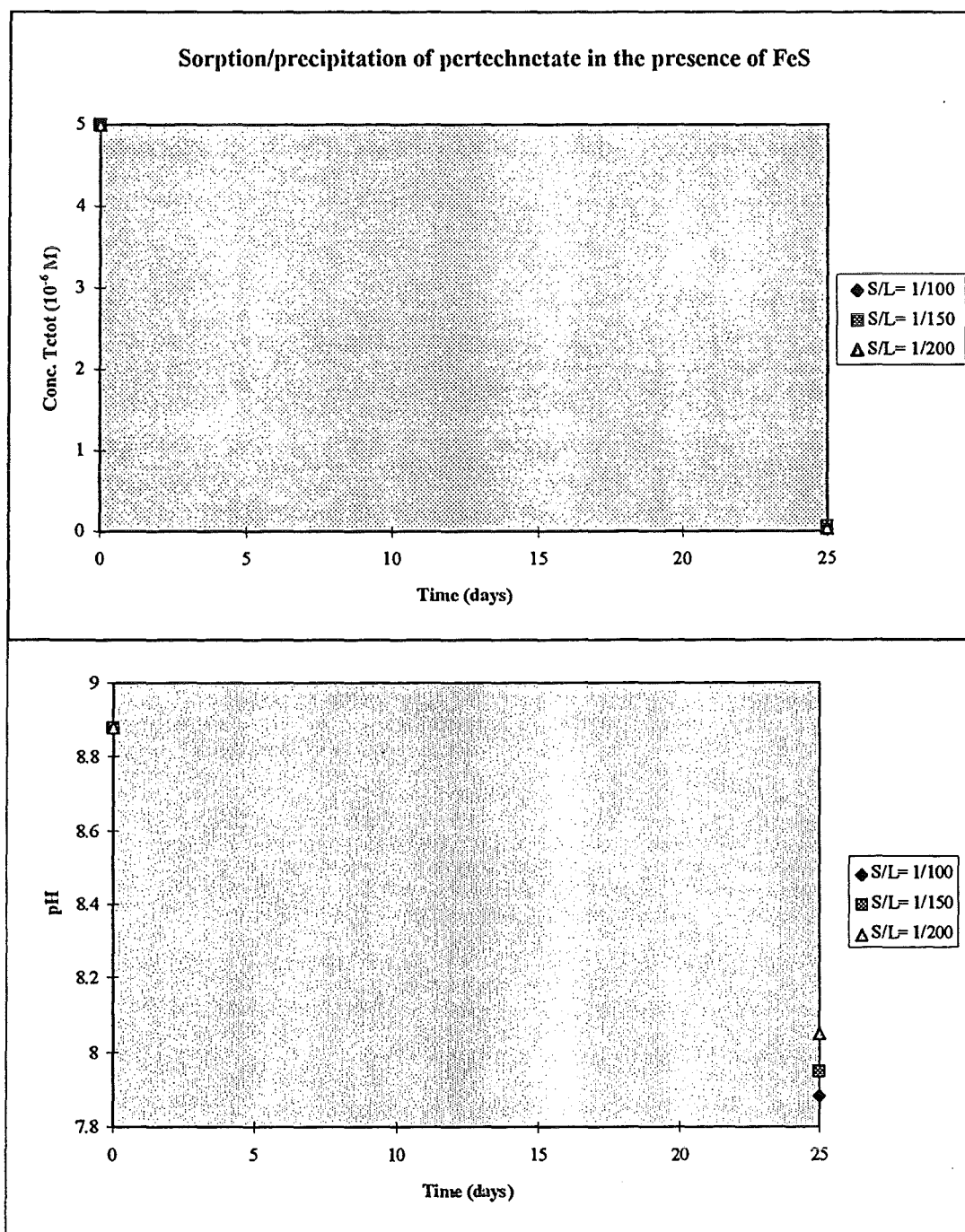


Figure 4: Sorption/Precipitation of pertechnetate in the presence of FeS

3.1.2. Sorption/precipitation of pertechnetate in the presence of FeS_2

A second series of experiments was executed with pyrite (FeS_2 , < 20 mesh) as Fe-containing mineral. The adsorption of Tc was studied as a function of time at two different solid/liquid ratios of 1/200 and 1/2000. The data from these experiments are shown in [Tc], pH and $[\text{Fe(III)}]$ vs time plots in figure 5 for the case of for the case of a solid/liquid ratio of 1/2000 and in figure 6 for the case of a S/L of 1/200.

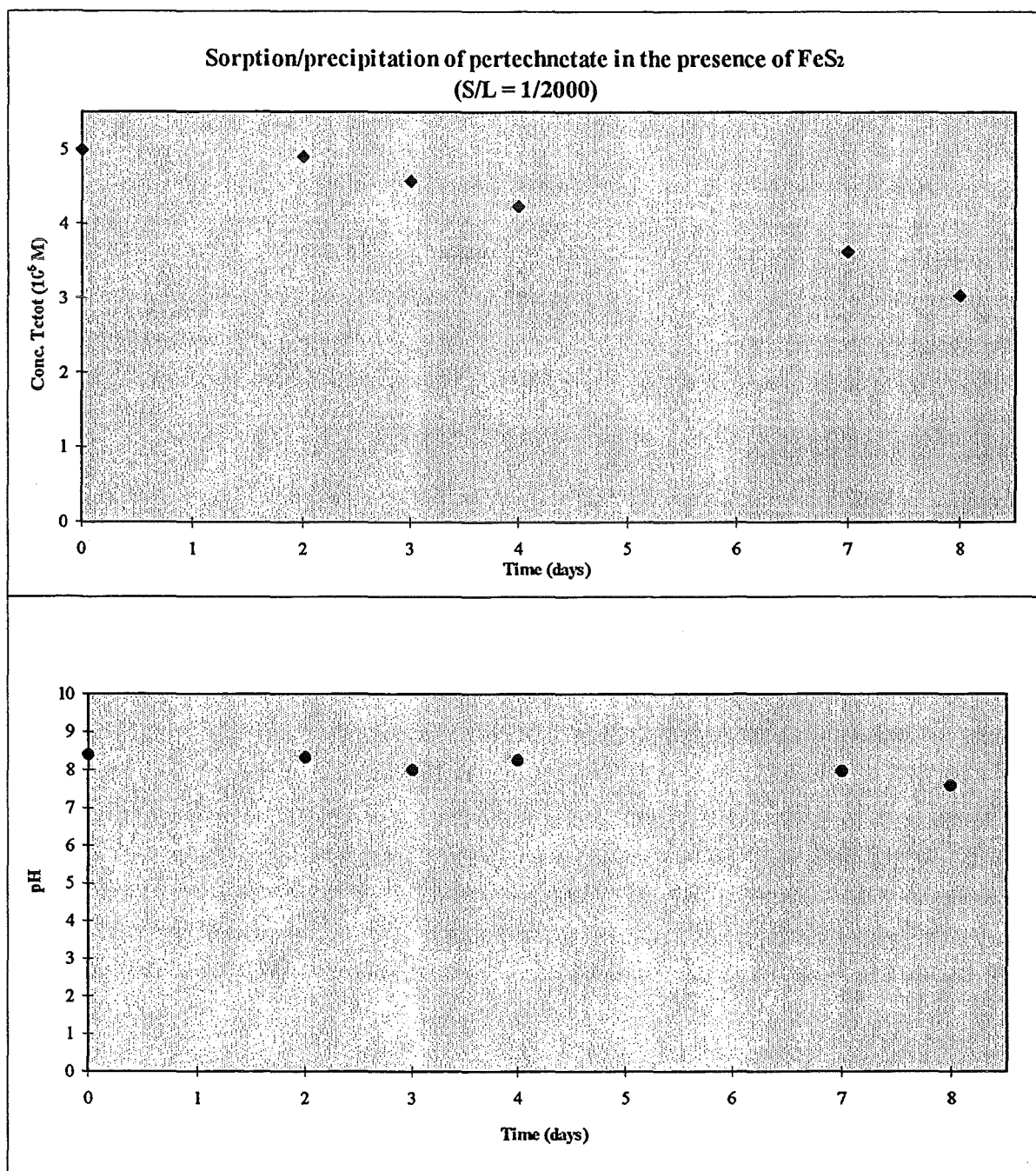


Figure 5: Sorption/Precipitation of pertechnetate in the presence of FeS_2 (S/L = 1/2000)

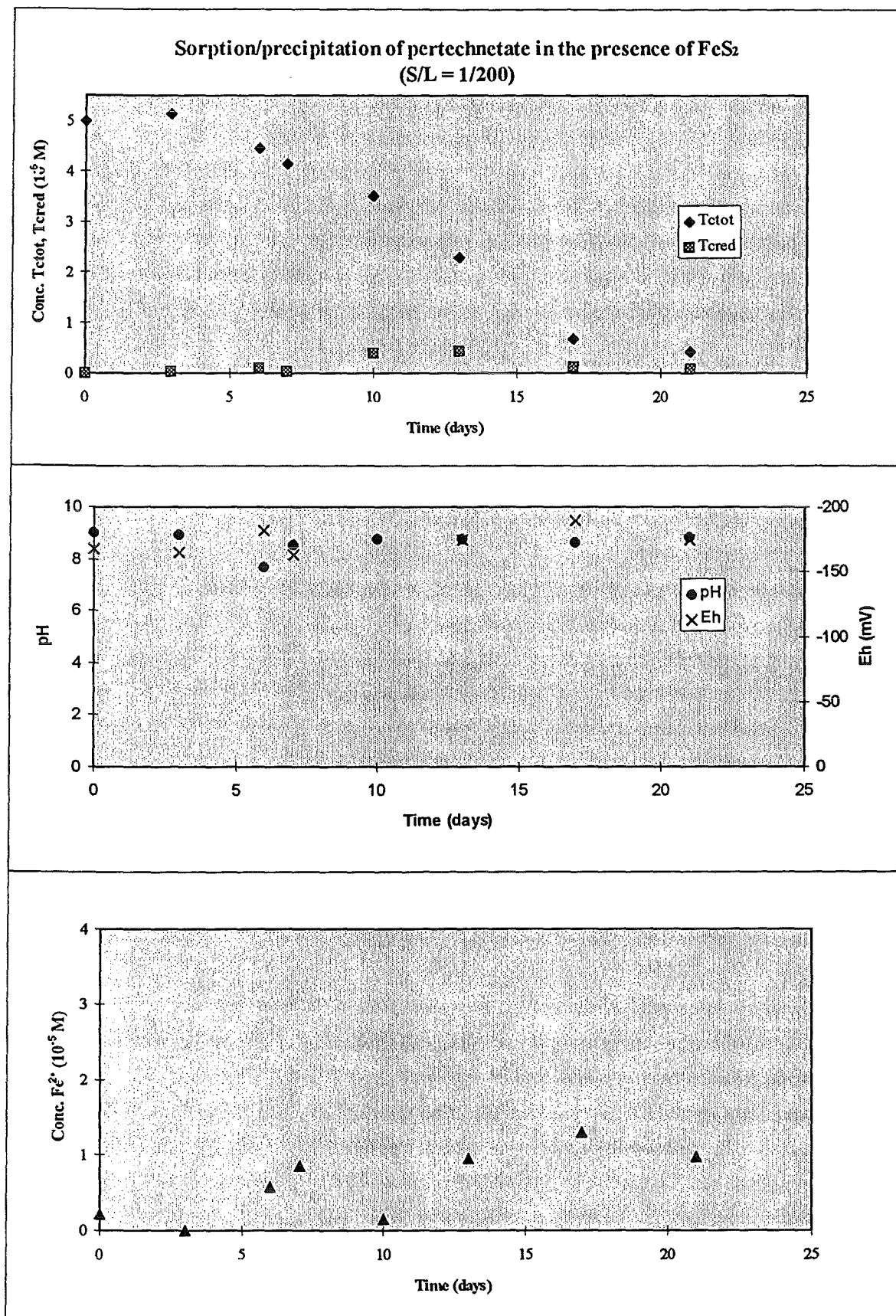


Figure 6: Sorption/Precipitation of pertechnetate in the presence of FeS₂ (S/L = 1/200)

For both solid/liquid ratios, a large difference in Tc removal was observed in comparison with results of FeS as Fe(II)-bearing mineral. In the case of a S/L of 1/2000 g/ml two third of the pertechnetate remained in solution after 1 week. In the case of a S/L of 1/200 g/ml all Tc was removed from solution but only after 20 days (vs FeS: 2 days).

By comparing the kinetics of FeS with those of FeS₂ at the same solid/liquid ratio (1/200 or 1/2000), it seems that the rate of disappearance is dependant of the Fe-containing mineral used. A possible explanation may be a different binding manner of Fe(II) in the solid phase, as well as the difference in specific surface area of the mineral, since the particle size of FeS₂ is larger than for FeS (higher specific surface area).

As can be seen from figure 6, Tc was efficiently (> 90 %) removed from solution within 21 days. During that time, pH and Eh remained stable at values around 8.5, respectively -170 mV. Iron was dissolved from pyrite (solubility FeS₂ = 4.9×10⁻³ g/l), giving values of upto 10⁻⁵ M Fe²⁺ in solution. No reduced Tc was found in solution, but Tc(VII) disappeared from solution and seemed to be sorbed on the mineral surface. Tc(VII) is probably reduced to Tc(IV) by a three-electron reduction process.

Further experiments were conducted with pyrite at a S/L ratio of 1/200 in the presence of bicarbonate (2 × 10⁻² M, pH 8.4) on the one hand to examine the influence of carbonate on the sorption of Tc on the mineral. On the other hand pyrite was pretreated with a dithionite-citrate solution in order to remove iron(III)oxides from the pyrite surface. Again, the adsorption of Tc was studied as a function of time.

For both experimental setups, no differences in kinetics were observed compared to the results obtained in the experiments shown in figure 6.

3.1.3. Sorption/precipitation of pertechnetate in the presence of FeS₂ and Fe²⁺

Further experiments were carried out to examine the effect of free Fe(II) on the behaviour of Tc in the presence of pyrite and as a function of time. An amount of 0.01 M FeCl₂ was added to 20 ml of the pertechnetate solution containing 100 mg of pyrite, in a way that an initial concentration of around 4 × 10⁻⁵ M Fe²⁺ was obtained.

Data from this experiment are shown in [Tc], pH and [Fe(II)] vs time plots in figure 7.

The main conclusion resulting from this experiment is that during the first six days only a small fraction (< 10 %) of the Tc is removed, while during the following 12 days the remainder of Tc is removed from solutions. At the end of the experiments (20 days) the technetium concentration in the aqueous solution was decreased to < 10⁻⁷ M. Additionally, the free iron concentration in the solution decreased from 4 × 10⁻⁵ M to lower values during the first week, while it increased during the further course of the experiment to values well above the initial

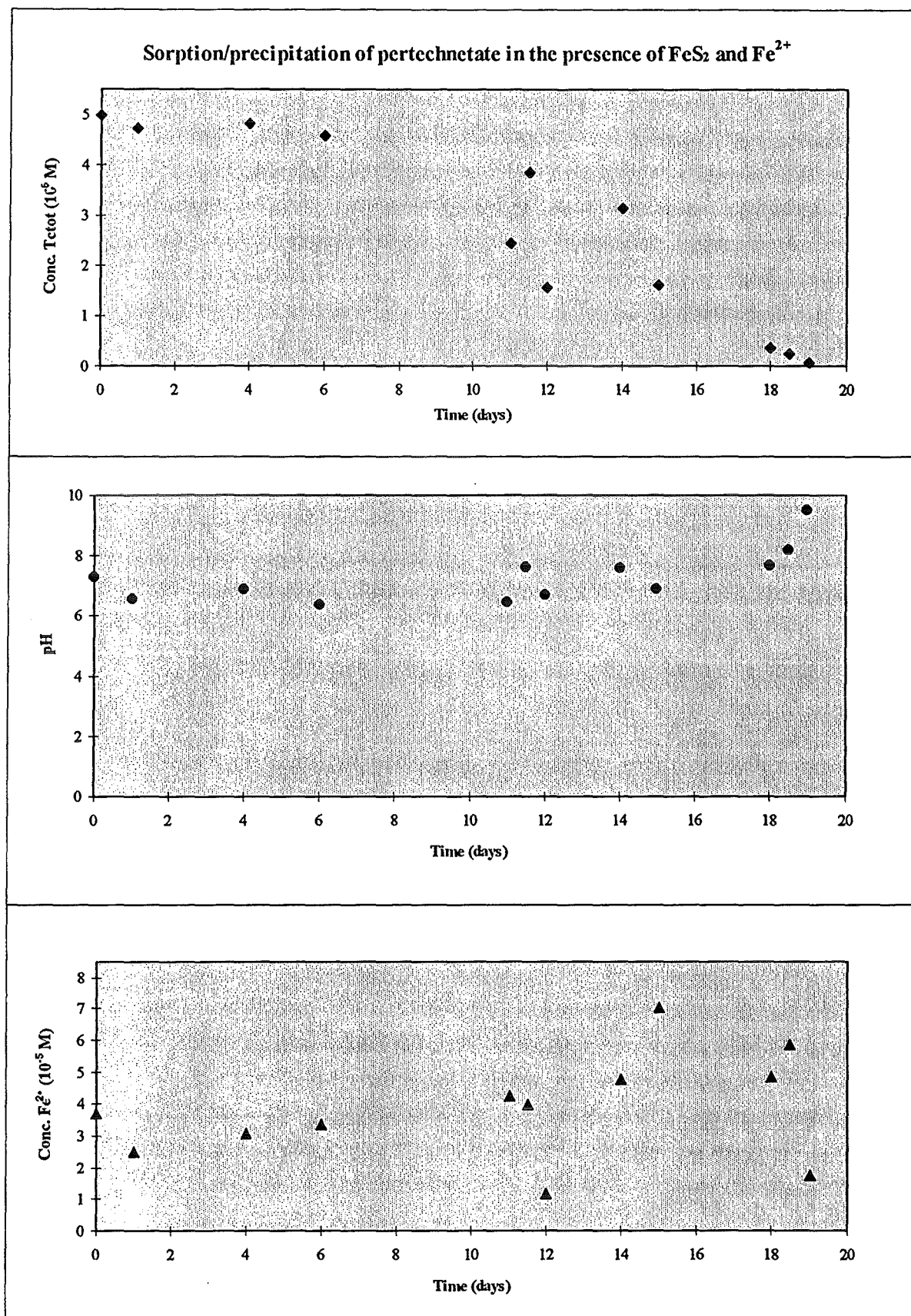


Figure 7: Sorption/Precipitation of pertechnetate in the presence of FeS_2 and Fe^{2+}

concentration (4×10^{-5} M) of the free iron. So Fe seemed to be released by the Fe-containing mineral.

No significant differences were observed compared to the results obtained from the reduction experiment with pyrite alone (see 3.1.2., figure 6). This would mean that the addition of Fe^{2+} as a free ion in solution has no effect on the removal/reduction of pertechnetate from solutions containing pyrite. This conclusion confirms the results from the first reductive complexation experiments (see 2.1., figure 1), in which it was demonstrated that TcO_4^- can not be reduced by Fe^{2+} (at the conditions studied), unless the iron is precipitated.

3.1.4. Conclusions

From the experiments described in section 3.1. we can conclude that Fe-containing minerals are capable to reduce pertechnetate from solutions efficiently. The presence of an additional amount of ferrous iron in solution has no significant influence on the kinetics of technetium disappearance, as noticed already in section 2.1. Furthermore, the observed rates of disappearance of Tc from solution in the presence of FeS is much faster than in the presence of FeS_2 .

3.2. Influence of clay minerals on the behaviour of technetium

3.2.1. Sorption/precipitation of pertechnetate in the presence of illite

Experiments were conducted in neutral to slightly alkaline solutions in the presence of illite as clay mineral. The polypropylene vials containing $100 (\pm 2)$ mg of the illite (< 0.2 mm) and 19 ml of a 10^{-3} M NaClO_4 -solution were shaken three days to stabilize the solution and to reach proper redox conditions. After those three days, 1 ml of a 10^{-4} M $^{99}\text{TcO}_4^-$ solution (in 10^{-3} M NaClO_4) was added to the polypropylene vials. So an initial concentration of 10^{-6} M pertechnetate was reached. The vials were turned slowly head over head to ensure good mixing. After certain periods of time the minerals and solutions were separated by centrifugation at 18000 rpm for half an hour before being analyzed. Experiments with the pertechnetate solution alone were also made to check for adsorption onto the container wall.

The data from this experiment are shown in $[\text{Tc}_{\text{tot}}]$, pH and $[\text{Fe}^{2+}]$ vs time plots in figure 8.

During the whole of the experiment (upto 2.5 months), the solution was alkaline at a constant pH of 8.5 - 9. All technetium in the solution remained present as pertechnetate (Tc(VII)). The fact that no reduction was noticed in the solution was probably due to the absence of any active sites on the clay mineral.

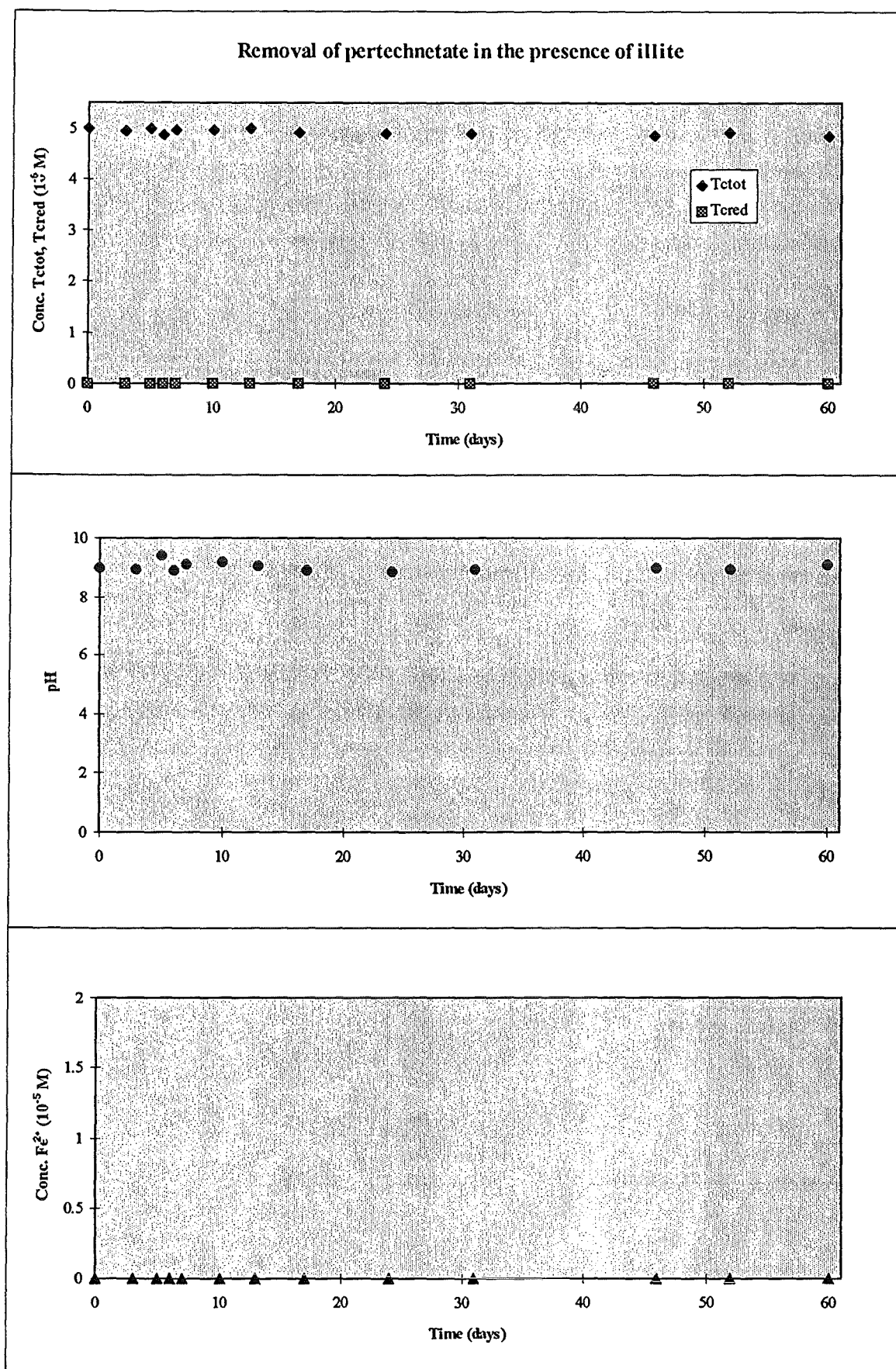
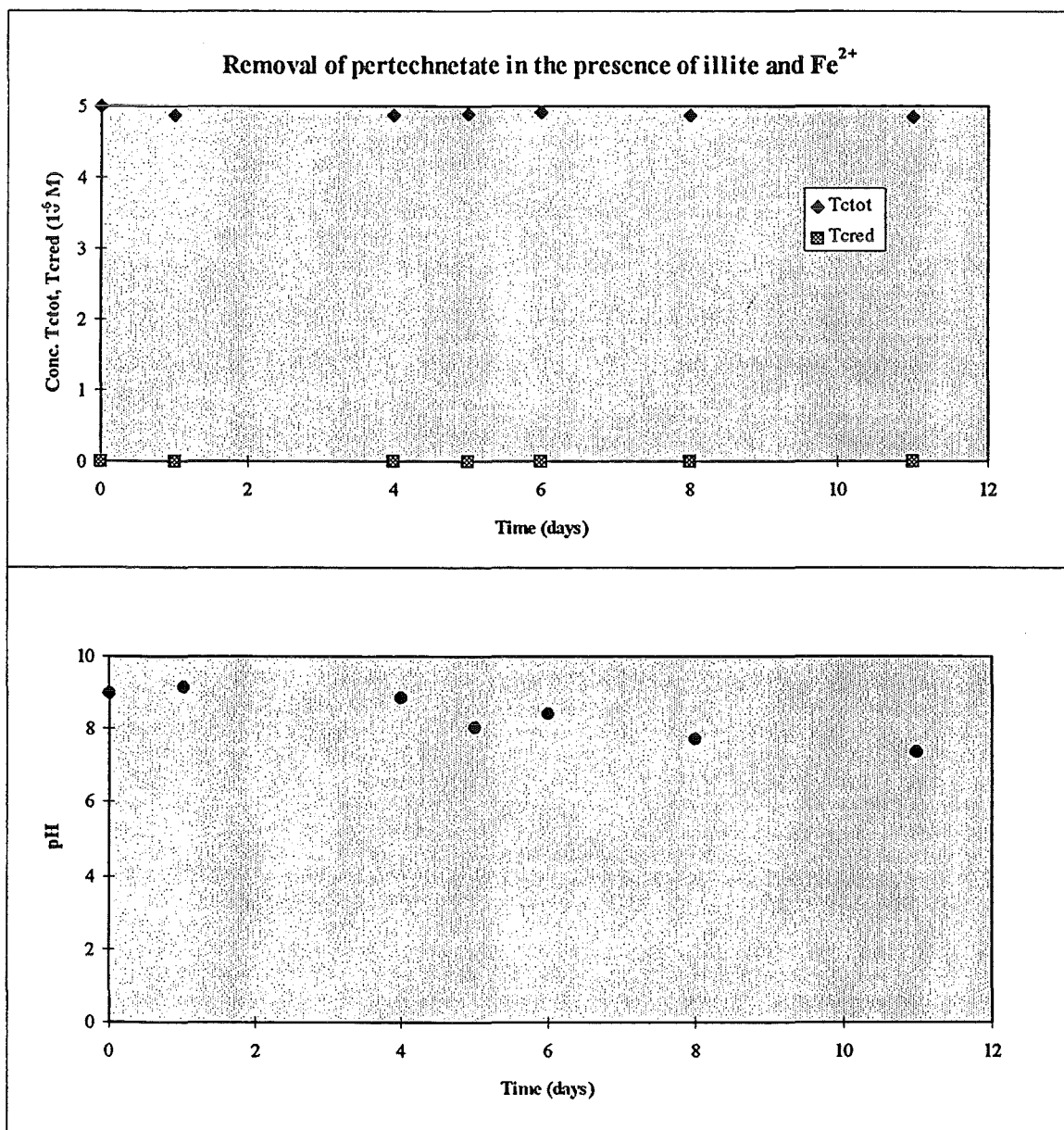


Figure 8: Sorption/Precipitation of pertechnetate in the presence of illite

3.2.2. Sorption/precipitation of pertechnetate in the presence of illite and Fe²⁺

In order to examine this hypothesis Fe²⁺ was added to the solution as FeCl₂ ([Fe²⁺]_{in} = 3.5 x 10⁻⁵ M) after two months. Experimental data are shown in figure 9. Again, all technetium in solution remained as Tc(VII) after two weeks. The free Fe(II) concentration in solution however was well below 10⁻⁵ M, which means that only 15 % of the added Fe²⁺ remained free in solution. Although Fe²⁺ was sorbed on the illite surface and active sites were present, no reduction of pertechnetate occurred.



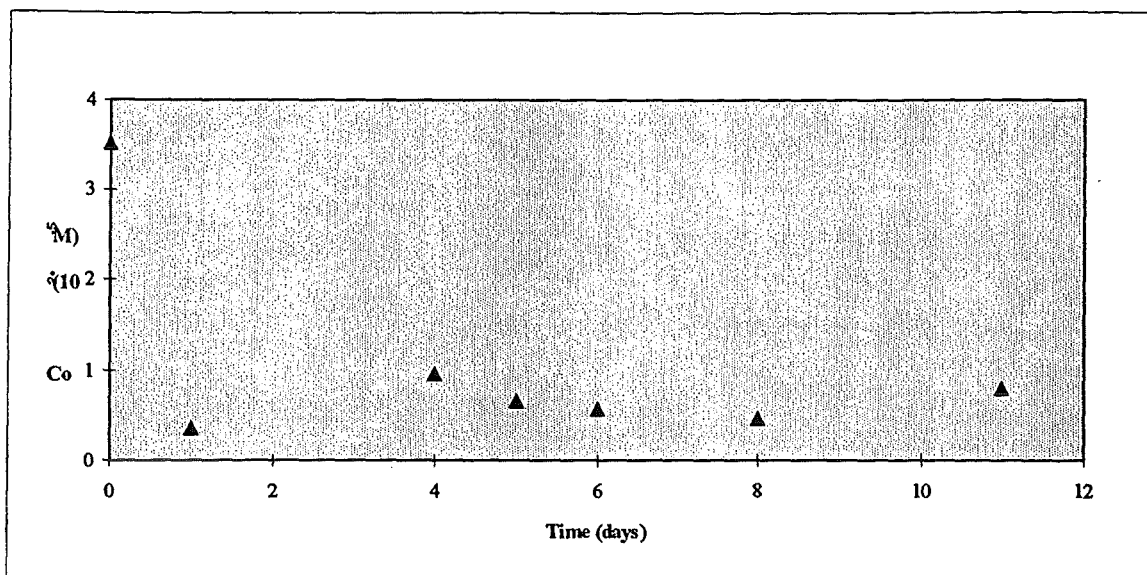
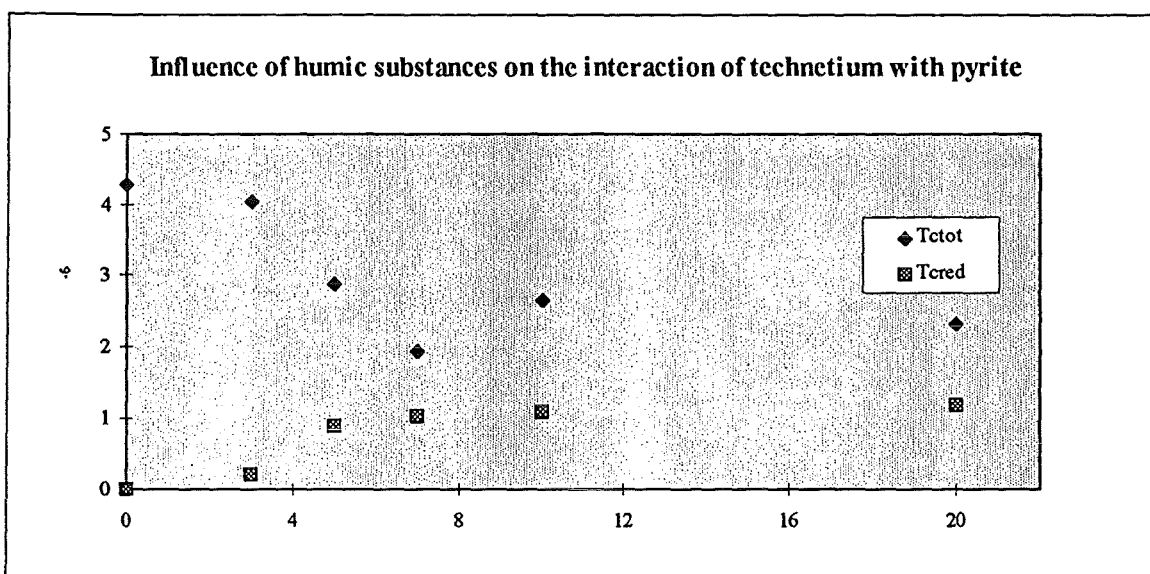


Figure 9: Sorption/Precipitation of pertechnetate in the presence of illite and Fe²⁺

3.3. Influence of humic substances on the interaction of Tc with mineral surfaces

In a final set of experiments the effect of humic substances on the interaction of Tc with pyrite was investigated. Extraction and decarbonation procedures, as described in section 1 and 2.2., were executed before adding the pyrite (100 mg) to the organic matter solution (S/L = 1/200). The initial concentration of pertechnetate in the organic matter solution (165 ppm) was 4.3×10^{-6} M.

In figure 10 data from this experiment are shown in [Tc], pH and Eh vs time plots as well as the different forms of Tc, which were chromatographically monitored.



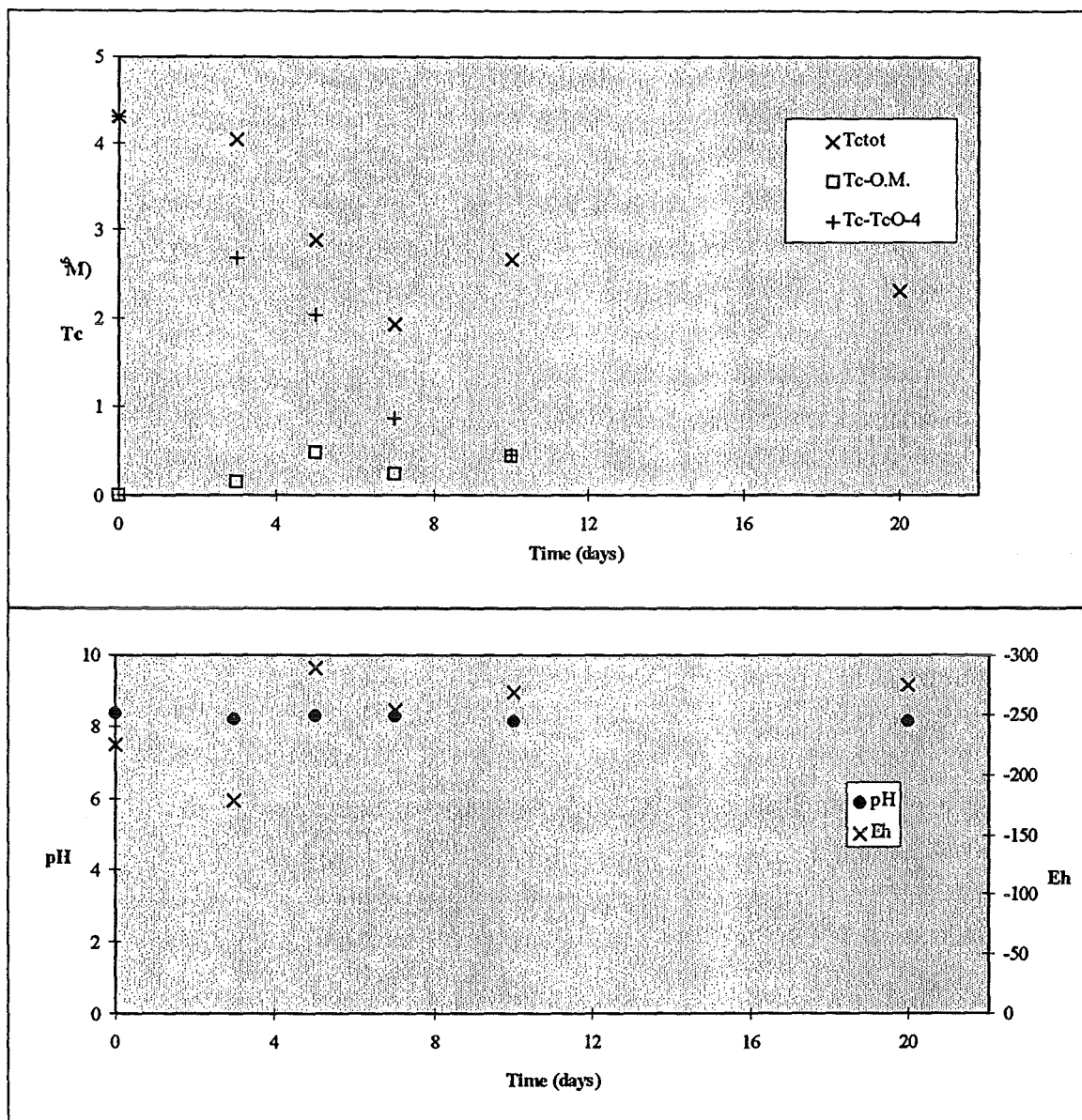


Figure 10: Influence of humic substances on the interaction of technetium with FeS_2

As can be seen from the different plots, redox potentials values (-180 to -290 mV) were always below those necessary for TcO_4^- reduction and the solution remained slightly alkaline ($\text{pH} \cong 8.2$). In the table below, the total and reduced forms as well as the different forms of Tc which were chromatographically monitored (Tc-TcO_4^- and Tc-O.M.) are presented. After 20 days only 54 % of the initial concentration of technetium was removed from solution, against more than 90 % in the case of pyrite alone (3.1.2.). However, as shown in the figure 50 % of the remaining fraction in solution was present as a reduced form of Tc. This reduced Tc doesn't correspond with the organic matter associated Tc alone since all the values of reduced Tc are higher than the ones for the Tc-O.M. Comparing however the residual Tc and the reduced Tc in solution at day 5 and 7, indicates that a fraction of this reduced technetium is in fact the technetium associated with the organic matter.

From the remaining fraction of technetium in solution, a constant amount of 15 % was associated with the humic substances.

Time (days)	T_{tot} (10 ⁻⁶ M)	Tc-TcO₄⁻ (10 ⁻⁶ M)	Tc-O.M. (10 ⁻⁶ M)	T_{Cresidual} = T_{tot} - Tc-O.M. - Tc-TcO₄⁻ (10 ⁻⁶ M)	T_{Cred} (10 ⁻⁶ M)
0	4.30	4.3	0	0	0.002
3	4.04	2.68	0.15	1.20	0.212
5	2.88	2.03	0.48	0.37	0.885
7	1.93	0.87	0.24	0.82	1.010
10	2.66	0.45	0.45	1.76	1.088
20	2.31	.25	.31	1.75	1.177

1st Technical Progress Report

EC Project:

"Effects of Humic Substances on the Migration of Radionuclides:
Complexation and Transport of Actinides"

LBORO Contribution to Task 2 (Complexation)

Studies of Metal Complexation with Humic and Fulvic Acid

Reporting period 1997

S.J. King and P. Warwick

Loughborough University
Department of Chemistry, Loughborough
GB-Leicestershire LE11 3TU
United Kingdom

CONTENTS

	<u>Page</u>
Executive Summary	221
1.0 Introduction	223
2.0 Preliminary Investigations	223
2.1 Eu sorption to Containing Vessel	223
2.2 Effect of Temperature on Humic Acid	223
3.0 Batch Experiments	225
3.1 Derivation of Stability Constants	225
3.2 Derivation of Thermodynamic Parameters	228
3.3 Discussion	228
4.0 Conclusion	229
5.0 Future Work	230
6.0 Aknowledgements	230
7.0 References	231
Figures	233
Tables	241

Effects of humic substances on the migration of radionuclides: Complexation and transport of actinides

CEC contract No F14W-CT96-0027

First Progress report covering the period January 97-December 97

Task 2: Complexation

Department of Chemistry, Loughborough University (LU) Leicestershire, UK.

S.J. King, and P. Warwick

Executive Summary

1.0 Introduction

The main objective of the project is to determine the influence of humic substances on the migration of radionuclides. One of the first steps taken in order to deepen this understanding was to investigate the complexation of Eu^{3+} with humic substances (Task 2).

There is concern that after disposal in underground repositories radionuclides may eventually come into contact with groundwaters containing humic acids at elevated temperatures. Preliminary investigations have therefore been undertaken to determine the effect of temperature on the stability constants for europium binding to humic acid by a series of batch experiments. Eu is used as an analogue of trivalent actinides.

2.0 Work Schedule

Task 2: Complexation

Temperature.

The effect of temperature on europium binding to humic and fulvic acid has been investigated by a series of batch studies at $\text{pH}=4.5$ and are close to completion. Developmental experiments have shown that sorption of Eu to the vessel walls at $\text{pH}=4.5$ and 6.5 is kept at a minimal level by the use of polysulfone tubes and $0.1 \text{ mol dm}^{-3} \text{ NaClO}_4$ solution. Similar experiments to those performed at $\text{pH}=4.5$ have been designed at $\text{pH}=6.5$.

Mixed species.

Experiments to investigate the presence of mixed species at high pH have been designed and preliminary studies are underway.

Task 3: Actinide transport

Batch and column experiments to investigate actinide transport are in the process of being designed, under close ongoing negotiations with migration model developers.

3.0 Summary of work carried out

The following experiments were conducted at LU during this reporting period.

1. Preliminary Investigations

Experiments were performed to determine the extent of Eu sorption to the containing vessel walls at $\text{pH}=4.5$ and $\text{pH}=6.5$. This was investigated with glass, polyethylene, polysulfone (PSF), Teflon FEP and Teflon PFA. Working stock Eu^{3+} solutions in the range 1.0×10^{-5} to 1.0×10^{-8} were prepared in NaClO_4 (0.01 mol dm^{-3}). At $\text{pH}=4.5$ PSF was found to be sufficiently non sorbing with no losses of Eu observed to the vessel walls even at 80°C . At $\text{pH}=6.5$ all materials showed significant sorption of Eu. However, sorption was significantly reduced at increased NaClO_4 concentrations and in the presence of cation exchange resin.

The stabilities of 50 mg/l HA solutions were investigated at temperatures of 25°C , 60°C and 80°C . By comparing UV absorbance at 254 nm of HA solutions held at different temperatures for a few days the change in HA concentration was investigated. Losses of less than 2% HA were observed when solutions were held at 60°C and 80°C .

A change in the degree of deprotonation of humic acid with increased temperature could be

expected to alter the loading capacity of the humic acid. A titrimetric method was therefore employed to investigate the effect of temperature on the deprotonation of the carboxylic acid groups of Aldrich humic acid^{1,2}. For a temperature change of 25°C to 60°C a change in pK_a of -0.01 would be expected for acetic acid, while for catechol a change of -0.43 pK_a units is expected. For humic acid no change was observed for the pK_a of 5. This is consistent with the very small change in pK_a for acetic acid.

2. Batch studies to determine the effect of temperature on Eu binding to humic /fulvic acid.

In the batch procedure Eu III solutions (1.0×10^{-6} , 1.1×10^{-7} , 2.4×10^{-8} mol dm⁻³) containing radioactive tracer quantities of Eu-152, were equilibrated with 0.004g (± 0.0001 g) of dry conditioned resin (Dowex 50x4, 100-200 mesh cation exchange resin). The experiments were performed in acid washed polysulfone centrifuge tubes with non-buffered NaClO₄ solution (0.1 mol dm⁻³) at pH=4.5, in the presence or absence of purified HA (2.5, 5, 7.5 and 10mg dm⁻³, Aldrich Chemical Co.). Samples were then left to equilibrate at temperatures between 20°C and 60°C for one week.

Similar batch studies were performed for Eu binding to fulvic acid (extracted from Derwent reservoir), at 20°C and 40°C. The fulvic acid used was provided and characterised (Task 1) by Jenny Higgo, at BGS.

3. Interpretation of results.

The stability constants were derived by three different approaches.

a) The Schubert method⁵, where the metal concentration remains fixed. The stability constants derived at Eu concentrations of 1.1×10^{-7} and 2.4×10^{-8} mol dm⁻³ were averaged at each temperature studied. These are shown in Table 1.

b) The Scatchard approach and the Charge neutralisation model⁷, where the humic acid concentration remains fixed. In both cases the results were first interpreted by the Ardakani and Stevenson approach⁴. The average stability constants over humic/fulvic acid concentration used at each temperature are shown in Table 1.

c) The derived stability constants for humic and fulvic acid binding Eu were found to be of similar magnitude, except those derived by the Schubert method.

4. Derivation of thermodynamic parameters

The thermodynamic parameters, ΔH , ΔG and ΔS were calculated from the stability constants determined from each of the three different model approaches. These derived parameters are shown in Table 2. The results by each different approach are in fairly good agreement and show that as the temperature increases the stability constant increases. However, the increase was not very significant, over the temperature range 20°C to 60°C. Overall the reaction of Eu binding to humic acid has been shown to be endothermic and entropy driven.

4.0 Planned activities for the next reporting period.

1. Eu batch studies.

It is envisaged that the investigation into the effect of temperature, from 4°C to 80°C, on Eu binding to HA and FA at pH=4.5 will be completed and presented in the next reporting period. It is also expected that results from experiments performed at pH=6.5 will be reported.

2. Uranium studies.

Similar batch experiments have been designed for Uranium. The results for Eu and U will then be used to derive thermodynamic constants for the interactions with HA and FA.

3. Mixed species EuHA(CO₃)_x

Experiments to determine the prevalence and stoichiometry of mixed species have been designed and preliminary investigations begun. Results are expected to be presented with in the next reporting period.

4. Mechanisms and kinetics

Studies are planned to study the mechanism and kinetics of HA association and dissociation to and from porous material.

1.0 Introduction

The main objective of the project is to determine the influence of humic substances on the migration of radionuclides. One of the first steps taken in order to deepen this understanding was to investigate the complexation of Eu^{3+} with humic substances (Task 2).

There is concern that after disposal in underground repositories radionuclides may eventually come into contact with groundwaters containing humic acids at elevated temperatures. Preliminary investigations have therefore been undertaken to determine the effect of temperature on the stability constants for specifically europium binding to humic acid by a series of batch experiments. Eu is used as an analogue of trivalent actinides.

2.0 Preliminary Investigations

2.1 Eu sorption to containing vessel

Preliminary experiments were performed to determine the extent of Eu sorption to the containing vessel walls at pH=4.5 and pH=6.5. This was investigated with glass, polyethylene (PE), polysulfone (PSF), Teflon FEP (fluorinated ethylene propylene) and Teflon PFA (perfluoroalkoxy).

Working stock Eu^{3+} solutions (1.0×10^{-5} , 1.0×10^{-6} , 1.0×10^{-7} , 1.0×10^{-8}) were prepared by successively diluting suitable solutions of A.R. grade $\text{EuCl}_3 \cdot 6\text{H}_2\text{O}$ with NaClO_4 solution (0.01 mol dm^{-3}). Tracer amounts of ^{152}Eu were added to the working stocks. Adjustment to pH=4.5 and pH=6.5 was achieved by the addition of small quantities of NaOH. Solutions at pH=6.5 were buffered with $10^{-3} \text{ mol dm}^{-3}$ MES(2-(N-Morpholino)ethansulphonic acid).

Solutions were left to equilibrate at room temperature or 80°C for a 3 to 5 days. Afterwards the activity of each supernatant solution was determined by taking a 1cm^3 aliquot for counting on Philips 4800 Gamma counter.

At pH=4.5 PSF was found to be sufficiently non sorbing with no losses of Eu observed to the vessel walls even at 80°C .

At pH=6.5 losses from solution were observed for all the following types of material tested, PE, PSF, FEP, PFA. Experiments were performed at room temperature for glass and at 80°C for all other materials. The percentage sorption of europium to the vessel walls for each material at varying europium concentrations are shown in Figure 1.

It was therefore decided to proceed with the studies at pH=4.5 using PSF tubes. However, PSF deteriorated after contact with HA. This meant that once PSF tubes had been used in the presence of HA the surface non-sorbing properties were reduced. Control experiments were therefore only performed in PSF centrifuge tubes which had not previously contained HA.

Different methods of overcoming sorption at the higher pH=6.5 were then investigated. The results from the preliminary experiments showed that by increasing the ionic strength of the solution from 0.01 mol dm^{-3} to 0.1 mol dm^{-3} the percentage of Eu in solution was observed to increase. The sorption of Eu to the PSF vessel walls was also observed to decrease in the presence of increased ionic strength at pH=6.5. In the presence of resin this was seen to be reduced to 2-3% at room temperature. In the presence of HA the sorption to the vessel walls would be expected to be further reduced due to competition for binding of Eu. It is therefore envisaged that experiments at pH=6.5 could be performed in NaClO_4 (0.1 mol dm^{-3}) by the Batch Method described later.

2.2 Effect of Temperature on Humic Acid

The effect of Temperature on the stability of HA.

Before embarking on experiments using HA (50mg/l) at elevated temperatures the stability of

HA at room temperature, 60°C and 80°C was compared. This was performed over a prolonged period of time by comparing the UV absorbance of the HA solutions at 254nm. It was found that there was negligible reduction in the concentration of HA at higher temperatures. A loss of 1.8% after 80 hours at 60°C and a 1.1% after 60 hours at 80°C.

The effect of Temperature on the acidity of HA.

The most important interaction between metals and humic acid materials in the pH range 4 to 9 is at the carboxylic acidic sites of the humic material. The formation of these metal-ligand complexes may be considered as the displacement of one or more acidic protons from the humic acid by the metal ion. A change in the degree of deprotonation of humic acid with increased temperature could therefore be expected to alter the loading capacity of the humic acid. A titrimetric method was therefore employed to investigate the effect of temperature on the deprotonation of the carboxylic acid groups of Aldrich humic acid^{1,2}.

Experimental method.

The cell used is shown in Figure 2. It consisted of a double walled glass cell through which thermostated water was pumped through to maintain a constant temperature. Inlets were provided for a burette, pH glass electrode and for passage of nitrogen gas. The experiments were performed at 25°C, 60°C and 80°C.

Validation of technique.

The method was first validated with two well characterised compounds: acetic acid and catechol (1,2-dihydroxybenzene), which have ΔH values of +0.4 and +25kJ/mol, respectively³.

Acetic acid (20ml of 0.1M) and catechol (20ml of 0.3M) were prepared in 0.1M NaCl as supporting electrolyte. Each solution was then titrated by the addition of 0.2ml increments of 0.1M NaOH. The system was then allowed to equilibrate and the pH reading recorded. The experiments were performed several times.

The raw data was used to calculate ($\Delta pH/\Delta$ volume added) as an approximation to the first differential dpH/dv . The ($\Delta pH/\Delta$ volume added) was then plotted against pH to obtain a graph where the maxima correspond to equivalence points, while the minima correspond to pK_a values.

The plots of $\Delta pH/\Delta v$ versus pH can be seen for acetic acid and catechol in Figures 3 and 4, respectively. The shift in pK_a is in agreement with that predicted from the rearranged form of the Van't Hoff equation shown below:

$$pK_{a2} - pK_{a1} = \frac{\Delta H^\ominus}{2.303R} \left(\frac{1}{T_2} - \frac{1}{T_1} \right) = \Delta pK_a \quad (1)$$

From equation (1) for a temperature rise from 27°C to 60°C a change in pK_a of -0.01 would be expected for acetic acid, while for catechol a change of -0.43 pK_a units.

Humic acid.

0.2g of Aldrich humic acid (unpurified) was dissolved in 10ml of 0.1M NaOH solution, then acidified to below pH 2.5 with 12ml of 0.2M HCl. The resulting solution was then titrated up to about pH =10.

It can be seen in Figure 5 that the pK_a values of humic acid for the carboxylic groups undergo minimal change with temperature. This observation is consistent with the small change in pK_a detected for other carboxylic acids, such as acetic acid, which is due to the low ΔH values of the deprotonation reaction.

3.0 Batch experiments

1. *Batch studies to determine the effect of temperature on Europium binding to humic acid.*

In the batch procedure Eu III solutions (1.0×10^{-6} , 1.1×10^{-7} , 2.4×10^{-8} mol dm⁻³) containing radioactive tracer quantities of Eu-152, were equilibrated with 0.004g (± 0.0001 g) of dry conditioned resin (Dowex 50x4, 100-200 mesh cation exchange resin). The resin was completely converted to the sodium form before use by washing successively with HCl (2 mol dm⁻³), distilled H₂O, NaCl (3 mol dm⁻³), distilled H₂O, NaOH (0.1 mol dm⁻³), distilled H₂O and finally with the appropriate pH solution before air drying.

The experiments were performed in acid washed polysulfone centrifuge tubes with non-buffered NaClO₄ solution (0.1 mol dm⁻³) at pH=4.5, in the presence or absence of purified HA (2.5, 5, 7.5 and 10mg dm⁻³, Aldrich Chemical Co.). Samples were then left to equilibrate at temperatures between 20°C and 60°C for one week. During this time samples were shaken at frequent intervals.

Afterwards the activity of each supernatant solution was determined by removing a 1cm³ aliquot for counting on Philips 4800 Gamma counter.

The pH of the solutions were checked at the end of the experiment and the measurement is rejected from any sample for which the pH had drifted considerably.

From knowing the amount of activity originally added and the total metal concentrations, the measured supernatant activities were used to calculate the concentration of metal remaining in each solution ([Eu]soln) and the amount sorbed by the resin ([Eu]res).

In order to obtain meaningful results it was important that samples contained sufficient activity for counting. It was therefore found necessary to reduce the amount of resin used in these experiments to 0.004g.

2. *Batch studies to determine the effect of temperature on Europium binding to fulvic acid.*

Similar batch studies were performed for Eu binding to fulvic acid (extracted from Derwent reservoir), so far only at 20°C and 40°C. The fulvic acid used was provided and characterised (Task 1) by Jenny Higgo, at BGS.

3.1 Derivation of Stability constants

The stability constants were derived by three different approaches.

- The Schubert method⁵, where the metal concentration remains fixed. The stability constants derived at Eu concentrations of 1.1×10^{-7} and 2.4×10^{-8} mol dm⁻³ were averaged at each temperature studied. These are shown in Table 1.
- The Scatchard approach and the Charge neutralisation model⁷, where the humic acid concentration remains fixed. In both cases the results were first interpreted by the Ardakani and Stevenson approach⁴. The average stability constants over humic/fulvic acid concentration used at each temperature are also shown in Table 1.

1. *Changing Metal Concentration*

This batch procedure was based on the Ardakani and Stevenson modification of the Schubert Method⁴. In the batch procedure Eu III solutions, containing radioactive tracer quantities of Eu-152, were equilibrated with cation exchange resin in the absence (controls) and presence of HA.

Results were interpreted by using the usual the Ardakani and Stevenson approach⁴, except log plots were used as the concentrations ranged over two orders of magnitude. Plots of log [Eu]res against log [Eu]soln were constructed, at each temperature, both for the controls and the solutions containing the HA. These plots were used to deduce the amounts of EuHA

present in each sample. At any [Eu]_{res} value, [EuHA] was found after anti logging and subtracting the control [Eu] solution value from the sample [Eu] soln value. This generated a large number of paired values of [EuHA] and [Eu]. This data was then interpreted further by two approaches, the Scatchard Method and the Charge Neutralisation Model.

Scatchard Approach.

The simple Scatchard approach is often used as it assumes a reaction stoichiometry of 1 cation to 1 site. This approach also does not require knowledge of the humic acid concentration. For the reaction,



the stability constant K is given by

$$K = \frac{[ML]}{[M][L]} \quad (3)$$

At equilibrium the free site concentration [L] equals the total site concentration [ML]_{MAX} minus the concentration of occupied sites [ML].

Hence

$$K = \frac{[ML]}{[M]([ML]_{MAX} - [ML])} \quad (4)$$

Therefore

$$\frac{[ML]}{[M]} = -K[ML] + K[ML]_{MAX} \quad (5)$$

A plot of [ML]/[M] versus [ML] has a slope of -K. Stability constants for the humic acid binding of Eu over the concentration range used of Eu were then estimated from fitting straight lines to plots of the experimental data. Scatchard plots in this case were found to be curved, as they invariably are for humic and fulvic acid. Therefore, two lines were fitted to the experimental data, to derive a stability constant over the Eu concentration of 1 x 10⁻⁶ to 1 x 10⁻⁷ mol dm⁻³ and 1 x 10⁻⁷ and 1 x 10⁻⁸ mol dm⁻³. A typical Scatchard plot for data obtained in this study is shown in Figure 6.

Charge Neutralisation Model.

The Charge Neutralisation Model as proposed by Kim and Czerwinski⁷ is based on the concept of metal ion charge neutralisation upon complexation to humic acid functional groups. Only a fraction of the total sites present on the humic acid are available for reaction under a given set of conditions. Hence the effective concentration of humic acid ([HA(z)]_{eff}) is calculated from its proton exchange capacity (PEC), metal ion charge (z) and loading capacity of the humic (LC), which changes as a function of pH, ionic strength and metal ion charge. It is defined as:

$$[HA(z)]_{eff} = \frac{(HA)(PEC)(LC)}{z} = [HA(z)]_t(LC) \quad (6)$$

where (HA) is the concentration of humic acid in g/l, [HA(z)]_t in mol/l and PEC in eq/g. The proton exchange capacity for Aldrich Humic acid and Derwent fulvic acid has been determined to be 5.43 ± 0.20 meq/g⁶ and 5.00 meq/g (under Task 1, at BGS).

The complexation reaction for a trivalent cation can be described as:



The free humate site concentration at equilibrium is given by

$$[\text{HA(III)}] = [\text{HA(III)}]_t \text{LC} - [\text{MHA(III)}] \quad (8)$$

Therefore

$$K = \frac{[\text{MHA}(z)]}{[\text{M}^{Z+}]_f ([\text{HA}(z)]_t \text{LC} - [\text{MHA}(z)])} \quad (9)$$

Rearranged

$$[\text{M}^{Z+}]_f = \text{LC} \left(\frac{[\text{M}^{Z+}]_f [\text{HA}(z)]_t}{[\text{MHA}(z)]} \right) - \frac{1}{K} = \text{LC} \times F - \frac{1}{K} \quad (10)$$

In the absence of knowledge of the loading capacity (LC) of HA under given conditions the stability constant K and LC can be determined from a plot of $[\text{M}^{Z+}]_f$ versus F has a slope of LC and a y intercept $-1/K$. A typical plot can be seen in Figure 7. It can be seen that these plots yielded curves. The model was used in the traditional manner and the best straight line fitted to this curve to determine a single stability constant.

2. Changing Ligand Concentration

Schubert Method.

The original Schubert method was also investigated for the determination of Eu-HA stability constants⁵. In this method the metal ion is regarded as the central group. This is only true when the concentration of metal ions is much smaller than that of the ligand. The experiments were performed at pH=4.5 with the Eu concentration (1.1×10^{-7} and $2.4 \times 10^{-8} \text{ mol dm}^{-3}$) fixed and the HA concentration varied (0, 2.5, 5, 7.5 and 10 mg dm^{-3}). In equation (11), $[\text{HA}]_f$ is the concentration of free humic acid ligands:

$$[\text{HA}]_f = [\text{HA}] - m[\text{M(HA)}] \quad (11)$$

where $[\text{HA}]$ is the initial concentration of humic acid and m the ligand to metal ratio. As the concentration of metal ions is very small compared with that of humic acid, $[\text{HA}]_f$ is essentially constant and equal to $[\text{HA}]$. For this reason results for $1.0 \times 10^{-6} \text{ mol dm}^{-3}$ were not used by this method.

The distribution coefficients of metal ions between resin and solution in the presence of humic acid (D) and absence of humic acid (D_0) are given by

$$D = \frac{[\text{M}]_{\text{RESIN}}}{[\text{M}]_{\text{AQ}} + [\text{ML}]} \quad (12)$$

$$D_0 = \frac{[\text{M}]_{\text{RESIN}}}{[\text{M}]_{\text{AQ}}} \quad (13)$$

As the distribution coefficient in the absence of HA (D_0) and in the presence of HA (D) is related to the concentration of HA (mol dm^{-3}) and the stability constant K by the following expression

$$\frac{D_o}{D} = 1 + K[HA] \quad (14)$$

It follows that

$$\log\left(\frac{D_o}{D} - 1\right) = \log K + m \log[HA] \quad (15)$$

Plots of $\log D_o/D-1$ versus $\log [HA]$ were used to derive the stability constant $\log K$ and m from the intercept and slope of the line. A typical graph can be seen in Figure 8.

3.2 Derivation of thermodynamic parameters

The thermodynamic parameters, ΔH , ΔG and ΔS were calculated from the stability constants determined from each of the three different model approaches. The enthalpy of the complexation reaction of Eu and HA is given by

$$-\frac{\Delta H}{R} = \frac{d \ln K}{d(1/T)} \quad (16)$$

The Gibbs free energy and the entropy of the complexation reaction were determined from

$$\Delta G = -RT \ln K \quad (17)$$

and

$$\Delta S = (\Delta H - \Delta G)/T \quad (18)$$

These derived parameters for EuHA and EuFA complex formation at 293K are shown in Table 2.

3.3 Discussion

The stability constants derived for EuHA and EuFA complexation were observed to increase as temperature increased.

LogK derived using Fixed Humic /Fulvic acid Concentration.

The $\log K$ values derived by the Charge Neutralisation Model and Scatchard Approach for both humic and fulvic acid are in good agreement. For example, measurements at 30°C with 2.5mg/l HA yielded stability constants of 8.03 (CN Model), 7.80 and 8.63 (Scatchard), as can be seen in Table 1. However, as can be seen in Figure 7 the plot produced from the Charge Neutralisation Model approach is curved. Therefore, two lines were also fitted to the curve to produce stability constants over the Eu concentration range of 1×10^{-6} to 1×10^{-7} mol dm⁻³ and 1×10^{-7} and 1×10^{-8} mol dm⁻³. Very similar stability constants to those derived by the Scatchard approach were calculated, i.e. 7.76 and 8.64.

In comparison the stability constants derived for humic and fulvic acid are very similar. In addition the loading capacity factor of humic and fulvic acid were also found to be similar, i.e. 0.065 ± 0.026 and 0.061 ± 0.009 , respectively.

LogK derived using Fixed Metal Concentration.

However, the $\log K$ values derived by the Schubert Method are between a factor of 4-200 times lower than those derived by the previously mentioned methods. This is probably due to the different values used for the concentration of humic acid in the Charge Neutralisation (CN) Model and Schubert Method. The CN Model makes the assumption that the effective

concentration of humic acid is dependent the loading capacity factor of a humic molecule for a particular metal and the charge on the metal ion. The Schubert Method makes no assumptions on the capacity of humic acid to bind metals rather than protons and the humic concentration is therefore expressed in terms of the proton exchange capacity of the humic acid (eq/l). If the effective concentration of humic acid is substituted into the Schubert Model the stability constants derived are of similar magnitude to those derived by the Scatchard approach and the CN model.

In contrast to the aforementioned approaches the similarity between the stability constants derived for humic and fulvic acid by the Schubert Method is poor. The measured stability constants suggest that the binding of Eu by fulvic acid is at least an order of magnitude stronger/higher than for humic acid. This appears to be an effect of varying the ligand concentration.

The slopes of the Schubert plots for the HA data were found to be very close to one, with the exception of the two temperature extremes, 20°C to 60°C producing slopes on average of 0.85 ± 0.03 and 1.24 ± 0.07 , respectively. For fulvic acid the slopes on average were determined to be 1.09 ± 0.16 and 1.30 ± 0.06 , for 20°C and 40°C respectively.

Derivation of Thermodynamic Parameters.

The enthalpy changes under standard atmospheric pressure were deduced from the slopes of the plots of $\log K$ against $1/T$ in accordance with equation (16). The plots were found to be linear and are shown in Figures 9, 10 and 11. The values for ΔG and ΔS were obtained using the equations (17) and (18). The thermodynamic parameters, ΔG , ΔS and ΔH , for EuHA and EuFA complexes at 293K are listed in Table 2. There is good agreement between the ΔH values derived by CN model and Scatchard approach, however the Schubert model suggests slightly higher values. The complexation reaction overall was found to be endothermic. The values indicate spontaneous changes (ΔG negative) with a large favourable entropy change (ΔS positive). In comparison the values for EuHA and EuFA are very similar. It has been suggested that the entropy increase results from the release of coordinated water molecules during complexation⁸.

In Table 3 the ΔG , ΔS and ΔH for EuHA complexation at 298K are shown compared to other published data for SrHA, ThHA and UO₂HA. The values derived for EuHA are of a similar order of magnitude to those derived for ThHA complexation. In contrast the complexation reaction for SrHA was found to be exothermic overall with a less favourable entropy than that derived for EuHA.

4.0 Conclusion

1. Batch studies investigating the binding of Eu to HA at pH=4.5 and 6.5 can be performed with minimal sorption of Eu to the vessel walls by using PSF centrifuge tubes and NaClO₄ solution (0.1 mol dm⁻³).
2. Humic acid is stable over the temperature range used in these projects experiments (25°C to 80°C). Negligible change was observed in concentrations and of pK_{as} of the humic acids carboxylic acid groups.
3. The stability constants derived by each different approach are in fairly good agreement and show that as the temperature increases the stability constant increases. However, the increase was not very significant, over the temperature range 20°C to 60°C.
4. Similar stability constants were derived for humic and fulvic acid by the Charge Neutralisation Model and Scatchard Approach. However, the Schubert model predicted stability constants of an order of magnitude higher for the fulvic acid than the humic acid.
5. Overall the reaction of Eu binding to humic and fulvic acid has been shown to be endothermic and entropy driven. Similar thermodynamic parameters were calculation for EuHA complexation to those cited for ThHA in Table 3.
6. The thermodynamic parameters calculated for humic and fulvic acid were similar. In both cases the ΔH and ΔS determined from stability constants derived by the Schubert model were slightly higher than those by the other two approaches.

5.0 Future Work

1. *Eu batch studies.*

It is envisaged that the investigation into the effect of temperature, from 4°C. to 80°C, on Eu binding to HA and FA at pH=4.5 will be completed and presented in the next reporting period. It is also expected that results from experiments performed at pH=6.5 will reported.

2. *Uranium studies.*

Similar batch experiments have been designed for Uranium. The results for Eu and U will then be used to derive thermodynamic constants for the interactions with humic and fulvic acid and will be included in the next reporting period.

3. *Mixed species $EuHA(CO_3)_x$*

Experiments to determine the prevalence and stoichiometry of mixed species have been designed and preliminary investigations begun. Results are expected to be presented with in the next reporting period.

4. *Mechanisms and kinetics*

Studies are planned to study the mechanism and kinetics of HA association and dissociation to and from porous material.

6.0 Acknowledgement

The European Community is thanked for funding this work.

7.0 References

- (1) Titrimetric Determination of Acidity and pK values of Humic Acid. O.K. Borggaard. *Acta Chem. Scand.* A28, No. 1, 121-122, (1974).
- (2) Studies of Selected Organic-Metal Interactions of Importance in the Environment. I.Mason. Ph.D. Thesis, Loughborough University.
- (3) Critical Stability Constants. A.E. Martell and R.M Smith. Volume 5, 1st Supplement, 1982, Plenum.
- (4) A Modified Ion Exchange Technique for the Determination of Stability Constants of Metal Soil Organic Matter Complexes. M.S. Ardakani and F.J Stevenson. *Soil Sci. Soc. Amer. Proc.* 36, 884-890, (1972).
- (5) The use of ion exchangers for the determination of physical-chemical properties of substances, particularly radio tracers in solution. J. Schubert. *Theoretical. J. Phys. Colloid Chem.* 52, 340-350, (1948).
- (6) Complexation of Americium(III) with Humic Acid. J.I. Kim, G. Buckau, E. Bryant and R. Klenze. *Radiochimica Acta*, 48, 135-143, (1989).
- (7) Complexation of Metal Ions with Humic Acid: Metal Ion Charge Neutralisation Model. J.I. Kim and K.R. Czerwinski. *Radiochimica Acta*, 73, 5-10, (1996).
- (8) Complexation Thermodynamics of Sr(II) and Humic Acid. M. Samadfam, Y. Niitsu, S. Sato and H. Ohashi. *Radiochimica Acta*, 73, 211-216, (1996).
- (8) Interaction of Humic and Fulvic Acids with Th(IV). K.L. Nash and G.R. Choppin. *J. Inorg. Nucl. Chem.*, 42, 1045-1050, (1980).
- (8) Binding of Uranyl by Humic Acids. P.M. Shanbhag and G.R. Choppin. *J. Inorg. Nucl. Chem.*, 43, 3369-3372, (1981).

Figure 1: Europium sorption to different surfaces at pH=6.5 and 80°C, (except glass at 13°C).

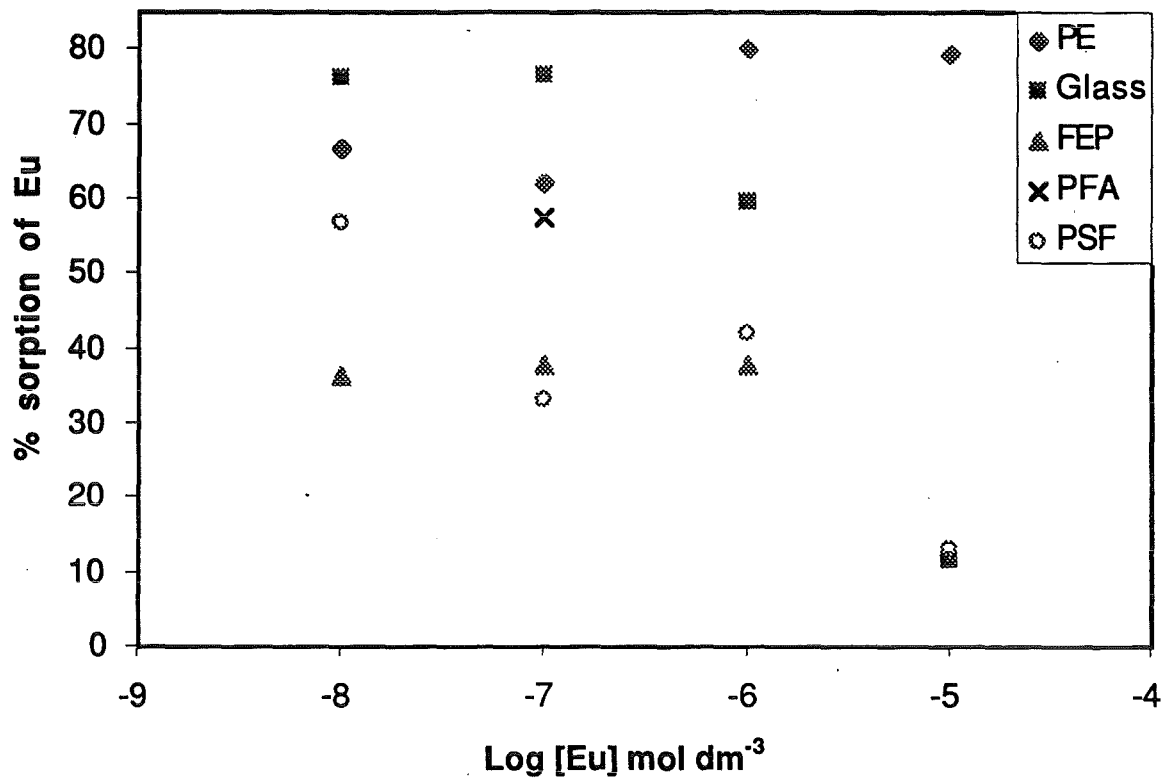


Figure 2: Apparatus for titration under nitrogen at constant temperature.

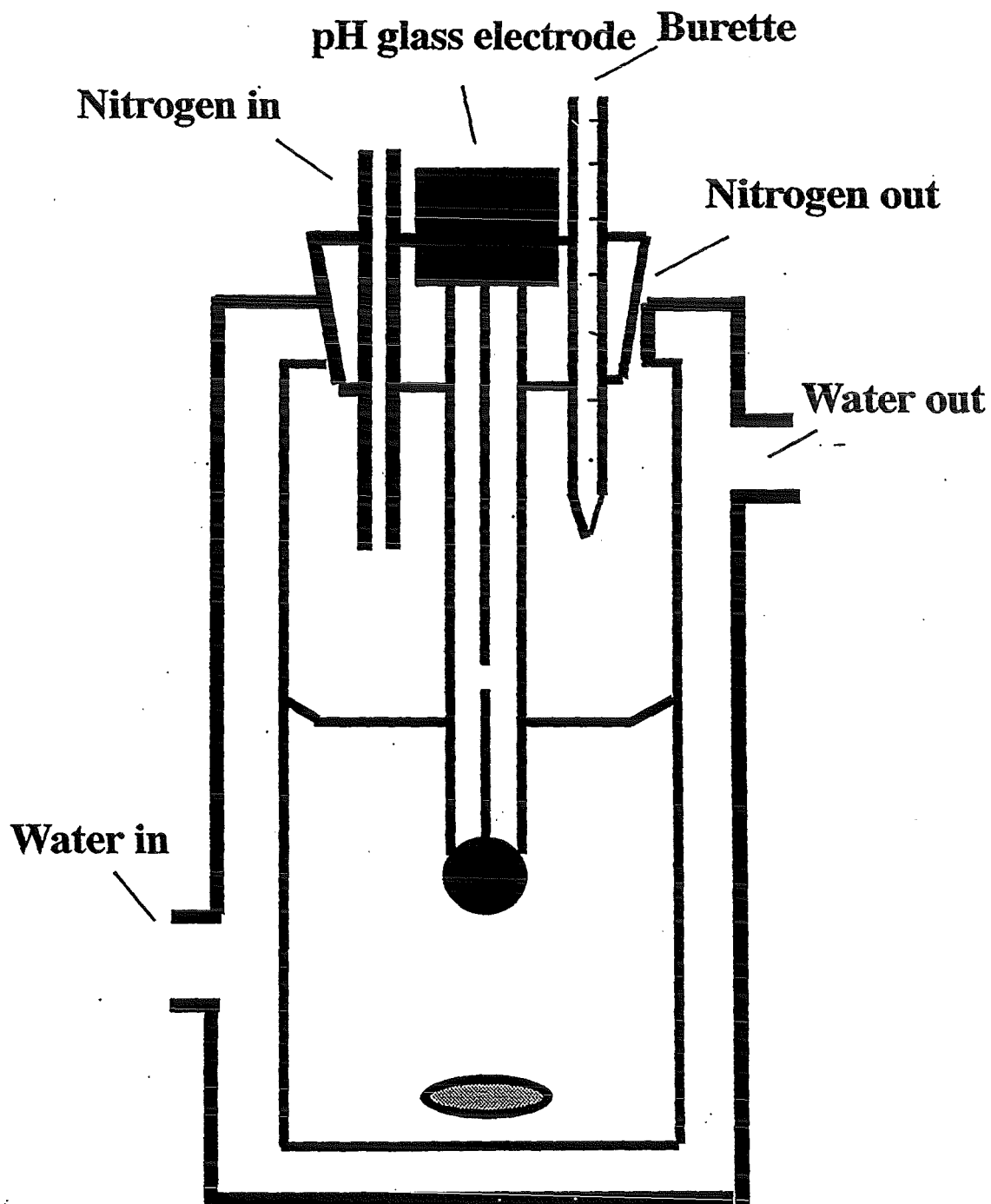


Figure 3: Averaged results of pH titration of Acetic acid (20ml of 0.1M) with 0.1M NaOH at various temperatures.

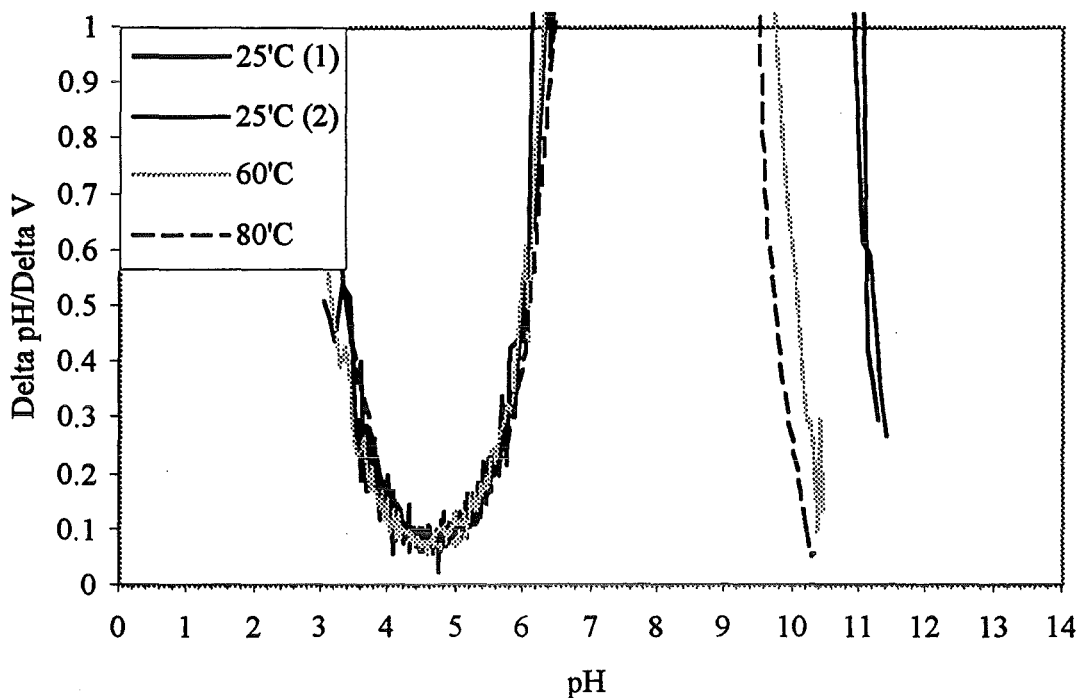


Figure 4: Averaged results of pH titration of Catechol (20ml of 0.3M) with 0.1M NaOH at various temperatures.

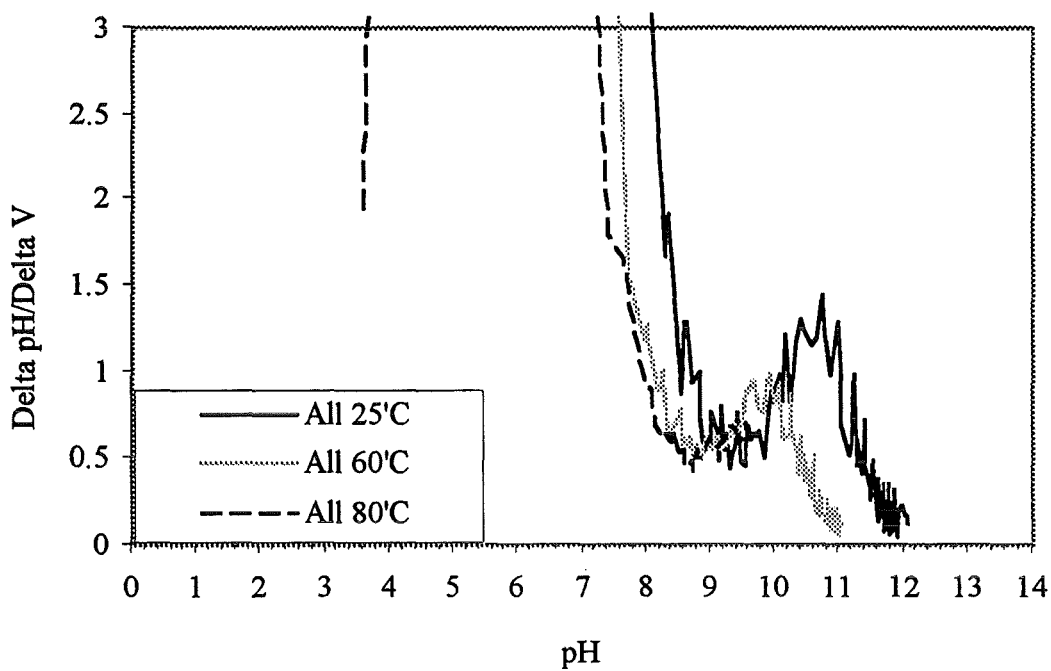


Figure 5: Averaged results from titration of 0.2g of Aldrich humic acid with 0.1M sodium hydroxide at various temperatures.

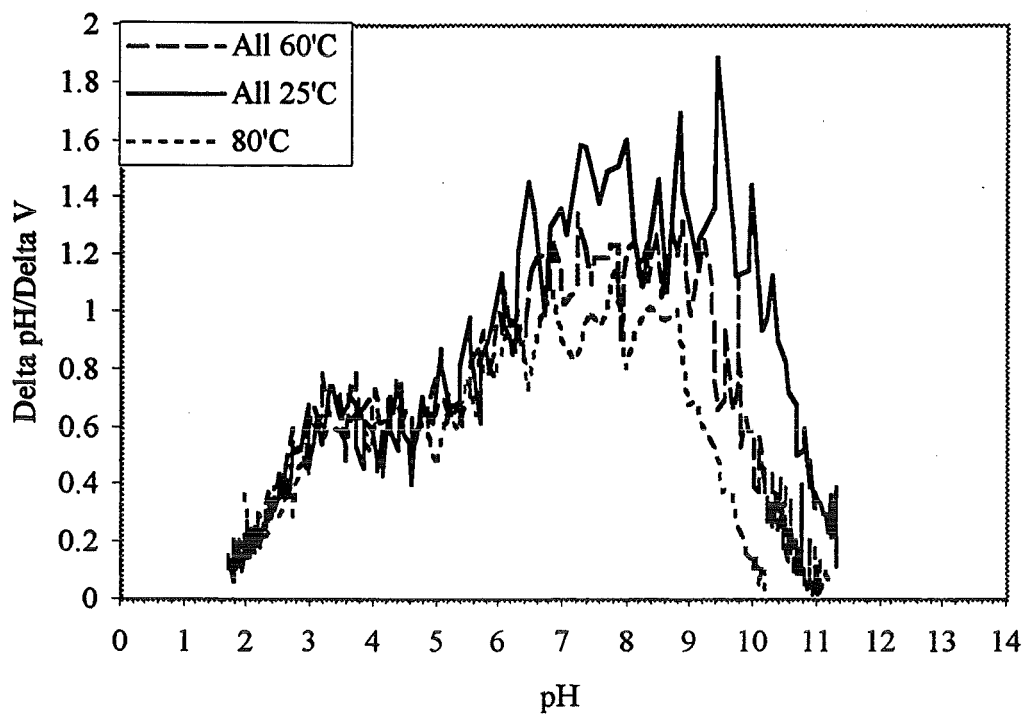


Figure 6: Determination of the stability constants $\log K_1$ and $\log K_2$ of EuHA by the Scatchard Approach.

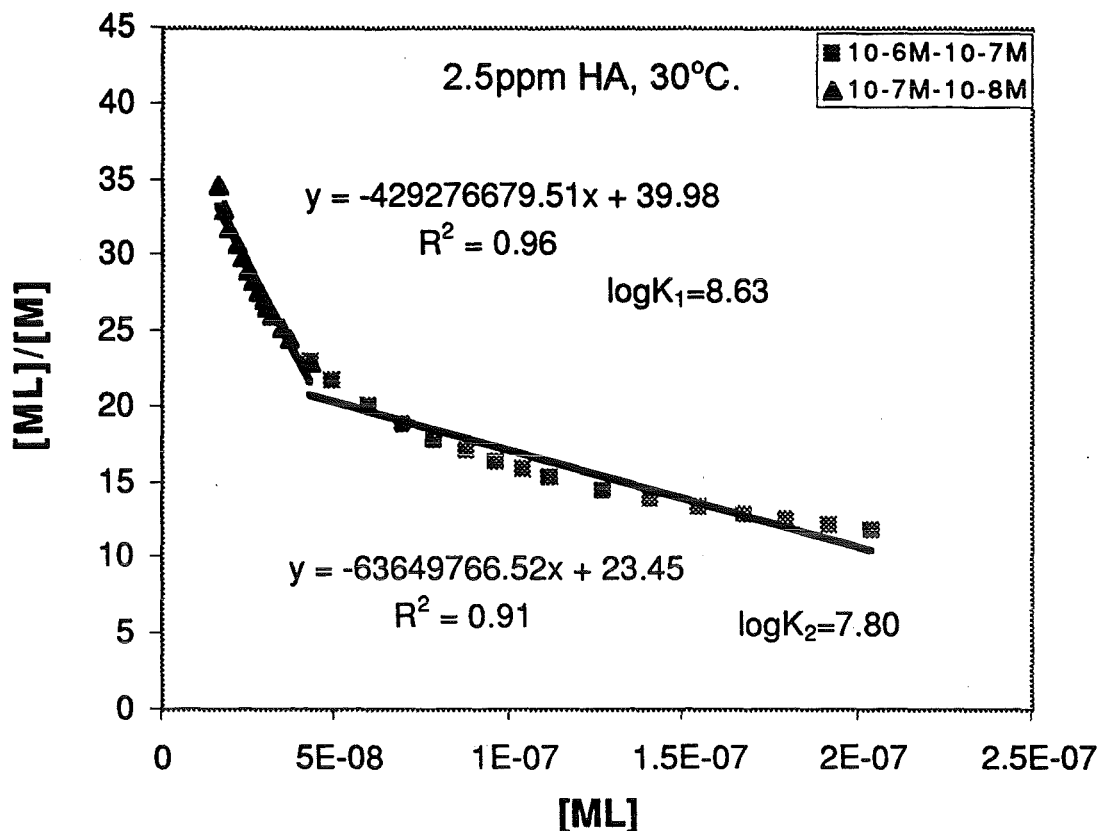


Figure 7: Determination of the stability constant $\log K$ of EuHA from the Charge Neutralisation Model.

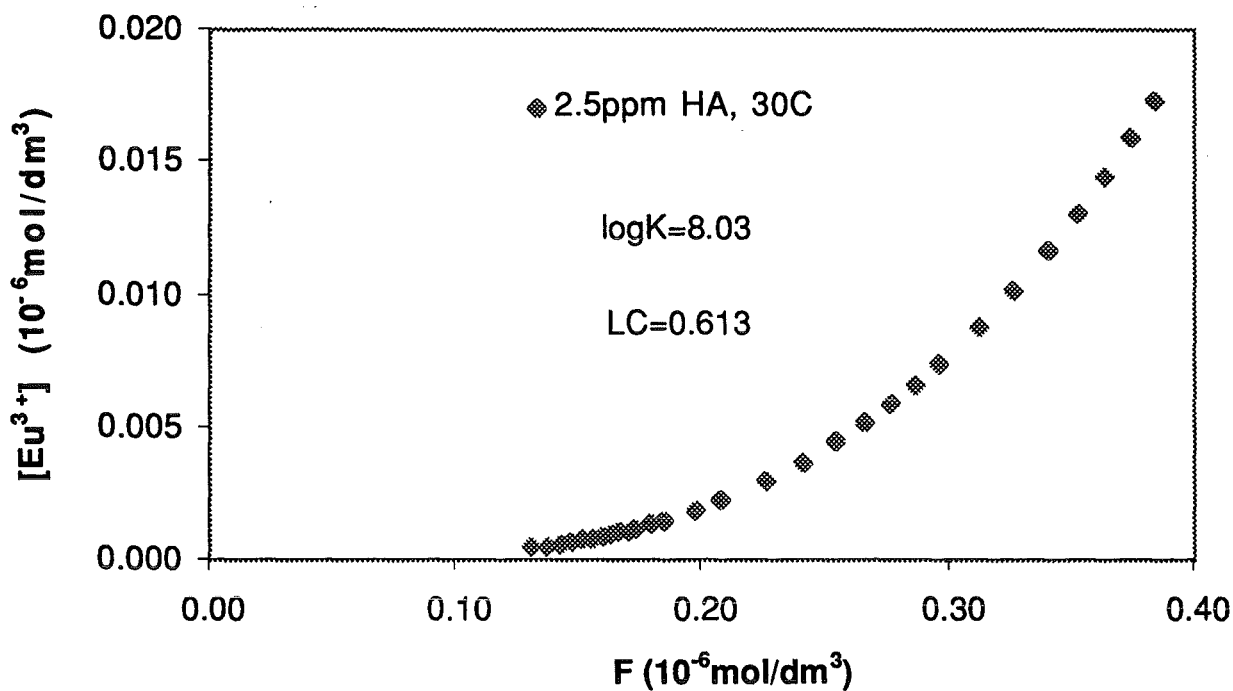


Figure 8: Determination of the stability constant logK of EuHA from the Schubert Model.

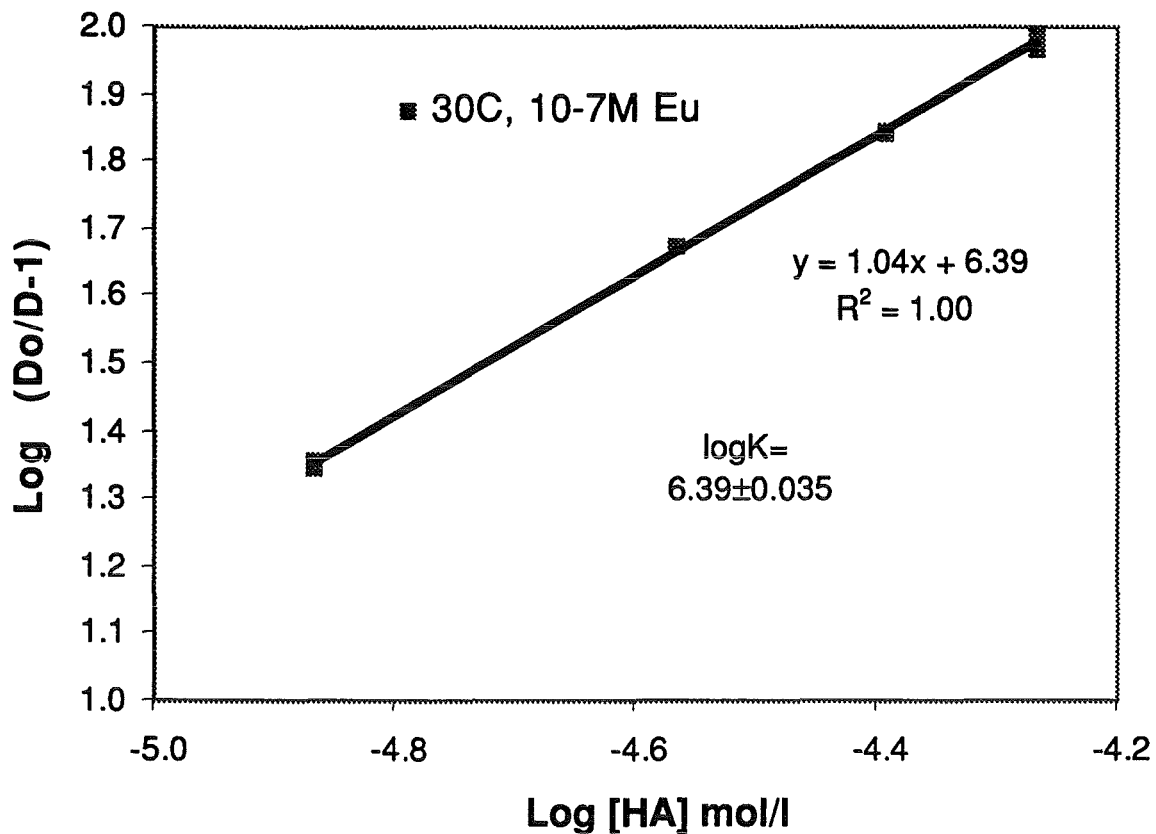


Figure 9: Temperature dependence of the stability constants lnK₁ and lnK₂ of EuHA as derived by the Scatchard Approach.

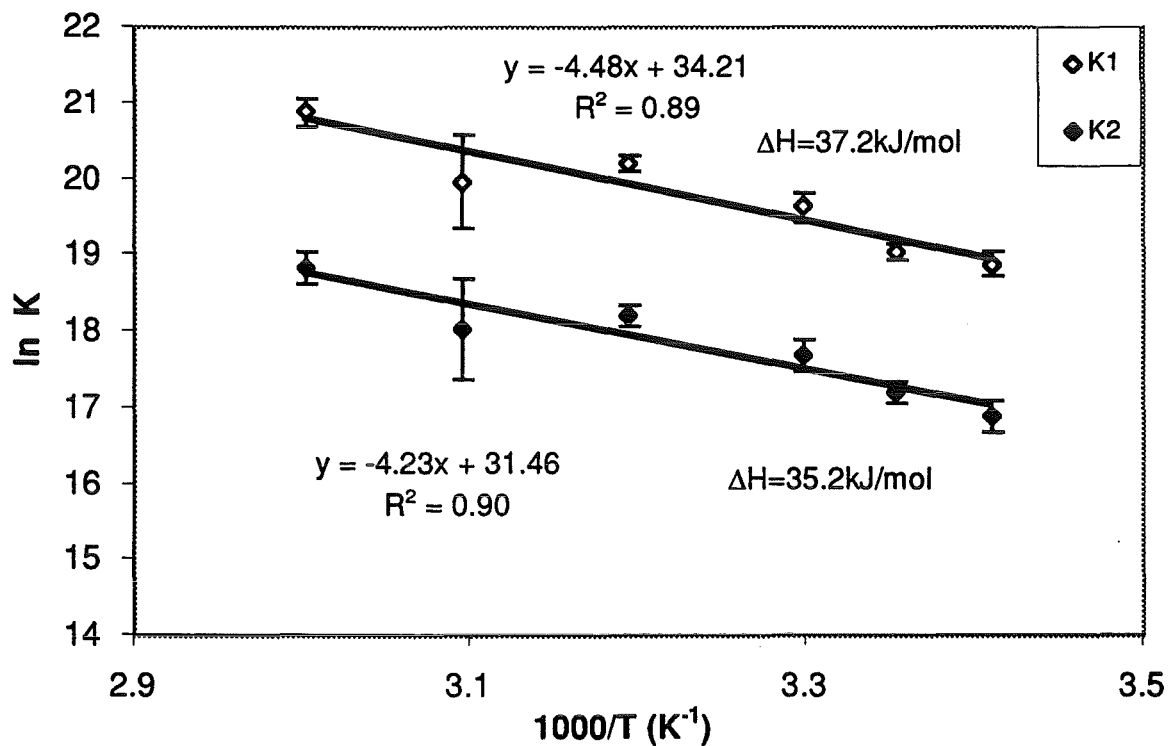


Figure 10: Temperature dependence of the stability constants $\ln K_1$ of EuHA as derived by the Charge Neutralisation Model.

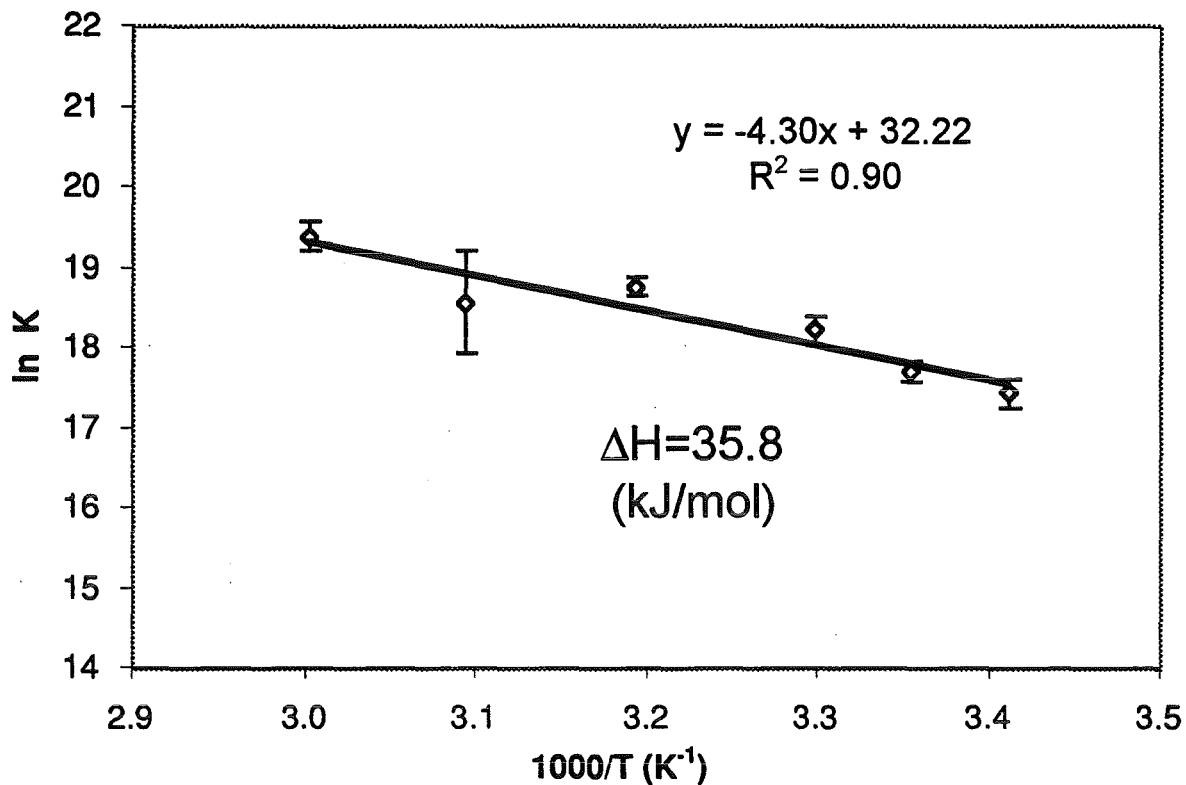


Figure 11: Temperature dependence of the stability constants $\ln K_1$ of EuHA as derived by the Schubert Model.

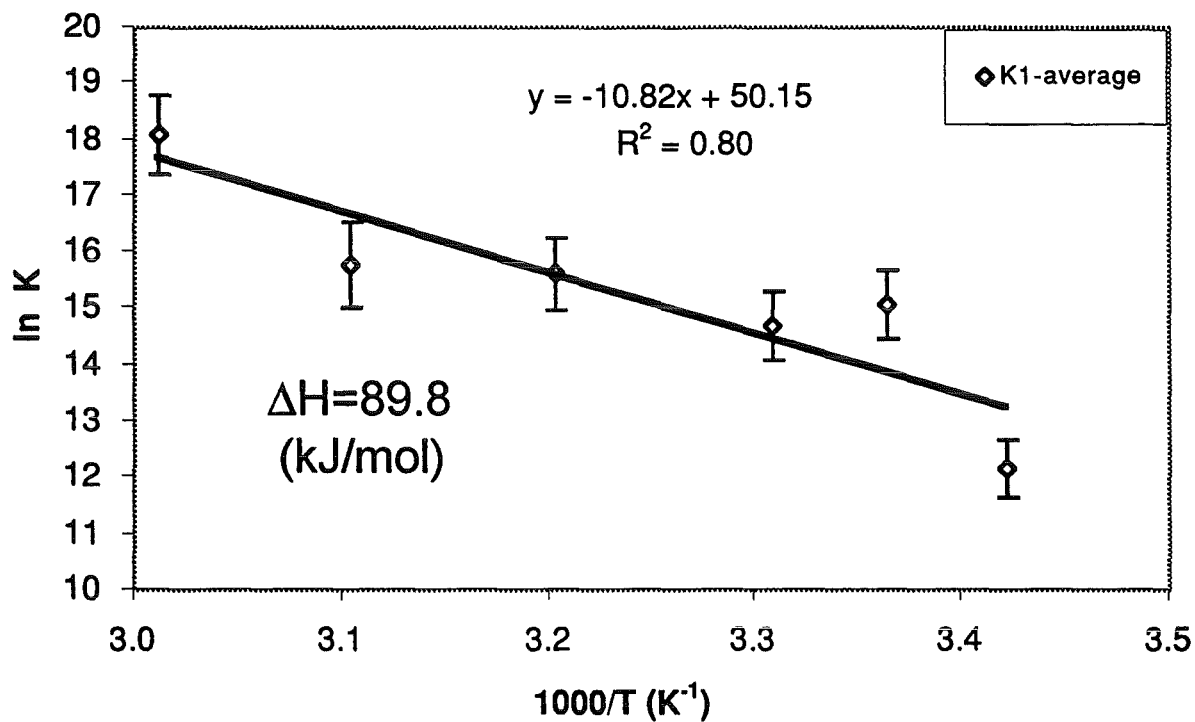


Table 1: Logarithmic stability constants, logK, for EuHA and EuFA complex derived at different temperatures.

Temperature	Schubert	Charge Neutralisation Model	Scatchard	
°C	logK	logK	logK ₁	logK ₂
Humic Acid				
20	5.28 ± 0.22	7.57 ± 0.08	8.20 ± 0.07	7.34 ± 0.09
25	6.55 ± 0.27	7.69 ± 0.05	8.27 ± 0.05	7.47 ± 0.06
30	6.38 ± 0.26	7.91 ± 0.08	8.52 ± 0.08	7.68 ± 0.09
40	6.78 ± 0.28	8.15 ± 0.05	8.77 ± 0.05	7.91 ± 0.06
50	6.85 ± 0.33	8.06 ± 0.28	8.67 ± 0.27	7.83 ± 0.29
60	7.85 ± 0.30	8.42 ± 0.08	9.07 ± 0.08	8.18 ± 0.09
Fulvic Acid				
20	6.58 ± 0.16	7.48 ± 0.03	8.33 ± 0.03	7.70 ± 0.04
40	7.95 ± 0.11	7.97 ± 0.05	8.83 ± 0.04	8.20 ± 0.04

*PEC used for Aldrich HA and Derwent FA were $5.43 \pm 0.20 \text{ meq/g}^7$ and 5.00 meq/g , respectively.

Table 2: Thermodynamic parameters of EuHA complex at 293K.

Model	ΔG	ΔH	ΔS
Approach	kJ eq^{-1}	kJ eq^{-1}	$\text{J T}^{-1}\text{eq}^{-1}$
EuHA			
CN model	-42.5 ± 0.3	35.8 ± 2.7	267 ± 20
Scatchard (K_1)	-46.0 ± 0.3	37.2 ± 3.0	284 ± 23
Scatchard (K_2)	-41.2 ± 0.3	35.2 ± 2.6	261 ± 20
Schubert	-37.4 ± 1.2	88.3 ± 15	407 ± 70
EuFA			
CN model	-43.2	43.9	297
Scatchard (K_1)	-46.8	43.9	309
Scatchard (K_2)	-42.0	32.4	254
Schubert	-37.0	66.8	354

Table 3: Thermodynamic Parameters of Metal HA complexes at 298K.

COMPLEX	ΔG	ΔH	ΔS	<u>Model approach</u>
	kJ eq^{-1}	kJ eq^{-1}	$\text{J T}^{-1}\text{eq}^{-1}$	
Sr(HA)	-15.0 ± 1.1	-1.5 ± 1.0	45.3 ± 7.0	Schubert (8)
Sr(HA) ₂	-26.7 ± 1.4	-13.3 ± 4.4	45.0 ± 16.1	
UO ₂ (HA)	-29.2 ± 0.1	-2.7 ± 0.4	89	Schubert (9)
UO ₂ (HA) ₂	-51.0 ± 0.2	$+8.0 \pm 4.0$	200	
Th(HA)	-63.56 ± 0.1	32.6 ± 3.2	323 ± 12	Schubert (10)
Th(HA) ₂	-92.23 ± 0.2	42.7 ± 3.3	453 ± 12	
EuHA				
	-43.9 ± 0.3	35.8 ± 2.7	267 ± 20	CN Model
K ₁	-47.2 ± 0.4	37.2 ± 3.0	283 ± 23	Scatchard
K ₂	-42.6 ± 0.5	35.2 ± 2.6	261 ± 20	Scatchard
	-37.4 ± 0.9	88.3 ± 15	427 ± 72	Schubert

1st Technical Progress Report

EC Project:

"Effects of Humic Substances on the Migration of Radionuclides:
Complexation and Transport of Actinides"

RMC-E Contribution to Task 4 (Model Development and Testing)

A Modelling Study of Humate Mediated Metal Transport

Reporting period 1997

N Bryan

RMC Environmental Ltd
Suite 7, Hitching Court, Albingdon Buisness Park, Albingdon
Oxfordshire OX14 1RA
United Kingdom

CONTENTS

	<u>Page</u>
List of Tables	249
List of Figures	249
1 Introduction	251
2 Static Modelling	251
3 Transport Modelling	255
4 Conclusions	260
5 References	260

LIST OF TABLES

Table No.	Title	<u>Page</u>
1	Current State of the Humics Complexation Database	252

LIST OF FIGURES

Figure No.	Title	
1	Effects of pH on Binding	253
2	Processes Included in PHREEQE97	257
3	PHAST: Program Structure	257
4	Loughborough Up-Flooding Experiment	258
5	BGS Pulsed Experiment Co/FA Injection	259

1. INTRODUCTION

The transport behaviour of actinides and their humate complexes in the environment is of crucial importance in radiological safety studies. Current models are unable to simulate observed behaviour, even in laboratory scale column experiments. Therefore, the aim of this on-going work is to attempt to develop models which are capable of simulating laboratory experiments. From there, the understanding which will have been gained about the nature of the physicochemical processes involved will enable field scale studies, which will answer questions such as: do humic substances significantly affect the migration behaviour of radionuclides in the environment; if so, overall do they tend to accelerate or retard migration; what will be their effects at certain specific sites. Hence, although the immediate aim is to simulate laboratory experiments, the final goal is to make a contribution to performance assessment studies.

Generally, two types of modelling study are attempted, static (or steady state) and transport (or transient). In a static experiment, one attempts to predict the speciation of a single solution, usually at equilibrium. Whilst in a transport study, the aim is to model the movement of a radionuclide down a column. Both types of modelling have been undertaken in this first twelve months.

2. STATIC MODELLING

The majority of metal/humate modelling studies in the literature are static studies, and a large number of approaches have been adopted. Model V of Tipping *et al* (Tipping and Hurley 1992) was selected by RMC-E as the thermodynamic model of choice for several reasons. It has already been extensively applied both to stable metals and more particularly actinides, and, primarily for this reason, had been recommended in the previous CHEMVAL II study. Also, Model V is included as part of the UKEA. speciation code, PHREEQE96. Most modelling studies have addressed conditions of moderate pH (<7) and low ionic strength (<0.1). However, in performance assessment studies, conditions of high ionic strength are often encountered. For example, the proposed Gorleben repository is located within a salt dome, and very high ionic

strengths are recorded in the groundwater. In other locations, the intrusion of saline waters can also result in high ionic strength. Also, one would not expect that all locations would have pH below 7. In particular, due to the use of cementitious materials in the construction of repositories, one might expect that the groundwater in the surrounding area might have raised pH. The first step in the static modelling was therefore to test the validity of the chosen model in high pH and high ionic strength (I) conditions. In order to assist in the development and refinement of these static models, a database of experimental data is being collated from the other partners in this project. The current state of the database is shown in Table 1.

**TABLE 1: CURRENT STATE OF THE HUMICS
COMPLEXATION DATABASE**

METAL	HUMIC	pH	I
Am	Aldrich	6.0	0.1
Am	Bradford	5.0 - 6.0	0.1, 1.0
Am	Gohy-573HA	4.0 - 6.0	0.01 - 5.0
Cm	Gohy-573HA	5.0 - 6.0	0.001 - 5.0
NpO ₂ ⁺	Gohy-573HA	6.0 - 9.0	0.1
UO ₂ ²⁺	Gohy-573HA	4.0	0.1
UO ₂ ²⁺	Broubster Fulvic	5.0 - 7.5	0.01 - 0.2
UO ₂ ²⁺	Needle's Eye Fulvic	5.0 - 5.5	0.04 - 0.1
UO ₂ ²⁺	Drigg Fulvic	3.5 - 7.0	0.005 - 0.2
Ca	Broubster Fulvic	5.0 - 7.0	0.01
Co	Drigg Fulvic	6.0 - 7.0	0.005 - 0.2
Co	Broubster Fulvic	6.0 - 7.0	0.005 - 0.2
Co	Broubster Humic	6.0 - 7.0	0.005 - 0.1
Co	Needle's Eye Fulvic	6.0 - 7.0	0.005 - 0.2
Ni	Needle's Eye Fulvic	6.0 - 7.0	0.005 - 0.2
Ni	Broubster Fulvic	6.0 - 7.0	0.01 - 0.2
Ni	Drigg Fulvic	6.0 - 7.0	0.005 - 0.2

The range of data collated thus far is representative of the data observed in the literature; typically moderate pH and low I. There is also a lack of information for the tetravalents. More data are required, however, there is a small amount of information at high pH (for NpO₂⁺) and high I (Am³⁺). This has enabled initial tests of Model V to be performed. Np data were

modelled across the pH range 6 to 9 and for two total humate concentrations: the results are shown in Figure 1.

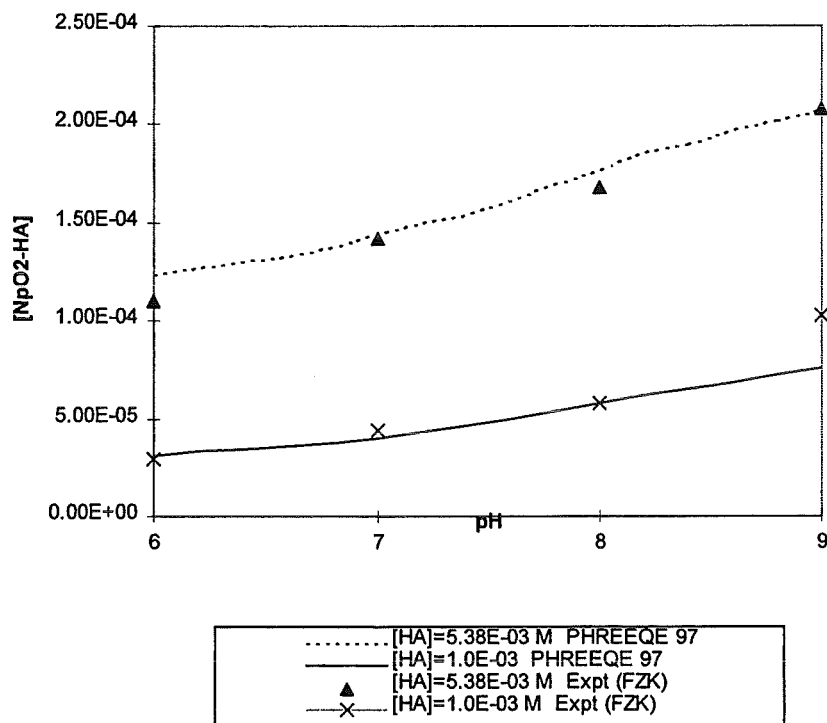


FIGURE 1: EFFECTS OF PH ON NP BINDING

It can be seen that the model seems to perform well in this pH region. This result must be treated with care for two reasons. Firstly, the metal, Np, in its oxidised form is the least hydrolysable of all of the actinides, and secondly, this is only a single dataset for one humic sample. More data/work are required before it is clear that the model is universally applicable in this pH range. In the case of high I, the model failed to perform. This is due to the simplistic form of the ionic strength correction equation implemented within the model:

$$w = \frac{P \log I}{1 + Q \log(I/|Z|)}$$

where w is the correction factor, P and Q are fitting parameters and Z is the charge on the humic. Even for simple inorganics, the effects of ionic strength become increasingly complex as ionic strength increases. For humics, one would expect the situation to be far more complicated. Indeed, several authors have found the need to apply the full Poisson-Boltzmann equation to describe the humic double layer (Bartschat *et al* 1992; Milne *et al* 1995). If the model is to be applied to high ionic strength conditions, then a more rigorous ionic strength correction mechanism is required. However, more data are required for such an adaptation.

PHREEQE96 has been adopted as the speciation code for use by RMC-E within this project. Although it contains Model V to describe the interaction of metals with dissolved humic substances and a routine to model the sorption of radionuclides onto solid surfaces, there are several important processes which were not considered. To address these gaps, the following additions have been made:

- a module has been added to describe the interaction of metals with colloids; more than one colloid may be considered at a time. This is the diffuse double layer model of Dzombak and Morel (1990), which is also used in the CEC CARESS colloids project;
- humics do not exist solely as either dissolved molecules or discrete pure phase solid: they may also sorb to solid surfaces, such as sand or iron containing minerals. These sorbed humic substances are also able to sequester metals from solution. In 'real' environmental situations, as well as in the column experiments, there will be large areas of surface for humic substances to leave solution and therefore these processes must be considered. These ternary complexes of mineral surface/humic substance/radionuclide have two aspects which need to be addressed: the model must first predict the extent of sorption of the humic substance and then the metal uptake onto the sorbed humic. To address the deposition of the humic, the isotherm equation of Gu *et al* (1994) has been adopted:

$$q = \frac{K \cdot e^{\left(\frac{-2q\theta}{RT}\right)} \cdot q_{\max} \cdot C}{K \cdot e^{\left(\frac{-2q\theta}{RT}\right)} \cdot C + 1}$$

where K is a constant, θ is the surface stress coefficient, q is the current surface concentration of the humic, q_{\max} is the maximum loading and C is the solution concentration. At a special modelling task meeting in May 1997, it was decided that the best way to treat the binding of metals by humic substances was to model them *via* the same method as for dissolved humic substances. Therefore, a second, but entirely independent, version of model V has been incorporated into the transport code;

- the static speciation code developed in this section was to be coupled with a transport code in order to model the column experiments. Before this could be achieved, the way in which precipitation and dissolution was treated needed to be addressed. PHREEQE was originally written to simulate the passage of groundwater across ore bodies. For this reason, it defines phase boundaries which, if the solution is not saturated, allows an unlimited amount of material to dissolve until the solution becomes saturated. This is clearly not applicable to a column experiment, and a version of the speciation code has been written which keeps account of the solid available.

This improved speciation code has been named PHREEQE97. The range of processes which are now described are shown in Figure 2.

3. TRANSPORT MODELLING

Previous attempts at modelling column experiments had proved unsuccessful. Therefore, in order to have the best possible chance of modelling the experiments, it was decided to produce a model which could address all of the processes involved in the column experiments. To this end, PHREEQE97 was taken and coupled with a 1-D transport code to produce the new code, PHAST; PHreeqe And Simple Transport. At each stage along the

column, the model assumes local equilibrium, *ie*, that all of the chemical processes are fast with respect to the movement of the solution through the column. This is common to virtually all such studies. Because the final goal of this project is performance assessment, the interface was written in such a way that it would be applicable to a field site study. In other words, the model transports humic and colloid bound metal separately to simple inorganic forms. The code also contains the humic sorption isotherm equation. A modified version of the advection dispersion equation is used to describe the transport of all the solution components:

$$\theta \Delta x A \frac{C_i(x)^{t+\Delta t} - C_i(x)^t}{\Delta t} = \Delta x A J_i(x - \Delta x / 2)^{t+\Delta t/2} - \Delta x A J_i(x + \Delta x / 2)^{t+\Delta t/2} - \theta \Delta x A W_i(x)^{t+\Delta t} + \theta \Delta x A W_i(x)^t - \theta \Delta x A S_i(x)^{t+\Delta t/2}$$

Here θ is the porosity, A is cross-sectional area of the column, J is total flux of component i and W is the immobile concentration (sorbed/precipitated) of component i . A source/sink term, S term has been introduced to account for the apparent appearance or disappearance of material, which arises directly as a result of transporting different chemical forms of the same element separately. The interaction of the various parts of the code are shown in Figure 3. The PHAST code is very complex and takes a very long time to produce a solution, especially when humic substances are included in the simulation. Therefore, in order to obtain a solution in a realistic time frame, a certain amount of up-scaling was required to model the column experiments. This was achieved by performing all of the speciation calculations prior to modelling the transport, and then using functions called by the code in order to provide an approximate solution to the chemistry of the system at each point in space and time. This is an indication of the complexity of the code, since up-scaling is not usually addressed until field sites are to be modelled.

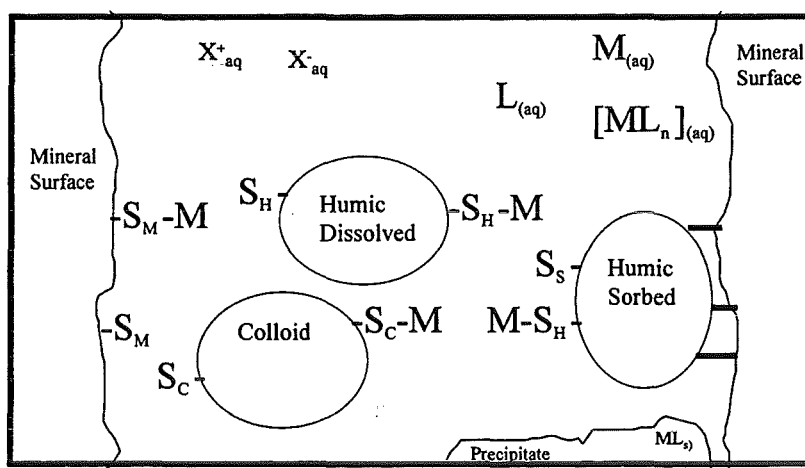


FIGURE 2: PROCESSES INCLUDED IN PHREEQE97

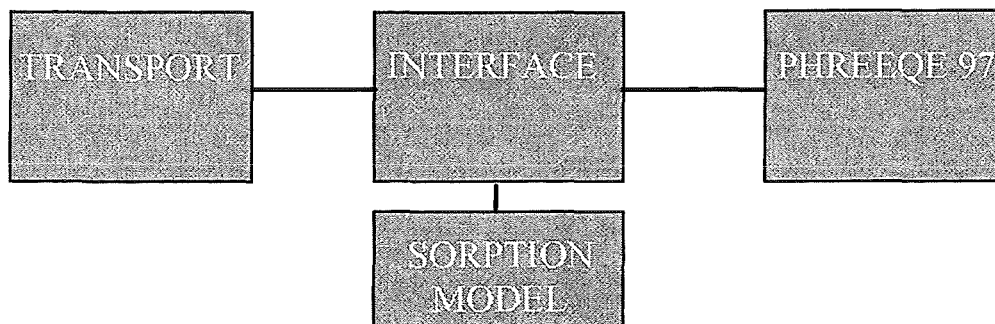


FIGURE 3 PHAST: PROGRAM STRUCTURE

The new model was initially tested against the results of column experiments from the University of Loughborough. These column experiments are 'up-flooding type', *ie*, the input metal solution is held at a constant level for a significant period of time (the equivalent of very many pore volumes), before the metal input is removed and the metal sorbed to the column leached: 'down-flooding'. The columns were permitted to come into equilibrium with humic acid before the injection of the metal. Also, silica colloids were present in all of the column feed solutions. An example of the results obtained is shown in Figure 4. This result is typical of the results obtained with the up-flooding experiments. It can be seen that the model is predicting the correct general behaviour. However, in the case of all the humic

acid columns, it was found that, although it was possible to get very impressive fits to the up-flooding and down-flooding sections separately, it was not possible to fit both portions with the same calibration. The results show that the humic acid is more effective at carrying the nuclide through the column than it is at cleaning the column once the input concentration has been removed. If local equilibrium were being achieved in the columns, then it would be possible to model both sections of the experiment simultaneously. These observations are consistent with the fact that the dominant reactions in the column are kinetically controlled.

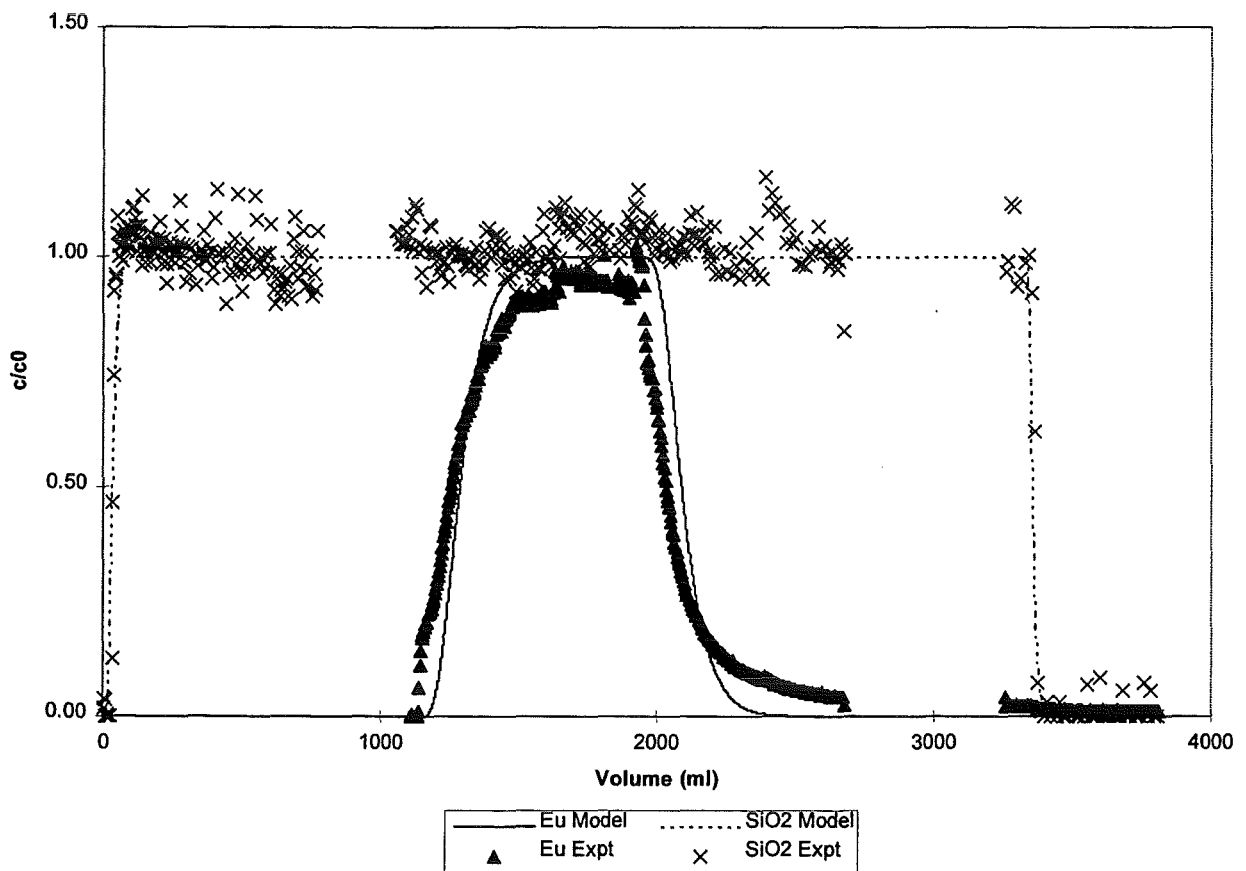


FIGURE 4: LOUGHBOROUGH UP-FLOODING EXPERIMENT

[EU]T=1.0E-08M SiO₂ COLLOIDS + HUMIC ACID

In this figure, the points represent the experimentally determined concentrations, and the lines the Eu and SiO₂ concentrations predicted by the PHAST code.

The model was also used to simulate pulsed injection experiments performed by BGS. Here, the humic and metal were injected as a single short pulse. An example of the results is shown in Figure 5.

Once again, the model simulates the general shape of the experimental plots, but with a visible discrepancy. The difference in position between the metal breakthrough and the model prediction can only be caused by kinetic effects within the column.

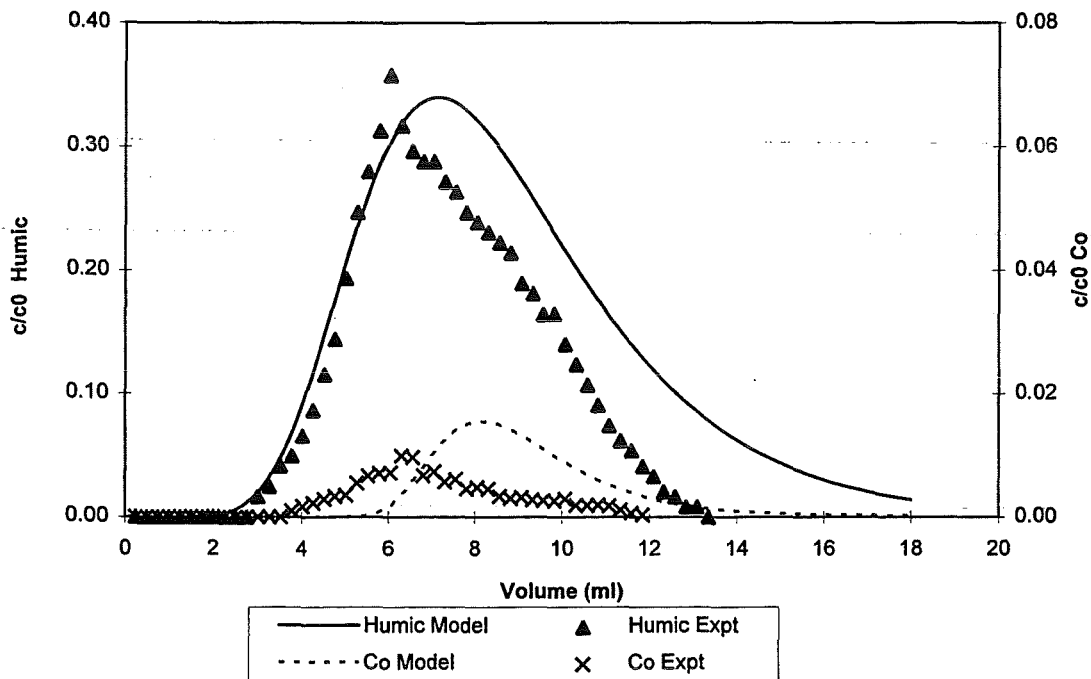


FIGURE 5: BGS PULSED EXPERIMENT CO/FA INJECTION (COLUMN 6)

Here the points represent the experimentally determined concentrations of humic and cobalt (Co). The lines represent the modelled values of humic and Co concentrations as predicted by the PHAST code.

4. CONCLUSIONS

More batch experimental data must be collected from the other partners to enable extension of the speciation model to conditions of higher ionic strength and pH. The resultant combined database will serve as a useful tool for future work in this subject area. Due to the extensions made in this first year, the speciation code, PHREEQE97, is now able to model all of the processes, at equilibrium, which are important in this project. However, the column data clearly shows that the columns are **not** in equilibrium. Therefore, a kinetic approach is required in order to correctly model these results. Hence, the next stage of this project will be to produce a coupled transport-kinetic-equilibrium code, which treats the humate reactions *via* the use of rate equations, whilst continuing to use equilibrium constants to describe any fast processes. Fortunately, the interface written for the code PHAST will also serve for the new kinetic model.

5. REFERENCES

Bartschat B M, Cabaniss S E, Morel F M M (1992). 'Oligoelectrolyte Model for Cation Binding by Humic Substances'. *Environmental Science and Technology* **26**, 284-294.

Dzombak D A and Morel F M M (1990). '*Surface Complexation Modelling: Hydrous Ferric Oxide*'. Wiley-Interscience, John Wiley and Sons.

Gu B, Schmitt J, Chen Z, Liang L, McCarthy J F (1994). 'Adsorption of Natural Organic Matter on Iron Oxide: Mechanisms and Models'. *Environmental Science and Technology*, **28**, 38-46.

Milne C J, Kinniburgh D G, de Wit J C M, van Riemsdijk W H and Koopal L K (1995). 'Analysis of Proton Binding by a Peat Humic Acid Using a Simple Electrostatic Model' *Geochimica et Cosmochimica Acta*, **59**, 1101-1112.

Tipping E and Hurley M A (1992). 'A Unifying Model of Cation Binding by Humic Substances'. *Geochimica et Cosmochimica Acta*, **56**, 3627-3641.

First Technical Progress Report

EC Project:

**"Effects of Humic Substances on the Migration of Radionuclides:
Complexation and Transport of Actinides"**

NERI Contribution to Task 3 (Actinide Transport)

(Reporting period 1997)

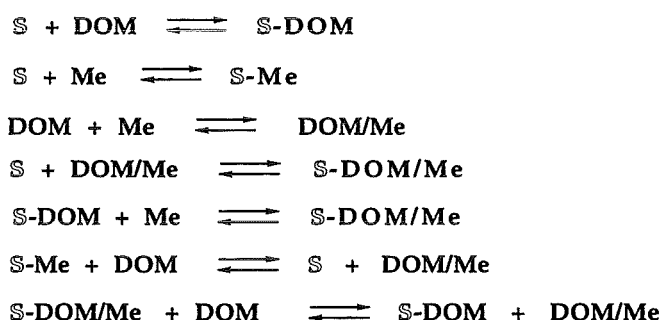
Interaction of Humic Acids with Mineral Surfaces

L. Carlsen

**NERI - National Environmental Research Institute
Department of Environmental Chemistry
Fredriksborgvej 399
P.O. Box 358
DK-4000 Roskilde**

Introduction

It is well known that humic substances interact with polyvalent metal ions and organic pollutants thereby altering the migration and sorption properties of the ions and pollutants. Further the interaction between humic substances and mineral surfaces may also play a crucial role in determining the fate of pollutants in e.g. the soil/ground water system due to significant changes in surface characteristics as a consequence of the surface coating with organic material. These interactions can be described by the following reactions:



where DOM is dissolved organic matter, e.g. humic substances, Me is a metal pollutant or an organic contaminant and S a binding site on a solid surface such as on a mineral or clay surface etc. The above equations represent a complex chemical system and in order to simplify this system, usually, only one or a maximum of two of the above equations are experimentally investigated at a time.

We have previously investigated the interactions between Al_2O_3 and humic acids (Lassen et al. 1996). In order to gain further information on the sorption of DOM onto solid surfaces, we currently investigate the sorption of humic acids (HA) onto other mineral surfaces, like Na-kaolinite and goethite, by focusing on the sorption process as well as the possible reversibility of the reaction. Further, a possible size fractionation of the humic material due to the sorption process is studied.

Results and discussion

<Preparation of goethite and kaolinite>

Preparation of goethite

A solution of 1 M $\text{Fe}(\text{NO}_3)_3$ was added 5 M KOH (ratio 1: 1.8) under stirring. The solution was diluted approximately 5 times with water and left for a minimum of 60 h at 70°C.

During this period ferrihydrite was converted to goethite. The precipitate was isolated by centrifugation and washed with water until the supernatant was colourless. The goethite was isolated by centrifugation and air dried. The final product was pulverised and stored in a closed container.

Preparation of Na-kaolinite

Kaolinite on Na-form was prepared by washing kaolinite with 1 M NaCl for 1 hour. The kaolinite was subsequently isolated by centrifugation and washed with 10^{-3} M NaCl 4 x 1 h corresponding to equilibrium (i.e. no change in the aqueous concentration), isolated by centrifugation and filtration. The final product was dried and stored in a closed container.

<Sorption experiments of humic acids on solid surfaces>

Humic acids solutions:

A stock solution of humic acid (HA), (Aldrich Chemical Co), was prepared by dissolving 1000 mg of HA per L in 10^{-3} M NaCl. After dissolution, the solution was filtered through a 0.45 μ m filter and the pH of the filtrate adjusted to a pH of 6 with 0.1 M HCl. Working solutions of HA were prepared by dilution of this stock solution using 10^{-3} M NaCl as diluent.

Sorption procedure:

10 mg of Na-kaolinite (in equilibrium with 10^{-3} M NaCl) was added to 5 mL of humic acid solution contained in a polyethylene vial. The vial was shaken for eighteen hours before centrifugation to separate the solid and solution phases. The supernatant was filtered through a 0.45 μ m filter in order to remove any remaining kaolinite. The humic acid concentration in the solution phase was determined by light absorption spectroscopy (400 nm).

The effect of humic acid concentration on the sorption of humic acid:

Solutions of humic acids in 10^{-3} M NaCl at pH 6 were prepared having concentrations of 0, 5, 10, 15, 20, 25, 50 and 75 mg HA/L. The preliminary results showed an increasing sorption with increasing humic acid concentration, an equilibrium being reached at 4 mg HA/g kaolinite (figure 1).

In previous investigations on the sorption of humic acids on Al_2O_3 have showed that the sorption of humic acid on Al_2O_3 reach an equilibrium approximately 10 times higher (within the humic acid concentration range of 0-500 mg/L) (Lassen et al. 1996). The

apparently lower sorption capacity of kaolinite may, however, be explained in form of fewer sorption sites available on kaolinite compared to Al_2O_3 .

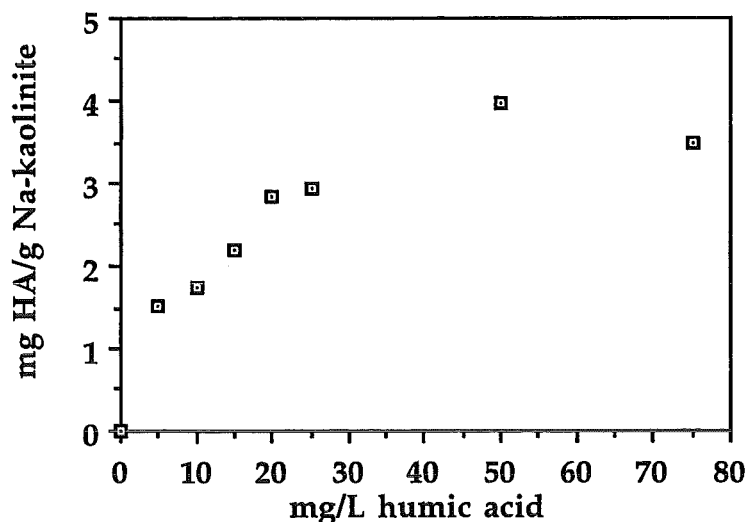


Figure 1: The effect of humic acid concentration on the sorption for humic acid to kaolinite.

Sorption sites is in the present context used as a general term reflecting the amount of humic material bound per gram solid material. Several research groups have found that the sorption mechanism for the interaction of humics with kaolinite and Al_2O_3 primarily can be explained as ligand exchange. Although no exact values concerning the available number of sorption sites available for ligand exchange, the larger amount of humics sorbed to Al_2O_3 relative to kaolinite can be elucidated by the difference of structure and site densities of the hydroxylated sites on the two solid materials. Thus, metal oxides and hydroxides like Al_2O_3 typically exhibit octahedral sheet structure, whereas the class of phyllosilicate minerals like kaolinite ($[\text{Si}](\text{Al}_4)\text{O}_{10}(\text{OH})_8$) exhibit a layered structure of tetrahedral and octahedral sheets. This structure shields most of the aluminol groups, thus leaving only aluminol groups at the edges of the layered silica sheets available for sorption by ligand exchange, where further steric hindrance may limit the humic acid sorption. In contrast to this the hydroxylated sites in Al_2O_3 are more evenly distributed across the mineral surface leaving a higher number of sites available for humic sorption.

In the present study it emphasized that the results are preliminary and need to be further investigated. It is planned to increase humic acid concentration up to 500 mg/L in order to verify if the observed equilibrium level.

References

Lassen, P., Carlsen, L. and Warwick, P. (1996). The interaction between humic acids and γ -Al₂O₃. *Theophrastus' Contributions*, 1, 3-17.

First Technical Progress Report

EC Project:

"Effects of Humic Substances on the Migration of Radionuclides:
Complexation and Transport of Actinides"

GSF/IfH Contribution to Task 3 (Actinide Transport)

**Effects of Humic Substances on the ^{152}Eu Migration in a Sandy Aquifer:
First Results from Column Experiments with 10 m Flow Distance**

Reporting period 1997

D. Klotz and M. Wolf

GSF - National Research Center for Environment and Health, Institute of Hydrology
D-85764 Neuherberg, Germany

1. Objectives

Objectives are the determination of the migration properties of ^{152}Eu (^{152}Eu humate) in water flowing through sandy sediments of different grain sizes as function of flow velocity and flow distance.

2. Accomplished work

In the reporting period 01.01. - 31.12.1997 the following work was carried out:

- a) Construction of two column systems (A and B) for the migration experiments with ^{152}Eu humate.
- b) Determination of the grain size parameters of the sediments used for the column experiments.
- c) Determination of the sediment parameters of systems A and B.
- d) Characterization of the GoHy 2227 humic acid by NMR spectroscopy.
- e) Migration experiment with ^{152}Eu humate in system B (flow distance 10 m).

3. Experimental set-up

For the migration experiments two column systems were constructed:

Column system A

is composed of five flow-through columns with the following characteristics:

Material:	Polymethyl methacrylate
Diameters:	50 mm
Length:	0.50 m,

installed with the accompanying equipment in an inert-gas box filled with 99% N_2 and 1% CO_2 (Fig. 1).

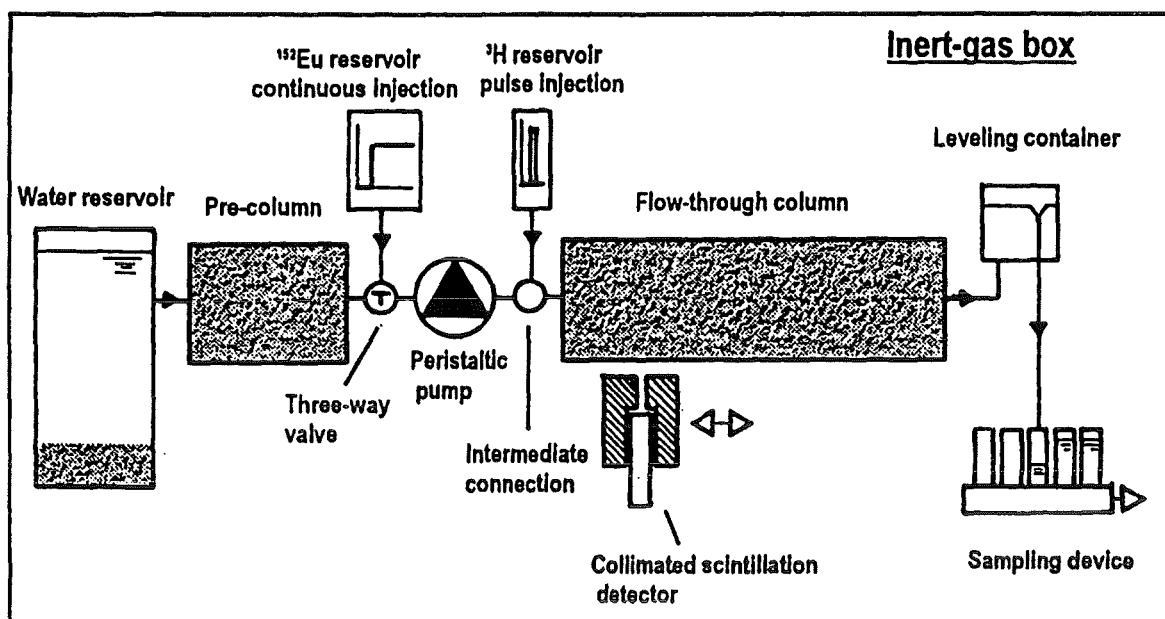


Fig. 1: Schematic diagram of the column set-up (system A) for the determination of the migration properties of ^{152}Eu humate.

The accompanying equipment is:

- groundwater reservoir,
- pre-columns,
- arrangements for the output of the flow (leveling container),
- collimated scintillation detector (movable along the columns) and
- sampling device for eluent.

The reservoir contains groundwater filtered with $0.45\ \mu\text{m}$ poresize. The function of the pre-column with graduated graining of coarse to fine sediments and a diameter of 50 mm and a length of 250 mm is to filter out larger humic particles (diameter some micrometers). The flow through in the columns according to natural flow velocities is regulated by a peristaltic pump in the column inflow and a leveling container in the column outflow. The concentration-space distribution is measured by scanning the gamma rays with the collimated scintillation detector at different times. The concentration-time distributions of the injected tritiated water and the ^{152}Eu humate are determined by analysis of the water samples taken at column's outflow.

Column system B

is composed of seven flow-through columns with the following characteristics:

Material:	Polymethyl methacrylate
Diameter:	50 mm
Length (total):	10.0 m,

of 0.5 m length (2x), 1.0 m length (1x) and 2.0 m length (4x), arranged in series (connected by PVC tubes with a diameter of 3 mm) and result in a total flow distance of 10 m (Fig. 2).

The columns are not installed in an inert-gas box, only the reservoir is hold under inert gas. The periphery corresponds to system A except the movable scintillation detector. In system B, in the outflow of each column it can be switched over by three-way valves to a flow-through arrangement equipped with a scintillation detector.

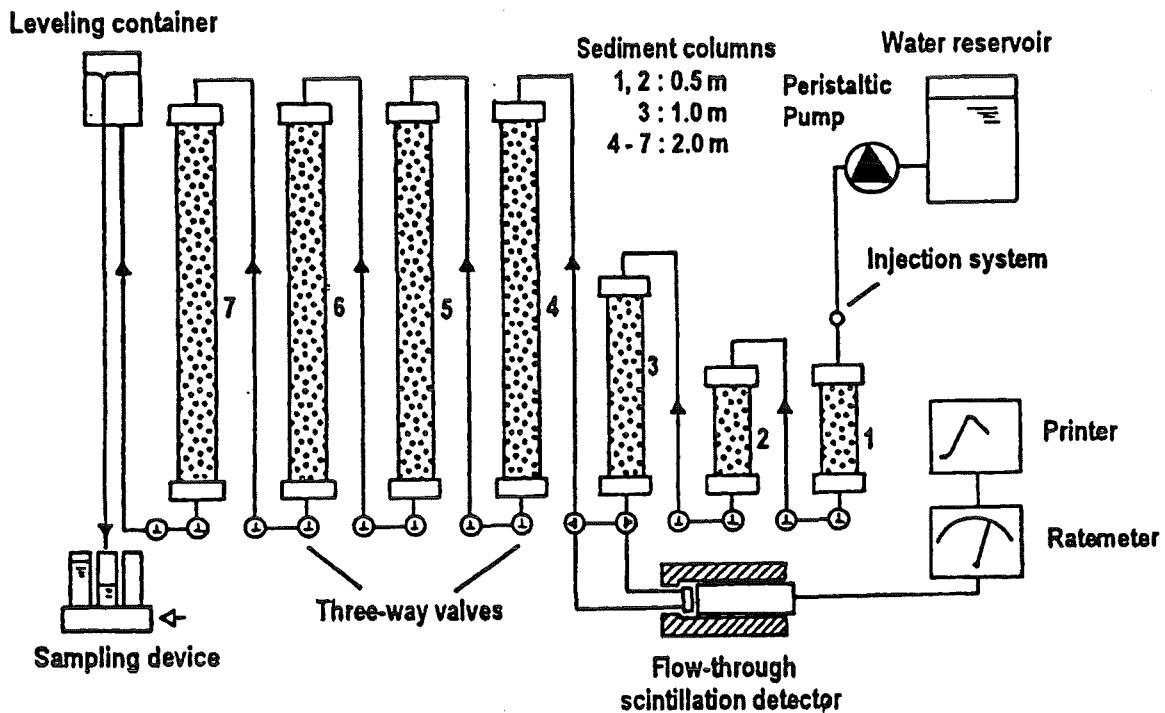


Fig. 2: Schematic diagram of the column set-up (system B) with a total flow distance of 10 m.

4. Grain size parameters of the sediments

The columns of the system A contain sands and gravel from different localities in Bavaria and Lower Saxony, the columns of the system B contain a fine sand from Lower Saxony. The grain size parameters (Tab. 1) were determined by sieve analyses.

Tab. 1: Sediment parameters in the columns of the system A and B.

(a), (b), (c): different localities

d_{10} = effective particle size, d_{50} = mean particle size, U = degree of dissimilarity,

n = total porosity, γ = bulk density (at dry-chamber conditions), G = gravel stone,

fS = fine sand, mS = medium sand, gS = coarse sand

System	No.	Locality	Grain size	d_{10} [mm]	d_{50} [mm]	U	n	γ [g/cm ³]
A	1	Dornach/Bavaria	G	0.67	3.9	7.0	0.200	2.23
	2	Gorleben(a)/Lower Saxony	fS	0.12	0.18	1.7	0.333	1.76
	3	Gorleben(b)/Lower Saxony	fS	0.11	0.15	1.5	0.343	1.78
	4	Gorleben(b)/Lower Saxony	mS	0.24	0.36	1.6	0.326	1.81
	5	Oberpfalz/Bavaria	gS	0.7	1.0	1.6	0.394	1.69
B	1	Gorleben(c)/Lower Saxony	fS	0.11	0.17	1.7	0.291	1.83
	2						0.293	1.83
	3						0.284	1.85
	4						0.286	1.84
	5						0.288	1.79
	6						0.295	1.83
	7						0.290	1.83
	(weighed mean)						0.290	1.83

5. Composition of the groundwater and NMR spectroscopy of the humic acid

The water used for the column experiments was sampled after filtration at 0.45 μ m poresize from the well GoHy 2227 (depth 128 -130 m) of the Gorleben aquifer in Lower Saxony. The main chemical composition of this water (data in mg/L) is: Na 959, K 8.1, Mg 4.4, Ca 18.9, Cl 1202, HCO₃ 482, SO₄ 26.3, HPO₄ 6.8, DOC 80 (KLOTZ et al. 1996).

The DOC is composed mainly of humic acids (approx. 80%) and fulvic acids (approx. 20%). The characterization of the main DOC component humic acid was carried out by ^1H and ^{13}C NMR spectroscopy by Dr. N. Hertkorn (GSF-Institute of Ecological Chemistry) and shows the following results (KLOTZ et al. 1996):

- Aromatic carbon: 50 % (about one half of these aromatic carbon atoms is C substituted;
- less than 10 % are phenolic groups).
- Aliphatic carbon: 35 % (methyl groups are dominant, the ratio of methylen groups vs. methylen groups which are bound to oxygen is 5 : 1; only a few C atoms which are H free are detectable).
- Carbonic acids: less than 10 %.
- Carbohydrates and ether groups: less than 10 %.

6. Sediments in the columns

The dry sediments were placed in the columns in a submerged state in thin layers and then compressed with a piston. The determined sediment parameters, i.e. total porosity and dry-chamber density resulting by this method, are well reproducible (Tab. 1) and are found to remain stable over the experimental period.

7. Migration experiment in system B

In order to obtain stable hydraulic conditions and conditions of the groundwater/sediment system, groundwater was pumped through the seven columns in series (approx. $30\text{ cm}^3/\text{h}$, corresponding to a flow velocity (Darcy velocity) v_f of approx. $4 \times 10^{-4}\text{ cm/s}$) for approx. 3 months. By tracer experiments, the hydraulic parameters (effective porosity n_{eff} and longitudinal dispersivity α) were determined on a monthly basis (Tab. 2).

For the determination of the Eu-migration behaviour, $500\ \mu\text{Ci } ^{152}\text{Eu}$ dissolved in 1 ml GoHy 2227 groundwater (equilibration time: approx. 3 months) was injected. Ultrafiltration shows, that more than 98 % of the ^{152}Eu in the injected tracer solution was bound to humic substances (mainly ^{152}Eu humate). The ^{152}Eu concentration-time distribution was registered after the column no. 1 (total flow distance: 0.5 m), the column no. 2 (1.0 m), the column no. 3 (2.0 m), the column no. 4 (4.0 m) and the column no. 7 (10.0 m) (Fig. 3). Evaluation of ^{152}Eu break-through curves is shown in Tab. 3 and plotted in Fig. 4.

Tab. 2: Hydraulic parameters effective porosity n_{eff} and longitudinal dispersivity α together with the flow velocity v_f in the system fine sand/humic water (total column length 10m).

Time [months]	v_f [cm/s]	n_{eff}	α [cm]
0	3.9×10^{-4}	0.262	0.16
1	4.1×10^{-4}	0.274	0.12
2	4.3×10^{-4}	0.296	0.11
3	4.4×10^{-4}	0.280	0.18

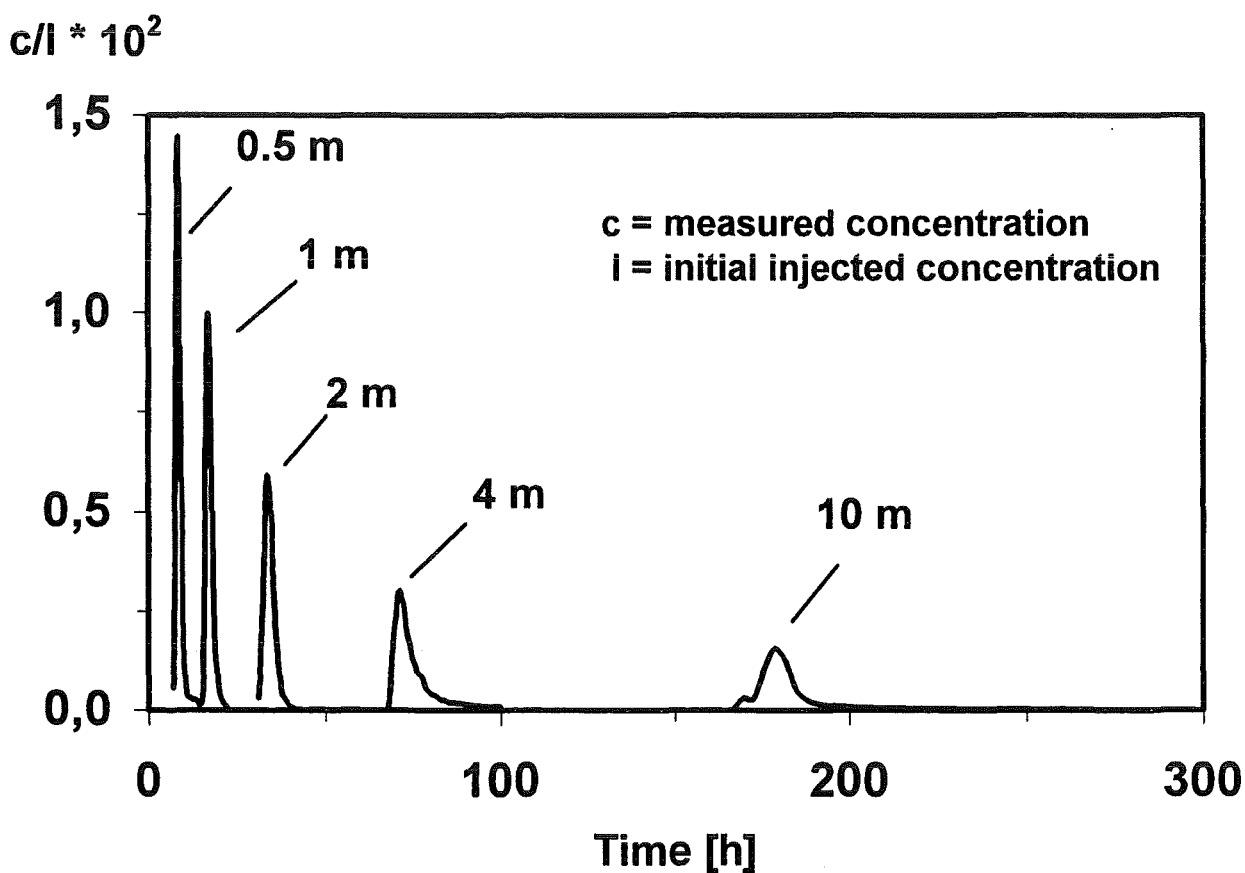


Fig. 3: Concentration-time distributions of ^{152}Eu in the system fine sand/humic water as function of the flow distance.

Tab. 3: Retardation factor R_f and recovery of ^{152}Eu humate in the system fine sand/ humic water as function of the flow distance (flow velocity $v_f = 4.5 \times 10^{-4}$ cm/s).

Flow distance [m]	Measurement	R_f	Recovery [%]
0.5	direct	1.00	82.3
1.0	direct	1.01	74.6
2.0	direct	1.02	68.5
2.0	sampling	1.04	72.1
4.0	direct	1.02	65.3
10.0	sampling	1.03	61.4

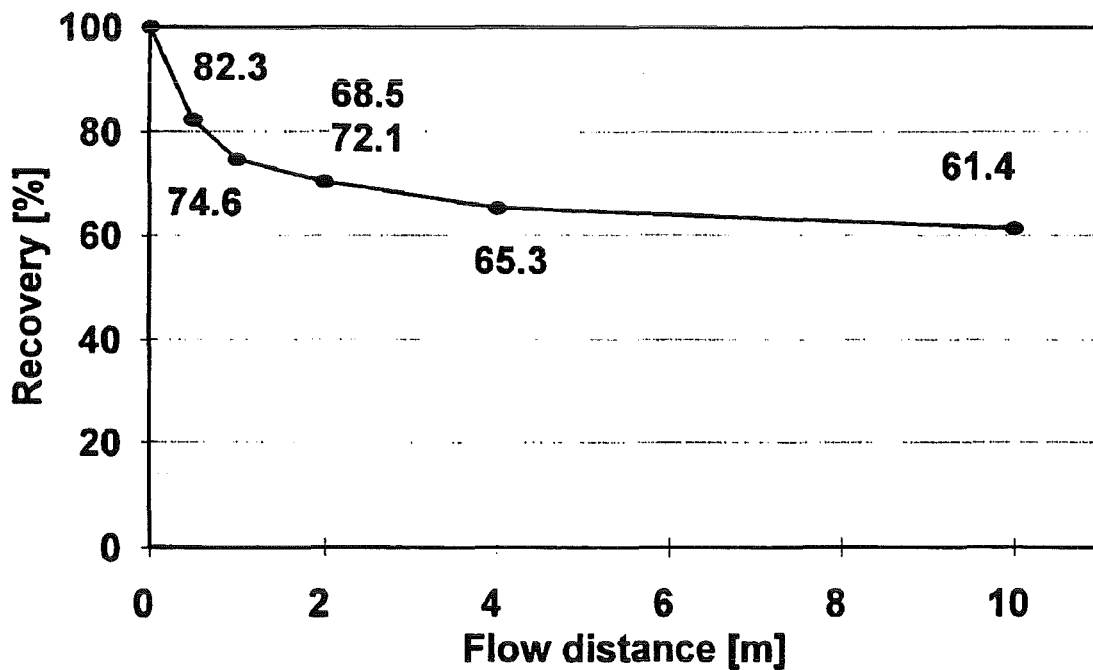


Fig. 4: Recovery of ^{152}Eu in the system fine sand/humic water as function of the flow distance (the numbers along the curve correspond to the recovery).

8. Conclusions

Part of ^{152}Eu humate is transported in the described fine sand/humic water system without retardation (retardation factor R_f approx. 1). The ^{152}Eu recovery decreases with flow distance. The reason for this decreasing recovery may be

- a) filtration of ^{152}Eu humate
- b) sorption of ^{152}Eu humate
- c) sorption of ^{152}Eu after dissociation of the ^{152}Eu humate.

A description of the ^{152}Eu recovery as function of flow distance or time is possible by assuming two first order reactions with different time constants (fast and slow kinetics) for the loss of ^{152}Eu from the solution (cf. FZK/INE contribution to task 4(I)).

Reference

KLOTZ, D., WOLF, M., HERTKORN, N., BUNZL, K., SCHIMMACK, W., ZEH, P. (1996):
Laborversuche zum Transport von ^{125}I -markierten Huminstoffen in einem Feinsand.
- Proc. Freiburger Isotopenkolloquium 1996, Freiberg, 137-146